Characterizing the structure of multiparticle entanglement in high-dimensional systems

DISSERTATION

zur Erlangung des Grades eines Doktors
der Naturwissenschaften

vorgelegt von

Christina Ritz

eingereicht bei der Naturwissenschaftlich-Technischen Fakultät
der Universität Siegen
Siegen 2018

Gutachter:

Prof. Dr. Otfried GÜHNE
Prof. Dr. Thomas MANNEL

Datum der mündlichen Prüfung: 14.12.2018

Prüfer:

Prof. Dr. Otfried GÜHNE
Prof. Dr. Thomas MANNEL
Prof. Dr. Christof WUNDERLICH
Prof. Dr. Ivor FLECK

Abstract

Quantum entanglement is a useful resource for many quantum informational tasks. In this context, enlarging the number of participating systems as well as increasing the system dimension has proven to enhance the performance. In order to successfully use this resource, it is crucial to have a consistent theoretical description of the different kinds of entanglement that can occur within those systems. This thesis studies the classification of entanglement in special families of multipartite and higher dimensional quantum systems. Furthermore, attention is put to the detection of entanglement within these systems.

There are three main projects addressed within this thesis. The first is concerned with the detection of entanglement between multiple systems based on the construction of entanglement witnesses. Here, a one-to-one connection between SLOCC-witnesses and entanglement witnesses within an enlarged Hilbert space is made. The form of the witness operator is such that it can be constructed from any representative state of the corresponding SLOCC class and its maximal overlap with the set of separable states or the set of states within another SLOCC class.

Within the second part, a special family of multipartite quantum states, the so-called qubit hypergraph states, is generalized to arbitrary dimensions. Following the definition of the basic framework, relaying strongly on the phase-space description of quantum states, rules to categorize qudit hypergraph states with respect to SLOCC- as well as LU-equivalence are determined. Interestingly, there exist close connections to the field of number theory.

Furthermore, a full classification in terms of SLOCC and LU is provided for tripartite systems of dimension three and four. Within the subsequent section, rules for local complementation within graph states of not-neccssarily prime dimension are presented. Finally, an extension to weighted hypergraphs is made and, for some particular cases, SLOCC equivalence classes are determined.

The third and last part of this thesis is dedicated to the question of how to reasonably define genuine multilevel entanglement. Starting from an example, a discrepancy of the widely used term of a maximally entangled state and the practical resources needed to produce such a state is shown. This motivates a definition of genuine multilevel entanglement that adapts to the fact that genuine d-level entangled states should need at least d-dimensional resource states. Based on this, the set of entangled multilevel states is then divided into three classes: decomposable (DEC-) states that can be generated from lower dimensional systems, genuine multilevel, multipartite entangled (GMME-) states, whose correlations cannot be reproduced by lower dimensional systems and multilevel, multipartite entangled (MME-) states which lie in between. That is, the last class covers the set of states, which are decomposable with respect to some bipartition. Naturally, within the bipartite scenario, the set of MME-states coincides with the set of decomposable states. Having set the framework, examples for all three classes are provided, as well as methods to distinguish between those. In the bipartite scenario, an analytical criterion is presented that additionally can be used to differ MME from GMME in the multipartite case. To distinguish MME-states from DEC- states has proven to be more involved, nonetheless there exist successful numerical optimization protocols as well as an necessary but not sufficient analytical criterion.

Zusammenfassung

Quantenverschränkung hat sich als eine wertvolle Ressource für viele Aufgaben der Quanteninformationstheorie etabliert. Eine zunehmende Zahl von miteinander verschränkten Systemen sowie eine größere Anzahl verfügbarer Dimensionen bewirkt in diesem Zusammenhang eine Steigerung des Leistungsvermögens und der Effizienz. Um diese Ressource erfolgreich zu nutzen, ist es zuvorderst notwendig, einen konsistenten theoretischen Formalismus zu entwickeln, der die verschiedenen Arten von Verschränkung korrekt beschreibt und zwischen ihnen differenziert. Die vorliegende Arbeit widmet sich der Klassifikation von Verschränkung in speziellen Familien hochdimensionaler Vielteilchensysteme sowie der Detektion von Verschränkung innerhalb dieser.

Diese Dissertation stellt die Forschungsergebnisse aus drei Projekten vor. Der erste Teil handelt von der Konstruktion eines Operators, eines sogenannten Verschränkungszeugen, der es ermöglicht Verschränkung innerhalb von Vielteilchensystemen zu detektieren. Der Hauptaspekt besteht hierbei in der Entwicklung einer Eins-zu-eins-Korrespondenz zwischen SLOCC-Zeugen und Verschränkungszeugen innerhalb eines erweiterten Hilbertraums. Die Form dieses Zeugen ist derart, dass er mit Hilfe eines Zustandes innerhalb der zu detektierenden SLOCC-Klasse und dem maximalen Überlapp dessen mit Zuständen einer inäquivalenten SLOCC-Klasse konstruiert werden kann.

Das zweite Projekt basiert auf der Erweiterung einer speziellen Familie von Vielteilchenzuständen, den Qubit-Hypergraphzuständen. Sie werden auf beliebige Dimensionen verallgemeinert und als Qudit-Hypergraphen definiert. Diese Zustände werden hinsichtlich SLOCC- und LU-Äquivalenzklassen untersucht und Methoden entwickelt um zwischen diesen zu unterscheiden. Interessanterweise konnte hier eine enge Verbindung zum Feld der Zahlentheorie festgestellt werden. Für tripartite Systeme in den Dimensionen drei und vier wird eine vollständige Klassifizierung unter SLOCC und LU angegeben. In den folgenden Abschnitten werden Regeln für die lokale Komplementation für Graphenzustände in nicht notwendigerweise Primzahl-Dimensionen entwickelt. Den Abschluss dieses Themas bildet eine Erweiterung der Qudit Hypergraphenzustände hin zu sogenannten gewichteten Hypergraphzuständen. Für spezielle Fälle davon werden SLOCC- und LU-Äquivalenzklassen determiniert.

Der dritte und letzte Teil dieser Arbeit beschäftigt sich mit der Frage, auf welche Art Mehrlevelverschränkung sinnvoll definiert werden kann. Die Motivation dazu resultiert aus der Tatsache, dass es Zustände gibt, die als maximal verschränkt hinsichtlich ihrer Dimension gelten, aber trotzdem durch Systeme niedrigerer Dimension generiert werden können. Basierend darauf werden drei inäquivalente Klassen von Mehrlevelverschränkung definiert: 1) Zerlegbare Zustände (DEC), deren Korrelationen vollständig durch niedriger-dimensionale Systeme reproduziert werden können, 2) Echt mehrlevel-, mehrteilchenverschränkte Zustände (GMME), für deren Produktion man Kontrolle über Systeme der entsprechenden Dimension haben muss, 3) Mehrlevel-, mehrteilchenverschränkte Zustände (MME), die zerlegbar bezüglich einer bestimmten Bipartition sind. Nach den grundlegenden Definitionen werden Beispiele für jede der drei Klassen diskutiert und Methoden entwickelt, die zwischen den Klassen unterscheiden können. Im bipartiten Fall, sowie für die Unterscheidung zwischen GMME und MME, kann die Frage der Klassenzugehörigkeit analytisch beantwortet werden. Die Differenzierung hinsichtlich MME und DEC basiert weitgehend auf numerischen Methoden, wobei auch ein analytisches Kriterium existiert, das notwendig, aber nicht hinreichend ist.

Contents

List of Figures

List of Tables

Chapter 1

Introduction

One of the most striking feature emerging from quantum mechanics is - next to the superposition principle - without doubt entanglement. Entanglement, named by Erwin Schroedinger in a paper published in 1935 [1], enables correlations between not locally connected parties, which are impossible to be described or reproduced within the realm of classical physics.
Earlier in the same year Einstein, Podolsky and Rosen published their famous EPR-paper [2] that deals with a hypothetical scenario regarding local measurement outcomes and their correlations within entangled systems. The results and possible explanations to solve the paradox emerging from the aforementioned scenario were discussed quite controversy among the scientific community. Einstein was an advocate of the concept that the worth and the correctness of any physical theory should be directly related to its connectivity regarding the elements building up physical reality. Thus, he was most inclined, out of the two elements, that were shown not to exists simultaneously (completeness (meaning: reality) and locality) to decline the completeness of quantum mechanics, proposing there had to exist *hidden variables* inherent in physical systems that are not encompassed by the quantum description.
In 1964 John Bell contributed an important milestone. In his paper [3], he pursued EPRs thought experiment, transferring it to spin measurements on electrons and formulating a mathematical framework for the locality - as well as the reality-assumption. Thereby he developed an inequality, consisting of the measurement outcomes of the two systems, that defines clear bounds on the values that can be reached within classical physics and furthermore even within local hidden variable theories. Solely quantum mechanics being able to produce theoretically predictable violation of those bounds. The CHSH inequality [4] specifies this original inequality and represents the nowadays most commonly used inequality. Since then, there have been many experimental tests, showing a violation of Bells, (i.e. the CHSH or some modified version [5]) inequality. The first one being done in 1972 by Freedman and Clauser [6] by measuring correlations in entangled photon pairs, which were also used in a series of experiments done by Alain Aspect et al. from 1981-1982 [7], [8]. In 1998 the locality loophole still present in the earlier experiments was closed for the first time [9]. A new level within this field of experimental Bell tests was reached by including systems consisting of more than two parties, e.g. by using the tripartite GHZ-entangled state [10] Even though not all experimental loopholes - concerning e.g. locality, detection and free choice of measurement - have been simultaneously fully closed yet, these experiments strongly emphasize the fact, that quantum mechanics does provide correct predictions of the measurable reality.
Once the existence of non local properties inherent in this special branch of quantum mechanics, manifesting themselves in entangled quantum states, was sufficiently proven, the question of utility came to the focus of the scientists: Is it possible to exploit the non local structure of entanglement and use it for technological tasks? The answer to this was a manifold “yes”.

The first application of entanglement was theoretically proposed by Wiesner [11] within the field of cryptography. In 1984 Bennet and Brassard extended Wiesners ideas and presented a practically feasible usage of quantum mechanics within this branch. They developed the first quantum key distribution (QKD) based on polarization states of a single photon, a technique to be used for producing secure keys for encrypting and decrypting messages. Within their famous BB84 protocol [12] they consistently show - based on the "No-Cloning-Theorem" [13], [14] - how it is actually possible to increase the classically accessible level of security within cryptographic mechanisms. Two years later, Bennetts B92 [15] protocol generalized the BB84 such that now it was possible to use non-orthogonal states, thereby simplifying the experimental implementation considerably. A new approach to quantum cryptography protocols was contributed by Ekert [16] in 1991, presenting the first quantum key distribution based on entangled states. Further applications of entanglement within the quantum communication sector were found to be, for example, in 1992 the concept of super dense coding [17]. Another growing field of applied entanglement can be found in the sector introduced in 1993 by Bennett [18] : quantum teleportation - the transfer of quantum states from one entangled partner particle to the, spatially separated, other. The first practical realizations, reporting a successful teleportation of quantum states, are going back to experiments done independently by two groups [19], [20] in 1997. Whereas at the beginning the teleportation distance was mere centimeters, the progress in recent years shows teleportation over tenth of kilometers and more [23], [24]. Furthermore, in 2004 teleportation of single atom states was experimentally shown to be possible [21], [22]. Today quantum cryptography poses as an important feature used by high security level organizations. The further development within this sector being of strong interest, as especially in modern times a secure way of transmitting information can become crucial. Another field, where entanglement has found an application, is quantum computing. In 1985, David Deutsch [25] laid the groundwork by showing that it is in principal possible to simulate important phenomena by a quantum computer. Further research resulted in the remarkable proof that a quantum algorithm, the Shor-Algorithm [26], can do the factorization of large numbers with higher efficiency than it is possible with any known classical algorithm. It has been practically realized with photonic qubits [27]. An algorithm providing a speedup compared to all classical accessible options was developed by Grover [28]. It covers the search of an unknown data base with N entries and was successfully tested experimentally with the aid of cluster states [29].

In conclusion, the importance and utility of quantum entanglement has, without doubt, been demonstrated by defining entanglement as physical resource that can help to overcome classical restrictions and thereby increase the profitableness of some important fields in the sector of technology and information theory.

From these manifold applications rises the urging need to understand entanglement in its essential structure. Especially, the question what kinds of entanglement exist and which of them may or may not be used for the same tasks is of interest. This is due to the fact that it might be practically more easy to prepare one special entangled state than another.

Additionally, for practical uses, the knowledge how to detect, if a given state is entangled and a way to quantify the entanglement within a state, is of interest. Those queries are mostly solved for low dimensional (2×2 *and* 2×3) systems built up out of not more than two parties, by the Peres-Horodecki-Criterion [30], [31].

Whereas the entanglement properties and structure of bipartite systems is quite well understood, the same is not true for high dimensional and multipartite systems. As multipartite

entanglement has the potential to further increase the efficiency of quantum information task and already has found practicable applications, for example in quantum cryptography [32], the interest in a mathematically sound description and its implications is strong.
The involved nature of the structure of multipartite and high dimensional entangled states eludes a general description that is analogous to the bipartite case up to now. Nonetheless, by restricting ourselves to special families of states, it is possible to reduce the complexity and hence the subclasses allow for full or partial characterization regarding their entanglement properties. Within this field, the graph states [33] and their generalization to hypergraph states [34] are a famous example that has already proven its usefulness in practical applications, i.e. in error correcting codes [36], measurement based quantum computation [35] and violation of realism in Bell inequalities [37].

This thesis is dedicated to the characterization and detection of entanglement in multipartite and high dimensional quantum systems. It is largely based on the following publications:

1. **'Qudit hypergraph states**, F.E.S. Steinhoff, C. Ritz, N. Miklin and O. Gühne, Phys. Rev. A **95**, 052340 (2017).

2. **'Characterizing genuine multilevel entanglement'**, C. Ritz, T. Kraft, N. Brunner, M. Huber and O. Gühne, Phys. Rev. Lett. **120**, 060502 (2018)

3. **'Tensor Witness'**, C. Ritz, C. Spee and O. Gühne: soon to be published

The focus is subdivided into three main parts: the detection of entanglement via entanglement witnesses (see 3.), the characterization of entanglement properties within the class of qudit hypergraph states (see 1.) and the definition of multilevel entanglement in an experimentally consistent context (see 2.)
Within the first topic, we establish a one-to-one connection from SLOCC witnesses to entanglement witnesses acting on a larger Hilbert space. Whereas entanglement witnesses are an important tool for verifying, if a given quantum state is entangled, SLOCC witnesses can give testimony of membership of a given state to a certain kind of SLOCC class, i.e. they distinguish between different kinds of entanglement. This is especially of importance for an increasing number of participating systems and dimensions. The relation between those types of witnesses enables us to reduce the question of entanglement type to verifying entanglement in general on a doubled Hilbert space. That is, from any SLOCC witness in a lower dimensional Hilbert space, a valid entanglement witness acting on the doubled Hilbert space can be constructed. The witness construction is based on the maximal squared overlap of a representative state of the respective SLOCC class we want to verify a state to be in and the set of states we want to separate this class from.
The second topic focuses on the generalization of qudit hypergraph states to systems of arbitrary dimension. The entangling multi- qudit operations are generalizations of the qubit Pauli-gates. A defining property emerging from the structure of those higher-dimensional Z-gates manifests itself in a rich structure of different kinds of hyperedges. To characterize equivalence classes with respect to LU-(local unitary) and SLOCC-(stochastic local operations and classical communication) operations, we exploit a close connection of the entangling operations, i.e. the associated hyperedge structure, to the field of number theory. Furthermore, we discuss a possible extension to so-called weighted hypergraphs. For qubits, a subclass of those were defined in [39] and found to be within the class of LME (locally maximal entangled) states [38]. For qubit graph states as well as qudit graphs of prime dimension [42] a

powerful tool to find LU equivalent states is a method denoted as local complementation (LC) [41]. We present a similar method, valid also for non-prime dimensions.
The last topic of this thesis is dedicated to a definition of multilevel entanglement that gives consideration to the experimental scenario. Up to now, a system was often times determined to possess high dimensional entanglement, when maximizing entanglement monotones, e.g. based on entropic measures. We show a contradiction based on the fact that in this way many states declared to be high dimensional are, in fact, reproducible by lower dimensional systems. Aiming to revoke this contraction, we define multilevel entangled states as those, whose correlations can not be reproduced, if one has not access to the corresponding multilevel systems. Based on this, the set of entangled multilevel states is divided into three classes: 1) decomposable (DEC-) states that can be generated from lower dimensional systems, 2) genuine multilevel, multipartite entangled (GMME-) states, whose correlations cannot be reproduced by lower dimensional systems and 3) multilevel, multipartite entangled (MME-) states, which lie in between. That is, the last class covers the set of states, which are decomposable with respect to some bipartition. We derive analytical as well as numerical methods to distinguish between the different classes. In the bipartite case, MME coincides with DEC and an analytical criterion that distinguishes between DEC and GMME, based on the rank of a matrix build up by the states Schmidt coefficients, is provided. The same criterion is naturally useful for deciding, if a multipartite state is within the MME- or GMME set. To distinguish MME-states from DEC-states has proven to be more involved, and though no general analytical criterion could be found, there exist successful numerical optimization protocols as well as an analytical criterion providing a necessary but not sufficient condition for decomposability. based on the subspace ranks of the coefficient matrix.

OVERVIEW of the THESIS

This thesis is organized as follows: Chapter 2 gives an introduction to the mathematical framework of quantum theory as well as a review of the most important results and tools used for characterizing quantum states, especially regarding their entanglement properties. Chapter 3 is based on the results of a joint work with Cornelia Spee and Otfried Gühne soon to be published. Following an introduction to semidefinite programming (SDP) in Sec. 3.1, Sec. 3.2 covers the main result, i.e. establishing a one-to-one connection of SLOCC witnesses and entanglement witnesses acting on a doubled Hilbert space. We discuss a possible relaxation to the set of PPT-states, which allows for a formulation as an SDP. Furthermore, we investigate a $2 \times 3 \times 3$ system in detail regarding SLOCC equivalence classes and their underlying hierarchic structure. We furthermore mention possible entanglement witnesses that can be constructed from the SLOCC representatives. Chapter 4 is dedicated to the theory of qudit hypergraphs. Following an introduction into the phase-space picture in Sec. 4.1, Sec. 4.2 presents the work done in collaboration with Frank E. S. Steinhoff, Nikolai Miklin and Otfried Gühne published in [185]. It covers the definition of qudit hypergraph states and their characterization with respect to SLOCC and LU equivalence classes. In Sec. 4.3, a method similar to LC in prime dimensions is derived for arbitrary dimensional graph states. Within Sec. 4.4, we extend the class of qudit graph states by introducing weights to the hyperedges. This corresponds to allowing for a more general version of Z-gates inhibiting complex phase parameters. Chapter 5 covers the definition and characterization of multilevel entanglement within bipartite as well as multipartite systems. In Sec. 5.1 the results published in [186], are presented. This work

was done in collaboration with Tristan Kraft, Nicolas Brunner, Marcus Huber and Otfried Gühne. In 5.2, a necessary but not sufficient analytical criterion to decide between DEC and MME is given. Sec. 5.3 shows a generic way to write graph states within a lower dimensional encoding and, finally, Sec. 5.3 discusses an alternative way of distributing subsystems within a lower dimensional encoding that is closely related to quantum networks. 6 concludes this thesis with a summary of the main results and an outlook concerning further questions of interest to be investigated.

Chapter 2

Preliminaries

Within this chapter, the fundamental concepts of quantum information theory are introduced. The main focus lies on the description of entangled systems and the mathematical tools needed to characterize, classify, quantify and detect entanglement in the bipartite as well as the multipartite- qudit scenario. Starting with the mathematical description of single quantum states in Hilbert spaces as well as the according operations that can be used to manipulate those, the focus is then shifted to multipartite systems. The notion of entanglement is introduced followed by the most important tools which allow for a characterization and detection. As they play an important role throughout large parts of this thesis, the last part of this introductory chapter is dedicated to a special class of multipartite quantum systems of arbitrary dimension: graph- and hypergraph states. In this context the stabilizer formalism, a useful way to describe quantum states from another perspective, is introduced.

2.1 Mathematical framework

This section will cover the basic mathematical notions and definitions of quantum states, the space they live in as well as the description of operations that can be applied to those. Here we differ between global and local operations with the main focus on different classes of local operation. These have the inherent property of preserving entanglement and as such are important and most useful in many aspects of entanglement characterization that are covered by this thesis. For a more detailed overview of those concepts, see [46], [47].

2.1.1 Hilbert space

The underlying mathematical structure that defines the operating framework of quantum mechanics is a complex vector space of finite or infinite dimension and an inner product that is complete with respect to the norm induced by said inner product: the Hilbert space $\mathcal{H}$. From the general definition of the dual space V^* of a vector space V over a field $\mathbb{K}$ as the space of linear functionals Λ over V that map elements of V back to $\mathbb{K}$

$$\Lambda(V, \mathbb{K}) : \; V \quad \longrightarrow \quad \mathbb{K} \tag{2.1}$$

one can infer that in case of $V = \mathcal{H}$ the inner product creates a bijection $V \longleftrightarrow V^*$ and thereby Dirac notation presents a valid formal language. The inner - or scalar- product hence is defined as the product of an element within the Hilbert space, some vector $|\psi\rangle$, and the complementary element $\langle\varphi| = (|\varphi\rangle)^\dagger$ of some vector $|\varphi\rangle$ within the dual space $\mathcal{H}^*$, such

that

$$\langle\varphi|\psi\rangle = \langle\psi|\varphi\rangle^* = \sum_{i=0}^{d-1} \varphi_i\psi_i \qquad \in \mathbb{C} \tag{2.2}$$

for $d = \dim(\mathcal{H}) = \dim(\mathcal{H}^*)$. The inner product is anti-linear in the first- and linear in the second argument:

$$\begin{aligned} \langle\alpha\varphi_1 + \beta\varphi_2|\psi\rangle &= \alpha^* \langle\varphi_1|\psi\rangle + \beta^* \langle\varphi_2|\psi\rangle \\ \langle\varphi|\alpha\psi_1 + \beta\psi_2\rangle &= \alpha \langle\varphi|\psi_1\rangle + \beta \langle\varphi|\psi_2\rangle . \end{aligned} \tag{2.3}$$

Furthermore, the inner product of a vector with its dual complement is positive semi-definite, that is $\langle\psi|\psi\rangle \geq 0$ and $\langle\psi|\psi\rangle = 0$ if and only if $|\psi\rangle = 0$.

From the definition and properties of the inner product a definition of the norm directly emerges as the square root of the inner product, allowing for geometrically based distance measures within the space:

$$|| \, |\psi\rangle \, || = \sqrt{\langle\psi|\psi\rangle} \qquad \in \mathbb{R} \tag{2.4}$$

Completeness then is satisfied if for any Cauchy sequence of elements $|\psi_n\rangle$ in $\mathcal{H}$ there exists an unique element $|\psi\rangle$ in $\mathcal{H}$ such that:

$$\lim_{n\longrightarrow\infty} || \, |\psi_n\rangle - |\psi\rangle \, || \longrightarrow 0. \tag{2.5}$$

In case of composite systems consisting of more that one party the operating space of the combined system can then be defined by the tensor product of all participating single-system Hilbert spaces, that is

$$\mathcal{H}_{composite} = \mathcal{H}_1 \otimes \mathcal{H}_2 \otimes ... \otimes \mathcal{H}_n = \bigotimes_n \mathcal{H}_n \tag{2.6}$$

for an n-partite system. The overall dimension of the total system is calculated to be

$$\dim[\mathcal{H}_{composite}] = \dim[\mathcal{H}_1] \times \dim[\mathcal{H}_2] \times ... \times \dim[\mathcal{H}_n] = \prod_n \dim[\mathcal{H}_n]. \tag{2.7}$$

At this point it is important to mention the fact that this work concentrates exclusively on the case of finite dimensions, many mathematical tools we will make use of are solely valid within this case.

2.1.2 Quantum states in Hilbert space

Pure quantum states

Normalized elements of the Hilbert space define the class of pure quantum states. For a single system, the vector $|\psi\rangle$ associated with a d-dimensional pure state can always be written as a decomposition w.r.t. a set of orthonormal basis vectors $|v\rangle$ of $\mathcal{H}$:

$$|\psi\rangle = \sum_{v=0}^{d-1} c_v \, |v\rangle \tag{2.8}$$

The weighting prefactor $c_v \in \mathbb{C}$ restricted to values satisfying $\sum_v |c_v|^2 = 1$ assures normalization of $|\psi\rangle$. In case of composite systems the associated vector describing a pure quantum state is the tensor product of the single system vectors. Then for n particles, the vector of a

pure state in some orthonormal basis $\{v_1, v_2, ..., v_n\}$ is

$$|\psi_n\rangle = |\psi_1\rangle \otimes |\psi_2\rangle \otimes ... \otimes |\psi_n\rangle = \sum_{v_1=0}^{d_1-1} \sum_{v_2=0}^{d_2-1} ... \sum_{v_n=0}^{d_n-1} c_{v_1 v_2 ... v_n} |v_1 v_2 ... v_n\rangle , \tag{2.9}$$

where we use $|v_1\rangle \otimes |v_2\rangle \otimes .... \otimes |v_n\rangle \equiv |v_1 v_2 ... v_n\rangle$ to keep the notation simple.

It is worth remarking that often times for simplicity in calculations, the choice of basis falls to a special kind of orthonormal basis, the so-called 'computational' basis, where the basis vectors γ_i are built such that they have zeros in all places except the $i-th$ position - thus $|\gamma_1\rangle = (1, 0, ..., 0)^T$, $|\gamma_2\rangle = (0, 1, ..., 0)^T$,..., $|\gamma_n\rangle = (0, 0, ..., 1)^T$ and

$$|\psi_\gamma\rangle = \sum_{\gamma_1=0}^{d_1-1} \sum_{\gamma_2=0}^{d_2-1} ... \sum_{\gamma_n=0}^{d_n-1} c_{\gamma_1 \gamma_2 ... \gamma_n} |\gamma_1 \gamma_2 ... \gamma_n\rangle . \tag{2.10}$$

The coefficient matrix of pure quantum states

From the decomposition of a multipartite pure quantum state in computational basis Eq. (2.10) we can construct a matrix with coefficients $c_{\gamma_1 \gamma_2 ... \gamma_n}$ which contains all information about the state. Because of the two-dimensionality of a matrix regarding its division into rows and columns, there is more than one way to define the coefficient matrix for systems that are composed of more than two subsystems.
In order to illustrate the general concept, let us start with two subsystems A and B and their combined system (AB)

$$|\psi_{AB}\rangle = \sum_{\gamma_A=0}^{d_A-1} \sum_{\gamma_B=0}^{d_B-1} c_{\gamma_A \gamma_B} |\gamma_A \gamma_B\rangle . \tag{2.11}$$

In this case, the row index of the coefficient matrix would correspond to the levels of system A, the column index to those of system B. The dimension of the matrix is determined by the dimension of the subsystems. The coefficient matrix $C_{\gamma_A \gamma_B}$ now takes the form:

$$C_{\gamma_A \gamma_B} = \sum_{\gamma_A, \gamma_B=0}^{d_A-1, d_B-1} c_{\gamma_A \gamma_B} |\gamma_A\rangle \langle\gamma_B| = \begin{pmatrix} c_{00} & c_{01} & \cdots & c_{0 d_B-1} \\ c_{10} & \ddots & & c_{1 d_B-1} \\ \vdots & & \ddots & \vdots \\ c_{d_A-1 0} & \cdots & \cdots & c_{d_A-1 d_B-1} \end{pmatrix} \tag{2.12}$$

where the convention is $\dim(A) = d_A = \#\ rows$
and accordingly $\dim(B) = d_B = \#\ columns$

Generalizing this concept to systems consisting of more than two parties, one immediately notices that there is more than one way to define its coefficient matrix, as the choice which systems are displayed by the rows and which ones by the columns is arbitrary. This origins therein that for multipartite states the equivalent of a coefficient matrix is a coefficient tensor. Such a tensor has different unfoldings, i.e. for a three partite state, the coefficient tensor T_{ijk} can be unfolded to the matrices in the respective bipartite splits $T_{ij|k}$, $T_{ik|j}$ and $T_{jk|i}$. Therefore all possible bipartite splits of the whole systems can be considered to define a valid

coefficient matrix, each of which can provide different complementary insights in the systems structure.

Schmidt decomposition

For the special case of bipartite pure states, any state of the form Eq. (2.9) can be written in the so-called Schmidt decomposition

Theorem 2.1. Schmidt decomposition [50], [49]
Let $|\psi_{AB}\rangle$ be a normalized state in $\mathcal{H}_{AB}$. Then there exist ortonormal bases $\{a_i\}_{i=0}^{d_A-1}$, $\{b_i\}_{i=0}^{d_B-1}$ of $\mathcal{H}_A$, $\mathcal{H}_B$ respectively such that

$$|\psi_{AB}\rangle = \sum_{i}^{min(d_A-1,d_B-1)} \sqrt{\lambda_i}\,|a_i\rangle\,|b_i\rangle \tag{2.13}$$

where the Schmidt coefficients $\{\sqrt{\lambda_i}\}$ are real, non-negative and satisfy the normalization condition ($\lambda_i \geq 0,\ \forall i,\ \ \sum_i \lambda_i = 1$).

Within Eq. (2.13), the number of non-zero Schmidt coefficients $\sqrt{\lambda_i} \neq 0$ is defined as the *Schmidt rank* of the state $|\psi_{AB}\rangle$. The Schmidt decomposition is an important tool in quantum information theory regarding the classification and characterization of entanglement of pure bipartite quantum states. Note that for more than two parties, the existence of a Schmidt decomposition is not given for arbitrary states [55]. This is due to the fact that the Schmidt decomposition necessarily demands equal spectra of the reduced density matrices which is not given in general.

Mixed quantum states

For practical uses, one needs to broaden the notion of pure quantum states. The description of a system by its pure state vector is only possible if perfect knowledge about which state was being prepared is accessible. In experiments, this knowledge is typically not available. Instead, one can only identify a set of possible states the system can be in, together with the relative probabilities of occurrence. Those states, which incorporate the incomplete knowledge about the system, are named mixed quantum states. The density matrix, a linear, bounded operator ρ on $\mathcal{H}$ has the mathematical properties which appropriately grasps the concept of a statistical ensemble $\{p_i, |\psi_i\rangle\}$ of potential states. It can be written as a weighted sum of projectors on all pure states within the ensemble:

$$\rho = \sum_i p_i\,|\psi_i\rangle\,\langle\psi_i|\,. \tag{2.14}$$

which is a quadratic matrix of the dimension of the Hilbert space they act on. Here the p_i define the probability with which the system actually is in state $|\psi_i\rangle$, thus they have to be real, they satisfy $0 \leq p_i \leq 1$ as well as $\sum_i p_i = 1$. Then the density matrix ρ is normalized, as $\mathrm{tr}(\rho) = \sum_i p_i = 1$ and positive semi-definite $\langle\varphi|\,\rho\,|\varphi\rangle \geq 0\ \forall\varphi \in \mathcal{H}$ leading to exclusively non-negative eigenvalues $\{\lambda_i\}$. From these properties hermiticity ($\rho = \rho^\dagger$) follows. Note that the decomposition of a density matrix in a statistical ensemble of pure states is not unique as the $\{|\psi_i\rangle\}$ need not be orthonormal. Though it is always possible to find a decomposition where the set of pure states $\{|\psi_i\rangle\}$ from a complete orthonormal basis, that is $\langle\psi_i|\psi_j\rangle = \delta_{ij}$ and $\sum_i(|\psi\rangle\,\langle\psi|)_i = \mathbb{1}$. Hence, within the orthonormal decomposition of ρ, the probabilities

p_i coincide with the eigenvalues of the density matrix, as: $\rho = \sum_i \lambda_i |\eta_i\rangle \langle\eta_i|$. From the density operator, one can deduce full information on the quantum state and all possible decompositions of ρ will lead to the same predictions in terms of measured observables. Thus two different ensembles which share the same density matrix are physically indistinguishable. Within the density operator formalism the class of pure states emerges as an ensemble where there is only one probability not equal to zero $p_i = 0\ \forall i \backslash \{i = j\}$. Thus only one element of the sum in (2.14) survives. As a direct consequence it follows that in case $\rho = \rho_{pure}$ the density matrix has rank one and thus

$$\rho_{pure} = |\psi_j\rangle \langle\psi_j| \qquad \text{with: } \rho\mathrm{tr}(\rho^2) = 1,\ \rho^2 = \rho \tag{2.15}$$

A tool to quantize the 'purity' of a density matrix is the trace of ρ^2. It takes the maximal value of one for pure states ($Tr(\rho^2_{pure}) = 1$) and its minimal value ($Tr(\rho^2_{mm}) = \frac{1}{d}$) for the state that displays equally weighted probabilities $p_i = \frac{1}{d}\ \forall\ i$ for a d-dimensional system. We call this the 'maximally mixed state' with respect to particle number and system dimension.

Reduced quantum states

The coupling of two or more quantum systems is achieved by the tensor product of the respective Hilbert spaces, e.g. their elements. Suppose now that, given a multiparticle system, one is interested in only one or some parts of the whole. For example, it may be that the systems are spartially divided and the accessibility is restricted to specified subsystems. Thus, the need for an operation contrary to the tensor product arises. It is called the **partial trace**, which maps an element of the whole Hilbert space to an element of the whole Hilbert space minus the outtraced subsystem. As such it disregards the parts of the systems, in which one is not interested in, by averaging them out. For example, if we have a tripartite quantum system ρ_{ABC}, consisting of the subsystems A, B and C, we can obtain a state that is an element of $\mathcal{H}_B \otimes \mathcal{H}_C$ by taking the partial trace over subsystem A. It is then denoted as a **reduced state** described by the reduced density matrix ρ_{BC}

$$\rho_{BC} = \mathrm{tr}_A(\rho_{ABC}) = \sum_{k=0}^{d_A-1} \langle\psi_A|_i\, \rho_{ABC}\, |\psi_A\rangle_i \tag{2.16}$$

where $\{|\psi_A\rangle_i\,,\ i \in [0, ..., d_A - 1]\}$ forms an orthonormal basis of $\mathcal{H}_\mathcal{A}$ and ρ_{BC} is now the **reduced density operator** describing the combined system BC.

Note that in case the state of the whole system is a pure state, the reduced states hold informations on the entanglement properties of the original system. For pure product states (for readability, let us look at a bipartite system, the generalization to more parties is straightforward) $|\psi_{AB}\rangle = |\psi_A\rangle \otimes |\psi_B\rangle$, the reduced state obtained by tracing out system A reads

$$\begin{aligned} \rho_B &= Tr_A(\rho_{AB}) = Tr_A((|\psi\rangle \langle\psi|)_{AB} = Tr_A(|\psi_A\rangle \langle\psi_A| \otimes |\psi_B\rangle \langle\psi_B|) \\ &= Tr(|\psi_A\rangle \langle\psi_A|)\, |\psi_B\rangle \langle\psi_B| = 1 \times |\psi_B\rangle \langle\psi_B| \\ &= |\psi_B\rangle \langle\psi_B|\,, \end{aligned} \tag{2.17}$$

which is again a density matrix for a pure quantum state of subsystem B.
Contrary to this for an (again bipartite) entangled state, say $|\psi_{AB}\rangle = \sum_{ij} c_{ij} |ij\rangle \neq |\psi_A\rangle \otimes$

$|\psi_B\rangle$, tracing out system A gives

$$\begin{aligned}\rho_B = Tr_A(\rho_{AB}) &= Tr_A(\sum_{iji'j'} c_{ij}c^*_{i'j'} |ij\rangle \langle i'j'|) \\ &= \sum_{ijj'} c_{ij}c^*_{ij'} |j\rangle \langle j'|\end{aligned} \tag{2.18}$$

which clearly describes a mixed state of system B.
Thus, by looking at the reduced states of a systems, one can decide on separability of the original system. It is important to again emphasize that this criterion works solely for pure states of the whole system.

2.1.3 Quantum operations

The term quantum operation defines the class of transformations that describe any valid evolution principally possible for a quantum system. The properties such an operation has to satisfy emerge from the condition that the evolved state still has to fulfill all qualities of a proper quantum state, e.g. the physicality is to be preserved. Within the density matrix formalism, this means that a quantum operation is an operation Λ on the space of density operators that maps one quantum state $\rho_{initial}$ to another quantum state $\rho_{evolved}$.

$$\Lambda[\rho_{initial}] = \rho_{evolved} \tag{2.19}$$

From the aforementioned condition of perseverance of physicality, the map Λ is necessarily characterized by the following properties:

- Due to the ensemble interpretation, it is to be demanded that the probabilistic interpretation of the initial density matrix is still valid for the evolved state. Therefore any map representing a valid quantum operation has to satisfy

$$\Lambda[\sum_i p_i\rho_i] = \sum_i p_i\Lambda[\rho_i] \tag{2.20}$$

  that is, the ensemble $\{p_i, \rho_i\}$ is be mapped to the ensemble $\{p_i, \Lambda[\rho_i]\}$. In other words, Eq. (2.20) demands Λ to be a **linear** map.

- Furthermore, as the prefactors $\{p_i\}$ in Eq. (2.14) refer to probabilities, a quantum operation generating evolution has to preserve the trace. In case of Λ describing a measurement, the trace does not need to be preserved, as the trace of the post measurement state $\mathrm{tr}(\rho') = \mathrm{tr}(\Lambda[\rho])$ then attribute to the probability with which the measurement outcome does occur and normalization restores the unit trace $\rho_n = \frac{\Lambda[\rho]}{\mathrm{tr}(\Lambda[\rho])}$. In summary, any quantum operation has to be non-trace-increasing

$$0 \leq Tr(\Lambda[\rho]) \leq 1 \qquad \forall \ \ \rho \in \mathcal{H} \tag{2.21}$$

- As the density matrix is an hermitean operator, a quantum operation has to preserve hermiticity

$$\Lambda[\rho] = [\Lambda[\rho]]^\dagger \qquad \forall\ \rho\ \in\ \mathcal{H} \tag{2.22}$$

- Any density operator ρ representing a quantum state is hermitean and has positive, real eigenvalues. To preserve this properties, Λ has to be **completely positive**. Positivity alone does not suffice for composite systems, as it can lead not negativity when considering exentions of the original system. Thus

$$\rho_{AB} \geq 0 \quad \Leftrightarrow \quad \Lambda_A[\rho_{AB}] = (\Lambda_A \otimes \mathbb{1}_B)[\rho_{AB}] \geq 0 \quad \forall\ \rho_{AB}\ \in\ \mathcal{H}. \tag{2.23}$$

Consequently, all operations describing a physical process a quantum state can undergo, are described by completely positive, trace preserving linear maps (CPTP-maps).

An elegant way to describe CPTP-maps is the operator-sum, or Kraus-, representation [54] [53]. To show this equivalence, firstly the Stinespring dilation theorem is needed

Theorem 2.2. Stinespring dilation theorem [52]
Let $\Lambda: \ S(\mathcal{H}) \longrightarrow S(\mathcal{H})$ be a completely positive, trace preserving linear map that maps density matrices to density matrices. Then there exists a unitary operation U and a Hilbert space $\mathcal{H}_E$ with U acting on the combined space $H \otimes H_E$ such that:

$$\Lambda(\rho) = Tr_E[U(\rho \otimes \rho_E)U^\dagger] \qquad \forall\ \ \rho\ \in\ S(\mathcal{H}) \tag{2.24}$$

where ρ_E is a fixed state within the extension Hilbert space $\mathcal{H}_E$ which can opted to be pure without loss of generality. Furthermore, considering the dimensionality of $\mathcal{H}_E$, it can chosen to be such that $dim(\mathcal{H}_E) \leq [dim(\mathcal{H})]^2$.

In other words, the Stinespring dilation theorem states that any valid quantum operation can be rewritten as a unitary evolution of an extended system and the consecutive tracing out of the extended part.
From Stinesprings theorem, the representation by Kraus operators readily follows. It reverses the representation of an CPTP map back to having to consider only the original system without having to take care of extensions.

Theorem 2.3. Kraus representation of CPTP-maps [54]
Let $\Lambda: \ S(\mathcal{H}) \longrightarrow S(\mathcal{H})$ be a linear map. Then Λ is completely positive if and only if its action on a density matrix ρ in $S(\mathcal{H})$ can be decomposed in terms of the Kraus operators K_i as follows:

$$\Lambda[\rho] = \sum_i K_i^\dagger \rho K_i \qquad\qquad \textit{with:}\ \sum_i K_i^\dagger K_i = \mathbb{1}. \tag{2.25}$$

Here the $\{K_i\}$ form a finite set acting on the systems Hilbert space. Note that the trace preserving property is assured by $\sum_i K_i^\dagger K_i = \mathbb{1}$ and for trace decreasing maps this condition will read $\sum_i K_i^\dagger K_i < \mathbb{1}$.

Proof. By Theorem 2.2, the state of the extended system can chosen to be pure. Hence, without loss of generality, let $\rho_E = |\eta_j\rangle \langle\eta_j|$ where the set $\{|\eta_i\rangle\}$ form an orthonormal basis (ONB) of $\mathcal{H}_E$, that is $\langle\eta_i|\eta_k\rangle = \delta_{ik}$ and $\sqrt{\langle\eta_i|\eta_i\rangle} = 1$ for $0 \leq (i,k) \leq d_E - 1$ with $d_E =$

$\dim(\mathcal{H}_E)$. Then Eq. (2.24) takes the form

$$\begin{aligned}\Lambda[\rho] &= Tr_E[U^\dagger(\rho\otimes\rho_E)U] \\ &= \sum_i \langle\eta_i|\,(U^\dagger\rho\otimes(|\eta_j\rangle\langle\eta_j|)U\,|\eta_i\rangle \\ &= \sum_i K_i^\dagger\rho K_i,\end{aligned} \tag{2.26}$$

where in the last equality the operator K_i is defined as $K_i = \langle e_i|Ue_j\rangle$ and acts on the Hilbert space $\mathcal{H}$ of the original system ρ. In order to be trace preserving, Λ has to satisfy

$$\begin{aligned}1 &\equiv Tr(\Lambda[\rho]) \\ &= Tr(\sum_i K_i^\dagger\rho K_i) = \sum_i Tr(K_i^\dagger\rho K_i) \\ &= \sum_i Tr(K_i K_I^\dagger\rho) = Tr(\sum_i K_i K_i^\dagger\rho),\end{aligned} \tag{2.27}$$

where the permutability of sum and trace as well as the invariance of the trace under cyclic permutations was used. As Eq. (2.27) has to hold for all density operators ρ on $\mathcal{H}$, it follows

$$\mathbb{1} = \sum_i K_i^\dagger K_i, \tag{2.28}$$

which proves the claim. Note that an analogous argumentation is valid for trace-decreasing maps. □

Furthermore, note that the operator-sum representation is not unique.
Consecutively, all valid quantum operations can be written in operator- sum representation and there are two main classes to consider:

- Trace preserving quantum operations with $\sum_i K_i^\dagger K_i = \mathbb{1}$
  Within this category all reversible operations can be found. As any unitary operator satisfies $U^{-1} = U^\dagger,\ \ UU^{-1} = \mathbb{1}$, they represent such reversible transitions, for example a change of basis, rotations or simply an identity transformation for U being the identity operator. Furthermore, trace operations of the form $\Lambda[\rho] = Tr(\rho\,|\psi\rangle\langle\psi|)$ fall into this class of CPTP maps.

- (Strictly) trace decreasing quantum operations with $\sum_i K_i^\dagger K_i < \mathbb{1}$
  These kind of operations describe measurements of all kinds, e.g. projective measurements, positive operator valued measurements (POVMs).

Global and local quantum operations on multipartite systems

Considering systems containing two or more subsystems, an important distinction to be made is between *global* and *local* quantum operations. As will be shown in Sec. 2.3, local operations cannot increase the amount of entanglement present within a system whereas global operations are necessary to create entanglement between two or more subsystems. Mathematically, one can formulate the class of quantum operations on an n-partite system transforming the state $\rho \longrightarrow \rho' = \frac{\Lambda[\rho]}{Tr(\Lambda[\rho])}$ as the action of the linear CP(TP)-map Λ on the whole Hilbert space e.g. its element ρ. In case of *local* operations, Λ can be written as tensor product of linear CP(TP)-maps $\Lambda_{(i)} : S(\mathcal{H}_{(i)}) \longrightarrow S(\mathcal{H}_{(i)})$ acting on all subsystems respectively, that is

$\Lambda = \Lambda_1 \otimes \Lambda_2 \otimes ... \otimes \Lambda_n$.
In the operator-sum representation, it follows that any *local* quantum operation on a density matrix ρ can be represented in terms of the Kraus operators $\{K_{i,t_i}\}$ by

$$\Lambda[\rho] = \sum_{t_1,...,t_n} K^7_{1,t_1}\dagger \otimes K^\dagger_{2,t_2} \otimes ... \otimes K^\dagger_{n,t_n} \rho K_{1,t_1} \otimes K_{2,t_2} \otimes ... \otimes K_{n,t_n} \tag{2.29}$$

Here in case of trace preserving operations $\sum_{t_i} K^\dagger_{i,t_i} K_{i,t_i} = \mathbb{1}$ and for trace decreasing operations $\sum_{t_i} K^\dagger_{i,t_i} K_{i,t_i} < \mathbb{1}$. The former are also named *deterministic* local operations, as the probability with which the transformation occurs is equal to one.
Following, local unitary (LU) operations and (stochastical) local operations assisted by classical communication ([S]LOCC) are discussed in more detail, as they are important tools for this thesis.

Measurements

Within the category of non-trace-preserving CP-maps, one can classify the quantum operations describing a measurement process. The most basic form of measurements are projective (or von-Neumann-) measurements [56]. When measuring an observable O, described by an hermitean operator in $\mathcal{H}$ with spectral decomposition $O = \lambda_i \Pi_i$, the Kraus operators describing a projective measurement are projectors $\Pi_i = \Pi_i^\dagger$ on the eigenvalues λ_i. The projectors can always be written as a sum of rank one projectors, $\Pi_i = \sum_j (|\varphi_j\rangle \langle\varphi_j|)_i$, of O. They sum up to identity, $\sum_i P_i = \mathbb{1}$, and are orthogonal, $\Pi_i \Pi_j = \delta_{ij} \mathbb{1}$. Then the probability with which a measurement outcome λ_i occurs is given by Borns rule [57]

$$p_i = \mathrm{tr}(\Pi_i \rho) \qquad \text{e.g. for pure states: } p_i = \langle\psi| \Pi_i |\psi\rangle . \tag{2.30}$$

The normalized state ρ', in which the system can be found after a projective measurement has been performed, is of the form

$$\rho' = \frac{\Pi_i \rho \Pi_i}{\mathrm{tr}(\Pi_i \rho)} = \frac{\Pi_i \rho \Pi_i}{p_i} \quad \text{e.g. for pure states: } |\psi'\rangle = \frac{\Pi_i |\psi\rangle}{\sqrt{\langle\psi| \Pi_i |\psi\rangle}} = \frac{\Pi_i |\psi\rangle}{\sqrt{p_i}} \tag{2.31}$$

The aforementioned projective measurements cover only a part of the whole class of possible measurements on a quantum system. The most general measures are positive operator valued measures (POVMs) [58]. They can be useful to distinguish non-orthogonal states, for which projective measurements provide no option for perfect distinctness [59], [60]. A POVM A is described by a set $A = \{E_i\}$ of positive semi-definite operators $E_i \geq 0$, also known as *effects*, that sum up to identity, $\sum_i E_i = \mathbb{1}$. Each effect E_i is associated with some outcome of the measurement, thus they can be decomposed as $E_i = A_i^\dagger A_i$. The main difference to projective measurements is that POVM elements, or effects need not be orthogonal. Then, the probability for a measurement outcome corresponding to E_i is:

$$p_i = \mathrm{tr}(E_i \rho), \qquad \text{e.g. for pure states: } p_i = \langle\psi| E_i |\psi\rangle \tag{2.32}$$

And the normalized post measurement state becomes

$$\rho' = \frac{A_i \rho A_i^\dagger}{Tr(E_i \rho)} = \frac{A_i \rho A_i^\dagger}{p_i}, \quad \text{e.g. for pure states: } |\psi'\rangle = \frac{A_i |\psi\rangle}{\sqrt{\langle\psi| A_i |\psi\rangle}} = \frac{A_i |\psi\rangle}{\sqrt{p_i}}. \tag{2.33}$$

As a consequence of non-orthogonality of the POVM elements, the same holds for ρ' in (2.33). Hence, POVM measurements are not repeatable, that is, another measurement round could produce different outcomes and thus it is obvious that the post measurement state is not accessible, as it is dependent on the POVM elements M_i. Of great importance, especially considering physical realizability, in context with POVMs is *Naimarks theorem* which states that every POVM can be performed as a projective measurement on an enlarged Hilbert space. More formally

Theorem 2.4. Naimarks theorem [61]
Let $A = \{E_i\}$ be a POVM acting on $\mathcal{H}_A$ with an element ρ_A. Then there exist a projective measurement $\{\Pi_i\}$ acting on the enlarged Hilbert space $\mathcal{H}_A \otimes \mathcal{H}_B$ and a pure state $\rho_B = |\psi_B\rangle\langle\psi_B|$ in $\mathcal{H}_B$ such that:

$$p_i = Tr[(\rho_A \otimes |\psi_B\rangle\langle\psi_B|)\Pi_i] = Tr[E_i\rho_A] \tag{2.34}$$

where for the projectors Π_i can be expressed as a unitary operation acting on the combined space, followed by a projective measurement on $\mathcal{H}_B$, that is $\Pi_i = U^\dagger_{i,AB}(\mathbb{1}_A \otimes \Pi_{i,B})U_{i,AB}$.

Local Unitary operations

Unitary operations belong to the class of deterministic operations as $U^{-1} = U^\dagger$, thus $\sum_i U_i^\dagger U_i = \mathbb{1}$, and are as such represented by trace preserving linear CP-maps. And important feature of unitaries acting on a quantum system is that they induce a change of basis. In case of local unitaries, this means a change of the local basis within the subsystem they are acting on. For global unitaries, the basis of the Hilbert space corresponding to the whole system is changed. As states as well as observables are subjected to this basis change, the systems description is invariant under such kind of local or global unitary transformations. A second fundamental role of unitaries is due to the nature of the Schroedinger equation which states that the systems dynamical behaviour is to be described by *unitary* time evolutions.

Definition 2.1. LU equivalence
Two n-partite states $\rho,\ \rho' \in \mathcal{H}$ are said to be equivalent under local unitary operations if and only if there exists a linear CPTP map Λ with $\Lambda[\rho] = \rho'$ which allows for an operator-sum-representations where all Kraus operators are zero except for one. By definition, this is then an unitary operator that can be written as a tensor product of unitaries with respect to all subsystems.

$$\rho \xleftrightarrow{LU} \rho' \qquad \text{iff: } \rho' = U^\dagger\rho U \quad \text{and: } U = U_1 \otimes ... \otimes U_n \tag{2.35}$$

If $\rho = |\psi\rangle\langle\psi|$ describes a system in a pure state, then local unitary equivalence between $|\psi\rangle$ and another pure n-partite state $|\psi'\rangle$ with $|\psi\rangle, |\psi'\rangle \in \mathcal{H}$ implies:

$$|\psi\rangle \xleftrightarrow{LU} |\psi'\rangle \quad \text{iff } \exists\ U_k,\ k \in [1,...n] \text{ such that: } |\psi'\rangle = U_1 \otimes ... \otimes U_n\,|\psi\rangle \tag{2.36}$$

Prominent examples for local unitary operations are e.g. the Pauli matrices $\sigma_i,\ i = x, y, z$ in case of qubits

$$\sigma_x = \begin{pmatrix} 0 & 1 \\ 1 & 0 \end{pmatrix}, \qquad \sigma_y = \begin{pmatrix} 0 & -i \\ i & 0 \end{pmatrix}, \qquad \sigma_z = \begin{pmatrix} 1 & 0 \\ 0 & -1 \end{pmatrix}, \tag{2.37}$$

which, together with $\sigma_0 \equiv \mathbb{1}$, form a complete basis for the vector space of complex matrices in $\mathbb{C}^2 \otimes \mathbb{C}^2$. Their generalizations to higher dimensional systems which will be discussed in more detail in Chapter 4 on the topic of qudit hypergraph states.

LOCC-Operations

An important class of operations to manipulate a given quantum state are local operations assisted by classical communication, called LOCC-operations. Those operations are able to answer the question whether it is possible to deterministically transform one quantum state ρ into another ρ' in case each party of a multipartite system has access exclusively to their own subsystem. Here, the local operations that can be applied include all quantum operations described by Eq. (2.29) that satisfy the trace-preserving property. That is, local unitary operations, local measurements and coupling to auxiliary systems and their removal. The classical part of those operations induces the option of classically correlated subsystem, where these correlations can be seen as a classical global operation on more than one subsystem. Thus the action a certain party decides to perform on their subsystem may depend on e.g. the classically communicated measurement outcome of another party. As a consequence, the Kraus operators of an LOCC map Λ_{LOCC} can depend on each other and consecutively such LOCC maps are in general very hard to formulate.

Definition 2.2. LOCC equivalence
Two quantum states ρ, ρ' are equivalent under LOCC operations if and only if they are deterministically interconvertible by the use of CPTP-maps inducing LOCC transformations. Formally

$$\rho \xleftrightarrow{LOCC} \rho' \qquad \text{iff: } \exists\ \Lambda_{LOCC},\ \Lambda'_{LOCC} \ \text{ such that: } \Lambda_{LOCC}[\rho] = \rho' \ \text{ and } \ \Lambda'_{LOCC}[\rho'] = \rho. \tag{2.38}$$

For the restricted set of pure quantum states it was shown in [62] that LOCC-equivalence coincides with LU-equivalence. Therefore two pure n-partite states $|\psi\rangle$, $|\psi'\rangle$ can be converted into each other with certainty if and only if they are LU-equivalent in terms of Definition 2.1

$$|\psi\rangle \xleftrightarrow{LOCC} |\psi'\rangle \qquad \text{iff: } |\psi'\rangle = (U_1 \otimes ... \otimes U_n)\,|\psi\rangle \tag{2.39}$$

The question of whether or not a bipartite pure state $|\psi\rangle$ can be transformed into another $|\psi'\rangle$ has been answered by Nielsons theorem [51]. Before stating the theorem itself, the definition of majorization is needed.

Definition 2.3. Majorization
Let $\vec{u} = (u_1, u_2, ..., u_{d_u})$, $\vec{v} = (v_1, v_2, ..., v_{d_v})$ be vectors in $\mathbb{R}^{d_u}$, $\mathbb{R}^{d_v}$ describing a probability distribution, that is $\sum_{i=1}^{d_u} u_i = \sum_{i=1}^{d_v} v_i = 1$ as well as $u_i, v_i \geq 0$. Furthermore, let $\vec{v}^{\downarrow}$, $\vec{u}^{\downarrow}$ denote the same vectors but with the entries ordered as a descending sequence, i.e. $u_1^{\downarrow} \geq ... \geq u_{d_u}^{\downarrow}$ and $v_1^{\downarrow} \geq ... \geq v_{d_v}^{\downarrow}$. Then $\vec{u}^{\downarrow}$ is majorized by $\vec{v}^{\downarrow}$, that is $\vec{u}^{\downarrow} \prec \vec{v}^{\downarrow}$, if and only if

$$\sum_{i=1}^{k} u_i^{\downarrow} \leq \sum_{i=1}^{k} v_i^{\downarrow} \qquad \forall\ k \in [1, ..., \min(d_u, d_v)] \tag{2.40}$$

Then Nielsons theorem can be formulated as follows

Theorem 2.5. Nielsons theorem [51]
A bipartite pure quantum state $|\psi\rangle$ is convertible to another state $|\varphi\rangle$ with certainty by LOCC-operations if an only if their ordered Schmidt coefficients satisfy

$$\sum_{i=1}^{n} \lambda_n^{\psi} \preceq \sum_{i=1}^{n} \lambda_n^{\varphi} \qquad \forall \; n \in [0,...,d] \text{ and } d = \min(\dim_{\psi}, \dim_{\varphi}) \tag{2.41}$$

that is, $|\psi\rangle$ has to majorize $|\varphi\rangle$.

Consecutively, from Nielsens theorem a criterion to classify entanglement can be introduced. States within the same LOCC class have to interconvertible by LOCC operations, thus majorization has to go both ways, leaving *equality* of Eq. (2.41) as the the only possible option. Then, it is obvious that LOCC equivalent states are those and only those, which possess the same Schmidt coefficients, which, in turn, means,they are related by local unitaries.

SLOCC-operations

Convertibility between two quantum states via LOCC is, as demonstrated in the section before, a hard task. This is due to the fact that their mathematical description is not easy to handle and often a clear statement regarding convertibility can not be made. Therefore, it is sensible to take a look at a broadened class of operations named stochastic local operations assisted by classical communication (SLOCC). Two states are convertible via SLOCC operation if they can be transformed into each other by using LOCC with non-vanishing probability.

Definition 2.4. SLOCC equivalence I [113]
Two quantum states ρ, ρ' are equivalent under SLOCC operations if and only if they are interconvertible with non-vanishing probability by the use of not necessarily trace preserving CP maps inducing LOCC transformations:

$$\begin{aligned} \rho \xleftrightarrow{SLOCC} \rho' \text{ iff: } \exists\, \Lambda_{LOCC}, \Lambda'_{LOCC} \text{ s.t.: } & \frac{\Lambda_{LOCC}[\rho]}{Tr(\Lambda[\rho])} = \rho',\ p = Tr(\Lambda[\rho]) > 0 \\ \text{and } & \frac{\Lambda'_{LOCC}[\rho']}{Tr(\Lambda'[\rho'])} = \rho,\ p' = Tr(\Lambda'[\rho']) > 0 \end{aligned} \tag{2.42}$$

where p and p' are not necessarily equal. referring to the fact that the probability of a successful transformation need not be equal in both directions.

Note that a SLOCC transformation, due to its probabilistic nature, converts any pure state, which it is applied to, into some mixture. SLOCC operations allow for post-selection of the various measurement outcomes and the LOCC map inducing the transformation can now be trace-decreasing. Within an SLOCC operation the LOCC protocol is divided in many different branches, where for each branch, post selection keeps only the desired outcome. Therefore only one Kraus operator is used per round. This poses as an enormous advantage, as it is now possible to characterize SLOCC-operations in a mathematically closed description. That is, they are induced by local operators only restricted by the demand of invertibility. For pure states it follows

Definition 2.5. SLOCC-equivalence II
Two pure n-partite quantum states $|\psi\rangle$, $|\psi'\rangle$ in $\mathcal{H} = \mathcal{H}_1 \otimes ... \otimes \mathcal{H}_n$ are interconvertible by stochastic local operations and classical communication if and only if there exist invertible

square matrices $\{A_i\}$ *acting on each subsystem, such that*

$$(A_1 \otimes ... \otimes A_n)\,|\psi\rangle = |\psi'\rangle \quad \text{and:} \quad (A_1^{-1} \otimes ... \otimes A_n^{-1})\,|\psi\rangle = |\psi'\rangle$$
$$\text{where: } \det(A_i) \neq 0 \;\; \forall\; i \;\in\; [1,...,n], \quad \text{and} \quad \dim[A_i] = d_i \times d_i, \quad d_i = \dim(\mathcal{H}_i) \tag{2.43}$$

Having set the formal framework of quantum states and quantum operations in Hilbert spaces, the next section of this chapter concentrates on the concept of entanglement, e.g. its definition, characterization, classification and quantization.

2.2 Entanglement

Entanglement is a feature possible for quantum states to own that in no way can be described or reproduced by classical means. Concretely, entanglement is a word to describe non-classical correlations between two or more systems. These kinds of correlations cannot be predicted within local classical models, not even when allowing for the inclusion of hidden variables, i.e. variables inherent to the systems but inaccessible to the observer.
This failure of local, classical probabilistic approaches to explain the character of entangled states, can be shown with e.g. Bell inequalities [3]. They bond certain combinations of probabilities originating from local measurement outcomes of two or more systems for all classical theories. Quantum mechanics is able to exceed those bounds due to their special kind of structure and correlations arising from it.
From a quantum mechanical point of view, combined systems are described by one single state vector. Thus any measurement causes an implicit state update of the whole system. It can be viewed as an actualization of the whole systems state using only information already present. Therefore, in quantum mechanics, unlike in attempts to find classical, local theories, there is no such thing as instant information transfer needed to explain the way measurement outcomes of entangled states display correlations.
Consecutively, entangled states are mathematically described by a single state vector, or a single density matrix for mixed states, combining two or more systems, that do not factorize as a product state. This can bee seen as follows: Factorizing as a product state means that a local measurement (quantum operation) acting on one subsystem gives a specific value for the measured observable, that is completely uncorrelated to the measurement results one would get when measuring the same observable on other subsystems of the whole system. That is, from measurement of one system we can infer nothing about the measurement results of the other systems. This very property is violated by entangled states.
For entanglement, there exists a vast field of applications, e.g. ultra-precise clocks [63], [64], quantum random number generators [66], [67], quantum computers [65] and enhanced interferometry techniques [68]. At the end of this section, the role of entangled states as a resource is illustrated for the field of quantum cryptography as well as quantum metrology processes.

2.2.1 Bipartite entanglement

Defining entanglement is usually done by defining *what it is not*. Or, in other words, by characterizing all bipartite states that originate from correlations which can be simulated classically. The set of entangled states emerges as those state not fitting within this category.

Consider two parties A and B each preparing a pure quantum state, $|\psi_A\rangle \in \mathcal{H}_A$ and $|\psi_B\rangle \in \mathcal{H}_B$ respectively, within their own laboratory. Then the whole system living on $\mathcal{H}_{AB} = \mathcal{H}_A \otimes \mathcal{H}_B$ is described by the tensor product of the uncorrelated single-system states, that is $|\psi_{AB}\rangle = |\psi_A\rangle \otimes |\psi_B\rangle$. States of this kind consist of totally independent subsystems and are called *product states*.
As mentioned before, the notion of pure states is a theoretical ideal which often times will fail for practical purposes. The situation when considering mixed states ρ_A, ρ_B gives an analogous description of the whole system as $\rho_{AB} = \rho_A \otimes \rho_B$. Furthermore, it is also possible to take statistical mixtures of product states without violating the classical nature of the used correlations. Then, the most general way to describe an exclusively classically correlated bipartite system is a convex combination of product states

$$\rho_{AB} = \sum_i p_i(\rho_{A,i} \otimes \rho_{B,i}) \qquad \text{with:} \quad p_i \geq 0, \quad \text{and} \quad \sum_i p_i = 1. \tag{2.44}$$

States of this type are called *separable states*. The class of pure states emerges from the class of separable state for only one non-zero weight, that is $p_i = 0 \;\; \forall \; i \neq j$. From the form of Eq. (2.44) it is obvious that the set of all separable states builds the convex hull to the set of all product states. Having found the condition any purely classically correlated bipartite state satisfies, it is now natural to define entangled state as those *not* fitting into the category defined by Eq. (2.44)

Definition 2.6. Bipartite entanglement
Let ρ_{AB} be a density operator on $\mathcal{H}_{AB}$ describing a bipartite quantum state. Then ρ_{AB} is said to be entangled if and only if it cannot be rewritten as convex combination of product states [48]

$$\begin{aligned} \rho_{AB} := \textit{entangled, iff: } \rho_{AB} \neq \sum_i p_i(\rho_{i,A} \otimes \rho_{B,i}) \quad & \forall \; \rho_{AB} \in \mathcal{H}_{AB} \\ & \forall \; p_i \quad \textit{with: } p_i \geq 0, \quad \sum_i p_i = 1 \end{aligned} \tag{2.45}$$

In case ρ_{AB} is a pure state, all possible classical correlations are included in the tensor product of the states of the subsystems. From Eq. (2.45), for $p_i = 0 \; \forall \; i \neq j$, it follows

$$|\psi_{AB}\rangle := \text{entangled, iff: } |\psi_{AB}\rangle \neq |\psi_A\rangle \otimes |\psi_B\rangle \quad \forall \; |\psi_{AB}\rangle \in \mathcal{H}_{AB} \tag{2.46}$$

The question if a given pure bipartite state $|\psi_{AB}\rangle$ is entangled or separable is fully answered by the Schmidt decomposition, see Theorem 2.1. Due to the fact that the Schmidt coefficients $\{\sqrt{\lambda_i}\}$ are unique and the Schmidt basis $\{|a_i, b_i\rangle\}$ is given by separable states, one can infer from the number of non-zero $\sqrt{\lambda_i}$ the entanglement properties of the state:

> A pure bipartite state is separable if and only if the Schmidt decomposition exhibits one and only one non-vanishing Schmidt coefficient. Otherwise the state is entangled.

Remark 2.1. *Evaluating the reduced density matrices $\rho_{A|B}$ of a pure bipartite state in Schmidt-decomposition gives:*

$$\begin{aligned}
\rho_A = Tr_B(\rho_{AB}) &= Tr_B[\sum_{ij}\sqrt{\lambda_i\lambda_j}\,|a_i\rangle\langle a_j|\otimes|b_i\rangle\langle b_j|] \\
&= \sum_n \langle b_n|\sum_{ij}\sqrt{\lambda_i\lambda_j}\,|a_i\rangle\langle a_j|\otimes|b_i\rangle\langle b_j|\,|b_n\rangle \\
&= \delta_{in}\delta_{jn}\sum_{ij}\sqrt{\lambda_i\lambda_j}\,|a_i\rangle\langle a_j| \\
&= \sum_i \lambda_i\,|a_i\rangle\langle a_i| \\
\text{and accordingly: } \rho_B &= \sum_i \lambda_i\,|b_i\rangle\langle b_i|
\end{aligned} \tag{2.47}$$

Thus the eigenvalue spectrum of the reduced states is given by the squared Schmidt coefficients. As separability demands all except one Schmidt-coefficient to be zero, entanglement can be related to the purity of the reduced density matrices

$$\begin{aligned}
\mathrm{tr}[(\rho_{A|B})^2) = 1 \quad &\Longleftrightarrow \quad |\psi_{AB}\rangle = \text{separable} \\
\mathrm{tr}[(\rho_{A|B})^2) < 1 \quad &\Longleftrightarrow \quad |\psi_{AB}\rangle = \text{entangled}
\end{aligned} \tag{2.48}$$

Prominent examples of entangled states are the *generalized Bell states*[3]

$$|\psi_{AB}^{BELL}\rangle = \frac{1}{\sqrt{d_{min}}}\sum_{i=0}^{d_{min}-1}|a_ib_i\rangle\,, \qquad \text{where: } d_min = \min(d_A, d_B). \tag{2.49}$$

For $d_A = d_B = 2$, e.g. two qubit states the original four orthogonal Bell states, realized e.g. in spin systems, emerge

$$\begin{aligned}
|\psi^+\rangle &= \frac{1}{\sqrt{2}}(|00\rangle + |11\rangle) & |\psi^-\rangle &= \frac{1}{\sqrt{2}}(|00\rangle - |11\rangle) \\
|\varphi^+\rangle &= \frac{1}{\sqrt{2}}(|01\rangle + |10\rangle) & |\varphi^-\rangle &= \frac{1}{\sqrt{2}}(|01\rangle - |10\rangle)
\end{aligned} \tag{2.50}$$

The set of Bell states additionally defines the *maximally* entangled states within a bipartite system. Maximally entangled here means that the reduced density operator is a multiple of the identity matrix, representing complete randomness, i.e. ignorance of the reduced state. In Chapter 5, the reasonableness of the term in connection with generalized Bell states in systems of dimension higher than three will be questioned and discussed.

In case of bipartite mixed states, the Werner state of two qubits, that is the probabilistic mixture of a Bell state and a completely mixed state:

$$\rho_W = p\,|\psi^+\rangle\langle\psi^+| + (1-p)\frac{1}{4}\mathbb{1} \tag{2.51}$$

may display entanglement. Whether this state is entangled or separable is decided by the value of p, that is, entanglement is present if $p > \frac{1}{3}$.

2.2.2 Multipartite entanglement

Turning to systems consisting of an arbitrary number of parties, a more complex structure emerges. Due to this involved composition, we consider pure states and statistical mixtures

in a separated discussion.

Pure states

Considering *pure states* first, the subsequent generalization of Definition 2.6,e.g. Eq. (2.45) gives [48]

Definition 2.7. Multipartite entanglement, pure states
An n-partite pure state $|\psi\rangle$ *in* $\mathcal{H} = \mathcal{H}_1 \otimes ... \otimes \mathcal{H}_n$ *is entangled if and only if it cannot be written as tensor product of single subsystem states* $|\psi_i\rangle$ *in* $\mathcal{H}_i$ *for all* $i \in [1, ..., n]$

$$|\psi\rangle := \text{entangled, iff:} \quad |\psi\rangle \neq \bigotimes_{i=1}^{n} |\psi_i\rangle \,. \tag{2.52}$$

Due to the richer structure of multipartite systems, Definition 2.7 does not take into account all possible scenarios. To be more precise one can think of it as follows: whereas for a bipartite system, there are in principle only two options - separable or entangled- this is not the case for more than two parties. Here, the situation could be that of an n-partite systems an arbitrary number of subsystems are entangled but no entanglement is present between other parts. As such, those systems are separable with respect to a certain partition but entangled with respect to another. These considerations lead to the definition of *k-separability* [69]:

Definition 2.8. k-separability
An n-partite pure state $|\psi\rangle$ *in* $\mathcal{H} = \mathcal{H}_1 \times ... \times \mathcal{H}_n$ *is said to be k-separable with respect to a specific k-partite split if and only if it can be written as tensor product of k factors of subsystem states, i.e.*

$$|\psi\rangle := \text{k-separable, iff:} \quad |\psi\rangle = \bigotimes_{i=1}^{k} |\psi_i\rangle \qquad k \in [1, ..., n]. \tag{2.53}$$

Note that here the factors $|\psi_i\rangle$ *may consist of more than one subsystem where the maximum is limited by the specific values of* n *and* k*, i.e.* $\max(n, k) = n - k + 1$*. This corresponds to the situation of* $(k-1)$ *single subsystems and one* $(n-k+1)$ *particle system.*

From Definition 2.8 it follows that Eq. (2.52) emerges as two special cases for $k = n$ and $k = 1$. States with the former property are called *fully separable* whereas the latter ones are called *genuinely multipartite entangled*.

Mixed states

For *mixed states* the definition of k-separability can be done in two different ways. Either going with the *conditioned* or the *unconditioned* option [70].
The conditioned separability defines a mixed state to be separable with respect to a certain partition P, if it can be written as convex sum of pure k-separable states, which are all separable with respect to the same partition P. Although this definition of separability is the logical and intuitive extension of bipartite separability, it does not give concrete information about the amount of entanglement within the state. Thus, it is no good candidate to bring forth a quantification of separability. From Definition 2.9

Definition 2.9. Conditioned k-separability of mixed states [70]
A mixed n-partite quantum state ρ *in* $\mathcal{H}^{\otimes n}$ *is called k-separable with respect to a specific k-partition P, if and only if it can be written as convex sum of pure states ,* $\{(\rho_{pure}^{k-sep|P})_i)\}$*, that*

are all k-separable with respect to the partition P

$$\rho := \text{k-separable, iff:} \quad \rho = \sum_{i=1}^{k} p_i (\rho_{pure}^{k-sep|P})_i \qquad \text{with: } k \leq n \tag{2.54}$$

one sees that this is due to the fact that states, which are k-separable conditioned on different partitions P and P', give rise to incomparable classes.Therefore, when talking about a definition for the separability of mixed states, which gives valid information within the quantification sector, the *unconditioned* k-separability is more useful:

Definition 2.10. Unconditioned k-separability of mixed states [70]
A mixed n-partite quantum state ρ in $\mathcal{H}^n$ is called k-separable if and only if it can be written as convex sum of pure states, where every one of those is k-separable with respect to some arbitrary partition P_i, e.g. $(\rho_{pure}^{k-sep|P_i})_i = (\rho_{pure}^{k-sep})_i$

$$\rho := \text{k-separable, iff:} \quad \rho = \sum_{i=1}^{k} p_i (\rho_{pure}^{k-sep})_i \qquad \text{with: } k \leq N \tag{2.55}$$

Of course, in this case one has to be careful with the notation and implications of k-separability. For the unconditioned option k-separability does not mean, that there exists a specific decomposition showing k-separability with respect to any specific partition.
The different classes of k-separable states build a convex set, with the cone of fully separable states lying in the middle, the cone of genuine multipartite states being the outermost one. This is due to the fact that any k-separable state has to be (k-1)-separable as well.

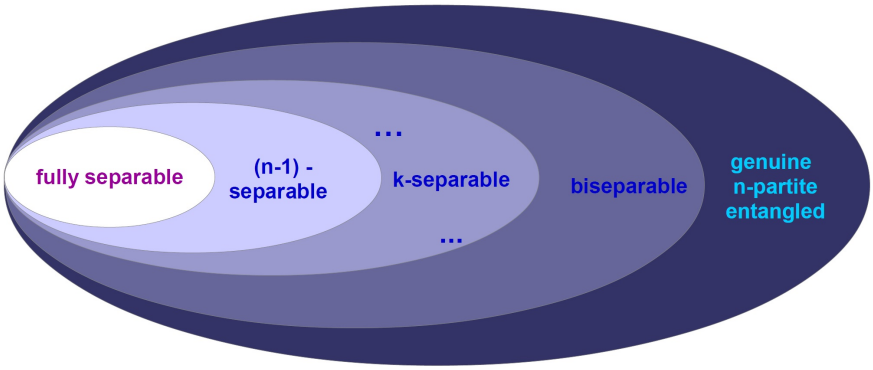

FIGURE 2.1: Convex Set of k-Separable States [71]

To conclude this section covering the basic definitions concerning entanglement, e.g. separability of pure and mixed multipartite quantum states, some prominent examples for entangled states in both categories are given:
For pure two-level systems, an example of a *genuine 3-partite entangled* state is the *W-state* [113]:

$$|W\rangle = \frac{1}{\sqrt{3}}(|001\rangle + |010\rangle + |100\rangle) \tag{2.56}$$

A pure state that is k-separable with $k = 2$ for a four level system could take, e.g., either one of the following forms:

$$\begin{aligned} |\psi_{1|3}\rangle &= (|0\rangle \otimes |W\rangle) && \text{bipartite split with 1 vs. 3 subsystems} \\ |\psi_{2|2}\rangle &= (|\psi^+\rangle \otimes |\varphi^-\rangle) && \text{bipartite split with 2 vs. 2 subsystems} \end{aligned} \tag{2.57}$$

Candidates for a mixed multipartite entangled states are the generalized n-partite Werner states [72] [73], given as

$$\rho_W = p\,|\psi_{maxE}\rangle\,\langle\psi_{maxE}| + (1-p)\frac{1}{2^n}\mathbb{1}. \tag{2.58}$$

Whereas in case of bipartite systems, the minimal value of p for ρ to still be entangled can be determined, it is not that easy in the multipartite case. Nonetheless, for example the [74] characterizes entanglement properties of three-qubit Werner states for $\psi_{maxE} = |GHZ\rangle$ that is: $\rho_{W,3qubit} = p\,|\psi_{GHZ}\rangle\,\langle\psi_{GHZ}| + \frac{1-p}{8}\mathbb{1}$.

2.2.3 Applications of entanglement

Following, there will be a short overview about two of the most important applications of entangled states nowadays: quantum cryptography, to be more precise, quantum key distribution and quantum metrology.

Quantum key distribution

Within the field of quantum cryptography, entanglement is a powerful tool within the field of quantum key distribution (QKD). Imagine two parties A and B wanting to exchange a private key to encode messages sent over an insecure classical information channel. Furthermore A and B are connected via a classical as well as a quantum channel, which may both be subjected to intervention of some third party E. The aim now is to create a private key in such a way that A and B are able to deduce any interference made by E and consecutively dismiss the key as insecure. The first method to generate such a private key by using quantum mechanics was proposed by Charles Bennett and Gilles Brassard in 1984 [12]. It is a measurement based protocol where security relies on the no-cloning theorem [46].
Here, the basic idea of another protocol using entangled pairs of photons proposed by Arthur Eckert in 1991 [16] will be reviewed. The Ekert protocol is based on quantum teleportation. That is, a source may create an Einstein Podolsky Rosen (EPR-)pair of photons, e.g. one of the four Bell states presented in Eq. (2.50). Then, both A and B, are sent one photon of each EPR-pair and, each randomly choosing a measurement basis, perform a polarization measurement on their own photon. The choice of basis may then be communicated through a classical channel. In case the bases coincide, the result, which displays perfect correlation or anti-correlation - depending on the state the source produces - is used for key generation. Otherwise, the result is discarded. The schematic setting of the protocol is illustrated in the Fig. 2.2

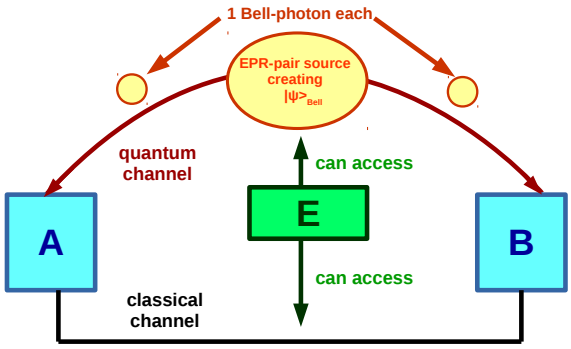

FIGURE 2.2: Schematic setting of a QKD protocol based on entanglement

The working principle of the protocol is based on some important properties of entangled states. First, the option to create perfectly correlated states in crucial. Then, the non-locality of entangled states enables A to deduce B's result of some polarization measurement with higher than average (random) probability leading to correlations strictly stronger than all classical limits. Furthermore regarding a possible intervention of E, any attempt to do so will weaken those correlations and thus any action of E can be detected by A and B. Hence, to verify security of the protocol, A and B test Bell inequalities. As entangled states should show a violation of those, if no violation is detected, A and B can infer that the original state was not entangled, which implies an intervention of E.

Quantum metrology

Within the field of metrology, quantum effects, like entanglement, can be used to enhance the precision of measurements on physical parameters. A promising and actual application is the detection of gravitational waves [75]. As an example for the usefulness of entangled states in quantum metrology, consider the estimation of the angel, or phase φ within a so special kind of entangled state of N particles, the so-called NOON-state [76]

$$|\psi_{NOON}\rangle = \frac{1}{\sqrt{2}}(|N\rangle_A \otimes |0\rangle_B + e^{iN\varphi}\,|0\rangle_A \otimes |N_B\rangle). \tag{2.59}$$

A NOON-state is a superposition of N particles in mode A and zero particles in mode B and vice versa. When used in an optical interferometer and measuring the observable $O = |0N\rangle\langle N0| + |N0\rangle\langle 0N|$, the NOON-state enables a highly precise measurement of the phase φ which beats classical limits by far. More detailed, the insecurity within φ is estimated to scale with the reciprocal particle number N:

$$\Delta(\varphi) = \frac{\Delta(O)}{|\frac{dO}{d\varphi}|} = \frac{1}{N} \leq \frac{1}{\sqrt{N}} \equiv \text{classical limit} \tag{2.60}$$

Thus, an entangled N-partite state was shown to exhibit far better scaling than possible when using any non entangled, N-partite state.

2.3 Entanglement classification and quantification

2.3.1 Classification

Due to entanglement being used as an important tool and resource for many processes in the field of quantum information theory, the need to identify states of identical entanglement properties arises from the fact that states inheriting an equivalent type of entanglement should possess the same complexity level regarding their producibility. For practical uses, in which the non-local properties of entanglement are exploited, oftentimes one has the situation of spatially separated, entangled states. Then, at each location the observer has access to one subsystem of the state, which he can manipulate via local operations. Additionally, the option of communication with the other observers at different locations is realizable via classical channels. Thus, it makes sense to classify the entanglement properties of a state based on those criteria.
As we know for a fact that an interaction described by a coherent quantum operation on all subsystems is necessary for the generation of entanglement, it is clear that operations applied on each system separately, i.e. purely local operations, cannot enhance the entanglement level of the whole system. Nonetheless, it is of course possible to transform one entangled state into another one by local means at hand for each subsystem respectively, if both states share the same kind and amount of entanglement. It is important to notice that the non-entanglement-generating property of locally applied quantum operations also implies that the entanglement level is not allowed to decrease under such local operations we want to use to categorize classes of the same kind of entanglement. This factum directly arises if one takes into account the need for the inverse transformation mapping the transformed state back to the original one. The operation initiating the reverse process would need to enhance entanglement, if the original one causes a decreasing.
As a consequence, those local operations that define an entanglement class as a class of states that can be transformed into each other back and forth, cannot manipulate the kind of entanglement within a given state in any direction. Therefore, as means for a proper and useful classification of entanglement, the equivalence of two quantum states under

- Local unitary operations (LU)
- Local operations and classical communication (LOCC)
- Stochastical local operations and classical communication (SLOCC)

are good and sensible candidates to define categories of states sharing the same entanglement. In the following, equivalence classes of states under the aforementioned local operations will be discussed for bipartite and multiparite systems. As will be shown, LU and LOCC-equivalence classes are in most cases hard to characterize in a mathematically closed way. Therefore SLOCC-equivalence takes an emphasized role in the discussions and will shown to be very useful to give deeper insight and better understanding of the structure and complexity of entangled states, especially in the multipartite scenario.

2.3.2 Quantification

As mentioned before, quantum entanglement is used as resource for various quantum informational tasks. From this, naturally the need for a tool that can quantify the amount of entanglement - and thereby give an important scale for the performance level of a state with

respect to a given task - arises. As seen in the previous section, entanglement cannot be generated by applying SLOCC-operations. Thus two states that are interconvertible via SLOCC should pricipally be able to perform the same quantum informational tasks. However, within an SLOCC class, not all states perform equally well at a given task. Hence, to quantify entanglement, behaviour under LOCC will first and foremost pose as the keystone towards quantifying the entanglement present within a given quantum state. Therefore, *entanglement monotones*, introduced by Vidal [77], will be defined before moving on to the definition of valid and good *entanglement measures* [78], [79], [80], [48]. Note that whereas there are some general conditions necessarily to be satisfied, there are additional ones, which might or might not be satisfied, depending on the task to be performed. Further note that whereas for bipartite states the existence of a maximally entangled state allows for a *unique* ordering, the same is not true for multipartite states.

Definition 2.11. Entanglement monotone
An entanglement monotone $\mathcal{M}$ is a function which maps density operators ρ in $\mathcal{H}$ to the field of real, positive numbers $\mathbb{R}^+$ and satisfies monotonicity:

$$\mathcal{M}[\Lambda_{LOCC}[\rho]) \leq \mathcal{M}(\rho) \quad \forall\ \rho,\ \Lambda_{LOCC} \quad \leftrightarrow \quad \mathcal{M} \text{ is non-increasing under LOCC} \tag{2.61}$$

One could impose an even stronger version of montonicity, i.e. demand $\mathcal{M}$ to be non-increasing under LOCC on average, *i.e.*

$$\sum_i p_p \mathcal{M}(\Lambda_{LOCC}[\rho])_i \leq \mathcal{M}(\rho) \quad \forall\ \rho,\ \Lambda_{LOCC} \tag{2.62}$$

where the LOCC-map Λ_{LOCC} maps the initial state ρ to the state $(\Lambda_{LOCC}[\rho])_i$ with probability p_i and naturally $\sum_i p_i = 1$.

For an entanglement monotone $\mathcal{M}$ to classify as a proper entanglement measure, additionally to monotonicity, a measure has to vanish on all separable states. Note that monotonicity already implies a constant value for any $\mathcal{M}$ as all states within the set of separable state are inteconvertible via LOCC.

Definition 2.12. Entanglement measure
An entanglement measure $\mathcal{M}$ is an entanglement monotone that vanishes on all separable states, that is

$$\begin{aligned} &1)\ \mathcal{M} \text{ is an entanglement monotone according to Definition 2.11} \\ &2)\ \mathcal{M}(\rho) = 0 \qquad\qquad \forall\ \rho \text{ in } \{\rho_{SEP}\} \end{aligned} \tag{2.63}$$

It is important to mention that a vanishing value for an entanglement measure does not imply separability per se. Thus, there can be entangled states for which $\mathcal{M} = 0$. Physically this indicates e.g. that such a state would not exhibit the kind of entanglement measured by the special respective measure, i.e. the state is not useful for some task (but could for some other measured by some other entanglement measure).
Additionally to the *necessary* conditions in Definition 2.12 , there are other properties desirable for entanglement measures that might or might not be satisfied depending on the specific measure, i.e.

3) Invariance under local unitary operations: [1]

$$\mathcal{M}(U^\dagger \rho U) = \mathcal{M}(\rho) \qquad \forall\ \rho \quad \text{and } \forall \text{ local unitaries: } U = \bigotimes_{i=1}^{n} U_i \tag{2.64}$$

4) Faithfulness, i.e. $\mathcal{M}$ is *tight* on the set of separable states:

$$\mathcal{M}(\rho) = 0 \quad \text{if and only if } \ \rho \text{ is separable} \tag{2.65}$$

5) Convexity, i.e. $\mathcal{M}$ is non-increasing under mixing of quantum states: [2]

$$\mathcal{M}(\sum_i p_i \rho_i) \leq \sum_i \mathcal{M}(\rho_i) \tag{2.66}$$

6a) Additivity under the tensor product, that is:

$$\mathcal{M}(\rho^{\otimes n}) = n \cdot \mathcal{M}(\rho) \tag{2.67}$$

6b) Sometimes, this is extended to *strong* additivity:

$$\mathcal{M}(\bigotimes_i \rho_i) = \sum_i \mathcal{M}(\rho_i) \tag{2.68}$$

7) Continuity, i.e. from closeness of the entanglement measure, closeness of the corresponding states necessarily follows:

$$\mathcal{M}(\rho) - \mathcal{M}(\rho') \longrightarrow 0 \quad \Longrightarrow \quad ||\rho - \rho'|| \longrightarrow 0 \tag{2.69}$$

An entanglement monotone defined for mixed states $\mathcal{M}'(\rho)$ has to reduce to the form defined for pure states in case $\rho \equiv \rho_{pure} = |\psi\rangle \langle\psi|$. Here, convexity is an important property, as this implies non-increasing of $\mathcal{M}$ under mixing of quantum states. A common way one can construct a mixed state entanglement monotone out of a valid one for pure states is by the *convex roof extension* [90]

$$\mathcal{M}'(\rho) = \inf_{\{p_i, \psi_i\}} \mathcal{M}(|\psi\rangle) \tag{2.70}$$

Where the minimization goes over all possible decompositions $\{p_i, \psi_i\}$ of ρ.

In the following, an overview considering some of the post popular and important entanglement measures is given [78]. For pure states, the **Entropy of Entanglement** [81] is defined as the von Neumann entropy of the reduced density matrix. That is

$$\mathcal{M}_E(\rho) = S(\rho_{RED}) = -Tr(\rho_{RED} log(\rho_{RED}) = -\sum_{i=0}^{n-1} \lambda_i log(\lambda_i) \tag{2.71}$$

where $\{\lambda_i\}$ denote the eigenvalues of ρ_{RED} and in case of a bipartite system those coincide with the Schmidt coefficients. Notice that for pure bipartite states $\mathcal{M}_E(\rho)$ has proven [91] to be the only existing 'good' measure in the sense that $\mathcal{M}_E(\rho) = 0$ if and only if ρ is separable.

[1] Note that LU invariance is satisfied by any entanglement monotone by definition. Deterministic interconvertibility as induced by local unitary transformations directly leads to $\mathcal{M}(\rho) = \mathcal{M}(\rho')$ if $\rho' = U^\dagger \rho U$.

[2] Convexity can be viewed as making note of the loss of information happening from the left to the right side of Eq.(2.3.2).

That is, $\mathcal{M}_E$ is a *faithful* measure (see Eq. (2.65)) and furthermore is gives its maximal value (normed to one) if and only if ρ is the density operator corresponding to the maximally entangled state $|\psi_{Bell}\rangle$: $\max(\mathcal{M}_E(\rho)) = \mathcal{M}_E(\rho_{Bell}) = 1$
[3]

The extension of M_E to mixed states via the convex roof construction gives the **Entanglement of Formation** [83], [82]:

$$\mathcal{M}_F(\rho) = \inf_{|\psi_i\rangle, p_i} \sum_i p_i \mathcal{M}_E(\psi_i), \qquad p_i \geq 0,\ \sum_i p_i = 1,\ \rho = \sum_i p_i |\psi_i\rangle \langle\psi_i| \tag{2.72}$$

Hence, $\mathcal{M}_F(\rho)$ gives the minimal averaged entanglement over all decompositions of ρ. One can interpret the entanglement of formation as a measure of how many maximally entangled states are needed to create one copy of ρ.
The **Distillable Entanglement** [83], [82] of a state ρ addresses the question of the rate at which maximally entangled states may be prepared from ρ using an LOCC-map Λ. Then:

$$\mathcal{M}_D(\rho) = \sup\{r : \lim_{n\to\infty} [\inf_{\Lambda} D(\Lambda[\rho^{\otimes n}], (|\psi_{max}\rangle \langle\psi_{max}|)^{rn})] = 0\} \tag{2.73}$$

where $|\psi_{max}\rangle$ is the maximally entangled state to be produced, D is some suitable distance measure, e.g. the trace, and r is some constant related to the dimension of the system. In a more compact form, Eq. (2.73), can be rewritten as ratio within the asymptotic limit for $n \to \infty$ between the number n of copies of the input state ρ and the number m of copies of the output state $|\psi_{max}\rangle$, i.e.: $\mathcal{M}_D(\rho) = \sup_{LOCC} \lim_{n\to\infty} \frac{m}{n}$.
The corresponding counterpart to $\mathcal{M}_D(\rho)$ is the **Entanglement Cost**. It targets the opposite problem of how many maximally entangled states are needed to prepare some noisy state. Thus it can be formalized as

$$\mathcal{M}_C(\rho) = \inf\{r : \lim_{n\to\infty} [\inf_{\Lambda} D(\rho^{\otimes n}, \Lambda[(|\psi_{max}\rangle \langle\psi_{max}|)^{rn})] = 0\}. \tag{2.74}$$

This corresponds to the rate between input- and desired output state in the asymptotic limit with m input states $|\psi_{max}\rangle$ and n output states ρ: $\mathcal{M}_C(\rho) = \inf_{LOCC} \lim_{n\to\infty} \frac{m}{n} = \lim_{n\to\infty} \frac{\mathcal{M}_F(\rho^{\otimes n})}{n}$. Note that for pure states, entanglement cost and entanglement of formation coincide.
Measures based on quantifying the distance of a given state to the set of all separable state are, e.g. the **Relative Entropy of Entanglement** [88] and the **Geometric Measure of Entanglement**. The former is defined as

$$\mathcal{M}_R(\rho) = \inf_{\sigma\in\{\rho_{SEP}\}} S(\rho||\sigma) = \inf_{\sigma\in\{\rho_{SEP}\}} [\mathrm{tr}(\rho\log(\rho) - \rho\log(\sigma))] \tag{2.75}$$

The latter, rather that on entropies, is based on the maximal squared overlap of a given pure state with the set of product states

$$\mathcal{M}_G(|\psi\rangle) = 1 - \max_{|\varphi\rangle\in\{|\psi_{product}\rangle\}} |\langle\psi|\varphi\rangle|^2 \tag{2.76}$$

The extension to a measure for mixed states can be done via the convex roof extension [90]
Another measure of entanglement introduced by Wooters is the **Concurrence** [86]. For a

[3] Note that with the entropy of entanglement, an **unique** measure of entanglement for pure bipartite state is provided. This can be seen by the fact that a pure bipartite state ρ can be converted into ρ' via LOCC if and only if the entropies satisfy: $\mathcal{M}_E(\rho') \geq \mathcal{M}_E(\rho)$.

two qubit system in a pure state it is defined as the overlap of a given state $|\psi\rangle$ with its respective spin-flipped state $|\tilde{\psi}\rangle$, that is

$$C(|\psi\rangle) = \langle\psi|\tilde{\psi}\rangle \qquad \text{where: } |\tilde{\psi}\rangle = \sigma_y \otimes \sigma_y |\psi^*\rangle \tag{2.77}$$

The concurrence can be extended to mixed ensembles $\rho = \sum_i p_i |\psi_i\rangle \langle\psi_i|$ via the convex roof construction

$$C(\rho) = \inf_{|\psi_i\rangle, p_i} \sum_i p_i C(|\psi_i\rangle) = \max(0, \sqrt{\lambda_1}, -\sqrt{\lambda_2}, -\sqrt{\lambda_3}, -\sqrt{\lambda_4}) \tag{2.78}$$

where λ_i are the eigenvalues sorted in decreasing order, $\sqrt{\lambda_i} \geq \sqrt{\lambda_{i+1}}$, of the hermitean matrix $\rho\tilde{\rho}$ with $\tilde{\rho} = \sigma_y \otimes \sigma_y \rho^* \sigma_y \otimes \sigma_y$. For dimensions $d > 2$ a possible generalization of the concurrence reads

$$C(\rho) = \sqrt{(2(1 - Tr(\rho_{RED}))} \tag{2.79}$$

Furthermore, based on the concurrence, an entanglement measure for multipartite states can be defined, the **n-tangle**[85]. In case of three qubit systems, the **three-tangle** [84] can be written in terms of the bipartite concurrences as follows

$$\tau_3(\rho) = C^2_{A|BC}(\rho) - C^2_{AB}(\rho) - C^2_{AC}(\rho) \tag{2.80}$$

The three-tangle is invariant under permutations of the three subsystems. The power of this criterion is shown by its ability to distinguish between the GHZ- and the W-state. To be more specific, the three-tangle is zero for the latter and gives its maximal value of $\tau_3 = 1$ for a pure GHZ-state. A non-zero value for τ_3 for any mixed $2 \times 2 \times 2$ state ρ then indicates that there is no decomposition of ρ without at least one summand of GHZ-nature.
An entanglement monotone measuring the amount of violation of the PPT-criterion [92] is the **Negativity** [87]:

$$N(|\psi\rangle) = \frac{||\rho^{T_A}||_1 - 1}{2} \qquad \text{with the trace norm: } ||\rho^{T_A}||_1 = \sqrt{(\rho^{T_A})^\dagger \rho^{T_A}} \tag{2.81}$$

It is possible to rewrite the negativity in terms of the eigenvalues of ρ^{T_A} which lead to the following formulation of N:

$$N(\rho) = \frac{\sum_i |\lambda_i| - \lambda_i}{2} \tag{2.82}$$

2.3.3 Classification of bipartite entanglement

The classification of entanglement within bipartite states is done by finding equivalence classes under SLOCC. As mentioned before, LU- as well as LOCC operations can also provide a useful division into different categories. But even for bipartite systems, a mathematically closed analysis is only possible in some lower dimensional cases. Some of these will be discussed shortly at the end of this subsection. In contrast to the aforementioned problems regarding LU and LOCC, SLOCC provides a way to fully characterize all different classes of entanglement in a neat way and as it turns out, bipartite entanglement classification under SLOCC is fully determined by the existence of the Schmidt decomposition and we can formulate the following statement:

Theorem 2.6. Bipartite entanglement classification
Let $\{|\psi_{AB}\rangle\}$ be the set of all bipartite pure quantum states in $\mathcal{H}_{AB}$ of dimension $d = d_A \times d_B$. Then, for a given state $|\psi_{AB}\rangle$ the SLOCC-class is completely determined by the Schmidt number n_S of the state. Furthermore, the total number of SLOCC inequivalent classes is equivalent to the value of n_S. As for $n_S = 1$ the state is of product form, the number of entanglement classes not interconvertible by SLOCC then is $(n_S - 1)$.

Proof. The most powerful tool when analyzing bipartite systems regarding their entanglement properties is the Schmidt decomposition, see Theorem 2.1. Recapitulating the main statement, any bipartite pure state $|\psi_{AB}\rangle$ of arbitrary dimension $d_{AB} = d_A \times d_B$ in $\mathcal{H}_{AB}$ can, by means of local basis transformations, be written in Schmidt form:

$$(U_A \otimes U_B)\,|\psi_{AB}\rangle = \sum_i \sqrt{\lambda_i}\,|a_i b_i\rangle := |\psi_{AB,S}\rangle \tag{2.83}$$

Furthermore, as was shown in [93], the free parameters $\{\lambda_i\}$ in Eq. (2.83) can be further reduced, more precisely they will disappear by the application of SLOCC-operations on each subsystem:

$$A \otimes B\,|\psi_{AB,S}\rangle = \frac{1}{\sqrt{n_S}} \sum_{i=0}^{n_S-1} |ii\rangle \tag{2.84}$$

Then, the number of non-vanishing Schmidt coefficients n_S is obviously sufficient to characterize the respective SLOCC class of the state, which proves Theorem 2.6. □

Note that Eq. (2.84) can be identified with the generalized Bell-state in arbitrary dimensions (Eq. (2.49)), which were mentioned to mark the *maximally* entangled state in each dimension. From the equation above it follows that any state can be mapped to $|\psi_{Bell}\rangle$ within the respective dimension by use of SLOCC, that is with non-vanishing probability depending on the Schmidt coefficients $\{\lambda_i\}$. For the other direction, i.e. mapping $|\psi_{Bell}\rangle$ to any state with the same n_S it holds that the transformation takes place with *certainty*. This poses as a reasonable argument for the generalized bipartite Bell states define the set of maximally entangled states. It is worth mentioning that the number of non-zero Schmidt coefficients is closely related to the rank of the coefficient matrix Eq. (2.12), which thereby can identified to be *invariant* under SLOCC as well.

Remark 2.2. Rank of the coefficient matrix and SLOCC classes
All bipartite states $|\psi_{AB}\rangle$ with equal rank r_C of their respective coefficient matrix $C_{|\psi_{AB}\rangle}$ belong to the same SLOCC-class. For $r_c = 1$ the corresponding state is a product state, for $r_C = \min(d_A, d_B)$ the state is SLOCC-equivalent to the generalized Bell state.

This connection will be used frequently in context with SLOCC classification of qudit hypergraph states in Chapter 4.
Finally, note that the notion of *maximally entangled states* will be revisited in Chapter 5. The need for discussion arises because, though the generalized Bell state is a sensible candidate for reasons shown above, there are scenarios that contradict the term in a fundamental way. Following, classification in terms of LU and LOCC equivalence classes are reviewed for two qubit states.

LU and LOCC classification of bipartite qubit states

As mentioned before, LU as well as LOCC operations in most cases fail to give a deeper insight into entanglement structures and properties of states simply due to either their number of

free paramters (LU) or the complex structure of the transformation protocol (LOCC).
For LUs, with increasing system dimension, the number of parameters of the general state vector rises much quicker then the number of parameter describing the LU. Thus, in most cases the equivalence classes under LU will contain families with one ore more free parameters. To illustrate the problem, the most simpe example of two qubits suffices. Obviously, the Schmidt decomposition of a two-qubit state has only one free parameter

$$|\psi_{AB}\rangle = \sqrt{\lambda_0}\,|00\rangle + \sqrt{\lambda_1}\,|11\rangle \quad \text{with: } \lambda_0 + \lambda_1 = 1 \tag{2.85}$$

Thus we can rewrite Eq. (2.85) in terms of a new parameter θ as

$$|\psi_{AB}\rangle = \cos(\theta)\,|00\rangle + \sin(\theta)\,|11\rangle \tag{2.86}$$

Therefore, any two qubit state can, under LU, be transformed to Eq. (2.86). Obviously there is still one continuous parameter, i.e. θ, left. Hence, even for the lowest possible dimension and particles, the number of equivalence classes under LU is *infinite*.

In terms of LOCC equivalence, it is known that LOCC equivalence coincides with LU equivalence for *single* copies of states.

For multiple round of LOCC-protocols it was shown in [18] that for an infinite number of copies there exist LOCC-protocols that transform every entangled two qubit state to the maximally entangled Bell state, i.e.

$$|\psi_{AB}\rangle^{\otimes n} \xrightarrow{LOCC-protocol} |\psi_{AB}\rangle_{Bell}^{\otimes m} = \frac{1}{\sqrt{2}}(|00\rangle + |11\rangle). \tag{2.87}$$

This process is called *entanglement distillation*. The transition rate, i.e. the number of maximally entangled states m that can be obtained from n copies of a lesser entangled state, is determined by the amount of entanglement within the original state. Likewise, the reverse process can be initiated, denoted as *entanglement dilution*. Therefore, the entanglement of any pure bipartite state can be seen as equivalent to that of the maximally entangled state in the asymptotic limit ($n \longrightarrow \infty$).

2.3.4 Classification of multipartite entanglement

In the multipartite case, entanglement classification is not solvable for arbitrary dimension and particle number. This is mostly due to the fact that there is no generalization of the Schmidt decomposition for systems consisting of more that two parties [55]. Nonetheless, special cases have been studied extensively and following an overview regarding those will be given.

Starting with the most simple multipartite system, that is a pure three-qubit state, it has been shown that any state $|\psi_{ABC}\rangle$ in $\mathcal{H} = \mathcal{H}_A \times \mathcal{H}_B \times \mathcal{H}_C$ of dimension $d = d_A \times d_B \times_C = 2 \times 2 \times 2$ is LU-equivalent to [95]

$$(U_A \otimes U_B \otimes U_C\,|\psi_{ABC}\rangle = \lambda_0\,|000\rangle + \lambda_1 e^{i\varphi}\,|100\rangle + \lambda_2\,|101\rangle + \lambda_3\,|110\rangle + \lambda_4\,|111\rangle \tag{2.88}$$

where $\{\lambda_i\}$ and φ are continuous real parameters. Notice that a consideration of the free parameters the three unitaries have in comparison with those inherent in a normalized three

qubit state already determines the appearance of continuous parameters in Eq. (2.88) [4]
Regarding equivalence under SLOCC, the seminal paper, published in 2000 [113] presents a full classification of entanglement of a multipartite system for the first time. It yielded the famous result stating that there are two inequivalent ways of genuine multipartite entanglement within a $(2 \times 2 \times 2)$ system - impossible to transform into each other via SLOCC operations: the *W-state* and the *GHZ-state*. [5].
The complete SLOCC classification, including the fully separable product state $(A|B|C)$ and biseparable states $(A|BC)$, $(B|AC)$, $(C|AB)$ was shown to encompass a total of six inequivalent SLOCC classes:

$$\begin{aligned} |\psi_{A|B|C}\rangle &= |000\rangle\,, \\ |\psi_{A|BC}\rangle = \frac{1}{\sqrt{2}}|000\rangle + |011\rangle),\ |\psi_{B|AC}\rangle &= \frac{1}{\sqrt{2}}(|000\rangle + |101\rangle),\ |\psi_{C|AB}\rangle = \frac{1}{\sqrt{2}}(|000\rangle + |110\rangle), \\ |GHZ\rangle = \frac{1}{\sqrt{2}}(|000\rangle + |111\rangle),\ |W\rangle &= \frac{1}{\sqrt{3}}(|001\rangle + |010\rangle + |100\rangle), \end{aligned} \tag{2.89}$$

The hierarchy of those, that is, the option of obtaining states from one SLOCC class with lower entanglement from one with higher entanglement when applying non-invertible local operations, was presented. Its conclusion being that every three qubit state can be generated from the W-or the GHZ-state, identifying them as the ones with the highest entanglement level. The hierarchy of those six classes is illustrated in Fig. 2.3

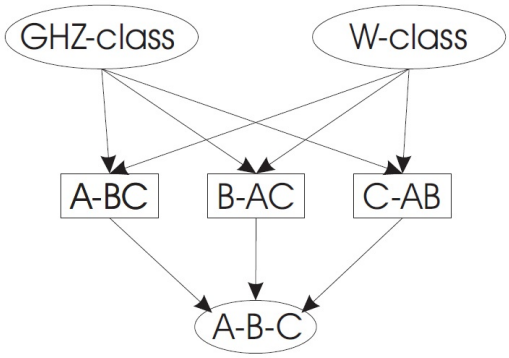

FIGURE 2.3: Hierarchy of three qubits SLOCC classes [113]. The arrows denote convertibility of two classes, that is the states within those classes, under non-invertible local operations. It is clear that from the GHZ and the W-state one can reach all states within the three qubits class.

The study of the maximally entangled state in the three qubit case is not as straightforward as in the bipartite case. This is due to the fact that there are the above-mentioned two classes, from which one can reach all states within the three qubit realm. It has been shown, that the GHZ-state maximizes entanglement monotones, like the three-tangle, whereas this measure vanishes for the W-state. Thus the GHZ state satisfies in many ways the properties a maximally entangled state should own. On the other hand, the W-state was identified as the one with the most residual bipartite entanglement. This refers to the amount of

[4] Each qubit unitary has four free, real valued parameters, factoring out a global phase reduces the number to three. This gives nine in total for U_A, U_B, U_C. A general three-qubit state however has $2 \times 2 \times 2 = 8$ complex parameters. Makes 16 real valued ones, minus one for global phase and normalization respectively gives 14.

[5] The method used by [113] to identify SLOCC classes is mainly based on the study of the rank of the reduced density matrices, which is known not to change under SLOCC. Additionally the range of the reduced density matrix is utilized, e.g. the inequivalent way the range can be built up. Further details: seeApp)

entanglement left within the state, when one subsystems is traced out. In contrast to the W-state, tracing out one party completely destroys all entanglement within the GHZ-state. Hence, the robustness of entanglement regarding the loss of one qubit is certainly higher within the W state. Therefore, one can conclude that the definition of the maximally entangled state is related to the question of maximal usefulness for quantum informational tasks, which can only be answered by: 'it depends'. Depends, on which feature one is interested in using.
Turning the focus to systems of higher dimension and more parties, it was shown that the last systems for which a finite classification under SLOCC is possible are those of the form $2 \times 3 \times n$ with n arbitrary but finite. In [126], representative states and hierarchy are given. The proof is based on the idea of matrix pencils. [6]. For the most simple four-partite system, i.e. four qubits, infiniteness under SLOCC was shown in [96]. For $3 \times 3 \times 3$ systems simple dimension arguments exclude the option of a finite classification. [7]

2.4 Entanglement detection

Despite the clear mathematical definition of entanglement as the impossibility of a decomposition into a convex sum of tensor products, it is by no means an easy task to decide whether a given state ρ is entangled or not. While for pure quantum states the Schmidt decomposition provides an operational method to detect entanglement, the task becomes more involved when considering mixed states. This whole topic is referred to as *separability problem in quantum information theory*. The complexity shows already in simple systems, in fact, even for the bipartite case, the question of separability was proven to be NP-hard [97]. Nonetheless, there exist approaches, both operational and non-operational, which tackle the problem and have proven to be useful tools. 'Operational' here means that a direct application to a given density matrix is possible. Separability criteria usually base on defining special properties satisfied by all separable states. A violation of the criterion thus indicates the presence of entanglement. Here, it is of importance to stress the fact that non-violation is not equal to separability, as it could likely be the case that the criterion is not 'strong' enough to detect the kind of possible entanglement within the state. A variety of some of the most successful and important separability criteria will be reviewed in the following section.

2.4.1 PnCP-maps

A non-operational criterion to detect entanglement within a given state ρ is based on the notion of *positive but not completely positive maps* (PnCP-maps)

Definition 2.13. PnCP-maps
A linear map Λ is said to be positive if and only if it preserves positivity of a positive (semi-) definite operator A, that is $\Lambda[A] \geq 0 \quad \forall\ A \geq 0$. Furthermore, Λ is k-positive if and only if positivity is preserved when acting on a subsystem of an enlarged Hilbert space, i.e.

$$(\mathbb{1}_k \otimes \Lambda)[A] \geq 0 \qquad \forall \quad A \geq 0 \tag{2.90}$$

Then, it follows that a map is completely positive if and only if it is k-positive for all k whereas a PnCP-map may lead to negative eigenvalues when acting on A.

[6] An alternative proof for $2 \times 3 \times 3$ systems can be found in Appendix A. Furthermore, a proof for infiniteness for $2 \times 4 \times 4$ and higher dimensions is given

[7] Each invertible 3×3 matrix has $2 \times (3 \times 3 - 1)$ real parameters, adding up to 48. A general three qutrit state possesses $2 \times (3 \times 3 \times 3 - 1) = 52$ free real parameters.

Recalling that density operators are positive semi-definite and considering the action of a positive but not completely positive map acting on a separable density operator of the form $\rho_{AB} = \sum_i p_i \rho_{A,i} \otimes \rho_{B,i}$, one finds

$$(\mathbb{1}_A \otimes \Lambda_B)\rho_{AB} = \sum_i p_i \rho_{A,i} \otimes \Lambda_B[\rho_{B,i}] \tag{2.91}$$

Then, as $\{\rho_{B,i}\}$ is the reduced density matrix with respect to subsystem B and therefore, as a valid density operator, positive semi-definite: $\Lambda[\rho_{B,i}] \geq 0$ for all i. Thus, $\rho_{A,i} \otimes \Lambda_B[\rho_{B,i}]$ is a positive semi-definite operator and finally the same is true for $\sum_i p_i \rho_{A,i} \otimes \Lambda_B[\rho_{B,i}]$. In conclusion, if the action of $(\mathbb{1}_A \otimes \Lambda_B)$ produces at least one negative eigenvalue, one can exclude separability of ρ_{AB} with certainty. Furthermore it has been shown [121] that preservation of positivity under *any* positive map is a necessary and sufficient criterion for separability.

Theorem 2.7. Preservation of positivity
*Let ρ_{AB} be a density operator on $\mathcal{H}_A \otimes \mathcal{H}_B$ and let Λ be a positive map acting on $\mathcal{H}_B$. Then ρ_{AB} is **separable** if and only if*

$$(\mathbb{1}_A \otimes \Lambda_B)\rho_{AB} \geq 0 \qquad \forall \;\; \Lambda \geq 0 \tag{2.92}$$

To see that this criterion, while mathematically giving a closed way to distinguish the set of separable states from entangled states, is non-operational, i.e. not directly computable, notice that there exists an infinite variety of PnCP-maps, whose set has not been characterized up to now.

PPT-criterion

One of the first and most known entanglement criteria based on PnCP-maps introduced by Peres and Horodecki [30], [121] is the *positive partial transpose (PPT) -criterion.* The positive map used in this case is the transposition map, T. Then the *partial* transposition-map, i.e. the transposition with respect to a certain subsystem of a composite density matrix ρ_{AB} can be written as $(\mathbb{1}_A \otimes T_B)$ (for the transposition to be performed on subsystem B). A density operator is said to have a positive partial transpose if and only if it stays positive under the action of the partial transpose map on any subsystem, i.e. $\rho_{AB}^{T_B} = (\mathbb{1}_A \otimes T_B)[\rho_{AB}] \geq 0$ and $\rho_{AB}^{T_A} = (T_A \otimes \mathbb{1}_B)[\rho_{AB}] \geq 0$. Moreover, positivity under transposition of one subsystem implies the same for the other subsystem: $\rho_{AB}^{T_A} \geq 0 \Leftrightarrow \rho_{AB}^{T_B} \geq 0$. The action of the partial transpose map on the density matrix can be illustrated best when decomposing ρ_{AB} into a certain product basis, i.e. $\rho = \sum_{ijkl} \rho_{ijkl} |i\rangle \langle j| \otimes |k\rangle \langle l|$. Then it follows

$$\rho_{AB}^{T_A} = \sum_{ijkl} \rho_{\mathbf{ji}kl} |i\rangle \langle j| \otimes |k\rangle \langle l|, \qquad \text{and} \quad \rho_{AB}^{T_B} = \sum_{ijkl} \rho_{ji\mathbf{lk}} |i\rangle \langle j| \otimes |k\rangle \langle l| \tag{2.93}$$

Theorem 2.8. PPT-criterion
Let ρ be the density matrix describing a mixed quantum state. If ρ is located within the set of separable states, its partial transpose with respect to any subsystem is positive definite, i.e.

$$\rho \;\in\; \{\rho_{SEP}\} \qquad \Longrightarrow \qquad \rho^{T_i} \geq 0 \;\; \forall \;\; i \tag{2.94}$$

Furthermore, if $\rho = \rho_{AB}$ corresponds to a bipartite system of dimension $\mathbb{C}^2 \times \mathbb{C}^2$ or $\mathbb{C}^2 \times \mathbb{C}^3$ it was shown in [30], [121] that the positivity of the partial transpose is a *necessary and sufficient* criterion for detecting entanglement. That is, from $\rho^{T_i} \geq 0$ with $i = A, B$ separability of ρ_{AB} follows. For higher dimensions the PPT-criterion is necessary, but not sufficient, the first example of an entangled state with positive partial transpose was found within a $\mathbb{C}^2 \times \mathbb{C}^4$ and a $\mathbb{C}^3 \times \mathbb{C}^3$ system by [117]. Those states fall into the category of *bound entangled* states. Bound entanglement defined as undistillable entanglement, i.e. no pure entangled states can be obtained by means of LOCC from a bound entangled state.

Reduction criterion

Theorem 2.9. Reduction criterion [99]
If a given bipartite state ρ_{AB} is separable, it stays positive under application of the reduction map $\Lambda_r(\rho) = \mathrm{tr}(\rho)\mathbb{1} - \rho$, i.e. $(\mathbb{1}_A \otimes \Lambda_{reduction,B})\rho_{AB} \geq 0$. Positivity under action of $\Lambda_{reduction}$ is equivalent to the fulfillment of the following conditions:

$$\mathbb{1}_A \otimes \rho_B - \rho_{AB} \geq 0 \qquad \textit{and} \qquad \rho_A \otimes \mathbb{1}_B - \rho_{AB} \geq 0 \tag{2.95}$$

where $\rho_{A,B}$ denote the reduced density matrices of ρ_{AB}. [8]

Majorization criterion

The majorization criterion is a necessary but not sufficient criterion for entanglement, it states:

Theorem 2.10. Majorization criterion [100]
For all separable states ρ_{AB} the sum of the decreasingly ordered eigenvalues of the reduced and full density matrices satisfy

$$\sum_{i=0}^{d-1} \lambda_i^{\downarrow}(\rho_{AB}) \leq \sum_{i=0}^{d-1} \lambda_i^{\downarrow}(\rho_{A,B}) \qquad \textit{where} \quad d = d_A \cdot d_B \tag{2.96}$$

Range criterion

The range criterion is one of the first criteria which was able to detect bound entangled states, that is state, which were not detected by the PPT-criterion.

Theorem 2.11. Range criterion [121]
If ρ_{AB} is a separable state, then there exists a set of product vectors $\{|\psi_i\rangle, |\varphi_i\rangle\}$ which spans the range [9] *of ρ_{AB}. Furthermore, the set $\{|\psi_i^*\rangle, |\varphi_i\rangle\}$ spans the range of $\rho_{AB}^{T_A}$. Here $|\psi_i^*\rangle$ is the ket whose entries are the complex conjugates of those within $|\psi_i\rangle$. Naturally the same is true under permutation $A \leftrightarrow B$, i.e. $\{|\psi_i\rangle, |\varphi_i^*\rangle\}$ spans the range of $\rho_{AB}^{T_B}$.*

Matrix realignement criterion

The matrix realignement criterion is a necessary but not sufficient criterion for separability. It has its origin in another, stronger separability criterion, which is necessary and sufficient but hard to compute, the cross norm criterion[ref] which states that for a separable state

[8] Similar to the PPT-criterion, the reduction criterion is necessary for all dimensions, but sufficient only for $d \leq 6$.

[9] The range of ρ is defined as the set of pure states $\{|\Psi\rangle\}$ for which there exists a pure state $|\Phi\rangle$ such that $|\Psi\rangle = \rho\,|\Phi\rangle$.

ρ the *cross norm* $||\rho||_\gamma = 1$ where $||\rho||_\gamma = \inf_{a_i,b_i} \sum_i ||a_i||_1 ||b_i||_1$ and a_i, b_i satisfying $\rho = \sum_i a_i \otimes b_i$. From this, a weaker version omitting the difficult search for the infimum, the matrix realignement criterion, also referred to as *computable* cross norm emerges:

Theorem 2.12. Matrix realignement criterion [101]
Any bipartite separable state ρ decomposed in a specific product basis $\rho = \sum_{ijkl} \rho_{ijkl} |ij\rangle \langle kl|$ has to satisfy

$$||\rho_R||_1 \leq 1 \qquad \text{with the realigned matrix: } \rho_R = \sum_{ijkl} \rho_{ikjl} |ij\rangle \langle kl| \tag{2.97}$$

2.4.2 Entanglement witnesses

Though there exists many different necessary criteria to distinguish entangled states form separable ones, computability and sufficiency remains a problem in many cases. Furthermore, there is one major disadvantage common to all separability criteria considered in the precedent parts of this section: the application of those require complete knowledge of the quantum state and as such the need for full state tomography arises. This, in turn, requires a large number of measurements. Detecting entanglement via entanglement witnesses reduces the measurement to one observable. Thus, if one is interested not in the concrete form of the given state but only in a statement regarding the entanglement properties, this constitutes as a big advantage, especially regarding practical realizability. Analytically based on the Hahn-Banach-Theorem [102],[103], entanglement witnesses can be defined as follows:

Definition 2.14. Entanglement witnesses [121]
Entanglement Witnesses are (non)-linear hermitean operators W that have at least one negative eigenvalue within their spectrum and satisfy

$$\begin{aligned} \forall \ \rho_{\text{SEP}} : &\qquad \text{tr}(W\rho_{\text{SEP}}) \ \geq \ 0 \\ \exists \ \rho_{\text{ENT}} : &\qquad \text{tr}(W\rho_{\text{ENT}}) \ < \ 0 \end{aligned} \tag{2.98}$$

As the set of separable states as well as the set of mixed states is convex and the expectation value of any observable $\langle A \rangle = \text{tr}(A\rho)$ is linear dependent on the state, the set of states for which $Tr(W\rho = 0$ defines a hyperplane within the whole state space. It divides the states in "left" and "right", the states on each side sharing the same algebraic sign "+" or "-". Thus the situation can be illustrated in a geometrical picture as shown in Fig. 2.4

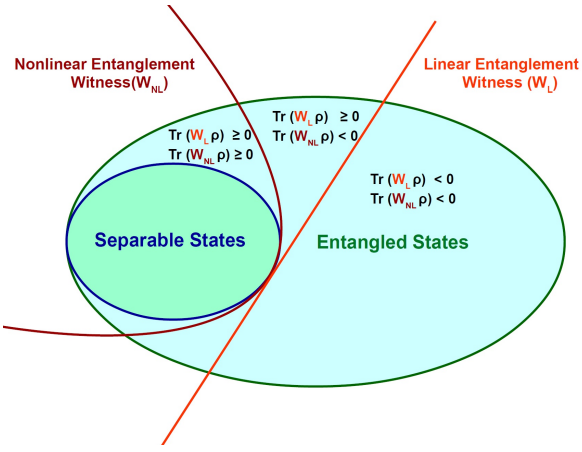

FIGURE 2.4: Entanglement witnesses. Illustrated are the *optimal* witnesses, which are defined by being tangent to the set of fully separable states

Construction of entanglement witnesses

There are different ways to construct an entanglement witness. One is by using the relation between PnCP-maps and witnesses via the Choi-Jamiolkowski-isomorphism [104]. It states that every linear map $\Lambda : \mathcal{L}(\mathcal{H}_A) \mapsto \mathcal{L}(\mathcal{H}_B)$ is associated to an operator R acting on $\mathcal{L}(\mathcal{H}_A \otimes \mathcal{H}_B)$ by the following relation

$$\Lambda(Y) = \mathrm{tr}_A(RY_A^T \otimes \mathbb{1}_B) \qquad \forall\, Y \in \mathcal{H}_A \tag{2.99}$$

The inverse relation to construct the operator from the map is

$$R = (\mathbb{1}_{A'} \otimes \Lambda_A)(|\psi\rangle\langle\psi|) \tag{2.100}$$

Where $|\psi\rangle = \sum_i |ii\rangle$ is the unnormalized maximally entangled state on $\mathcal{H}_{A'} \otimes \mathcal{H}_A$. Then the connection between CnCP-maps and entanglement witnesses follows from the properties of the isomorphism. That is, Λ is a CP-map if and only if R is a positive semidefinite operator and Λ is a PnCP-map if and only if R is an entanglement witness, i.e. the following relations for a witness operator W and a PnCP-map Λ hold

$$\begin{aligned} \Lambda(\rho) &= \mathrm{tr}_A(W\rho_A^T \otimes \mathbb{1}_B) \\ W &= (\mathbb{1}_{A'} \otimes \Lambda_A)(|\psi\rangle\langle\psi|) \end{aligned} \tag{2.101}$$

Another powerful and simple way to construct an entanglement witness for any given pure entangled state $|\psi_{\mathrm{ENT}}\rangle$ uses the maximal overlap with the set of separable states $\{|\psi_{\mathrm{SEP}}\rangle\}$. The idea being that states close to $|\psi_{\mathrm{ENT}}\rangle$ should be entangled as well. Witnesses of such form are also referred to as *projector based witnesses* and will be used frequently within subsequent parts of this thesis.

Definition 2.15. Projector based entanglement witness
Let $|\psi_E\rangle$ be an n-partite, entangled state of arbitrary dimension and let α denote the maximal squared overlap of $|\psi_E\rangle$ with the set of all separable states. Then one can define an operator W with

$$W = \alpha\mathbb{1} - |\psi_E\rangle\langle\psi_E| \qquad \text{with: } \alpha = \max_{|\varphi\rangle \in \{|\psi_{\mathrm{SEP}}\rangle\}} |\langle\varphi|\psi_E\rangle|^2 \tag{2.102}$$

that hence witnesses for $\mathrm{tr}(\rho W) < 0$ non-membership with respect to the convex set of separable states.

Due to the fact that large parts of this thesis deal with entanglement classification via SLOCC operations, following, the generalization of the concept to operators witnessing membership to a specific SLOCC-class is described.

SLOCC witnesses

Based on the notion of projector based entanglement witnesses, one can generalize the idea to construct an SLOCC witness, that is, an operator, which can decide if for a given state $|\varphi\rangle$ it is possible to be an element of $S_{|\psi\rangle}$, i.e. the SLOCC-class corresponding to the representative state $|\psi\rangle$.

Definition 2.16. SLOCC-witness
A hermitian operator W is a SLOCC witness for class $S_{|\psi\rangle}$ if and only if

$$\begin{aligned} \mathrm{tr}(\rho_{S_{|\psi\rangle}} W) \geq 0 \qquad & \text{for all states } \rho_{S_{|\psi\rangle}} \text{ in the SLOCC orbit of } |\psi\rangle \\ \mathrm{tr}(\rho W) < 0 \qquad & \text{for at least one state not in the SLOCC orbit of } |\psi\rangle \end{aligned} \tag{2.103}$$

holds.

Thus, in this case W detects for $\mathrm{tr}(\rho W) < 0$ states that are not within the convex set of all states within $S_{|\psi\rangle}$. The concrete form of the $(|\varphi\rangle, S_{|\psi\rangle})$-SLOCC witness then reads $W = \lambda \mathbb{1} - |\varphi\rangle\langle\varphi|$, where λ denotes the maximal squared overlap

$$\lambda = \sup_{|\eta\rangle} |\langle\varphi|\eta\rangle|^2. \tag{2.104}$$

Here, the supremum is taken over all states $|\eta\rangle = \bigotimes_i A_i |\psi\rangle$ in the SLOCC class $S_{|\psi\rangle}$, where $\{A_i\}$ denote ILOs on the respective subsystem, and $|\varphi\rangle$ is a representative state of SLOCC class $S_{|\varphi\rangle}$. A special class of witnesses are those verifying the Schmidt rank of a given pure state. As the Schmidt rank is invariant under SLOCC, such witnesses are very useful to distinguish between SLOCC classes of biparite systems or bipartite splits of multipartite systems.

2.5 Graph states, Hypergraph states and the Stabilizer formalism

The last section is dedicated to a special family of (multipartite) quantum states referred to as *graph states* [33], e.g. their generalization to *hypergraph states* [34], which will be frequently used within Chapter 4 and Chapter 5. As has been shown in the previous sections, entanglement within the multipartite (and high dimensional) regime is highly non-trivial and a closed classification and characterization is, due to the fast growing number of free parameters, not possible in general. Hence, it is sensible to redirect the focus on particular systems, circumventing the difficulty of high parameter quantity by enforcing restrictions on initial state and/or entanglement generating operations. Furthermore, graph - and hypergraph states are are so-called *stabilizer states*, thus, within this context, the stabilizer formalism is reviewed as an alternative way to describe a quantum state by the operations leaving it unchanged rather than by the traditional way of the common state vector. The diverse perspective on the characterization of a quantum system is in some cases easier to handle as no complete knowledge of the state is necessary. Furthermore it has proven to be useful in a vast field of applications, e.g. in the area of quantum error codes.

2.5.1 Graph states

A qudit *graph state* [105]-[109] is a multipartite quantum state of n qudits that can be represented by a graph G of n vertices $\{V_i\}$ and a set of edges $\{E_{ij}\} = \{(V_i, V_j)\}$ connecting vertices V_i an V_j, in short one writes $G(V, E)$. A crucial difference to qubit graph states and graph states in *prime* dimensions, occurs when considering non-prime dimensions. Here, additionally to the options of either an edge or no edge between two vertices, edges may appear with a certain *multiplicity* m_e. This is a consequence of the behaviour of powers of

the generalized Pauli-Z-gate. Whereas in prime dimension Z^k just gives permutations of the diagonal elements of the original Z-gate, in non prime dimension the situation is more evolved. [10]

To connect the graphical description with the formal state vector, the following rules are applied: at each vertex, there is initially a qudit in an equal superposition of all levels in computational basis, i.e. $|+_d\rangle = \frac{1}{d}\sum_{i=0}^{d-1}|i\rangle$ which is an eigenstate of the generalized Pauli-X-operator in d dimensions, that reads

$$X = \sum_k |(k+1) \bmod d\rangle\langle k| \overset{\text{for d=4}}{=} \begin{pmatrix} 0 & 0 & 0 & 1 \\ 1 & 0 & 0 & 0 \\ 0 & 1 & 0 & 0 \\ 0 & 0 & 1 & 0 \end{pmatrix}. \tag{2.105}$$

Then, the initial state $|G_0\rangle$, i.e. the state corresponding to an *empty* graph with no edges, can be written as the tensor product of the single vertex states, i.e.

$$|G_0\rangle = \bigotimes_{i=0}^{n-1} |+_d\rangle_i \tag{2.106}$$

for an n-partite graph of dimension d. The edges representing the entangling operation are described by the controlled Pauli-Z-operators Z_{ij} in d dimensions, depending on the multiplicity m_e of the edge, that is

$$\begin{aligned} Z_{ij}^{m_e} &= \sum_{k=0}^{d-1} |k\rangle\langle k|_i \otimes (Z_j^{m_e})^k \\ &= (|0\rangle\langle 0|)_i \otimes \mathbb{1}_j + (|1\rangle\langle 1|)_i \otimes Z_j^{m_e} + ... + (|n-1\rangle\langle n-1|)_i \otimes (Z_j^{m_e})^{n-1} \end{aligned} \tag{2.107}$$

where Z_i is the generalized Pauli-Z-gate in d dimensions applied to the qudit at the $i-th$ vertex defined as

$$Z = \sum_k \omega^k |k\rangle\langle k| = \begin{pmatrix} 1 & 0 & \cdots & 0 \\ 0 & \omega & \ddots & \vdots \\ \vdots & \ddots & \ddots & 0 \\ 0 & \cdots & 0 & \omega^{d-1} \end{pmatrix} \qquad \text{with the root of unity } \omega = e^{\frac{2\pi i}{d}} \tag{2.108}$$

The generalized Pauli-X-and Z-gates satisfy, in an analogous fashion to the two dimensional matrices $X^d = Z^d = \mathbb{1}$, $Z_{ij}^d = \mathbb{1}_{ij}$. Additionally, one can define the commutation relation between the single vertex X and Z gates as

$$Z^a X^b = X^b Z^a \omega^{ab}. \tag{2.109}$$

If one wishes to switch from computational (Z-) basis, $\{|k\rangle\}$, to the eigenbasis of the X operator denoted by $\{|\tilde{k}\rangle\}$, the transformation is mediated by the fourier operator defined as

$$F = \frac{1}{\sqrt{d}} \sum_{k,\tilde{k}=0}^{d-1} |k\rangle\langle\tilde{k}| \qquad \text{and thus: } |\tilde{k}\rangle = F^\dagger |k\rangle \tag{2.110}$$

[10] For a detailed derivation of the characteristic behaviour and rules of Z^k w.r.t the dimension, see introductory part of Chapter 4.

A more detailed overview regarding the phase space representation, the Heisenberg-Weyl group containing the symplectic operations, which will be of importance when considering operations on- and local equivalence of higher dimensional (hyper-)graph states, will be given in the introductory part of Chapter 4.
Finally, an arbitrary graph state can be defined as:

Definition 2.17. Graph state
Given a d-dimensional graph $G(V, E)$ consisting of a set of n vertices and edges of multiplicity m_e connecting two vertices $(v_i, v_j)0$, the associated graph state $|G\rangle$ takes the form

$$|G\rangle = \prod_{e\in E} (Z_e^{m_e}) \, |+_d\rangle^V \,, \qquad \text{where: } |+_d\rangle^V = |+_d\rangle^{\otimes n} = \bigotimes_{i=0}^{n-1} |+\rangle_i \,. \tag{2.111}$$

Alternatively, one can rewrite Eq. (2.121) in computational basis as

$$|G\rangle = \sum_{ijkl...=0}^{d-1} \prod_{e_a\in E} \omega^{m_{e_a} e_a} \, |ijkl...\rangle \,. \tag{2.112}$$

Exemplary, a six-dimensional graph of five vertices and a set of edges of multiplicity $m_e = 1, 2, 3$ is illustrated in Fig. (2.5). The corresponding graph states can be determined to be

$$\begin{aligned} |G\rangle &= Z_{12}^2 Z_{34} Z_{25} Z_{35}^3 \, |+_6\rangle^{\otimes 5} \\ &= \sum_{ijklm=0}^{5} \omega^{2ij} \omega^{kl} \omega^{im} \omega^{3km} \, |ijklm\rangle \end{aligned} \tag{2.113}$$

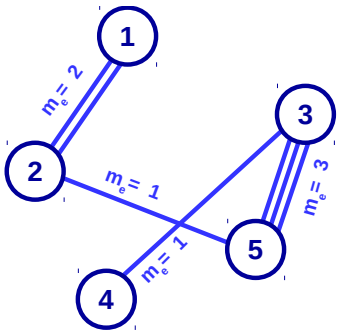

FIGURE 2.5: Qudit graph of five vertices with dimesnionality six.

Graph states as stabilizer states

As mentioned, there exists an alternative way to characterize a quantum state. Instead of using state vectors themselves, the operators leaving them unchanged can be utilized. This works as follows: first defined for qubits, a stabilizer group $\mathcal{S}^{(n)}$ is a commutative subgroup of the Pauli group $\mathcal{P}$, e.g. $\mathcal{P}^{\setminus}$ for an n-partite state, which does not contain $-\mathbb{1}$ an thus guarantees hermiticity of its elements $S_i = S_i^\dagger$. Generalization to qudits are based on the generalized Pauli group. The *generator* of a stabilizer group is the set of elements within $\mathcal{S}$ defined by the maximal number of independent S_i, that is, every element of $\mathcal{S}$ can be generated by multiplying elements of the generator. The qubit Pauli group $\mathcal{P}_2$ is generated by $\mathcal{G}_2 = \{cX^a Z^b | a, b \in (\mathbb{Z} \bmod d), \; c \in [\pm 1, \pm i]\}$ and the generalized Pauli group $\mathcal{P}_g$ has

the generator $\mathcal{G}_g = \{\omega^c X^a Z^b | a, b, c \in \mathbb{Z} \bmod d,\ \omega = e^{\frac{2\pi i}{d}}\}$. Then, for a given state $|\psi\rangle$ the stabilizer group is defined by all operators S_i *stabilizing* the state, i.e. all S_i have $|\psi\rangle$ as a common eigenstate with eigenvalue $+1$:

$$S_i |\psi\rangle = +1 |\psi\rangle \qquad \forall\ S_i \ \in \ \mathcal{S} \tag{2.114}$$

For an n partite qudit-system, a cardinality of d^n for $\mathcal{S}$ is needed to define the state *uniquely*. Graph states are a special kind of stabilizer states, their definition in terms of stabilizers is formulated in the following Definition 2.18.

Definition 2.18. Stabilizer of graph states [134]
For a graph $G(V, E)$, the associated graph state $|G\rangle$ is the unique common eigenvector with eigenvalue $+1$ of the set of commuting operators $\{K_i\}$ defined as

$$K_i = X_i \prod_{j \in \mathcal{N}(i)} Z_j^{m_e^{(ij)}} \qquad \forall\ i \in V^{11} \tag{2.115}$$

where $\mathcal{N}(i)$ denotes the neighbourhood of vertex i, i.e. all vertices connected to vertex i via an edge.

As an example, consider the graph in Fig. (2.5). The five stabilizer generators K_i, $i \in [1, ..., 5]$ are then given by

$$\begin{aligned} K_1 &= X_1 Z_2^2 \qquad K_2 = X_2 Z_1^2 Z_2 \qquad K_3 = X_3 Z_4 Z_5^3 \\ K_4 &= X_4 Z_3 \qquad K_5 = X_5 Z_3^3 Z_4 \end{aligned} \tag{2.116}$$

Associated with a certain graph $G(V, E)$ is a *graph state basis* defined as the collection of orthonormal states of the form

$$|a\rangle = Z^a |G\rangle = \prod_i Z_i^{a_i} |G\rangle \tag{2.117}$$

where a is the n-tuple $(a_0, a_1, ..., a_{n-1})$ with each a_i taking integer values within $[0, ..., d-1]$ and the d^n different states $|a\rangle = |a_o, a_1, ..., a_{n-1}\rangle$ form an orthonormal basis of the corresponding Hilbert space. Furthermore, the states $|a\rangle$ are the eigenstates of the stabilizers K_i according to different eigenvalues ω^k, $k \in [0, ..., d-1]$ defined by the value a_i, i.e. $K_i |a\rangle = \omega^{a_i} |a\rangle$. The projector onto a certain graph state $|G\rangle \langle G|$ can be written in terms of the stabilizing operators:

$$P_G = |G\rangle \langle G| = \frac{1}{d^n} \sum_{s_i \ \in \ S} s_i, \qquad S = \text{stabilizer group of } |G\rangle \tag{2.118}$$

Concluding this subsection, it is worth mentioning that it was shown in [41] that each stabilizer state corresponds to certain graph. Hence, when analyzing the properties of stabilizer states, it suffices to do so for graph states.

Local complementation of qubit graph states

For qubit graph states, there exists a powerful tool to identify graph states that are equivalent under local unitaries, local complementation (LC) [110]. Generally, according to Definition (2.1), two n-partite graph states $|G\rangle$ and $|G'\rangle$ are LU-equivalent if and only if $|G'\rangle =$

[11] The influence of the multiplicity on the form of the stabilizer will be proven in the introductory part of Chapter 4

$\bigotimes_{i=1}^{n} U_n |G\rangle$. An interesting subgroup of the group of local unitaries are the local *Clifford operations* denoted here and in the following by C. The Clifford group is the normalizer of the Pauli group, which means it is build up by those operations mapping elements of the Pauli group to elements of the Pauli group. The Pauli group $\mathcal{P}$ is build up by the n-fold tensor products of the three Pauli matrices and the identity together with the prefactors ± 1 and $\pm i$ for group closure:

$$\mathcal{P} = \{\pm\mathbb{1}, \pm i\mathbb{1}, \pm\sigma_x, \pm i\sigma_x, \pm\sigma_y, \pm i\sigma_y, \pm\sigma_z, \pm i\sigma_z\} \tag{2.119}$$

Formally, the Clifford group then consist of two matrices mapping $\mathcal{P}$ to itself, that is

$$\mathcal{C} = \{\frac{1}{\sqrt{2}}\begin{pmatrix}1 & 1\\ 1 & -1\end{pmatrix}, \begin{pmatrix}1 & 0\\ 0 & i\end{pmatrix}\} \quad \text{then: } C\sigma_i C^\dagger = \sigma_j \quad \text{for } C \in \mathcal{C} \text{ and } \sigma_i, \sigma_j \in \mathcal{C}. \tag{2.120}$$

The local Clifford group then consists of the tensor product of all single Clifford groups of all participating qubits. Practically, local complementation of a graph can be done solely by staying in 'graph-language', i.e. one need not do any mathematical calculation on the state vectors but rather follow the *graphical rules for local complementation*. Those rules were proven to be quite simple [40]: local complementation on a certain vertex v_i of a graph goes as follows: for each pair of unconnected vertices in the *neighbourhood* of v_i, a new edge is created. Consequently, a previously existing one is then deleted, as applying the edge twice is nothing but the identity matrix acting on those two vertices. Here, the *neighbourhood* of a vertex v_i is defined as the set of vertices that are connected to v_i via an edge.
Then, two graph states $|G\rangle$, $|G'\rangle$ are said to be LC-equivalent if and only if there exists a *finite* sequence of local complementations converting one into the other. Exemplary the local complementation rule is illustrated in Fig. (2.6)

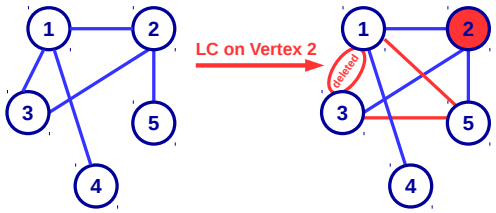

FIGURE 2.6: Local complementation, graphical rule.

In the case of qudit graph states, local complementation rules can be derived as will be shown in Chapter 4. These are based on studying the action of the generalized local Clifford operations, denoted as *symplectic* operations, on qudit graph states. Without going into detail at this point, it is worth mentioning that due to the multiplicity of edges within non-prime dimensions, LC rules for those state show a more complex structure and are difficult to derive in a general framework.

Concluding the graph state section, two special kinds of graph states which will be frequently used during this thesis are to be mentioned:

- Star graph states: graph states, where there is one distinguished vertex to which all other vertices are connected and where there is no other edge between the other vertices of the graph.

- Cluster states: graph states, which are aligned in a one-or two dimensional lattice. Edges then are necessarily and exclusively present between neighbouring qudits in horizontal as well as vertical direction.

2.5.2 Hypergraph states

Hypergraph states emerge from the family of graph states as a natural generalization, in which edges are allowed that may connect an *arbitrary* number of vertices, named *hyperedges*. In analogy to qubit graph states, a qubit hypergraph state can be defined as follows:

Definition 2.19. Hypergraph state
Given a two-dimensional hypergraph H consisting of a set of n vertices, V, and a set of (hyper-)edges, E, connecting an arbitrary number of vertices, the associated hypergraph state $|H\rangle$ takes the following form:

$$|H\rangle = \prod_{e\in E}(Z_e)\,|+_d\rangle^V \qquad \textit{where: } |+_d\rangle^V = |+_d\rangle^{\otimes n} = \bigotimes_{i=0}^{n-1}|+\rangle_i \tag{2.121}$$

that is, the difference to graph states lies purely within the refined and broadened set of edges.
The entanglement generating gate of an hyperedge connecting m vertices is the controlles Z-gate for m qubits, which is recursively defined based on the two-qubit controlled Z gate, which takes the form

$$Z_I = \sum_{k=0}^{d-1}(|k\rangle\langle k|)_i \otimes Z_{I\setminus i}, \tag{2.122}$$

where I denotes the index set of all m vertices. Again, in analogy to the graph state case, qubit hypergraph states are stabilizer states.

Definition 2.20. Stabilizer of qubit hypergraph states
For a hypergraph H described by a set of vertices and edges, (V,E), the associated hypergraph state $|H\rangle$ is the unique common eigenvector with eigenvalue $+1$ to the set of commuting operators $\{K_i\}$ defined as:

$$K_i = X_i \prod_{j\in\mathcal{N}(i)} Z_j \qquad \forall\ i \in V \tag{2.123}$$

However, due to the multi-qubit edges, the stabilizing operators of a hypergraph state are no longer local: the Z-gates acting on the neighbourhood of the $i-th$ vertex are again acting on more then one qubit depending on the number of qubits the original edge had enclosed. Thus many advantages present in the smooth description and characterization of graph states in terms of stabilizers are no longer accessible. In Fig. (2.7) an example of a hypergraph of seven qubits is given, associated with the hypergraph state

$$|H\rangle = Z_{125}Z_{23567}Z_{26}Z_{45}Z_{46}\,|+_2\rangle^{\otimes 7} = \sum_{ijklmno=0}^{1}\omega^{ijm}\omega^{jkmno}\omega^{jn}\omega^{lm}\omega^{ln}\,|ijklmno\rangle\,. \tag{2.124}$$

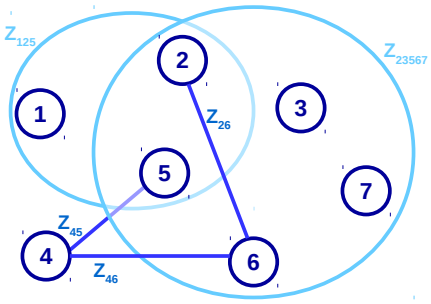

FIGURE 2.7: Qudit hypergraph of seven vertices.

Concerning LU-equivalence classes of hypergraph states, a rule for hypergraph states similar to the local complementation within the field of graph states was proposed in [43].[12] Furthermore, it can give useful insight to consider all hypergraph states which can be transformed into each other by application of local X-gates on a qubit. For example, in case of hypergraphs that have one big hyperedge connecting all vertices, successive application of Pauli-X on the participating qubits can generate arbitrary (hyper-)edges between any number of qubits.
The generalization of hypergraph states to arbitrary dimensions, i.e. *qudit* hypergraph states is a main topic of this thesis and will be presented in detail in Chapter 4.

2.5.3 One way quantum computer - a graph state application

Graph states are the resource for an important application of quantum phenomena paving the way to a quantum computer. Here, the key points regarding the mode of operation of a so-called *one way quantum computer* [133] are reviewed shortly. One way quantum computation is viewed as a basic and fundamental concept among the general idea referred to as *measurement based quantum computation*, which uses measurements rather than unitary transformations (as in quantum circuit models) as main computational force. Within a one-way quantum computer, a highly entangled graph state, to be more precise a two-dimensional *cluster state* [13], is used as initial resource state. By a sequence of measurements on single qubits within the lattice of the cluster along different measurement axis, it is possible to achieve universal quantum computation. That is, all qubit gates can be simulated by this method. The next measurement step, i.e. the next choice of measurement basis, within the sequence may be dependent on the measurement results of the foregoing one. For universality, e.g. the Hadamard gate (H), a single qubit rotation gate, the ($\frac{\pi}{8}$)-gate $R_Z(\frac{\pi}{4})$ and a CNOT-gate (controlled X-gate), are needed with:

$$H = \frac{1}{\sqrt{2}}\begin{pmatrix}1 & 1\\ 1 & -1\end{pmatrix}, \quad R_Z(\frac{\pi}{4}) = \begin{pmatrix}1 & 0\\ 0 & e^{\frac{i\pi}{4}}\end{pmatrix}, \quad CNOT = X_{12} = \begin{pmatrix}1 & 0 & 0 & 0\\ 0 & 1 & 0 & 0\\ 0 & 0 & 0 & 1\\ 0 & 0 & 1 & 0\end{pmatrix}. \quad (2.125)$$

[12] Note that in general the complementation of a hypergraph demands the presence of nonlocal gates. Though there are special configurations where all non-local gate chancel out and therefore the total operation can again be performed by exclusively local gates. (see [44] for examples)
[13] A cluster state is a special kind of graph state, where the vertices are arranged in a kind of lattice. In the one dimensional case these state are also called chain-graph states or linear cluster.

Whereas for realizing arbitrary one qubit gates, a linear cluster state is sufficient, realizing two qubit gates demands a two-dimensional arrangement of the cluster. The term *one-way* quantum computation pays respect to the nature of the computing process that results in the destruction of the resource state as any measurement disentangles the corresponding qubit on which it is preformed upon from the cluster. In Fig. (2.8) the schematic principle of a cluster state used for one way quantum computation is illustrated.

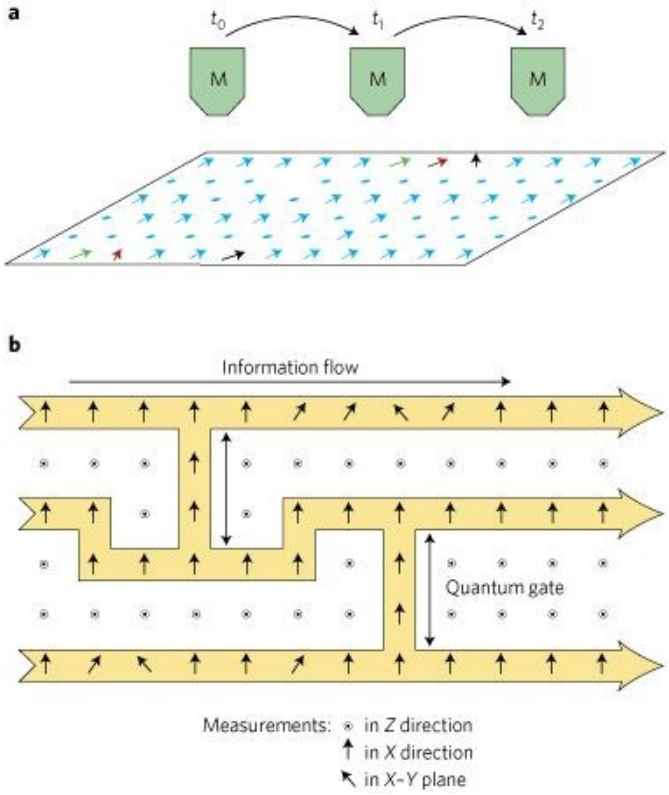

FIGURE 2.8: Schematic procedure of one way quantum computing [111]. (a): A sequence of adaptive one-qubit measurements M is implemented on certain qubits in the cluster state. (b): Within each step of the computation, the measurement bases depend on the utilized program (that is specified by the classical input) and on the outcomes of the previous measurements.

Chapter 3

Tensor witness

This chapters covers the first project of this thesis, the construction of a SLOCC-witness that is one-to-one correspondent to an associated entanglement witness in a Hilbert space of doubled dimensionality. Before presenting the main result in section 3.2, there will be a short introduction to semidefinite programming, which we used in context with the PPT-relaxation in the following parts of this chapter.

3.1 SDP - introduction

Within this section, we give a short introduction into the field of semidefinite programming [151]. In the field of convex optimization problems, semidefinite programming (SDP) is a subclass that seeks to optimize a linear function over the cone of positive semidefinite matrices. That is, an SDP can be seen as a generalization of a linear program where the inequality constraints are exchanged for semidefinite constraints on matrix variables. In its primal form, a semidefinite program for an optimization of a vector x can be written as

$$\begin{aligned} \min_x \quad & c^T x \equiv p \\ \text{subject to:} \quad & F(x) \geq 0, \\ & F_0 + \sum_{i=1}^{m} x_i F_i \geq 0 \end{aligned} \tag{3.1}$$

Here, the vector $c \in \mathbb{R}^m$ as well as the $(m+1)$ elements in the set $\{F_i\}$ of symmetric matrices with $F_i \in \mathbb{R}^n \times \mathbb{R}^n$ represent the data of the specific problem. The constraint $F(x) \geq 0$ ensures that $F(x)$ is positive semidefinite, i.e. for any vector $z \in \mathbb{R}^n$ $z^T F(x) z \geq 0$ holds. The optimization is performed over all vectors $x \in \mathbb{R}^m$. To any primal SDP, a dual problem of the following form can be constructed

$$\begin{aligned} \max_Z \quad & -\operatorname{Tr}(F_0 Z) \equiv d \\ \text{subject to:} \quad & \operatorname{Tr}(F_i Z) = c_i \quad \forall\ i\ \in [1, m] \\ & Z \geq 0 \end{aligned} \tag{3.2}$$

where now the optimization is performed over the cone of all positive semidefinite $n \times n$-matrices Z. The importance of the dual problem becomes clear when considering the implications of feasibility. Consider both, the primal and the dual problem to be feasible, i.e. there exists a solution to both, then $\min(p) \geq \max(d)$ which can be seen by calculating

$$
\begin{aligned}
p - d &= c^T x + \mathrm{Tr}(F_0 Z) = \mathrm{Tr}(cx^T) - \mathrm{Tr}(F_0 Z) = \mathrm{Tr}(cx^T + F_0 Z) \\
&= \sum_i c_i x_i + \mathrm{Tr}(F_0 Z) \overset{c_i = \mathrm{Tr}(F_i Z)}{=} \sum_i (\mathrm{Tr}(F_i Z) x_i + \mathrm{Tr}(F_0 Z)) \\
&= \mathrm{Tr}(\sum_i ([F_i x_i + F_0] Z)) \\
&= g \geq 0 \qquad\qquad \text{as: } F_0 + \sum_i F_i x_i \geq 0
\end{aligned}
\tag{3.3}
$$

Eq. (3.3) is the weak duality theorem and the value g of the difference is called duality gap. By this, one can see that the primal an the dual problems impose bounds on each other, if and only if feasibility is presumed. Concretely, the primal problem imposes an upper bound on the dual problem and the dual problem a lower bound on the primal one. In case $g = 0$, that is the primal and dual problem reach the same optimal value $p = d$, then we have strong duality. This is the case for strong feasibility for both, the primal and the dual problem, which means the semidefinite constrains become definite: $F(x) > 0$ and $Z > 0$.

3.2 Tensor witness

Witness operators serve as a prominent tool to detect entanglement or to distinguish among the equivalence classes under stochastic local operations assisted by classical communication (SLOCC) which represent different classes of entanglement. We show a one-to-one correspondence between SLOCC witnesses and entanglement witnesses in an extended Hilbert space for arbitrary multipartite systems. As a concrete application we use this relation to (re)derive the maximal squared overlap between a n-qubit GHZ state and an arbitrary state in the n-qubit W class. Possible issues and perspectives of the relaxation of the set of separable states to states with positive partial transpose for the construction of the considered type of entanglement witnesses are discussed. Considering $2 \times 3 \times 3$-dimensional systems we numerically evaluate the maximal squared overlap between the representative state of a SLOCC class and arbitrary states of another SLOCC class. This does not only provide information about the hierarchical structure of the SLOCC classes in such systems but also allows to construct projector-based SLOCC witnesses and (employing the relation shown in this work) entanglement witnesses for $4 \times 6 \times 6$-dimensional systems.

3.2.1 Introduction

Entanglement has proven to be an important resource for a vast field of applications and processes within quantum information theory. This includes the task of its characterization, to distinguish between principally different classes of entanglement, and its quantification. Entanglement is a resource if parties are spatially distributed and therefore restricted to local operations assisted by classical communication (LOCC). It can neither be generated nor increased by (deterministic) LOCC transformations. Hence, convertibility via LOCC imposes a partial order on the entanglement of the states. A sensible way to define entanglement classes for pure states is then their equivalence under Stochastic local operations assisted by classical communication (SLOCC). That is, an SLOCC-class is formed by those states that can be converted into each other via local operations and classical communication with non-zero probability of success [113]. SLOCC classes have been characterized for small system

sizes [113, 114, 115] and it has been shown that for multipartite systems there are finitely many SLOCC classes for tripartite systems with local dimensions of up to $2 \times 3 \times m$ (m arbitrary but finite) and infinitely many otherwise [116].

Another important problem in entanglement theory is the separability problem, i.e., the task to decide whether a given quantum state is entangled or separable. Even though several criteria have been found (see e.g. [117, 118, 119]), which can decide separability in many instances, the question whether a general multipartite mixed state is entangled or not, remains highly non-trivial. On the contrary, the separability problem has been proven to be computationally NP-hard [120].

One method to certify entanglement within a physical system is by using entanglement witnesses [121, 122]. An entanglement witness is a hermitian operator which has a positive expectation value for all product states but gives a negative value for at least one entangled state. In opposition to other criteria, one main advantage of witnesses lies in the fact that in principle no prior knowledge of the state is necessary as the certification is being done by measuring an accordingly constructed observable - the witness operator. A special type of witnesses are projector based witnesses of the form $W = \lambda \mathbb{1} - |\xi\rangle\langle\xi|$, with λ being the maximal squared overlap between the entangled state $|\xi\rangle$ and the set of all product states. Such projector based witnesses can also be used to distinguish between different SLOCC classes [123, 124]. In that case λ is the maximal squared overlap between a given state $|\xi\rangle$ in SLOCC-class $S_{|\xi\rangle}$ and the set of all states within another SLOCC class $S_{|\varphi\rangle}$. The witness then decides if for a given state $|\psi\rangle$ it is possible to be within $S_{|\varphi\rangle}$ or if it is definitely not an element of $S_{|\varphi\rangle}$. In this context it is important to note that without extensive knowledge about the hierarchic structure of SLOCC-classes in the respective system, it is not possible to draw any conclusions of $|\psi\rangle$ to be in class $S_{|\xi\rangle}$ upon measuring an negative expectation value or class $S_{|\varphi\rangle}$ in case of positive or zero value.

In this section, we establish an one-to-one correspondence between SLOCC-witnesses for multipartite systems of arbitrary dimension and entanglement witnesses within a higher (doubled) dimensional system built by two copies of the original one. This extends the results of [125] from the bipartite setting to the multipartite one. Such equivalence provides not only a deeper insight in the structure of SLOCC classes but enables to construct whole sets of entanglement witnesses for high dimensional systems from the SLOCC-structure of lower dimensions and vice versa. As such, from the solution for one problem, the solution to the related one readily follows.

The section is organized as follows. In Section 3.2.2, we will briefly revise the notion of SLOCC-operations, entanglement witnesses and SLOCC-witnesses. Section 3.2.3 will state the main result of our work, the one-to-one correspondence among entanglement-and SLOCC witnesses. Starting from the equation for the maximal overlap between two states under SLOCC this section will take the reader step by step through all key points of our method. Furthermore, as optimizing the overlap λ is in general a hard problem and as such often not feasible analytically, a possible relaxation of the set of separable states to states with positive partial transpose is discussed. Section 3.2.4 focuses on systems consisting of one qubit and two qutrits. Using numerical optimization, we find the maximal overlaps between all pairs of representative states of one SLOCC class and arbitrary states of another SLOCC class. The implications of these results for the hierarchic structure of SLOCC classes are then discussed. Section 3.2.5 concludes the section and provides an outlook.

3.2.2 Preliminaries

In this section the basic notions and definitions needed in the following sections of the chapter are briefly reviewed. We start with the notion of SLOCC equivalence of two states and then move on to the definition of entanglement witnesses. Finally, we will relate both concepts by recapitulating the notion of witness operators that are able to separate between different SLOCC classes.

SLOCC classes

As mentioned before two pure states are within the same SLOCC class if one can convert them into each other via LOCC with a non-zero probability of success. It can be shown that this implies the condition phrased in the following definition [113].

Definition 3.1. SLOCC-equivalence
Two n-partite pure quantum states $|\psi\rangle$, $|\varphi\rangle$ are equivalent under SLOCC if and only if there are matrices $\{A_i|\ \det(A_i) \neq 0;\ i \in [1,n]\}$ such that:

$$|\varphi\rangle = \bigotimes_{i=1}^{n} A_i |\psi\rangle \quad \text{and due to invertibility of all } A_i\text{:} \quad |\psi\rangle = \bigotimes_{i=1}^{n} A_i^{-1} |\varphi\rangle$$

That is, an SLOCC class - or orbit- includes all states that are related by local, invertible operators. To extend this definition to mixed states one defines the class $S_{|\Psi\rangle}$ (containing a representative state $|\Psi\rangle$) as those states that can be built as convex combinations of pure states within the SLOCC orbit of $|\Psi\rangle$ and of all pure states that can be approximated arbitrarily close by states within this orbit [123, 124].

Entanglement witnesses

An operator acting on a Hilbert space $\mathcal{H}$ that can be used to distinguish between different classes of entanglement is called a witness operator. A witness operator that can certify entanglement has to fulfill the following properties [121, 122]:

Definition 3.2. Entanglement witness
A hermitian operator W is an entanglement witness if and only if

$$\begin{aligned} \mathrm{tr}(\rho_s W) &\geq 0 && \text{for all separable states } \rho_s \\ \mathrm{tr}(\rho_e W) &< 0 && \text{for at least one entangled state } \rho_e \end{aligned}$$

holds.

Hence, W witnesses non-membership with respect to the convex set of separable states. If $\mathrm{tr}(\rho W) < 0$ for some state ρ, then W is said to detect ρ. A special class of witness operators are projector based witnesses. Their construction is based on the maximal value λ of the squared overlap between a given entangled state $|\psi\rangle$ with the set of all product states $\{|\psi_s\rangle\}$. More precisely, $W = \lambda \mathbb{1} - |\psi\rangle\langle\psi|$ with $|\psi\rangle$ being some entangled state and $\lambda = \sup_{\{|\psi_s\rangle\}} |\langle\psi|\psi_s\rangle|^2$ is a valid entanglement witness.

SLOCC witnesses

Based on the notion of projector based entanglement witnesses, one can generalize the idea and thereby construct an SLOCC witness. An SLOCC-witness then is an operator, which

can decide if for a given state $|\varphi\rangle$ it is possible to be an element of $S_{|\psi\rangle}$ with representative state $|\psi\rangle$ [123, 124].

Definition 3.3. SLOCC witness
A hermitian operator W is a $(|\varphi\rangle, S_{|\psi\rangle})$-SLOCC witness if and only if

$$\begin{aligned} \mathrm{tr}(|\eta\rangle\langle\eta| W) &\geq 0 \quad \text{for all states } |\eta\rangle \text{ in the SLOCC orbit of } |\psi\rangle \\ \mathrm{tr}(|\varphi\rangle\langle\varphi| W) &< 0 \quad \text{for at least one state } |\varphi\rangle \text{ not in the SLOCC orbit of } |\psi\rangle \end{aligned}$$

holds.

Thus W detects for $Tr(\rho W) < 0$ states that are not within $S_{|\psi\rangle}$. One can construct a $(|\varphi\rangle, S_{|\psi\rangle})$ SLOCC witness via $W = \lambda \mathbb{1} - |\varphi\rangle\langle\varphi|$, where λ denotes the maximal squared overlap between all states in the SLOCC class $S_{|\psi\rangle}$, that is $|\eta\rangle = \bigotimes_i A_i |\psi\rangle$ and the representative state $|\varphi\rangle$ of SLOCC class $S_{|\varphi\rangle}$, i.e. $\lambda = \sup_{|\eta\rangle} |\langle\varphi|\eta\rangle|^2$. A special class of witnesses are those verifying the Schmidt rank of a given pure state. As the Schmidt rank is an SLOCC- invariant, such witnesses are very useful to distinguish between SLOCC classes of bipartite systems and a one-to-one correspondence between Schmidt number witnesses and entanglement witnesses in an extended Hilbert space has been found [125]. In the next section we will show that in fact there is a one-to-one correspondence between SLOCC- and entanglement witnesses for arbitrary multipartite systems.

3.2.3 One-to-one correspondence between SLOCC- and entanglement witness

In the following we will show how to establish a one-to-one correspondence between SLOCC witnesses and entanglement witnesses within a higher dimensional Hilbert space for arbitrary multipartite systems. In order to improve readability, our method will be presented for the case of tripartite systems, however, the generalization to more parties is straightforward.

Let us start with formulating the problem as follows: Consider the pure state $|\psi\rangle$, which is a representative state of the SLOCC-class $S_{|\psi\rangle}$. Then all pure states, $|\eta\rangle$, within the SLOCC-orbit of $S_{|\psi\rangle}$ can be reached by applying local invertible operators A, B and C, that is $|\eta\rangle = A \otimes B \otimes C |\psi\rangle$. The aim will be to maximize the overlap between a given state $|\varphi\rangle$ and a pure state $|\eta\rangle$ within $S_{|\psi\rangle}$:

$$\sup_{|\eta\rangle \in S_{|\psi\rangle}} |\langle\varphi|\eta\rangle| = \sup_{A,B,C} \frac{|\langle\varphi|A \otimes B \otimes C|\psi\rangle|}{||A \otimes B \otimes C |\psi\rangle||} \tag{3.4}$$

Or stated differently, the quantity of interest is the minimal value λ, such that:

$$\sup_{A,B,C} \frac{|\langle\varphi|A \otimes B \otimes C|\psi\rangle|}{||A \otimes B \otimes C |\psi\rangle||} \leq \sqrt{\lambda} \tag{3.5}$$

It can easily be seen that this equation holds if and only if:

$$\begin{aligned} \lambda \langle\psi|A^\dagger A \otimes B^\dagger B \otimes C^\dagger C|\psi\rangle \\ - \langle\psi|A^\dagger B^\dagger C^\dagger |\varphi\rangle\langle\varphi| ABC|\psi\rangle \geq 0 \end{aligned} \tag{3.6}$$

One can then define an (witness-)operator $W = \lambda \mathbb{1} - |\varphi\rangle\langle\varphi|$ which, with the definition of $|\eta\rangle$ from before, satisfies:

$$\langle\eta|W|\eta\rangle \geq 0 \tag{3.7}$$

Thus, in case the maximal overlap between $|\varphi\rangle$ and $|\psi\rangle$ under SLOCC is smaller than one ($\lambda < 1$), which implies $|\varphi\rangle$ and $|\psi\rangle$ belong to different SLOCC-classes, the operator W is not positive semidefinite and is able to distinguish between the representative state of class $S_{|\varphi\rangle}$, that is $|\varphi\rangle$ and the SLOCC-class $S_{|\psi\rangle}$. It is hence a $(|\varphi\rangle, S_{|\psi\rangle})$ witness. It is important to note that whereas the witness enables a discrimination between the chosen representative state $|\varphi\rangle$ and $S_{|\psi\rangle}$, it is clearly not possible to distinguish all states within the SLOCC-orbit of $S_{|\varphi\rangle}$. Furthermore, note that the hierarchy of the SLOCC classes plays an important role here. If $S_{|\psi\rangle} \subset S_{|\varphi\rangle}$, then starting from $|\varphi\rangle$ it is possible to get arbitrary close to any state in $S_{|\psi\rangle}$ via SLOCC.

Let λ_{max} be the maximal overlap of $S_{|\psi\rangle}$ and $|\varphi\rangle$. Then, if $\lambda > \lambda_{max}$ (where λ is the maximal overlap between a given state $|\alpha\rangle$ and $|\varphi\rangle$ under SLOCC operations on $|\alpha\rangle$), one can exclude $|\alpha\rangle$ to be element of $S_{|\psi\rangle}$ but from $\lambda > \lambda_{max}$ it is not possible to deduce that $|\alpha\rangle$ is in $S_{|\varphi\rangle}$. This is due to the fact that there could be some intermediate class $S_{|\xi\rangle}$ (see Fig. 3.1).

Hence, one cannot obtain from this a finer distinction of classes in between $S_{|\varphi\rangle}$ and $S_{|\psi\rangle}$ as it does not provide the necessary information about the structure and depends on the exact geometrical position of the witness.

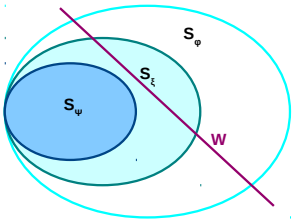

FIGURE 3.1: Witness that distinguishes $|\varphi\rangle \in S_{|\varphi\rangle}$ and $S_{|\psi\rangle}$ in case that some intermediate class $S_{|\xi\rangle}$ exists

In the next step, we establish a connection between the SLOCC-witness W and an entanglement witness $\widetilde{W}$ for a suitable extended system. More precisely, as stated in the following theorem, one can show that if Eq.(3.7) holds, then there exists an operator $\widetilde{W} = W \otimes |\psi^*\rangle\langle\psi^*|$, which is positive on all separable states $|\xi\rangle_{SEP}$ and vice versa.

Theorem 3.1. *The operator $W = \lambda\mathbb{1} - |\varphi\rangle\langle\varphi|$ is a $(|\varphi\rangle, S_{|\psi\rangle})$-SLOCC witness, if and only if the corresponding operator $\widetilde{W} = W \otimes |\psi^*\rangle\langle\psi^*|$ is an entanglement witness with respect to the split $(A_1A_2|B_1B_2|C_1C_2)$:*

$$\langle\eta|W|\eta\rangle \geq 0 \quad \Leftrightarrow \quad \langle\xi_{SEP}|\widetilde{W}|\xi_{SEP}\rangle \geq 0 \tag{3.8}$$

where $|\xi_{SEP}\rangle$ are product states within an enlarged system consisting of two copies of each original system, that is they are of the form $|\xi_{SEP}\rangle = |\xi_{A_1A_2}\rangle \otimes |\xi_{B_1B_2}\rangle \otimes |\xi_{C_1C_2}\rangle$ and $|\eta\rangle \in S_{|\psi\rangle}$.

Proof. The "only if" part("$\Longrightarrow$") of the proof can be shown as follows:
We will use that one can always write the witness operator W in some diagonal basis, i.e. $W = \sum_n \lambda_n |\alpha^n\rangle\langle\alpha^n|$, and therefore (neglecting normalization and with the definition of $|\eta\rangle$

from before)

$$\langle\eta|W|\eta\rangle = \sum_n \lambda_n |\langle\psi|A^\dagger \otimes B^\dagger \otimes C^\dagger|\alpha^n\rangle|^2 \geq 0. \tag{3.9}$$

Moreover, it holds that

$$\langle\psi|A^\dagger \otimes B^\dagger \otimes C^\dagger|\alpha_n\rangle = \mathrm{tr}(A^\dagger \otimes B^\dagger \otimes C^\dagger |\alpha_n\rangle\langle\psi|). \tag{3.10}$$

Using then the following representation of the SLOCC operations A, B, C and the state $|\psi\rangle$, rewritten as $A = \sum_{ij} A_{ij}|i\rangle\langle j|$, $B = \sum_{i'j'} B_{i'j'}|i'\rangle\langle j'|$, $C = \sum_{i''j''} C_{i''j''}|i''\rangle\langle j''|$,$|\alpha^n\rangle = \sum_{kk'k''} \alpha^n_{kk'k''}|kk'k''\rangle$ and $|\psi\rangle = \sum_{ll'l''}\psi_{ll'l''}|ll'l''\rangle$, one can rewrite each summand in Eq. (3.9) via

$$\begin{aligned}
\mathrm{tr}(A^\dagger \otimes B^\dagger \otimes C^\dagger |\alpha^n\rangle\langle\psi|) &= A^*_{ij}B^*_{i'j'}C^*_{i''j''}\alpha^n_{ii'i''}\psi^*_{jj'j''} \\
&= A^*_{ij}B^*_{i'j'}C^*_{i''j''}\alpha^n_{ii'i''}\psi^*_{jj'j''}(\langle ii'i''|\otimes\langle jj'j''|)(|ii'i''\rangle\otimes|jj'j''\rangle) \\
&\equiv \langle\langle A_{12}\otimes B_{12}\otimes C_{12}|\alpha^n_1,\psi^*_2\rangle\rangle \qquad (3.11)
\end{aligned}$$

and in the same way:

$$\mathrm{tr}(|\psi\rangle\langle\alpha^n| A\otimes B\otimes C) \equiv \langle\langle\alpha^n_1,\psi^*_2|A_{12}\otimes B_{12}\otimes C_{12}\rangle\rangle \tag{3.12}$$

where here and in the following the ket-vectors $|Y_{12}\rangle\rangle = \sum_{ij} Y_{ij}|ij\rangle = (Y\otimes\mathbb{1})|\Phi^+\rangle$ with $|\Phi^+\rangle = \sum_{i=0}^{\dim[\mathcal{H}(Y_1)]-1}|ii\rangle$ are elements of the two-copy Hilbert space of the first subsystem, that is $\mathcal{H}(Y_1)\otimes\mathcal{H}(Y_2)$ for $Y\in\{A,B,C\}$. Thus, Eq.(3.9) can now be written as

$$\begin{aligned}
\langle\langle A_{12}\otimes B_{12}\otimes C_{12}|\, X_1\otimes(|\psi^*\rangle\langle\psi^*|)_2\,|A_{12}\otimes B_{12}\otimes C_{12}\rangle\rangle \\
\geq 0.
\end{aligned} \tag{3.13}$$

Note that the operators A, B and C leading to the states $|\xi_{SEP}\rangle = \bigotimes_{Y=A,B,C}|Y_{12}\rangle\rangle$ with $|Y_{12}\rangle = (Y\otimes\mathbb{1})|\Phi^+\rangle$ in the equation above are invertible. Note further that any state in $\mathcal{H}(Y_1)\otimes\mathcal{H}(Y_2)$ can be written as $|Y_{12}\rangle = (Y\otimes\mathbb{1})|\Phi^+\rangle$, however, Y might be not invertible. It hence remains to show that the equation above holds true also for states $|\xi_{SEP}\rangle$ whose structure corresponds to some non-invertible matrix Y. In order to do so, it is sufficient to show that for such states $|\xi_{SEP}\rangle$ there always exists an invertible $|\xi'_{SEP}\rangle$ for which the expectation value of $X_1\otimes(|\psi^*\rangle\langle\psi^*|)_2$ is arbitrarily close. Making use of the singular value decomposition, one finds that for each $Y = UDV$ that is non-invertible, there exists an invertible $Y' = UD'V$ for which the entries of D' are arbitrary close to those of D. As the expectation value of $X_1\otimes(|\psi^*\rangle\langle\psi^*|)_2$ is a continuous (polynomial) function in the entries of D [1]. This shows that Eq. (3.13) has to hold true for an arbitrary product state $|\xi_{SEP}\rangle$. Let us finally note that it is straightforward to see that if W is not positive semidefinite ($\lambda<1$) then $\widetilde{W} = W\otimes|\psi^*\rangle\langle\psi^*|$ is not positive semidefinite as well which completes the "only if" part of Theorem 3.1.

In order to see that the "if" part of theorem ($\Longleftarrow$) holds true first recall that any state in $\mathcal{H}(Y_1)\otimes\mathcal{H}(Y_2)$ can be written as $|Y_{12}\rangle = (Y\otimes\mathbb{1})|\Phi^+\rangle$. Using then the relations in Eqs. (3.11) and (3.12) and that $\widetilde{W} = W\otimes|\psi^*\rangle\langle\psi^*|$ being not positive semidefinite implies that W is not positive semidefinite the "if" part readily follows.

With this we have shown a one-to-one correspondence between W as SLOCC-witness and $\widetilde{W}$ as entanglement witness which completes the proof of Theorem 3.1. □

[1] Note that we do not assume here that the states are normalized.

In addition to etablishing a connection between the SLOCC-witness W acting on the Hilbert space $\mathcal{H}$ and the entanglement witness $\widetilde{W}$ operating on an enlarged Hilbert space $\widetilde{\mathcal{H}} = \mathcal{H} \otimes \mathcal{H}$, Theorem 3.1 provides the possibility to consider the problem of maximizing the overlap of two states under SLOCC from a different perspective. That is, by solving the problem of finding the minimal value of λ, for which $\widetilde{W} = (\lambda \mathbb{1} - |\varphi\rangle\langle\varphi|) \otimes |\psi^*\rangle\langle\psi^*|$ is an entanglement witness for the respective partition, we likewise have found the value of the maximal overlap between $|\varphi\rangle$ and $|\psi\rangle$ under SLOCC-operations. In order to provide a concrete application of Theorem 3.1, we derived the maximal squared overlap between a n-qubit GHZ state and an arbitrary state in the n-qubit W class using the relation derived above (see Section 3.2.6) which is shown to be $3/4$ for $n = 3$ (see also [123]) and $1/2$ for $n \geq 4$ [2]. Note that the separability problem as well as the problem of deciding whether two tripartite states are within the same SLOCC class are both computationally highly non-trivial. In fact, they were shown to be NP-hard [120, 126]. In the following section we will discuss the relaxation of the set of separable states to states having a positive partial transpose for the construction of entanglement witnesses of the form $\widetilde{W} = (\lambda \mathbb{1} - |\varphi\rangle\langle\varphi|) \otimes |\psi^*\rangle\langle\psi^*|$.

PPT-relaxation

In general it can be very difficult to find an analytical solution for the minimal value of λ such that the expectation value of $\widetilde{W}$ is positive on all product states $|\xi_{SEP}\rangle$. To circumvent this problem without resorting to numerical optimization protocols, one can try to broaden the restrictions on the set of states on which $\widetilde{W}$ is positive in a way that the new set naturally includes the original set of separable states. One way to do this would be to demand that $\widetilde{W}$ is positive on the whole set of states which have positive partial transposition (are PPT) with respect to all subsystems in the considered bipartite splittings, i.e.,

$$\begin{aligned} \mathrm{tr}(\rho\widetilde{W}) = \mathrm{tr}(\rho(W \otimes |\psi^*\rangle\langle\psi^*|)) \geq 0 \\ \forall\ \rho_{A_{12}B_{12}C_{12}} \quad with: \ \rho^{T_{Y_{12}}} \geq 0,\ Y = \{A, B, C\}. \end{aligned} \tag{3.14}$$

Though the set of PPT-states is known to include PPT-entangled states, this relaxation of the initial conditions offers an advantage, as we are now able to formulate the problem of minimizing λ as a semi-definite program and as such provides a way for an analytical result:

$$\begin{aligned} \text{minimize} \quad & \mathrm{tr}(\rho\widetilde{W}) \\ \text{subject to} \quad & \rho \geq 0, \\ & \rho^{T_i} \geq 0, \quad i = A, B, C \end{aligned} \tag{3.15}$$

It should, however, be noted that states of the form

$$\begin{aligned} \sigma_p(|\phi\rangle, |\psi^*\rangle) = \tfrac{1-p}{(d_1-1)(d_2-1)} (\mathbb{1}_1 - |\phi\rangle_1\langle\phi|) \otimes (\mathbb{1}_2 - |\psi^*\rangle_2\langle\psi^*|) \\ + p\,|\phi\rangle_1\langle\phi| \otimes |\psi^*\rangle_2\langle\psi^*|, \end{aligned} \tag{3.16}$$

are in general PPT-entangled (with respect to bipartite splittings $\Gamma_1\Gamma_2|A_1A_2\ldots Z_1Z_2$ with $\Gamma \in \{A, \ldots, Z\}$) for a suitable choice of $1 > p > 0$ [128]. More precisely, it has been shown in [128] if for a considered bipartition $\Gamma_1\Gamma_2|A_1A_2\ldots Z_1Z_2$ the Schmidt coefficient of $|\phi\rangle$ and $|\psi^*\rangle$ do not coincide and neither of the two states is separable with respect to

[2] For 4-qubit states this value has been already found in [124].

that splitting, then the state $\sigma_p(|\phi\rangle, |\psi^*\rangle)$ with a suitable choice of $1 > p > 0$ is positive under the partial transpose with respect to subsystems $\Gamma_1\Gamma_2$, but it is not separable with respect to the considered splitting. Note that states of the form given in Eq. (3.16) lead to $\mathrm{tr}\{(\lambda\mathbb{1}_1 - |\phi\rangle_1\langle\phi|) \otimes |\psi^*\rangle_2\langle\psi^*|)\sigma_p(|\phi\rangle, |\psi^*\rangle)\} < 0$ for any $\lambda < 1$. Hence, the relaxation to states that are PPT does not allow to determine possible values of λ for which $\widetilde{W}$ (with the above mentioned conditions on $|\phi\rangle$ and $|\psi^*\rangle$) is an entanglement witness. However, note that considering other relaxations of the set of separable states might provide a way to estimate the maximal SLOCC overlap using a semi-definite program. Note further that if the Schmidt coefficients of $|\phi\rangle$ and $|\psi^*\rangle$ coincide for at least one bipartite splitting, using the relaxation to PPT-states, one still might be able to provide a non-trivial upper bound on λ using the semidefinite program specified above.

Let us finally mention that in [128] operators of the form $(\lambda\mathbb{1} - |\phi\rangle\langle\phi|)_1 \otimes (|\psi^*\rangle\langle\psi^*|)_2$ with an appropriate choice of λ have been shown to be bipartite entanglement witnesses for the case where the local Schmidt rank of $|\psi^*\rangle$ is smaller than the Schmidt rank of $|\phi\rangle$ for the considered bipartite splitting. This can be easily understood using our result (see also [125]) as in this case $|\phi\rangle$ and $|\psi\rangle$ are in different bipartite SLOCC classes and $|\phi\rangle$ cannot be approximated arbitrarily close by a state in the SLOCC class of $|\psi\rangle$.

3.2.4 Numerical values for $2 \times 3 \times 3$

Systems consisting of one qubit, one qutrit and one system of arbitrary dimension mark the last cases, which still have a finite number of SLOCC-classes. For one qubit and two qutrits there are 17 different classes with 12 of these being truly tripartite entangled and six of them containing full-rank entangled states [116]. Finding the maximal overlap of the representative states of the different classes not only indicates towards a hierarchy among them but, as shown in Section 3.2.3, can give insight in the entanglement properties of states in an enlarged (two-copy) system. To be precise, by evaluating $\lambda_{max}(|\psi_n\rangle, S_{|\psi_m\rangle})$, in addition to the SLOCC-witness for $(|\psi_n\rangle, S_{|\psi_m\rangle})$, $W = \lambda_{max}(|\psi_n\rangle, S_{|\psi_m\rangle})\mathbb{1} - |\psi_n\rangle\langle\psi_n|$ with $\langle\kappa|W|\kappa\rangle \geq 0$ for all $|\kappa\rangle$ in $S_{|\psi_m\rangle}$ and lower classes, one can construct an entanglement witness, $\widetilde{W} = W \otimes |\psi_m^*\rangle\langle\psi_m^*|$ which detects entanglement within states of dimension $4 \times 6 \times 6$, that is $\langle\xi|\widetilde{W}|\xi\rangle \geq 0$ for all separable $|\xi\rangle = |\xi_{A_1A_2}\rangle \otimes |\xi_{B_1B_2}\rangle \otimes |\xi_{C_1C_2}\rangle$. Thus, for all pairs of representatives and SLOCC classes where $\lambda_{max} \neq 1$ one can construct a specific $\widetilde{W}$. The unnormalized representative states of the SLOCC classes (not including the (bi-)separable classes) within a $2 \times 3 \times 3$ system are [116],(see also Appendix A)

$$
\begin{aligned}
|\psi_6\rangle &= |000\rangle + |111\rangle \\
|\psi_7\rangle &= |000\rangle + |011\rangle + |101\rangle \\
|\psi_8\rangle &= |000\rangle + |011\rangle + |102\rangle \\
|\psi_9\rangle &= |000\rangle + |011\rangle + |120\rangle \\
|\psi_{10}\rangle &= |000\rangle + |011\rangle + |122\rangle \\
|\psi_{11}\rangle &= |000\rangle + |011\rangle + |101\rangle + |112\rangle \\
|\psi_{12}\rangle &= |000\rangle + |011\rangle + |110\rangle + |121\rangle \\
|\psi_{13}\rangle &= |000\rangle + |011\rangle + |102\rangle + |120\rangle \\
|\psi_{14}\rangle &= |000\rangle + |011\rangle + |112\rangle + |120\rangle \\
|\psi_{15}\rangle &= |000\rangle + |011\rangle + |100\rangle + |122\rangle \\
|\psi_{16}\rangle &= |000\rangle + |011\rangle + |022\rangle + |101\rangle \\
|\psi_{17}\rangle &= |000\rangle + |011\rangle + |022\rangle + |101\rangle + |112\rangle\,.
\end{aligned}
\tag{3.17}
$$

The values of the numerical maximization of the SLOCC-overlap for the different SLOCC classes with respect to the representative states from above is given in the following cross table: Note, that we rely on numerical precission of 10^{-12}.

from \ to	$\|\psi_6\rangle$	$\|\psi_7\rangle$	$\|\psi_8\rangle$	$\|\psi_9\rangle$	$\|\psi_{10}\rangle$	$\|\psi_{11}\rangle$	$\|\psi_{12}\rangle$	$\|\psi_{13}\rangle$	$\|\psi_{14}\rangle$	$\|\psi_{15}\rangle$	$\|\psi_{16}\rangle$	$\|\psi_{17}\rangle$
$\|\psi_6\rangle$	1	1	$\frac{2}{3}$	$\frac{2}{3}$	$\frac{2}{3}$	$\frac{3}{4}$	$\frac{3}{4}$	$\frac{3}{4}$	0,5625	$\frac{3}{4}$	$\frac{3}{4}$	0,65
$\|\psi_7\rangle$	$\frac{3}{4}$	1	$\frac{2}{3}$	$\frac{2}{3}$	$\frac{2}{3}$	$\frac{3}{4}$	$\frac{3}{4}$	0,5433	0,5625	0,7	$\frac{3}{4}$	0,6129
$\|\psi_8\rangle$	1	1	1	$\frac{2}{3}$	$\frac{2}{3}$	0,875	$\frac{3}{4}$	$\frac{3}{4}$	$\frac{3}{4}$	$\frac{3}{4}$	$\frac{3}{4}$	0,7252
$\|\psi_9\rangle$	1	1	$\frac{2}{3}$	1	$\frac{2}{3}$	$\frac{3}{4}$	0,875	$\frac{3}{4}$	$\frac{3}{4}$	$\frac{3}{4}$	$\frac{3}{4}$	0,7252
$\|\psi_{10}\rangle$	1	1	1	1	1	0,875	0,875	0.8333	$\frac{3}{4}$	0,9045	1	0,7955
$\|\psi_{11}\rangle$	1	1	1	$\frac{2}{3}$	$\frac{2}{3}$	1	$\frac{3}{4}$	$\frac{3}{4}$	$\frac{3}{4}$	$\frac{3}{4}$	$\frac{3}{4}$	0,8
$\|\psi_{12}\rangle$	1	1	$\frac{2}{3}$	1	$\frac{2}{3}$	$\frac{3}{4}$	1	$\frac{3}{4}$	$\frac{3}{4}$	$\frac{3}{4}$	$\frac{3}{4}$	0,8
$\|\psi_{13}\rangle$	1	1	1	1	0,8333	1	1	1	1	0,95	1	1
$\|\psi_{14}\rangle$	1	1	1	1	$\frac{2}{3}$	0,875	0,875	0,8125	1	$\frac{3}{4}$	$\frac{3}{4}$	0,8
$\|\psi_{15}\rangle$	1	1	1	1	1	1	1	1	1	1	1	1
$\|\psi_{16}\rangle$	1	1	1	1	0,7357	0,875	0,875	0,7706	$\frac{3}{4}$	$\frac{3}{4}$	1	0,8
$\|\psi_{17}\rangle$	1	1	1	1	0,795	1	1	0,8958	1	0,875	1	1

TABLE 3.1: Numerical values for the maximal squared overlap $\alpha = |\langle\psi_i|\psi_j\rangle|^2$ for $i, j \in [6, 17]$. Here, $|\psi_i\rangle$ (column) denotes the initial state (representative state of SLOCC class $S_{|\psi_i\rangle}$), which, under application of SLOCC operations, can be transformed to the final state $|\psi_j\rangle$ (representative state of SLOCC class $S_{|\psi_j\rangle}$ (row) with probability accordingly to α.

From Table 3.1, we can deduce a hierarchy of SLOCC classes, illustrated in Fig. 3.2.

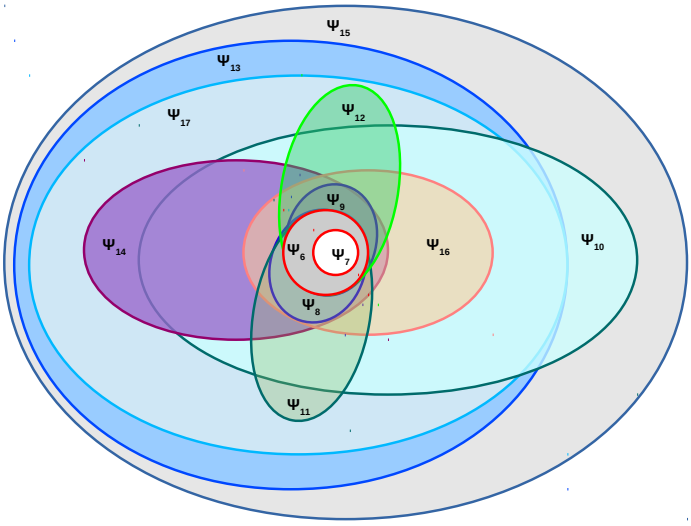

FIGURE 3.2: Hierarchic structure of SLOCC-classes within a $2 \times 3 \times 3$ system. If the orbit of one class is completely within the orbit of another one, all states belonging to the class of the inner orbit can be reached by the representative state of the class of the outer orbit via SLOCC with probability numerically close to one. Furthermore, if a state ρ can be found outside the SLOCC- orbit of a certain state, one needs terms proportional to the representative state of the respective outer orbit to construct this state. As can be seen from Table (3.1), $|\psi_{15}\rangle$ is the most powerful class in the sense that any other state $|\psi_i\rangle$ with $6 \leq i \leq 16$ can be reached from $|\psi_{15}\rangle$ via SLOCC operation with certainty, that is $\alpha = 1$ within the numerical limits.

3.2.5 Conclusions

For arbitrary numbers of parties and local (finite) dimensions we showed a one-to-one correspondence between an operator W able to distinguish between different SLOCC classes of a system and another operator $\widetilde{W}$ that detects entanglement within a system which consists of two copies of the original system. This correspondence thereby enables us to directly transfer a solution for one problem to the other. Though the relaxation to PPT-states in order to construct the entanglement witness did not prove to be helpful for reasons stated in Section 3.2.3, it very well might be that other possible relaxations on the set of separable states will give more insight and a good approximation for an upper bound on the maximal overlap. As an concrete application of the presented relation we derived the maximal overlap between the n-qubit GHZ state and states within the n- qubit W class. The numerical calculations in section IV for the qubit-qutrit-qutrit system do not only indicate a hierarchy among the SLOCC classes but also provides us with the option to construct a whole set of entanglement witnesses for the doubled system of dimensions $4 \times 6 \times 6$.

3.2.6 Appendix

Example

In this Appendix we will provide an example of how the relation among SLOCC witnesses and EWs can be employed and compute the maximal squared overlap between the GHZ-state of n-qubits, $|GHZ_n\rangle = 1/\sqrt{2}(|00\ldots0\rangle + |11\ldots1\rangle$, and a normalized n-qubit state in the W-class (with representative $|W_n\rangle = 1/\sqrt{n}(|10\ldots0\rangle + |010\ldots0\rangle + \ldots + |0\ldots010\rangle + |0\ldots01\rangle)$). We show that for $n = 3$ the maximal squared overlap is given by $\frac{3}{4}$ (see also [123]), whereas for $n \geq 4$ it is given by $\frac{1}{2}$ [2].

In order to do so we consider $\mathcal{W}_n = (\lambda_n \mathbb{1} - |GHZ_n\rangle\langle GHZ_n|) \otimes |W_n\rangle\langle W_n|$ and show that it is an EW (for $2n$-qubit states) with respect to the splitting $(A_1A_2|B_1B_2|C_1C_2|\ldots|Z_1Z_2)$ iff $1 > \lambda_3 \geq \frac{3}{4} \equiv \lambda_3^C$ and $1 > \lambda_n \geq \frac{1}{2} \equiv \lambda_n^C$ for $n \geq 4$. Using Theorem 3.1 this implies that $\langle \Psi_W^n | (\lambda_n \mathbb{1} - |GHZ_n\rangle\langle GHZ_n|) |\Psi_W^n\rangle \geq 0$, where $|\Psi_W^n\rangle$ denotes a normalized state in the n-qubit W-class, iff $1 > \lambda_n \geq \lambda_n^C$. Recall that $\langle \Psi_W^n | (\lambda_n \mathbb{1} - |GHZ_n\rangle\langle GHZ_n|) |\Psi_W^n\rangle \geq 0$ is equivalent to $\lambda_n \geq |\langle GHZ_n|\Psi_W^n\rangle|^2$ and therefore the maximal squared overlap is given by λ_n^C.

Before considering the problem of finding the range of λ for which $\mathcal{W}_n$ is an EW let us first present a parametrization of states in the W-class that will be convenient for our purpose and then relate it to the parametrization of product states that have to be considered. It is well known that any state in the W-class [3] can be written as [113] $\bigotimes_i U_i(x_0|00\ldots0\rangle + x_1|10\ldots0\rangle + x_2|010\ldots0\rangle + \ldots + x_{n-1}|0\ldots010\rangle + x_n|0\ldots01\rangle)$ with $x_0 \geq 0$, $x_i > 0$ for $i \in \{1,\ldots,n\}$ and U_i unitary or equivalently as $U_1D_1 \otimes U_2D_2 \otimes \ldots \otimes U_{n-2}D_{n-2} \otimes U_{n-1}g_{n-1} \otimes U_nD_n|W_n\rangle$ where $D_i = \mathrm{diag}\,(1, \tilde{x}_i)$ with $\tilde{x}_i = x_i/x_n > 0$ and

$$g_{n-1} = \begin{pmatrix} x_n & x_0 \\ 0 & x_{n-1} \end{pmatrix}. \tag{3.18}$$

For the local unitaries we will use the parametrization $U_i = U_{ph}(\gamma_i)X(\alpha_i)U_{ph}(\beta_i)$ with $X(\delta) = e^{i\delta X}$, $U_{ph}(\delta) = \mathrm{diag}\,(1, e^{i\delta})$ and $\alpha_i, \beta_i, \gamma_i \in \mathbb{R}$. In order to simplify our argumentation we will use that $\otimes_i U_{ph}(\delta)|W_n\rangle = e^{i\delta}|W_n\rangle$ and choose $\beta_n = 0$, $\beta_i = \beta_i - \beta_n$ for

[3] Note that we will consider unnormalized states.

$i \in \{1,\dots,n-2\}$ and $x_j = x_j e^{-i\beta_n}$ for $j = 0, n-1$. Using that $(U_{ph}(\delta_1) \otimes U_{ph}(\delta_2) \otimes \dots \otimes U_{ph}(\delta_{n-2}) \otimes U_{ph}(-\sum_{i\in I_0}\delta_i) \otimes U_{ph}(\delta_n)\,|GHZ_n\rangle = |GHZ_n\rangle$ where here and in the following $I_0 = \{1,2,\dots,n-2,n\}$ one can easily see that when computing the maximal SLOCC overlap between the GHZ state and a W-class state one can equivalently choose $\gamma_i = 0$ for $i \in I_0$ and $\gamma_{n-1} = \sum_{i=1}^{n}\gamma_i$.

We will now make use of the fact that $\langle\eta|\,(\lambda_n \mathbb{1} - |GHZ_n\rangle\langle GHZ_n|)\,|\eta\rangle \geq 0$ for $|\eta\rangle = A\otimes B\otimes \dots \otimes Z\,|W_n\rangle$ iff $\langle\xi_{SEP}|\,[\lambda_n\mathbb{1} - (|GHZ_n\rangle\langle GHZ_n|)_1] \otimes (|W_n\rangle\langle W_n|)_2\,|\xi_{SEP}\rangle \geq 0$ for $|\xi_{SEP}\rangle = |A_{12}\rangle\otimes|B_{12}\rangle\otimes\dots|Z_{12}\rangle$ with $|\Gamma_{12}\rangle = (\Gamma_1\otimes\mathbb{1}_2)\,|\Phi^+\rangle$, $\Gamma \in \{A,B,\dots Z\}$ and $|\Phi^+\rangle = \sum_{i=0}^{1}|ii\rangle$ (see proof of Theorem 3.1). As any state in the W-class can be parametrized as explained above we only have to consider product states of the form $|\xi_{SEP}\rangle = \otimes_{i=1}^{n}|\phi_i\rangle$ with $|\phi_i\rangle = (U_iD_i\otimes\mathbb{1})\,|\Phi^+\rangle = (U_i\otimes\mathbb{1})(|00\rangle + \tilde{x}_i\,|11\rangle)$ for $i\in I_0$ and $|\phi_{n-1}\rangle = (U_{n-1}g_{n-1}\otimes\mathbb{1})\,|\Phi^+\rangle$ [4]. Note that $\langle\xi_{SEP}|\,\mathcal{W}_n\,|\xi_{SEP}\rangle \geq 0$ for all $|\xi_{SEP}\rangle$ as defined above iff $\tilde{w}_n \equiv \langle\zeta_{SEP}|\,\mathcal{W}_n\,|\zeta_{SEP}\rangle \geq 0$, that is $\tilde{w}_n$ is positive semidefinite, for all $|\zeta_{SEP}\rangle = \otimes_{i\in I_0}|\phi_i\rangle$ with $|\phi_i\rangle$ as defined above. This is due to the fact that the parameters of $|\zeta_{SEP}\rangle$ and $|\phi_{n-1}\rangle$ can be chosen independently and $|\phi_{n-1}\rangle$ is an arbitrary state. One obtains for the respective terms of $\tilde{w}_n$ that

$$\langle\zeta_{SEP}|\,[\mathbb{1}_1\otimes(|W_n\rangle\langle W_n|)_2]\,|\zeta_{SEP}\rangle = \frac{1}{n}\mathbb{1}_{\Gamma_1}\otimes[\mathbb{1}_{\Gamma_2} + \sum_{i=1}^{n-2}\tilde{x}_i^2(|0\rangle\langle 0|)_{\Gamma_2}], \tag{3.19}$$

where Γ refers to party $n-1$ and $\langle\zeta_{SEP}|\,(|GHZ_n\rangle\langle GHZ_n|)_1\otimes(|W_n\rangle\langle W_n|)_2\,|\zeta_{SEP}\rangle = (|\varphi\rangle\langle\varphi|)_{\Gamma_1\Gamma_2}$ with

$$\begin{aligned}|\varphi\rangle_{\Gamma_1\Gamma_2} &= \tfrac{1}{\sqrt{2n}}\{[\textstyle\sum_{j\in I_0}(-i\sin(\alpha_j)\tilde{x}_j e^{-i\beta_j}\prod_{k\in I_0\setminus\{j\}}\cos(\alpha_k))\,|0\rangle_{\Gamma_1}\\ &+\textstyle\sum_{j\in I_0}(\cos(\alpha_j)\tilde{x}_j e^{-i\beta_j}\prod_{k\in I_0\setminus\{j\}}(-i\sin(\alpha_k)))\,|1\rangle_{\Gamma_1}]\otimes|0\rangle_{\Gamma_2}\\ &+[\textstyle\prod_{j\in I_0}\cos(\alpha_j)\,|0\rangle_{\Gamma_1} + \prod_{j\in I_0}(-i\sin(\alpha_j))\,|1\rangle_{\Gamma_1})]\otimes|1\rangle_{\Gamma_2}\}\\ &\equiv |\varphi_0\rangle_{\Gamma_1}|0\rangle_{\Gamma_2} + |\varphi_1\rangle_{\Gamma_1}|1\rangle_{\Gamma_2}\,.\end{aligned} \tag{3.20}$$

Hence, we have that $\tilde{w}_n = \frac{\lambda_n}{n}\mathbb{1}_{\Gamma_1}\otimes[\mathbb{1}_{\Gamma_2} + \sum_{i=1}^{n-2}\tilde{x}_i^2(|0\rangle\langle 0|)_{\Gamma_2}] - (|\varphi\rangle\langle\varphi|)_{\Gamma_1\Gamma_2}$. Defining $\mu = ||\varphi_0||$ and $\nu = ||\varphi_1||$ we can write $|\varphi\rangle = \mu\,|\Phi_0\rangle_{\Gamma_1}|0\rangle_{\Gamma_2} + \nu\,|\Phi_1\rangle_{\Gamma_1}|1\rangle_{\Gamma_2}$ where $||\Phi_i|| = 1$. We construct now the following orthonormal basis

$$|\Psi_0\rangle = \tfrac{\mu}{\sqrt{\mu^2+\nu^2}}\,|\Phi_0\rangle_{\Gamma_1}|0\rangle_{\Gamma_2} + \tfrac{\nu}{\sqrt{\mu^2+\nu^2}}\,|\Phi_1\rangle_{\Gamma_1}|1\rangle_{\Gamma_2} \tag{3.21}$$

$$|\Psi_1\rangle = \tfrac{\nu}{\sqrt{\mu^2+\nu^2}}\,|\Phi_0\rangle_{\Gamma_1}|0\rangle_{\Gamma_2} - \tfrac{\mu}{\sqrt{\mu^2+\nu^2}}\,|\Phi_1\rangle_{\Gamma_1}|1\rangle_{\Gamma_2} \tag{3.22}$$

$$|\Psi_2\rangle = |\Phi_0^{\perp}\rangle_{\Gamma_1}|0\rangle_{\Gamma_2} \tag{3.23}$$

$$|\Psi_3\rangle = |\Phi_1^{\perp}\rangle_{\Gamma_1}|1\rangle_{\Gamma_2}\,, \tag{3.24}$$

where $\langle\Phi_i|\Phi_i^{\perp}\rangle = 0$ for $i\in\{0,1\}$. It can be easily seen that $\tilde{w}_n = \sum_{i,j=0}^{1}\Lambda_{ij}\,|\Psi_i\rangle\langle\Psi_j| + \frac{\lambda_n}{n}(1+\sum_{i=1}^{n-2}\tilde{x}_i^2)\,|\Psi_2\rangle\langle\Psi_2| + \frac{\lambda_n}{n}\,|\Psi_3\rangle\langle\Psi_3|$ with

$$\Lambda = \begin{pmatrix} \frac{\lambda_n}{n}(1+\sum_{i=1}^{n-2}\tilde{x}_i^2\frac{\mu^2}{\mu^2+\nu^2}) - (\mu^2+\nu^2) & \sum_{i=1}^{n-2}\tilde{x}_i^2\frac{\lambda_n\mu\nu}{n(\mu^2+\nu^2)} \\ \sum_{i=1}^{n-2}\tilde{x}_i^2\frac{\lambda_n\mu\nu}{n(\mu^2+\nu^2)} & \frac{\lambda_n}{n}(1+\sum_{i=1}^{n-2}\tilde{x}_i^2\frac{\nu^2}{\mu^2+\nu^2}) \end{pmatrix}. \tag{3.25}$$

Note that as we consider the case $\lambda_n > 0$ (otherwise $\mathcal{W}_n \leq 0$ which implies that it cannot be an EW) and as $\tilde{x}_i \in R$ we have that $\tilde{w}_n \geq 0$ iff $\Lambda \geq 0$. In order to determine for which values of

[4] As before the expectation value of $\mathcal{W}^n$ for states with some separable $|\phi_i\rangle$ can be approximated arbitrarily close by the expectation value for a state $|\xi_{SEP}\rangle$ for which all $|\phi_i\rangle$ are entangled.

λ_n the matrix Λ is a positive semidefinite matrix we impose that $Tr(\Lambda) \geq 0$ and $\det(\Lambda) \geq 0$. It can be easily seen that $\det(\Lambda) \geq 0$ implies $Tr(\Lambda) \geq 0$ and one straightforwardly obtains that $\Lambda \geq 0$ iff $\frac{\lambda_n}{n} \geq \frac{\mu^2}{\sum_{i\in I_0} \tilde{x}_i^2} + \nu^2$. Hence, the minimal λ_n for which $\mathcal{W}_n$ is an EW is given by

$$\lambda_n^C = \sup_{\tilde{x}_i,\alpha_i,\beta_i\in\mathbb{R}} n\left(\frac{\mu^2}{\sum_{i\in I_0} \tilde{x}_i^2} + \nu^2\right). \tag{3.26}$$

One can easily derive from Eq. (3.20) that

$$\mu^2 = \frac{1}{2n}\left[\left|\sum_{j\in I_0} \sin(\alpha_j)\tilde{x}_j e^{-i\beta_j} \prod_{k\in I_0\setminus\{j\}} \cos(\alpha_k)\right)\right|^2 + \left|\sum_{j\in I_0} \left(\cos(\alpha_j)\tilde{x}_j e^{-i\beta_j} \prod_{k\in I_0\setminus\{j\}} \sin(\alpha_k)\right)\right|^2\right] \tag{3.27}$$

and

$$\nu^2 = \frac{1}{2n}\left[\prod_{j\in I_0} \cos^2(\alpha_j) + \prod_{j\in I_0} \sin^2(\alpha_j)\right]. \tag{3.28}$$

Note that as $|\sum_i a_i| \leq \sum_i |a_i|$ for any complex numbers a_i (and as any possible pair of values of $|\sin(\delta)|$ and $|\cos(\delta)|$ is attained for $\delta \in [0, \pi/2]$ and $\sin(\delta) \geq 0$ and $\cos(\delta) \geq 0$ for this parameter range) one obtains that the supremum in Eq. (3.26) is attained for $\beta_i = 0$ and $\alpha_i \in [0, \pi/2]$.

We will in the following distinguish between $n = 3$ and $n \geq 4$ and first discuss the case $n = 3$. Inserting the corresponding expressions for μ^2 and ν^2 in Eq. (3.26) and using $\beta_1 = \beta_3 = 0$ one straightforwardly obtains that

$$\lambda_3^C = \sup_{x,\alpha_1,\alpha_3\in\mathbb{R}} \frac{1}{2}\left(1 + \frac{x}{1+x^2}\sin(2\alpha_1)\sin(2\alpha_3)\right). \tag{3.29}$$

It is easy to see that therefore the supremum is obtained for $\alpha_1 = \alpha_3 = \pi/4$ and $x = 1$ which implies that $\lambda_3^C = \frac{3}{4}$. Hence, if λ_3 is larger than $\frac{3}{4}$ $\tilde{w}_3$ is positive semidefinite. However, it should be noted that $\mathcal{W}_3$ is only an EW if $\lambda_3 < 1$ as for $\lambda_3 \geq 1$ $\mathcal{W}_3$ is positive semidefinite and there exists no state, $|\Psi\rangle$, such that $\langle\Psi|\mathcal{W}_3|\Psi\rangle < 0$. A state that attains the maximum overlap of $3/4$ is given by $1/\sqrt{3}(|+++\rangle + |--+\rangle + |+--\rangle)$ with $|\pm\rangle = 1/\sqrt{2}(|0\rangle \pm |1\rangle)$. Using $\lambda_3 = 3/4$, $\beta_1 = \beta_3 = 0$, $x = 1$ and $\alpha_1 = \alpha_3 = \pi/4$ the remaining parameters for a state in the W-class that attains the maximum can be obtained by calculating the eigenvector of $\tilde{w}_3$ for the eigenvalue 0 [5].

We will proceed with $n \geq 4$ and will use that the supremum is attained for $\beta_i = 0$. Note that then $\frac{\mu^2}{\sum_{i\in I_0} \tilde{x}_i^2}$ can be equivalently written as

$$(\vec{v}_0 \cdot \vec{v}_1)^2 + (\vec{v}_0 \cdot \vec{v}_2)^2, \tag{3.30}$$

[5] In order to obtain the state presented here symmetries of the GHZ and W state are used.

where

$$\begin{aligned}
\vec{v}_0 &= \frac{1}{\sqrt{\sum_{i\in I_0}\tilde{x}_i^2}}(\tilde{x}_1,\tilde{x}_2,\ldots,\tilde{x}_{n-2},\tilde{x}_n)\\
\vec{v}_1 &= (y_1,\ldots,y_{n-2},y_n) \quad \text{with: } y_j = \frac{1}{\sqrt{2n}}\sin(\alpha_j)\prod_{k\in I_0\setminus\{j\}}\cos(\alpha_k)\\
\vec{v}_2 &= (z_1,\ldots,z_{n-2},z_n) \quad \text{with:} z_j = \frac{1}{\sqrt{2n}}\cos(\alpha_j)\prod_{k\in I_0\setminus\{j\}}\sin(\alpha_k).
\end{aligned} \tag{3.31}$$

Hence, one obtains

$$\lambda_n^C = \sup_{\tilde{x}_i,\alpha_i\in\mathbb{R}} n[(\vec{v}_0\cdot\vec{v}_1)^2+(\vec{v}_0\cdot\vec{v}_2)^2+\nu^2] \leq \sup_{\alpha_i\in\mathbb{R}} n[|\vec{v}_1]^2+|\vec{v}_2|^2+\nu^2] \tag{3.32}$$

as $\vec{v}_0$ is a normalized vector. Inserting the expressions for $\vec{v}_1,\vec{v}_2$ and ν we have that

$$\begin{aligned}
\lambda_n^C &\leq \sup_{\alpha_i\in\mathbb{R}}\frac{1}{2}\Big(\sum_{j\in I_0}\cos^2(\alpha_j)\prod_{k\in I_0\setminus\{j\}}\sin^2(\alpha_k)+\sum_{j\in I_0}\sin^2(\alpha_j)\prod_{k\in I_0\setminus\{j\}}\cos^2(\alpha_k)\\
&\qquad +\prod_{j\in I_0}\cos^2(\alpha_j)+\prod_{j\in I_0}\sin^2(\alpha_j)\Big)\\
&= \sup_{\alpha_i\in\mathbb{R}}\frac{1}{2}\Big(\sum_{j\in I_0\setminus\{n\}}\cos^2(\alpha_j)\prod_{k\in I_0\setminus\{j\}}\sin^2(\alpha_k)+\sum_{j\in I_0\setminus\{n\}}\sin^2(\alpha_j)\prod_{k\in I_0\setminus\{j\}}\cos^2(\alpha_k)\\
&\qquad +\prod_{j\in I_0\setminus\{n\}}\cos^2(\alpha_j)+\prod_{j\in I_0\setminus\{n\}}\sin^2(\alpha_j)\Big)\\
&\leq \sup_{\alpha_i\in\mathbb{R}}\frac{1}{2}\Big(\sum_{j\in I_0\setminus\{n\}}\cos^2(\alpha_j)\prod_{k\in I_0\setminus\{j,n\}}\sin^2(\alpha_k)+\sum_{j\in I_0\setminus\{n\}}\sin^2(\alpha_j)\prod_{k\in I_0\setminus\{j,n\}}\cos^2(\alpha_k)\\
&\qquad +\prod_{j\in I_0\setminus\{n\}}\cos^2(\alpha_j)+\prod_{j\in I_0\setminus\{n\}}\sin^2(\alpha_j)\Big)\\
&\leq \sup_{\alpha_i\in\mathbb{R}}\frac{1}{2}\Big(\sum_{j\in\{1,2,3\}}\cos^2(\alpha_j)\prod_{k\in\{1,2,3\},k\neq j}\sin^2(\alpha_k)+\sum_{j\in\{1,2,3\}}\sin^2(\alpha_j)\prod_{k\in\{1,2,3\},k\neq j}\cos^2(\alpha_k)\\
&\qquad +\prod_{j\in\{1,2,3\}}\cos^2(\alpha_j)+\prod_{j\in\{1,2,3\}}\sin^2(\alpha_j)\Big)\\
&= \frac{1}{2}.
\end{aligned} \tag{3.33}$$

Note that for the second inequality we used that $0\leq\cos^2(\alpha_i)\leq 1$ and $0\leq\sin^2(\alpha_i)\leq 1$ and then repeatedly applied the same argumentation. Note further that the upper bound obtained in the last line is equal to $1/2$ independent of the value of the parameters α_i for $i\in\{1,2,3\}$. As the state $|00\ldots0\rangle$ which can be approximated arbitrarily close by a state in the W-class has a squared overlap with the GHZ-state of $1/2$ we also have that $\lambda_n^C\geq 1/2$. Hence, one obtains $\lambda_n^C = 1/2$ for $n\geq 4$. Note that this is also the maximal squared overlap between the GHZ-state and an arbitrary separable state.

Chapter 4

Hypergraph states in arbitrary, finite dimension

Within this chapter, the second main result of this thesis, encompassing the definition, characterization and classification of hypergraph states in arbitrary dimension, is presented. Qubit hypergraph states have been introduced in [34] as a generalization of qubit graph states. For practical applications, hypergraph states were proven to pose an advantage compared to graph states within the field of measurement based quantum computation [133]. Furthermore, qubit hypergraph states are really equally weighted states and as such have applications within the Grover-[28] and Deutsch-Joza [25] algorithm. As a part of the broader class of locally maximally entangled (LME-) states, qubit hypergraph states can be used for fingerprint protocols [143]. A special class of qubit hypergraph states, the k-uniform qubit hypergraph states, are useful for applications in quantum metrology. Additionally inequalities, e.g. Bell inequalities, have been constructed and a violation for some hypergraph states which is exponentially increasing with the number of qubits has been shown [140, 141].
This chapter is organized as follows. First, there will be an introductory part in Section 4.1 covering the structure of quantum states in finite Hilbert spaces and their representation in phase space based on the work of [144]. Within this framework, the emergence of position- and space operators as well as the characterization of important groups of transformations are derived to explain the structure of the generalized X-, Z- and symplectic operations, which are of crucial importance within the following parts of the chapter. Furthermore, it highlights the reason for the fundamental difference between qudit hypergraph states in prime and in non-prime dimensions as a consequence of the basic properties of those structures. The second part will mainly cover the work published in [185] on the definition of qudit hypergraph states as well as their classification in terms of LU- and SLOCC equivalence. The following sections deal with unpublished results in the field of local complementation rules for qudit graph states of arbitrary dimension 4.3 as well as with weighted qudit hypergraph states 4.4.

4.1 Phase space representation of quantum systems in finite Hilbert spaces

A harmonic oscillator is a well studied system within the quantum mechanical context. Characterized by the dual variables position and momentum, methods were developed to successfully analyze and use the structure of the related phase space. Within this realm, those variables usually are continuous, that is, they are allowed to take values within the field of real numbers $\mathbb{R}$. Due to the well working formalism it seems a promising idea to try and

transfer it to a more restricted class of quantum systems and thereby gain powerful tools to better understand and describe those. The work of, e.g. Vourdas [144] develops an analogous formalism for quantum systems within a finite Hilbert space, where the restriction to discrete values of X (position) and P (momentum) demands them to be *integers modulo* d where d refers to the ring denoted as $\mathcal{Z}(d)$. The phase-space structure of those systems is a toroidal lattice $\mathcal{Z}(d) \times \mathcal{Z}(d)$. Note, that the existence of a finite geometry is an exclusive a property in case the dimension of the Hilbert space is a *prime number*. Then, $\mathcal{Z}(d)$ is a field (instead of a ring for non-prime dimension) and the additional structure allows for e.g. the formation of groups of certain operators acting in phase-space.

Within this setting, through position and momentum two orthonormal bases can be defined which are related by the finite Fourier transformation with the dimension-related phase parameter ω defined as

$$\mathcal{F} = \frac{1}{\sqrt{d}} \sum_{m,n=0}^{d-1} \omega^{mn} |X_m\rangle \langle X_n| \qquad \text{where: } \omega^x = e^{\frac{2\pi i}{d}x}, \quad x \in \mathcal{Z}(d) \tag{4.1}$$

and the set $\{|X_m\rangle\}$ is an orthonormal basis in position space, that is $\langle X_m|X_n\rangle = \delta_{mn}$ and $\sum_n |X_n\rangle \langle X_n| = \mathbb{1}$. The dual basis of momentum states $\{|P_m\rangle\}$ can be reached from $\{|X_n\rangle\}$ via $\mathcal{F}$:

$$|P_m\rangle = \mathcal{F}|X_m\rangle = \frac{1}{\sqrt{d}} \sum_{m',n=0}^{d-1} \omega^{m'n} |X_n\rangle \langle X_{m'}| |X_m\rangle = \frac{1}{\sqrt{d}} \sum_{n=0}^{d-1} \omega^{mn} |X_n\rangle \tag{4.2}$$

and an arbitrary state within $\mathcal{H}^d$ then always has a decomposition in position and momentum basis, e.g. $|\psi\rangle = \sum_n \lambda_n |X_n\rangle = \sum_m \mu_m |P_m\rangle$. The coefficients $\{\lambda_n\}$, $\{\mu_n\}$ are directly related by Eq. (4.2). The operators of position and momentum, x, p read

$$x = \sum_{n=0}^{d-1} n |X_n\rangle \langle X_n|, \qquad p = \sum_{n=0}^{d-1} n |P_n\rangle \langle P_n| \tag{4.3}$$

and again the Fourier transformation conducts the conversion between those two:

$$\begin{aligned} \mathcal{F}X\mathcal{F}^\dagger &= \frac{1}{d} \sum_{m=0}^{d-1} m\mathcal{F}|X_m\rangle \langle X_m|\mathcal{F}^\dagger \\ &= \frac{1}{d} \sum_{m=0}^{d-1} m \sum_{m',n,o,p=0}^{d-1} \omega^{m'n} |X_n\rangle \langle X_{m'}| |X_m\rangle \langle X_m| |X_o\rangle \langle X_p| (\omega^{op})^* \\ &= \frac{1}{d} \sum_{m=0}^{d-1} m \sum_{n,p=0}^{d-1} \omega^{mn} |X_n\rangle \langle X_p| (\omega^{mp})^* \\ &\overset{\text{Eq. (4.2)}}{=} \sum_{m=0}^{d-1} m |P_m\rangle \langle P_m| = P \end{aligned} \tag{4.4}$$

and, vice versa , $\mathcal{F}P\mathcal{F}^\dagger = -X$. Position and momentum operators are principally generators of infinitesimal displacements along position the and momentum axis in phase space. For this reason, to describe a displacement within a finite dimensional Hilbert space, discrete quantum systems related operators are used that fit into this kind of phase-space structure.

As mentioned, of importance for the remainder of this section, that is, the description of

qudit hypergraph states, are primarily those operators, which conduct finite displacements along the $x-$ and $p-$ axis of the underlying phase space they are embedded in - the generalization of the Pauli-operators: $\sigma_{(x|z)} \rightarrow (X|Z)$ acting on a single system as well as the corresponding controlled gates as their multi-system pendant. The single qudit displacement operators are defined as

$$Z = e^{\frac{2\pi i}{d}x} \qquad \text{and:} \qquad X = e^{\frac{2\pi i}{d}p} \tag{4.5}$$

with x, p defined as in Eq. (4.3) and naturally $XX^\dagger = ZZ^\dagger = \mathbb{1}$. Then, the action of X and Z on states in position- and momentum basis gives those displacements on the respective axis that show the right properties to be in analogy to the qubit case. Precisely, one has the following relations, symmetric when exchanging basis and associated operators simultaneously:

$$\begin{aligned} Z^a |X_m\rangle &= \omega^{am} |X_m\rangle & \qquad Z^a |P_m\rangle &= |P_{m+a}\rangle \\ X^a |X_m\rangle &= |X_{m+a}\rangle & \qquad X^a |P_m\rangle &= \omega^{-ma} |P_m\rangle \end{aligned} \tag{4.6}$$

Obviously, the $d-th$ power of X and Z return identity $X^d = Z^d = \mathbb{1}$ and in general:

$$Z^a = Z^{a \mod d} \qquad \text{and:} \qquad X^a = X^{a \mod d} \qquad \text{for a } \in \mathbb{Z} \tag{4.7}$$

Furthermore, the commutation rule between X and Z is of utmost significance when working with qudit hypergraph states, especially within the area of determining equivalence classes under local unitaries. For the single system operators, one finds:

$$X^b Z^a = \omega^{-ab} Z^a X^b \qquad \forall\ a, b\ \in \mathbb{Z} \tag{4.8}$$

which can be generalized to controlled $X-$ and $Z-$ gates acting on arbitrary index sets[1]. Eq. (4.6) enables a compact form of the X- and Z- operators which will we used frequently in many calculations and proofs later on:

$$\begin{aligned} Z^a &= \sum_{n=0}^{d-1} \omega^{aq} |q\rangle \langle q| & \qquad Z^a &= \sum_{n=0}^{d-1} |p \oplus a\rangle \langle p| \\ X^a &= \sum_{n=0}^{d-1} |q \oplus a\rangle \langle q| & \qquad X^a &= \sum_{n=0}^{d-1} \omega^{-ap} |p\rangle \langle p| \end{aligned} \tag{4.9}$$

Where from now on, for better readability, the double indexing is dropped and the position- and momentum states are denotes by bases $|X_m\rangle \rightarrow |q\rangle$ and $|P_m\rangle \rightarrow |p\rangle$, respectively. The values of p and q are in analogy to m dimension dependent and reach from 0 to $d-1$. Again, $q = q \mod d$ and in the following, $\oplus$ denotes the modular addition, that is, $q \oplus a = (q + a) \mod d$. $X^a,\ Z^a,\ a \in [0, .., d-1]$ are referred to as generalized Pauli operators and are generators of the generalized Pauli group.

An important set of transformation within this phase-space description are operators from the *symplectic* group. They go back to the Bogoliubov-transformations [129] for an harmonic oscillator. Within a $\mathbb{Z}(d) \times \mathbb{Z}(d)$ phase-space, the symplectic transformations denoted by S, $X \xrightarrow{S} X'$ and $P \xrightarrow{S} P'$, can be defined by their action on the displacement operators along

[1] The generalization is part of the main section for some special cases. Additionally, section 3.4. proves a commutation rule for the most general case of arbitrary index sets and arbitrary powers of X and Z.

the axis, X and P:

$$\begin{aligned} X' &= SXS^\dagger = X^\kappa Z^\lambda \omega^{2^{-1}\kappa\lambda} \\ P' &= SPS^\dagger = X^\mu Z^\nu \omega^{2^{-1}\nu\mu} \end{aligned} \tag{4.10}$$

Where $S^{-1} = S^\dagger$, i.e. S is a unitary operator and the parameters $\lambda, \kappa, \mu, \nu$ are element of $\mathbb{Z}(d)$ and additionally have to satisfy:

$$\kappa\nu - \lambda\mu \overset{mod\ d}{=} 1 \tag{4.11}$$

This restriction on the transformation parameters is necessary to ensure that all possible displacements are *finite*. Furthermore, in Eq.(4.10) the factor '2^{-1}' denotes the *multiplicative inverse* of 2. In general the *multiplicative inverse* of some arbitrary number k in $\mathbb{Z}^d$ is defined as the corresponding number k^{-1} such that $kk^{-1} \overset{mod\ d}{=} 1$. To systematically calculate the multiplicative inverse of some d, with d being prime, one can use the *Carmichael function* [159] $\lambda(d)$.

Definition 4.1. Carmichael function
The Carmichael function has its origin within the field of number theory. It assigns to every integer d with $d \geq 0$ a positive integer $\lambda(d)$, which is defined as the smallest $\lambda(d)$ such that

$$k^{\lambda(d)} \overset{mod\ d}{=} 1 \qquad \forall\ k\ with\ \ gcd(k,d) = 1 \tag{4.12}$$

Notice that $gcd(k,d) = 1$ is always true for $d = prime$ and $d > 2$. Using Eq. (4.12) one finds $k^{-1} = k^{\lambda(d)-1}$. As an example, consider the case $d = 3$. Then the multiplicative inverse is given by $k^{-1} = k^{\lambda(3)-1} = k^{2-1} = k$. For a value of $k = 2$, one can calculate $kk^{-1} = 2 \times 2 = 4$ and going backwards, one verifies $4 \overset{mod\ 3}{=} 1$ as demanded.
For $d \neq prime$ the multiplicative inverse cannot be defined in such a way for an arbitrary value of k, which is clear from the definition (k and d must not have a common divisor). If a multiplicative inverse does not exist, it is, in some cases, possible to broaden the termination over the field of rational numbers. Then, with the usual definition of a negative exponent, we have that $k^{-1} = \frac{1}{k}$. Thus, the expression for k^{-1} becomes independent of the dimension, for example for $k = 3$, one finds $k^{-1} = \frac{1}{3}$ for any d with $gcd[3,d] \neq 1$. It is important to state that for the non-prime case, according to the missing geometrical structure of the phase-space, one has to be careful when transferring methods and operations defined for prime dimensions. It is necessary to consider each case separately and determine structure and rules, as e.g. the one referring to the multiplicative inverse defined by the fraction, individually step by step .
Furthermore, notice that the operators X', P' can be written in terms of a general displacement operator $D(a,b)$ with $D(a,b) = Z^a X^b \omega^{2^{-1}ab}$ and $[D(a,b)]^\dagger = D(-a,-b)$ which are again unitary operators referring to the Heisenberg-Weyl[2] group for finite quantum systems. Concluding the section concerning the phase-space description of finite quantum systems, in the realm of symplectic transformations, there are three special operations $S(\kappa,\lambda,\mu)$, which play an important role for the classification of qudit hypergraph states.

- $S(\kappa,\lambda,\mu) = S(\xi,0,0)$: when applied to X (Z), they create the $\xi - th$ $(\xi^{-1} - th)$ power of the original gate

[2] for further details on the Heisenberg-Weyl group in the context of finite quantum systems, see [144]

- $S(\kappa,\lambda,\mu) = S(1,0,\xi)$: when applied to Z, they will leave Z unchanged and additionally create a $X-$gate of $\xi - th$ power.
- $S(\kappa,\lambda,\mu) = S(1,\xi,0)$: when applied to X, they will leave X unchanged and additionally create a $Z-$gate of $\xi - th$ power.

As will be shown, $S(\xi,0,0)$ refers to permutations of elements for diagonal matrices within X-or P-basis and thus is a helpful tool for the classification of qudit hypergraphs w.r.t. local unitary equivalence. $S(1,0,\xi)$ and $S(1,\xi,0)$ will prove to pose as a mediator for local unitary transformations between qudit- graph states that are in analogy to the local complementation rule [40] valid in the qubit case. In fact, for $d=2$ and $\xi = \frac{1}{2}$, $S(1,0,\xi)$ corresponds to the operation conducting the local complementation, that is, application of $\sqrt{X}$ on the LC-vertex and $\sqrt{Z}$ on all vertices within the neighbourhood. The concrete form of the aforementioned symplectic transformations can be calculated by Eq. (4.10) and their action on the basis states $|q\rangle$ and $|p\rangle$. Thus, using Eq. (4.2) and the relation

$$\frac{1}{d}\sum_{n=0}^{d-1}\omega^{n(m-l)} = \delta_{m,l} \qquad \text{as:} \sum_{n=0}^{d-1}\omega^{d} = 0 \tag{4.13}$$

one finds in position-and momentum basis, respectively:

$$\begin{aligned}
S(\xi,0,0) &= \sum_q |\xi q\rangle\langle q| & S(\xi,0,0) &= \sum_p |\xi^{-1}p\rangle\langle p| \\
S(1,0,\xi) &= \sum_q \omega^{-2^{-1}\xi p^2}|q\rangle\langle q| & S(1,0,\xi) &= \sum_p \omega^{-2^{-1}\xi p^2}|p\rangle\langle p| \\
S(1,\xi,0) &= \sum_q \omega^{2^{-1}\xi q^2}|q\rangle\langle q| & S(1,\xi,0) &= \sum_p \omega^{2^{-1}\xi q^2}|p\rangle\langle p|
\end{aligned} \tag{4.14}$$

One easily verifies that Eq.(4.14) implies:

$$\begin{aligned}
S(\xi,0,0)XS(\xi,0,0)^\dagger &= X^\xi & S(\xi,0,0)ZS(\xi,0,0)^\dagger &= Z^{-\xi} \\
S(1,0,\xi)XS(1,0,\xi)^\dagger &= X & S(1,0,\xi)ZS(1,0,\xi)^\dagger &= ZX^\xi\omega^{-2^{-1}\xi} \\
S(1,\xi,0)XS(1,\xi,0)^\dagger &= XZ^\xi\omega^{2^{-1}\xi} & S(1,\xi,0)ZS(1,\xi,0)^\dagger &= Z
\end{aligned} \tag{4.15}$$

where the displacement operators X and P are defined according to Eq. (4.9). In case of non-prime dimensions or $d=2$, one can find analogous representations of the symplectic operators. Starting with Eq. (4.15) as desired transformation rules and using a slightly changed version of Eq. (4.14), where the phase factor is arbitrary, i.e. $2^{-1} \longrightarrow \alpha$ with α being from the field of rational numbers, one can verify the mentioned re-definition of the multiplicative inverse as a simple fraction.[3]

With the basic framework and most important operators and relations within the phase-space of finite quantum systems in general and their useful applications on the way towards defining hypergraph states in arbitrary dimension explained, the next subsection will cover the main results regarding definition and classification of qudit hypergraph states.

[3] Concrete examples for $d = 3, 4$ can be found in Section 4.2.

4.2 Qudit hypergraph states

The results within this subsection are based on the work of [185]
The main goal of this project was the generalization of the class of hypergraph states defined for qubits [34] to systems of arbitrary dimension. To define hypergraphs for multipartite systems of qudits, we use constructions based on the d-dimensional Pauli group and its normalizer within a phase-space description of finite quantum systems. For simple hypergraphs, the different equivalence classes under local operations are shown to be governed by a greatest common divisor hierarchy. Moreover, the special cases of three qutrits and three ququarts are analysed in detail and equivalence classes under local unitary transformations as well as SLOCC transformations are listed.

4.2.1 Introduction

The physical properties of multipartite systems are highly relevant for practical applications as well as foundational aspects. Despite their importance, multipartite systems are in general very complex to describe and little analytical knowledge is available in the literature. Well-known examples in many-body physics are the various spin models, which are simple to write down, but where typically not all properties can be determined analytically. The entanglement properties of multipartite systems are no exception and already for pure states it is known that a complete characterization is, in general, not a feasible task [130, 174]. This motivates the adoption of simplifications that enable analytical results or at least to infer properties in a numerically efficient way.

One approach in this direction with broad impact in the literature is that based on a graph state encoding [132]. Mathematically, a graph consists of a set of vertices and a set of edges connecting the vertices. Graph states are a class of genuinely multipartite entangled states that are represented by graphs. This class contains as a special case the whole class of cluster states, which are the key ingredients in paradigms of quantum computing, e.g. the one-way quantum computer [133] and quantum error correction [134] or for the derivation of Bell inequalities [135]. Interestingly, results and techniques of the mathematical theory of graphs can be translated into the graph state framework: one prominent example is the graph operation known as local complementation. The appeal of graph states comes in great part from the so-called stabilizer formalism [134]. The stabilizer group of a given graph state can be constructed in a simple way from local Pauli operators and is abelian; the stabilizer operators associated to a given graph state are then used in a wide range of applications such as quantum error correcting codes [134], in the construction of Bell-like theorems [135], entanglement witnesses [136], models of topological quantum computing [137] and others.

Recently, there has been an interest in the generalization of graph states to a broader class of states known as *hypergraph states* [138]. In a hypergraph, an edge can connect more than two vertices, so hypergraph states are associated with many-body interactions beyond the usual two-body ones. Interestingly, the mathematical description of hypergraph states is still very simple and elegant and in Ref. [140] a full classification of the local unitary equivalence classes of hypergraphs states up to four qubits was obtained. Also, in Refs. [140, 141], Bell and Kochen-Specker inequalities have been derived and it has been shown that some hypergraph states violate local realism in a way that is exponentially increasing with the number of qubits. Finally, recent studies in condensed matter theory showed that this class of states occur naturally in physical systems associated with topological phases [139].

Originally, hypergraph states were defined as members of an even broader class of states known as locally maximally entangleable (LME) states [142], which are associated to applications such as quantum fingerprinting protocols [143]. Hypergraph states are then known as π-LME states and display the main important features of the general class of LME states.

Up to now, hypergraph states were defined only in the multi-qubit setting, while graph states can be defined in systems with arbitrary dimensions. In higher dimensions, graph states have many interesting properties not present in the two-dimensional setting. For instance, there are considerable differences between systems where the underlying local dimensions are prime or non-prime [144]. Another difference is the construction of Bell-like arguments for higher-dimensional systems [145].

In the present work, we extend the definition of hypergraph states to multipartite systems of arbitrary dimensions (qudits) and analyse their entanglement properties. Especially, we focus on the equivalence relations under local unitary (LU) operations and under stochastic local operations assisted by classical communication (SLOCC). In particular, the possible local inter-conversions between different entangled hypergraph states are governed by a greatest-common-divisor hierarchy. Note that the whole class of qudit graph states is a special case of our formulation.

This section is organized as follows: In Section 4.2.2, we start by giving a brief review of the concepts and results that are at the basis of our formulation. This includes a description of the Pauli and Clifford groups in a d-dimensional system, as well as a general look on qudit graph states. In Section 4.2.3, we introduce the definitions associated with qudit hypergraph states. Section 4.2.4 presents some properties of the stabilizer formalism used for qudit hypergraph states. Sections 4.2.5 and 4.2.6 introduce the problem of classifying the SLOCC and LU classes of hypergraph states, first describing the different techniques employed and then proving a series of results on this classification. Finally, we present some concrete examples in low dimensional tripartite systems in Sections 4.2.7 and 4.2.8, where already the main differences between systems of prime and non-prime dimensions become apparent. We reserve the related subjects of a phase-space description and local complementation of qudit graphs for the Appendices 4.2.10.

4.2.2 Background and basic definitions

Let us give a short review of the definition of graph-and hypergraph states given in Chapter 2. We consider an N-partite system $\mathcal{H} = \bigotimes_{i=1}^{N} \mathcal{H}_i$, where the subsystems $\mathcal{H}_i$ have the same dimension d. A graph is a pair $G = (V, E)$, where V is the set of vertices and E is a set comprised of 2-element subsets of V called edges. Likewise, a hypergraph is a pair $H = (V, E)$, where V are the vertices and E is a set comprised of subsets of V with arbitrary number of elements; a n-element $e \in E$ is called a n-hyperedge. Thus, in some sense, a hyperedge is an edge that can connect more than two vertices. A multi-(hyper)graph is a set where the (hyper)edges are allowed to appear repeated. An example of a multi-graph can be found in Fig. 4.1, while one of a multi-hypergraph can be found in Fig. 4.2. Given two integers m and n, their greatest common divisor will be denoted by $gcd(m, n)$. The integers modulo n will be denoted as $\mathbb{Z}_n$.

The Pauli group and its normalizer

Taking inspiration in the formulation of qubit hypergraph states, we adopt here the description based on the Pauli and Clifford groups in finite dimensions. In a d-dimensional system with

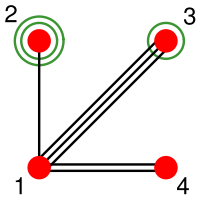

FIGURE 4.1: Example of a graph state represented by the multi-graph $G = (V, E)$, where $V = \{1, 2, 3, 4\}$ and $E = \{\{1, 2\}, \{1, 3\}, \{1, 3\}, \{1, 3\}, \{1, 4\}, \{1, 4\}, \{2\}, \{2\}, \{3\}\}$. The graph state in this case is $|G\rangle = Z_{12}Z_{13}^3Z_{14}^2Z_2^2Z_3|+\rangle^V$.

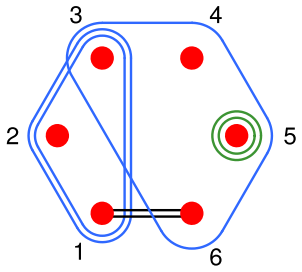

FIGURE 4.2: Hypergraph state represented by the multi-hypergraph $H = (V, E)$, with $V = \{1, 2, 3, 4, 5, 6\}$ and $E = \{\{1, 2, 3\}, \{1, 2, 3\}, \{1, 6\}, \{1, 6\}, \{5\}, \{5\}, \{3, 4, 5, 6\}\}$. The corresponding hypergraph state is then $|H\rangle = Z_{123}^2Z_{16}^2Z_5^2Z_{3456}|+\rangle^V$.

computational basis $\{|q\rangle\}_{q=0}^{d-1}$, let us consider the unitary operators given by

$$Z = \sum_{q=0}^{d-1} \omega^q |q\rangle\langle q|; \;\; X = \sum_{q=0}^{d-1} |q \oplus 1\rangle\langle q| \tag{4.16}$$

with the properties $X^d = Z^d = I$ and $X^m Z^n = \omega^{-mn} Z^n X^m$, where $\omega = e^{2\pi i/d}$ is the d-th root of unity and $\oplus$ denotes addition modulo d. The group generated by these operators is known as the Pauli group and the operators $X^\alpha Z^\beta$, for $\alpha, \beta \in \mathbb{Z}_d$ are referred to as Pauli operators. For $d = 2$, these operators reduce to the well-known Pauli matrices for qubits. In general, these operators enable a phase-space picture for finite-dimensional systems, via the relations $Z = e^{\frac{2\pi i}{d}Q}$, $X = e^{-\frac{2\pi i}{d}P}$, where $Q = \sum_{q=0}^{d-1} q|q\rangle\langle q|$ and $P = \sum_{q=0}^{d-1} q|p_q\rangle\langle p_q|$ are discrete versions of the position and momentum operators; here, $|p_q\rangle = F|q\rangle$ and $F = d^{-1/2}\sum_{q',q=0}^{d-1} \omega^{q'q}|q'\rangle\langle q|$ is the discrete Fourier transform. Thus, X performs displacements in the computational (position) basis, while Z performs displacements in its Fourier transformed (momentum) basis.

Another set of important operators are the so-called Clifford or symplectic operators, defined as

$$S(\xi, 0, 0) = \sum_{q=0}^{d-1} |\xi q\rangle\langle q|; \tag{4.17}$$

$$S(1, \xi, 0) = \sum_{q=0}^{d-1} \omega^{\xi q^2 2^{-1}} |q\rangle\langle q|; \tag{4.18}$$

$$S(1, 0, \xi) = \sum_{q=0}^{d-1} \omega^{-\xi q^2 2^{-1}} |p_q\rangle\langle p_q|. \tag{4.19}$$

These operators are invertible and unitary whenever the values of ξ and d are coprime (see proof of Lemma 4.1) and generate the normalizer of the Pauli group, which is usually referred as the Clifford group. Throughout the text, if not stated otherwise, by a symplectic operator (or Clifford operator) S we will mean an arbitrary symplectic operator, which can be decomposed as a product of operators from Eqs. (4.17,4.18,4.19). The interested reader can check a more broad formulation in terms of a discrete phase-space in the Appendix A, Section 4.1 or in the Ref. [144].

Qudit graph states

We briefly review the theory of the so-called qudit graph states, which is well established in the literature [146]. The mathematical object used is a multi-graph $G = (V, E)$; we call $m_e \in \mathbb{Z}_d$ the multiplicity of the edge e, i.e., the number of times the edge appears. Given a multigraph $G = (V, E)$, we associate a quantum state $|G\rangle$ in a d-dimensional system in the following way:

- To each vertex $i \in V$ we associate a local state $|+\rangle = |p_0\rangle = d^{-1/2} \sum_{q=0}^{d-1} |q\rangle$.
- For each edge $e = \{i, j\}$ and multiplicity m_e we apply the unitary

$$Z_e^{m_e} = \sum_{q=0}^{d-1} |q_i\rangle\langle q_i| \otimes (Z_j^{m_e})^q \tag{4.20}$$

  on the state $|+\rangle^V = \bigotimes_{i\in V} |+\rangle_i$. Thus, the graph state is defined as

$$|G\rangle = \prod_{e\in E} Z_e^{m_e} |+\rangle^V. \tag{4.21}$$

We allow among the edges $e \in E$ the presence of "loops", i.e., an edge that contains only a single vertex. A loop of multiplicity m on vertex k means here that a local gate $(Z_k)^m$ is applied to the graph state. An example of a qudit graph state in a system with dimension $d > 3$ is shown in Fig. 4.1.

An equivalent way of defining a qudit graph state is via the stabilizer formalism [146]. Given a multi-graph $G = (V, E)$, we define for each vertex $i \in V$ the operator $K_i = X_i \prod_{e\in E^*} Z_{e\setminus\{i\}}$, where E^* denotes all edges containing i. The set K_i generates an abelian group known as the stabilizer. The unique $+1$ common eigenstate of these operators is precisely the state $|G\rangle$ associated to the multi-graph G. Moreover, the set of common eigenstates of these operators forms a basis of the global state space, the so-called graph state basis.

The local action of the generalized Pauli group on a graph state is easy to picture and clearly preserves the graph state structure. As already said, the action of Z_l^m corresponds to a loop of multiplicity m on the qubit l, while the action of X_l^m corresponds to loops of multiplicity m on the qubits in the neighbourhood of the qubit m; this last observation is a corollary of Lemma 4.1.

The action of the local Clifford group is richer and enables the conversion between different multi-graphs in a simple fashion. For prime dimensions, the action of the gate $S_k(\xi, 0, 0)$ enables the conversion between edges of different multiplicities, while the gate $S_k(1, -1, 0)$ is associated to the operation known as local complementation - see Appendix B. Moreover,

in non-prime dimensions, the possible conversions between edges are governed by a greatest common divisor hierarchy, as shown in more generality ahead - see Proposition 4.1 and Theorem 4.1.

4.2.3 Qudit hypergraph states

We now introduce the class of hypergraph states in a system with underlying finite dimension d. Before proceeding, we first need a concept of controlled operations on a multipartite system. From a given local operation M, one can define a controlled operation M_{ij} between qudits i and j as

$$M_{ij} = \sum_{q=0}^{d-1} |q_i\rangle\langle q_i| \otimes M_j^q \tag{4.22}$$

Likewise, a controlled operation between three qudits i, j and k is defined recursively as

$$M_{ijk} = \sum_{q=0}^{d-1} |q_i\rangle\langle q_i| \otimes M_{jk}^q \tag{4.23}$$

and, in general, the controlled operation between n qudits labeled by $\mathcal{I} = \{i_1 i_2 \dots i_n\}$ is given by

$$M_{\mathcal{I}} = M_{i_1 i_2 \dots i_n} = \sum_{q=0}^{d-1} |q_{i_1}\rangle\langle q_{i_1}| \otimes M_{i_2 \dots i_n}^q \tag{4.24}$$

A prominent example is the CNOT operation, which is simply the bipartite controlled operation generated by the X gate - $CNOT = \sum_q |q\rangle\langle q| \otimes X^q$. Although our formulation can be done in terms of this gate and its multipartite versions, it is preferable to use an equivalent formulation in terms of controlled-phase gates $Z_{\mathcal{I}}$, since these gates are mutually commuting and thus are easy to handle. Explicitly, the controlled phase gate for a hyperedge e on n particles is given by

$$\begin{aligned} Z_e &= \sum_{q_1=0}^{d} \dots \sum_{q_{n-1}=0}^{d} |q_1 \dots q_{n-1}\rangle \langle q_1 \dots q_{n-1}| \, Z^{q_1 \cdot \dots \cdot q_{n-1}} \\ &= \sum_{q_1=0}^{d} \dots \sum_{q_n=0}^{d} |q_1 \dots q_n\rangle \langle q_1 \dots q_n| \, \omega^{q_1 \cdot \dots \cdot q_n} \end{aligned} \tag{4.25}$$

The mathematical object used here to represent a given state is a multi-hypergraph $G = (V, E)$; as usual, we call $m_e \in \mathbb{Z}_d$ the multiplicity of the hyperedge e, i.e., the number of times the hyperedge appears. Given a multi-hypergraph $H = (V, E)$, we associate a quantum state $|H\rangle$ in a d-dimensional system in the following way:

- To each vertex $i \in V$ we associate a local state $|+\rangle = d^{-1/2} \sum_{q=0}^{d-1} |q\rangle$.
- For each hyperedge $e \in E$ with multiplicity m_e we apply the controlled-unitary $Z_e^{m_e}$ on the state $|+\rangle^V = \bigotimes_{i \in V} |+\rangle_i$. Thus, the hypergraph state is defined as

$$|H\rangle = \prod_{e \in E} Z_e^{m_e} |+\rangle^V. \tag{4.26}$$

Among the hyperedges $e \in E$, we allow the presence of "loops", i.e., an edge that contains only a single vertex. Also empty edges are allowed, they correspond to a global sign. A loop of multiplicity m on vertex k means here that a local gate $(Z_k)^m$ is applied to the graph state. An example of hypergraph state is illustrated in Fig. 4.2.

Equivalently, one can define a hypergraph state as the unique $+1$ eigenstate of a maximal set of commuting stabilizer operators K_i which can be defined in a similar way as for graph states. The principal concept was already introduced in the Chapter 2. We will explain this approach and the concrete formulation for the case of qudit hypergraph states within the next section, that is, directly following the proof of Lemma 4.1 below.

For completeness, we cite alternative formulations of hypergraph states that are potentially useful in other scenarios. First, we notice that the multiplicities of the hyperedges can also be encoded in the adjacency tensor Γ of the multi-hypergraph H, defined by $\Gamma_{i_1 i_2 \ldots i_n} = m_{\{i_1,i_2,\ldots,i_n\}}$, where $\{i_1, i_2, \ldots, i_n\} \in E$. For graph states, for example, the Γ tensor is a matrix, the well-known adjacency matrix of the theory of graphs. Many local quantum operations, especially those coming from the local Clifford group, are elegantly described as matrix operations over the adjacency matrix of the multi-graph G.

One can also work in the Schrödinger picture: the form of the state in the computational basis is then given by:

$$|H\rangle = \sum_{\mathbf{q}=\mathbf{0}}^{\mathbf{d-1}} \omega^{f(\mathbf{q})} |\mathbf{q}\rangle, \tag{4.27}$$

where $\mathbf{q} \equiv (q_1, q_2, \ldots, q_n)$. f is a function from $\mathbb{Z}_d$ to $\mathbb{Z}_d$ defined by $f(\mathbf{q}) = \bigoplus_{\{q_1,\ldots,q_k\}\in E} \bigwedge_k q_k$. For qubits, for example, the function f is a Boolean function and this encoding is behind applications such as Deutsch-Jozsa and Grover's algorithms [138]. Furthermore, we can identify $f(q)$ within the framework of an n-partite qudit hypergraph-states as

$$|H\rangle = \prod_{a=1}^{k} Z_{I_a}^{m_a} |+\rangle^{\otimes n} = \sum_{c_i=0,\ i\in[1,\ldots,n]}^{d-1} \prod_{a=1}^{k} \omega^{\left(m_a \prod_{i,\ i\in I_a} c_i\right)} \bigotimes_{i=1}^{n} |c_i\rangle\,, \tag{4.28}$$

where I_a denotes the index set on which the different (hyper-)edges are applied to with the corresponding multiplicity m_a. For clearity, let us consider a concrete example:

Example 4.1. Hypergraph of $n = 4$ qudits in dimension $d = 6$
Consider the hypergraph given in Fig. (4.3), that is, a system of four qudits, where certain subsets are connected by three (hyper-)edges of some multiplicity. Precisely, we have an hyperedge of multplicity $m_e = 5$ connecting all four qubits, an hyperedge of multiplicity $m_e = 1$ connecting qudits 1,2 and 4 and finally a two-edge of multiplicity $m_e = 2$ between qudits 1 and 3. Then the whole state, according to Eq. (4.26), can be written as

$$|H\rangle = Z_{1234}^5 Z_{124} Z_{13}^2 |++++\rangle = \sum_{ijkl=0}^{3} \omega^{5ijkl} \omega^{ijl} \omega^{2ik} |ijkl\rangle \tag{4.29}$$

where the controlled Z-gates, the phase ω and the initial qudits in state $|+\rangle$ are of the form given in Fig. (4.3).

An important special class of hypergraph states are the so-called *n-elementary hypergraph states*, which are those constituted of exclusively one single hyperedge e between all n qudits of the system. Thus, such a state has the simple form $|H\rangle = Z_e^{m_e} |+\rangle^V$. For this subclass,

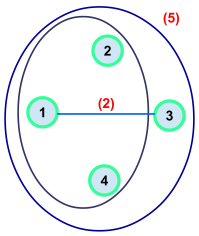

- $Z = diag(1, e^{\frac{i\pi}{3}}, e^{\frac{2i\pi}{3}}, e^{\frac{4i\pi}{3}}, e^{\frac{5i\pi}{3}})$
- $|+\rangle = |0\rangle + |1\rangle + |2\rangle + |3\rangle + |4\rangle + |5\rangle$
- $Z_{124} = (|0\rangle\langle 0|)_1 \mathbb{1}_{24} + (|1\rangle\langle 1|)_1 Z_{24} + ... + (|5\rangle\langle 5|)_i Z_{24}^5$
  $Z_{1234}^5 = (|0\rangle\langle 0|)_1 \mathbb{1}_{234} + (|1\rangle\langle 1|)_1 Z_{234}^5 + ... + (|5\rangle\langle 5|)_i Z_{234}^{(5\cdot 5=25 \overset{mod\ 6}{=} 1)}$
  $Z_{13}^2 = (|0\rangle\langle 0|)_1 \mathbb{1}_2 + (|1\rangle\langle 1|)_1 Z_2^2 + ... + (|5\rangle\langle 5|)_i Z_2^{(2\cdot 5=10 \overset{mod\ 6}{=} 4)}$

FIGURE 4.3: Four qudit hypergraph in dimension six

the main entanglement properties depend on the multiplicity m_e of the hyperedge, as shown in the next sections.

4.2.4 Properties of hypergraph states and the stabilizer formalism

In the following sections, we derive some properties of hypergraph states, the controlled-Z operation on many qudits and the stabilizer formalism. These tools will later be used for the SLOCC and LU classification.

Local action of Pauli and Clifford groups

We now consider the effect of unitaries from the Pauli and Clifford groups on a hypergraph state. First, we need some simple relations:

Lemma 4.1. *The following relations hold:*

$$X_k^\dagger Z_{\mathcal{I}} X_k = Z_{\mathcal{I}\setminus\{k\}} Z_{\mathcal{I}} \tag{4.30}$$

$$Z_{\mathcal{I}} X_k Z_{\mathcal{I}}^\dagger = X_k Z_{\mathcal{I}\setminus\{k\}} \tag{4.31}$$

Proof. We prove the lemma by induction on the cardinality n of the index set $\mathcal{I}$, i.e., on the number of qudits. For $n = 2$, remembering the relation $X^\dagger Z X = \omega Z$, we see that

$$\begin{aligned}
X_k^\dagger Z_{jk} X_k &= X_k^\dagger \left(\sum_{q=0}^{d-1} |q_j\rangle\langle q_j| \otimes Z_k^q \right) X_k \\
&= \sum_{q=0}^{d-1} |q_j\rangle\langle q_j| \otimes (X_k^\dagger Z_k^q X_k) \\
&= \sum_{q=0}^{d-1} |q_j\rangle\langle q_j| \otimes (\omega^q Z_k^q) \\
&= \left(\sum_{q=0}^{d-1} \omega^q |q_j\rangle\langle q_j| \otimes I_k \right) \left(\sum_{q=0}^{d-1} |q_j\rangle\langle q_j| \otimes Z_k^q \right) \\
&= Z_j Z_{jk}
\end{aligned}$$

and the relations are valid. Now, let us consider the set $\mathcal{I}$ having cardinality n and the set $\mathcal{I}' = \mathcal{I} \cup \{j\}$, with $j \neq k$. Then we have

$$
\begin{aligned}
X_k^\dagger Z_{\mathcal{I}'} X_k &= X_k^\dagger \left(\sum_{q=0}^{d-1} |q_j\rangle\langle q_j| \otimes Z_{\mathcal{I}}^q \right) X_k \\
&= \sum_{q=0}^{d-1} |q_j\rangle\langle q_j| \otimes (X_k^\dagger Z_{\mathcal{I}}^q X_k) \\
&= \sum_{q=0}^{d-1} |q_j\rangle\langle q_j| \otimes (Z_{\mathcal{I}\setminus\{k\}} Z_{\mathcal{I}})^q \\
&= \left(\sum_{q=0}^{d-1} |q_j\rangle\langle q_j| \otimes Z_{\mathcal{I}\setminus\{k\}}^q \right) \left(\sum_{q=0}^{d-1} |q_j\rangle\langle q_j| \otimes Z_{\mathcal{I}}^q \right) \\
&= Z_{\mathcal{I}'\setminus\{k\}} Z_{\mathcal{I}'}
\end{aligned}
$$

i.e., if the relations are valid for n, then they are also valid for $n+1$. The proof of the second statement, i.e. Eq. (4.31), then follows straightforward. □

The effect of applying the gate $X_k^\dagger$ on an elementary hypergraph is then given by the creation of a hyperedge of same multiplicity on the neighbourhood of the qudit k:

$$
X_k^\dagger |H\rangle = X_k^\dagger Z_e^{m_e} |+\rangle^V = Z_{e\setminus\{k\}}^{m_e} Z_e^{m_e} X_k^\dagger |+\rangle^V = Z_{e\setminus\{k\}}^{m_e} |H\rangle.
$$

It is important to note that the hyperedges induced on the neighbourhood of k by repeated applications of $X_k^\dagger$ have multiplicities that are divisible by m_e. Depending on the primality of the underlying dimension d, there are restricted possibilities of inducing hyperedges on neighbouring qudits via this procedure, a difference in relation to the qubit case.

Moreover, since the local Z_k gate commutes with any $Z_{\mathcal{I}}$, it can always be locally removed by applying $Z_k^\dagger$. As explained previously, we adopt the convention of representing any Z_k acting on a hypergraph state as a loop - a 1-hyperedge - around the vertex k; higher potencies $(Z_k)^m$ are represented by m loops around k. Thus, the action of the local Pauli group constituted of the unitaries $X_k^m Z_k^n$ is to create n loops on the vertex k and m-hyperedges on the neighbourhood of k.

Let us now turn to the action of the local Clifford group. The local gate from Eq. (4.17) performs (see also Eq. (4.15)) permutations on the computational basis via the mapping $S(\xi^{-1},0,0)ZS^\dagger(\xi^{-1},0,0) = Z^\xi$, where Z acts on a single particle. Based on this, we can derive the action on multiparticle Z_e gates, corresponding to a hyperedge e. It turns out that for d prime, it is always possible to convert a k-hyperedge of multiplicity m ($m \neq 0 \mod d$) to another k-hyperedge of multiplicity m' ($m' \neq 0 \mod d$). For non-prime d, the k-hyperedges that are connectable via permutations are those whose multiplicities have an equal greatest common divisor with the dimension d. In detail, we can formulate

Proposition 4.1. *Let $k, k' \in \mathbb{Z}_d$ be such that $gcd(d,k) = gcd(d,k') = g$. Then there exists a Clifford operator S defined in Eq. (4.17) such that $S(Z_e)^k S^\dagger = (Z_e)^{k'}$.*

Proof. One can find the proof of this proposition in Ref. [147]. For completeness, we provide alternative proofs of this Proposition in Appendix C. □

As an example, consider a system of dimension six. There, we have three different classes with respect to the greatest common divisor, that is $gcd(m_e, d) = [1,2,3]$. This then relates to permutation-equivalence of the Z-gates of multiplicity $m_e = [1,..,5]$ within the same

$gcd-$class; precisely, we have: for $gcd(m_e, d) = 1$, the class includes the gates Z^1 and Z^5, for $gcd(m_e, d) = 2$ we have the gates Z^2 as well as Z^4 and finally the class for $gcd(m_e, d) = 3$ has only one element, namely Z^3.
Furthermore, the symplectic operator conducting the permutation of diagonal elements within Z-power gates according to Proposition (4.1) is, as defined in Eq. (4.17), given by $S(\xi, 0, 0)$. To find the corresponding value of ξ for given k, k' with $gcd(k, d) = gcd(k', d)$, we use the first line in Eq. (4.15) and deduce from $S(\xi, 0, 0)ZS(\xi, 0, 0)^\dagger = Z^{\xi^{-1}}$

$$S(\xi,0,0)Z^kS(\xi,0,0)^\dagger = \underbrace{(\xi,0,0)ZS(\xi,0,0)^\dagger S(\xi,0,0)ZS(\xi,0,0)^\dagger ...}_{k-times} = Z^{k\xi^{-1}} \equiv Z^{k'} \quad (4.32)$$

and thus, $k\xi^{-1} = k'$. For the example above, exemplary the operator transforming Z^2 to Z^4 in dimension $d = 6$ has a $\xi-$value satisfying $2\xi^{-1} \overset{mod\ 6}{=} 4$. Thus, $\xi^{-1} = 5$ and as $\xi\xi^{-1} \overset{mod\ 6}{=} 1$, it follows that $\xi = 5$. Notice, that per definition of the Carmichael function, i.e. Eq. (4.12), $\xi^{-1} = 2$ does not work properly as $gcd(2, 6) \neq 1$.
Let us anticipate the next section and already mention at this point that Prop.(4.1) is of great importance when considering local equivalence of elementary hypergraphs in arbitrary dimension. This is mainly due to the fact that it is possible to directly connect the $gcd-$hierarchy to the entanglement properties of the state via the reduced rank, which will be shown in the section covering local measurements. The subsequent consequences regarding local equivalences of n-elementary hypergraph states are given in section 2.1.5.
For a more detailed discussion on the Clifford group see Ref. [148]. As mentioned in Chapter 2, the local Clifford gates, or sympletic operators, in Eq. (4.18) and Eq. (4.19) are associated with the local complementation of qudit graphs, which is explained in detail in the next section as well as in Appendix B. Furthermore, rules for local complementation of qudit graph states within a more general framework are derived in Section 4.3.

Stabilizer formalism

From relation (4.31) we can construct the stabilizer operator on a vertex i:

$$|H\rangle = \prod_{e\in E} Z_e|+\rangle^V = \prod_{e\in E} Z_eX_iZ_e^\dagger Z_e|+\rangle^V \quad (4.33)$$

$$= X_i \prod_{e\in E^*} Z_{e\setminus\{i\}}|H\rangle = K_i|H\rangle \quad (4.34)$$

with $K_i = X_i \prod_{e\in E^*} Z_{e\setminus\{i\}}$ and where E^* denotes all edges containing i. Hence, the operators K_i stabilize the hypergraph state $|H\rangle$. An equivalent way is expressing the stabilizer operator in the compact form $K_i = X_iZ_{N_i}$, where $Z_{N_i} \equiv \prod_{j\in N_i} Z_j$, where N_i is the neighbourhood of i. Moreover, these operators are mutually commuting:

$$K_iK_j = (X_i \prod_{e\in E} Z_{e\setminus\{i\}})(X_j \prod_{e\in E} Z_{e\setminus\{j\}}) \quad (4.35)$$

$$= (\prod_{e\in E} Z_eX_i \prod_{e\in E} Z_e^\dagger)(\prod_{e\in E} Z_eX_j \prod_{e\in E} Z_e^\dagger) \quad (4.36)$$

$$= \prod_{e\in E} Z_eX_iX_j \prod_{e\in E} Z_e^\dagger \quad (4.37)$$

$$= \prod_{e\in E} Z_eX_jX_i \prod_{e\in E} Z_e^\dagger = K_jK_i \quad (4.38)$$

Indeed, these operators generate a maximal abelian group on the number n of qudits. The group properties of closure and associativity are straightforward, while the identity element comes from $K_i^d = I$ and the inverse of K_i simply being $K_i^\dagger$. Each operator in this group has eigenvalues $1, \omega, \omega^2, \ldots, \omega^{d-1}$ and their d^n common eigenvectors form an orthonormal basis of the total Hilbert space, the hypergraph basis with elements given by

$$|H_{k_1,k_2,\ldots,k_N}\rangle = Z_1^{-k_1} Z_2^{-k_2} \ldots Z_N^{-k_N} |H\rangle \tag{4.39}$$

where the k_is attain values in $\mathbb{Z}_d$. Notice also that

$$|H\rangle\langle H| = \frac{1}{d^N} \prod_{i \in V} (I + K_i + K_i^2 + \ldots + K_i^{d-1}) \tag{4.40}$$

In the qubit case, these non-local stabilizers are observables and were used for the development of novel non-contextuality and locality inequalities [140, 141]. For $d > 2$, these operators are no longer self-adjoint in general, but we believe techniques similar to Ref. [155] could be used to extend the results of the qubit case to arbitrary dimensions. We conclude the topic of defining (hyper-)graph states within the stabilizer formalism by giving two short examples:

1) three qudit graph in dimension d=3

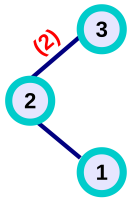

- state: $|G\rangle = Z_{12}^2 Z_{23} |+++\rangle$
- stabilizers: $K_1 = X_1 Z_2^2 \;\; K_2 = X_2 Z_1^2 Z_3 \;\; K_3 = X_3 Z_2$
- e.g. look at:

$$\begin{aligned} K_1 |G\rangle &= Z_2^2 \underbrace{X_1 Z_{12}^2}_{= Z_2 Z_{12}^2 X_1} Z_{23} |+++\rangle \\ &= Z_2^2 Z_2 Z_{12}^2 Z_{23} X_1 |+++\rangle = |G\rangle \end{aligned} \tag{4.41}$$

2) four qudit hypergraph in dimension d=6

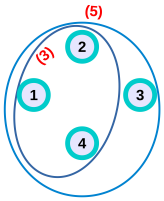

- state: $|H\rangle = Z_{1234}^5 Z_{124}^3 |++++\rangle$
- stabilizers: (non-local)
  $K_1 = X_1 Z_{24}^3 Z_{234}$
  $K_2 = X_2 Z_{14}^3 Z_{134}$
  $K_3 = X_3 Z_{124}$

Local measurements in Z basis and ranks of the reduced states

It is possible to give a graphical description of the measurement of a non-degenerate observable $M = \sum_q m_q |q\rangle\langle q|$ on a hypergraph state in terms of hypergraph operations. Obtaining outcome m_q when measuring M on the qudit k of the hypergraph state $|H\rangle = \prod_e Z_e^{m_e} |+\rangle^V$ amounts to performing the projection $P_q^{(k)} |H\rangle$, where $P_q^{(k)} = |q_k\rangle\langle q_k|$. The state after the measurement is then $|q_k\rangle \otimes |H'\rangle$, where $|H'\rangle = \prod_e Z_{e\setminus\{k\}}^{m_e q} |+\rangle^{V\setminus\{k\}}$. For the example shown in Fig.(4.4) with $|H\rangle = Z_{123}^2 Z_{13}^2 |+\rangle^{\otimes 3}$ and local dimension $d = 4$, when measuring in Z-basis

on qudit 2, we have the post measurement states:

$$|q_2\rangle \otimes |H'_{13}\rangle = |q_2\rangle \otimes Z_{13}^{2q} Z_{13}^{2} |{+}{+}_{13}\rangle = |q_2\rangle \otimes Z_{13}^{2(q_2+1)} |{+}{+}_{13}\rangle . \tag{4.42}$$

Therefore, for outcomes m_q with $q = [0, ..., 3]$ the reduced states $|H'\rangle (m_q)$ are

- $q_2 = 0$: $|0_2\rangle \otimes |H'(m_0)_{13}\rangle = |0_2\rangle \otimes Z_{13}^{2} |{+}{+}_{13}\rangle$
- $q_2 = 1$: $|1_2\rangle \otimes |H'(m_0)_{13}\rangle = |1_2\rangle \otimes Z_{13}^{(4 \overset{mod\ 4}{=} 0)} |{+}{+}_{13}\rangle = |1_2\rangle \otimes |{+}{+}_{13}\rangle$
- $q_2 = 2$: $|2_2\rangle \otimes |H'(m_0)_{13}\rangle = |2_2\rangle \otimes Z_{13}^{(6 \overset{mod\ 4}{=} 2)} |{+}{+}_{13}\rangle = |2_2\rangle \otimes Z_{13}^{2} |{+}{+}_{13}\rangle$
- $q_2 = 3$: $|3_2\rangle \otimes |H'(m_0)_{13}\rangle = |3_2\rangle \otimes Z_{13}^{(8 \overset{mod\ 4}{=} 0)} |{+}{+}_{13}\rangle = |3_2\rangle \otimes |{+}{+}_{13}\rangle$

and a subsequent measurement on qudit 1 gives for the cases $q_1 = 0$ and $q_1 = 2$

$$|q_1\rangle \otimes |q_2\rangle \otimes |H''_3\rangle = |q_1\rangle \otimes |q_2\rangle \otimes Z_3^{2(q_2+1)q_1} |{+}_3\rangle , \tag{4.43}$$

and the fully separable states after measurements on qudits 1 and 2 are

- $q_1 = q_2 = 0$: $|0_1\rangle \otimes |0_2\rangle \otimes Z_3^{0} |{+}_3\rangle = |00{+}_{123}\rangle$
- $q_1 = 2,\ q_2 = 0$: $|2_1\rangle \otimes |0_2\rangle \otimes Z_3^{(4 \overset{mod\ 4}{=} 0)} |{+}_3\rangle = |00{+}_{123}\rangle$
- $q_1 = 0,\ q_2 = 2$: $|0_1\rangle \otimes |2_2\rangle \otimes Z_3^{0} |{+}_3\rangle = |02{+}_{123}\rangle$
- $q_1 = 2,\ q_2 = 2$: $|2_1\rangle \otimes |2_2\rangle \otimes Z_3^{(4 \overset{mod\ 4}{=} 0)} |{+}_3\rangle = |20{+}_{123}\rangle$
- $q_1 = 1,\ q_2 = 0$: $|1_1\rangle \otimes |0_2\rangle \otimes Z_3^{2} |{+}_3\rangle$
- $q_1 = 3,\ q_2 = 0$: $|3_1\rangle \otimes |0_2\rangle \otimes Z_3^{(6 \overset{mod\ 4}{=} 2)} |{+}_3\rangle$
- $q_1 = 1,\ q_2 = 2$: $|1_1\rangle \otimes |2_2\rangle \otimes Z_3^{2} |{+}_3\rangle$
- $q_1 = 3,\ q_2 = 2$: $|3_1\rangle \otimes |2_2\rangle \otimes Z_3^{(6 \overset{mod\ 4}{=} 2)} |{+}_3\rangle$

Hence, the reduced density matrix ρ_3 consists of a superposition of two linear independent terms: $\rho_3 \propto |{+}_3\rangle \langle{+}_3| + (Z_3^2 |{+}_3\rangle \langle{+}_3| Z_3^2) = |{+}_3\rangle \langle{+}_3| + |{+}_1\rangle \langle{+}_1|$ and thus, $\mathrm{rank}(\rho_3) = 2$.

Moreover, the calculation of ranks of reduced states can be done graphically as shown in Fig.(4.4). Now, we prove a lemma that will be important in future derivations:

Lemma 4.2. *For a d-dimensional system, the rank of any reduced state of an n-elementary hypergraph state is $d/gcd(d, m_e)$ where m_e is the multiplicity of the hyperedge.*

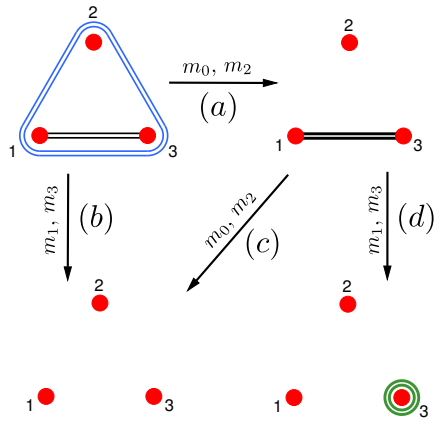

FIGURE 4.4: Measurements in Z-basis on the hypergraph state $|H\rangle = Z^2_{123}Z^2_{13}|+\rangle^V$ $(d=4)$. Measurement on qudit 2 results in (a) for outcomes m_0 or m_2 and (b) for outcomes m_1 or m_3. Now, measuring on qudit 1 results in (c) for outcomes m_0 or m_2 and (d) for outcomes m_1 or m_3. It is clear that any reduced state has rank 2.

Proof. An n-elementary hypergraph state is given by

$$|H\rangle = Z_e^{m_e}|+\rangle^V = \sum_{q=0}^{d-1} |q\rangle\langle q| \otimes (Z_{e\setminus\{1\}}^{m_e})^q |+\rangle^V, \tag{4.44}$$

where $e = \{12\ldots n\}$ is the n-hyperedge. Let us first consider the case where only a single system is traced out. Tracing out subsystem 1, we arrive at

$$\rho_{e\setminus\{1\}} = Tr_1(|H\rangle\langle H|) = \sum_{q=0}^{d-1} \langle q|H\rangle\langle H|q\rangle \tag{4.45}$$

$$= \frac{1}{d}\sum_{q=0}^{d-1} |H_q^{(1)}\rangle\langle H_q^{(1)}| \tag{4.46}$$

where

$$|H_q^{(1)}\rangle = (Z_{e\setminus\{1\}})^{qm_e}|+\rangle^{V\setminus\{1\}}. \tag{4.47}$$

The number of different values (modulo d) of the product qm_e, with $q = 0, 1, 2, \ldots, d-1$ is $d/gcd(d, m_e)$, since in $\mathbb{Z}_d$ one has $m_e q = m_e q'$ iff $q = q'$ modulo $d/gcd(d, m_e)$.

Moreover, the $d/gcd(d, m_e)$ different vectors $|H_q^{(1)}\rangle$ are linearly independent. We prove this via induction on the number of vertices of $V \setminus \{1\}$. For $V \setminus \{1\}$ composed of one vertex, we see that $|H_q^{(1)}\rangle = Z_2^{qm_e}|+_2\rangle$ and

$$\sum_q \alpha_q |H_q^{(1)}\rangle = (\sum_q \alpha_q Z_2^{qm_e})|+\rangle_2 \tag{4.48}$$

where α_q are arbitrary complex numbers. Then, $\sum_q \alpha_q |H_q^{(1)}\rangle = 0$ iff $(\sum_q \alpha_q Z_2^{qm_e}) = 0$. To see this, note that the operators $Z_2^{qm_e}$ are diagonal in the computational basis and the vector $|+\rangle_2$ is an equal superposition of all basis elements. Therefore, $(\sum_q \alpha_q Z_2^{qm_e})|+\rangle_2 = 0$. already implies $(\sum_q \alpha_q Z_2^{qm_e}) = 0$.

Since the Pauli operators form a basis of the Lie algebra $sl_d(\mathbb{C})$ and are thus linearly independent, and given that the operators Z^{qm_e} are Pauli operators, we have that $(\sum_q \alpha_q Z_2^{qm_e}) = 0$ implies that $\alpha_q = 0$ for all q, i.e., the vectors $|H_q^{(1)}\rangle$ are linearly independent.

For $V \setminus \{1\}$ composed of two vertices, $|H_q^{(1)}\rangle = Z_{23}^{qm_e}|+,+\rangle_{2,3}$. By the same argument as above, $|H_q^{(1)}\rangle$ are linearly independent iff $Z_{23}^{qm_e}$ are linearly independent operators. We have

$$\sum_q \alpha_q Z_{23}^{qm_e} = \sum_{q,q'} |q_2'\rangle\langle q_2'| \otimes (\alpha_q Z_3^{q'qm_e}) \tag{4.49}$$

$$= \sum_q{}' |q_2'\rangle\langle q_2'| \otimes (\sum_q \alpha_q Z_3^{q'qm_e}) \tag{4.50}$$

$$= |0_2\rangle\langle 0_2| \otimes (\sum_q \alpha_q I_3) \tag{4.51}$$

$$+ \quad |1_2\rangle\langle 1_2| \otimes (\sum_q \alpha_q Z_3^q) + \ldots \tag{4.52}$$

and hence, $\sum_q \alpha_q Z_{23}^{qm_e} = 0$ can be satisfied only if $\alpha_q = 0$ for all q, since this is the only way to have a null term $|1_2\rangle\langle 1_2| \otimes (\sum_q \alpha_q Z_3^q)$, given that the Z_3^q operators are linearly independent. Thus, $|H_q^{(1)}\rangle$ are linearly independent for $V \setminus \{1\}$ composed of two vertices as well. The general induction argument is now clear and it is obvious that the vectors $|H_q^{(1)}\rangle$ are linearly independent in general. Hence, the rank of $\rho_{e\setminus\{1\}}$ is $d/gcd(d, m_e)$.

One can directly check, using the representation in Eq. (4.25), that if more than one qudit is traced out, the same arguments apply. Thus, the rank of any reduced state is $d/gcd(d, m_e)$. □

4.2.5 SLOCC and LU classes of hypergraphs

SLOCC and LU transformations

Let us shortly review the basic definitions of equivalence of quantum states under local unitary and SLOCC operations. For more details, the Chapter 2 provides a broader overview. The phenomenon of entanglement is a consequence of the physical restriction to local operations by agents separated by space-like distances. It is thus important to identify when it is possible to inter-convert two different quantum states by means of local operations or, more specifically, characterize their equivalence under SLOCC or LU operations. Finding the SLOCC/LU classes to which a given hypergraph state belongs is in general a cumbersome task even in the qubit case. However, in the following, we will present several results and ideas that can be used for tackling this task.

Let us first define the basic notation. Two pure n-partite states $|\phi\rangle$ and $|\psi\rangle$ are equivalent under local unitaries if one has a relation like

$$|\phi\rangle = \bigotimes_{i=1}^{n} U_i |\psi\rangle, \tag{4.53}$$

where the U_i are unitary matrices, acting on the i-th particle. The question whether two multiqubit states are LU equivalent or not can be decided by bringing the states into a normal form under LU transformations [156].

More generally, the states are equivalent under stochastic local operations and classical communication (SLOCC) iff there exist invertible local operators (ILOs) A_i such that

$$|\phi\rangle = \bigotimes_{i=1}^{n} A_i |\psi\rangle. \tag{4.54}$$

Physically, this means that $|\phi\rangle$ can be reached starting from $|\psi\rangle$ by local operations and classical communication with a non-zero probabilitiy.

Although general criteria for SLOCC equivalence of multiparite states do not exist, it is possible to find necessary conditions that are useful as exclusive constraints. For instance, SLOCC transformations clearly can not change the rank of a reduced state ρ_i. Moreover, for special classes of states, sufficient conditions for SLOCC-equivalence can be found.

Tools for SLOCC classification

In this section, we will explain some more refined criteria for proving or disproving SLOCC equivalence. As already mentioned, the rank of the reduced states, $r(\rho_i) = r(\mathrm{tr}_{S\setminus\{i\}}(\rho_S))$ (where S denotes the set of all subsystems) is a simple way of identifying inequivalences.

To find a finer distinction we employ a method based on Ref. [152] that uses a $(1|23\ldots n)$ split of the system to identify types of inequivalent bases of the $(2,3,\ldots,n)$-subspace, which results in a lower bound on the number of actual SLOCC-classes. As we want to infer for a given state its SLOCC-class, there remains the following problem to be solved: identifying the basis which has minimal entanglement in its basis vectors. Accordingly, we refer to this tool as minimally entangled basis (MEB) criterion. A major disadvantage of this method is that with growing number n of subsystems, the entanglement structure within the bases becomes more complex, as it arises recursively from the total number of SLOCC-classes of the $(n-1)$-partite systems.

The MEB of an n-partite quantum state is defined as follows:

Definition 4.2. MEB
Consider a state

$$|\psi_{12\ldots n}\rangle = \sum_{a_1,a_2,\ldots,a_n=0}^{d-1} c_{a_1,a_2,\ldots,a_n} |a_1, a_2, \ldots, a_n\rangle$$

in a $d^{\otimes n}$ system. According to Ref. [152], we define the $d \times (d^{n-1})$ coefficient-matrix $C_{1|2\ldots n}$ as follows:

$$C_{1|2\ldots n} = \sum_{a_1,a_2,\ldots,a_n=0}^{d-1} c_{a_1,a_2,\ldots,a_n} \vec{a}_1 (\vec{a}_2^{\,T} \otimes \ldots \otimes \vec{a}_n^{\,T})$$

where the basis $\{\vec{a}_i\}_{i=0}^{d-1}$ in $\mathbb{R}^d$ represents the basis $\{|a_i\rangle\}_{i=0}^{d-1}$ of a d-dimensional Hilbert space. In other words, $C_{1|2\ldots n}$ is a reshaped matrix of coefficients $c_{a_1,a_2,\ldots,a_n}$ with rows corresponding to the same value of a_1. This matrix holds all information about the entire state. From the singular value decomposition (SVD) of this matrix, $C_{1|2\ldots n} = U_1 D V_{2\ldots n}^{\dagger}$, we can identify a basis $\{v_k\}$ of the right subspace $(2,\ldots,n)$, where individual basis vectors $|v_k\rangle$ might be entangled.
Within this framework, we define a **minimally entangled basis (MEB)** $\{v_k\}_{MEB}$ *of*

$|\psi_{12\ldots n}\rangle$ as the one within which the number of full product vectors is maximal under the condition that it spans the same subspace as $\{v_k\}$.

With this definition, we can state:

Lemma 4.3. *Two n-partite quantum states $|\phi\rangle, |\psi\rangle$ of the same subsystem-dimensionality and equal reduced ranks are SLOCC-inequivalent, if their MEBs have a different number of product vectors.*

Proof. The action of the ILOs A_i, where $i = 1, 2, \ldots n$, on $C_{1|2\ldots n}$ in its SVD is identified to be

$$A_1 U_1 D[(A_2 \otimes \ldots A_n) V_{2\ldots n}]^\dagger. \tag{4.55}$$

We analyse the basis $\{v_k\}$ of the right subspace. The Schmidt rank of each basis vector can be changed by A_1 exclusively, which corresponds to a basis transformation of the subspace. If the states $|\phi\rangle, |\psi\rangle$ are SLOCC equivalent, by definition, there exist ILOs A_i which map $|\phi\rangle$ into $|\psi\rangle$ and thus, map the basis of the right subspace of $|\phi\rangle$ into the basis of the right subspace of $|\psi\rangle$. The MEB of $|\psi\rangle$ will be then a valid MEB for $|\phi\rangle$, implying that the number of product vectors is the same. □

In the above Lemma, we consider states $|\phi\rangle, |\psi\rangle$ that have equal reduced ranks, because otherwise these states are automatically SLOCC-inequivalent and there is no point in calculating their MEBs.

Notice that inequivalent MEBs can exclude SLOCC equivalence, but an equivalence of MEBs does not, in general, guarantee SLOCC-equivalence. An exception is the case where the right subspace is spanned by a complete product basis. The reason is that in this case, they are SLOCC equivalent to a generalized GHZ state:

Lemma 4.4. *Two genuine n-partite entangled quantum states $|\phi\rangle$, $|\psi\rangle$ of the same subsystem-dimensionality and equal reduced single-particle ranks are SLOCC-equivalent, if their MEBs are complete product bases.*

Proof. We show that the existence of a complete product basis within the right subspace is sufficient to find ILOs that transform $|\psi\rangle$ (and $|\phi\rangle$) to the GHZ type state $|\psi_{GHZ}\rangle \sim \sum_{k=0}^{r} \bigotimes_{i=1}^{n} |k\rangle_i$, where r is the rank of the reduced single-particle states.

Let us assume that the basis vectors $|v_k\rangle$ are all product vectors. Therefore, they can be written as

$$|v_k\rangle = \bigotimes_{i=2}^{n} |\phi_i^{(k)}\rangle \tag{4.56}$$

In order to map this onto the GHZ state, we only have to find ILO $A^{(i)}$ on the particles $i = 2, \ldots, n$ such that for any particle the set of states $\{|\phi_i^{(k)}\rangle\}$ is mapped onto the states $\{|k\rangle_i\}$. This is clearly possible: since the reduced state ranks are all r, the set $\{|\phi_i^{(k)}\rangle\}$ consists of r linearly independent vectors. Finally, on the first particle, we have to consider the left basis $|u_k\rangle$. These vectors are orthogonal, and hence, we can find a unitary transformation that maps it to $\{|k\rangle_1\}$. □

Based on the Lemmata presented in this subsection, we wrote computer programs which we regard as tools which we use later for classification of tripartite hypergraphs of dimension 3 and 4. A coarse overview follows about the structure of those programs, for further details on the structure of such programs, see [161].

- **Program 1:**
  The first program checks whether there exist a state ϱ in the subspace spanned by a given set of pure states $|v_i\rangle$ for $i = 1, \ldots, K,\ K \leq d$ that has a positive partial transpose (PPT) with respect to any bipartition [157]. This problem can be formulated as an SDP:

$$\begin{aligned} \min_{\lambda} \quad & 0 \\ \text{subject to} \quad & \varrho = \sum_{ij}^{K} \lambda_{ij} |v_i\rangle\langle v_j|, \\ & \varrho \geq 0, \\ & \forall \text{ bipartitions } M|\overline{M},\ \varrho^{T_M} \geq 0, \\ & \lambda^\dagger = \lambda,\ Tr(\lambda) = 1, \end{aligned} \tag{4.57}$$

  where last condition means λ is a hermitian $K \times K$ matrix with trace 1, and ϱ^{T_M} denotes partial transpose of matrix ϱ with respect to the subsystem M. We use this to prove nonexistence of a product vector in the right subspace $(2, \ldots, n)$ of an n-partite state $|\phi\rangle$, where K is the number of basis vectors in the right subspace. If the above SDP is infeasible, it implies that there is no separable state in the subspace $(2, \ldots, n)$, which in turns implies that there is no product vector. If for some other n-partite state $|\psi\rangle$ there is a product vector in the right subspace $(2, \ldots, n)$, the two states $|\phi\rangle$ and $|\psi\rangle$ are SLOCC-inequivalent according to Lemma 4.3.

- **Program 2**
  The second program is a slight modification of the first one and it checks whether there exists a PPT state of rank K in the subspace spanned by K linearly independent vectors $|v_i\rangle,\ i = 1, \ldots, K,\ K \leq d$. If the optimal value ϵ of the following semidefinite program

$$\begin{aligned} \min_{\lambda, \epsilon} \quad & \epsilon \\ \text{subject to} \quad & \varrho = \sum_{ij} \lambda_{ij} |v_i\rangle\langle v_j|, \\ & \varrho \geq 0, \\ & \forall \text{ bipartitions } M|\overline{M},\ \varrho^{T_M} \geq 0, \\ & \varrho \geq \epsilon \left(\sum_i |v_i\rangle\langle v_i| \right), \\ & \lambda^\dagger = \lambda,\ Tr(\lambda) = 1, \end{aligned} \tag{4.58}$$

  is greater than 0, and if the found PPT state ϱ can be proven to be (fully) separable, then by the range criterion (see Ref. [158]) it means that in the subspace spanned by $|v_i\rangle$, there are K product states which span the same subspace. This program can be used to prove SLOCC-equivalence of states $|\phi\rangle$ and $|\psi\rangle$ according to Lemma 4.4, if for both states the above conditions are satisfied for their right subspace of at least one bipartition.

- **Program 3**
  Finally, it is convenient to perform a numerical optimization in order to find product states $|v_i^p\rangle,\ i = 1, \ldots, K',\ K' \leq K$ in the subspace spanned by the given set of vectors $|v_i\rangle$ for $i = 1, \ldots, K,\ K \leq d$. This can be done by maximizing the purity of the

reduced states (that is, $1 - Tr(\varrho_M^2)$, where $\varrho_M = Tr_M(\varrho)$ is the reduced state of the subsystem M) for each bipartition and minimizing the scalar product $\left|\langle v_i^p | v_j^p \rangle\right|^2$ between the product vectors for each unique pair $\{i, j\}$, $i, j \in \{1, \ldots, K'\}$. Minimizing the scalar products makes the program look for linearly independent vectors which, in the best case, are orthogonal.

As we will see in the next section, for most of the tripartite hypergraph states of dimension 3 and 4, numerical optimization (**Program 3**) gives an explicit form of product states in the right subspace if they exist. Moreover, knowing the exact form of product states for the case where a full product basis exists for both states $|\phi\rangle$ and $|\psi\rangle$ allows us to find an explicit SLOCC transformation between these states.

Tools for LU-classification

Let us now discuss how LU equivalence can be characterized. In principle, this question can be decided using the methods of Ref. [156], but for the examples in the next section some other methods turn out to be useful.

If LU equivalence should be proven, an obvious possibility is to find the corresponding LU transformation directly. This has been used in Theorem 4.1. For proving non-equivalence, one can use entanglement measures such as the geometric measure [149], since such measures are invariant under LU transformations. Another possibility is the white-noise tolerance of witnessing entanglement [150]. The latter method works as follows: For an entangled state which is detected by a witness one can assign an upper limit of white noise which can be added to the state, such that the state can still be detected by that witness. Clearly, if two states are equivalent under LU, they have the same level of white-noise tolerance of entanglement detection. Now, if one considers a class of decomposable witnesses, the estimation of this level for a given state can be accomplished effectively by means of semidefinite programming [151]. Below, we use a method described in Ref. [150] to witness genuine multipartite entanglement of hypergraph states and to determine the corresponding white-noise tolerance of that witness.

4.2.6 Classification of qudit hypergraphs under SLOCC and LU

Using the tools described above and Lemmata 4.2,4.3,following, we present a classification in terms of SLOCC- and LU-equivalence. For special classes of qudit hypergraphs, e.g. elementary hypergraphs, we develop general rules valid for any number of particles and arbitrary dimension. Additionally, for tripartite hypergraph states in dimensions 3 and 4, a full classification of all states within this category considering LU- as well as SLOCC- equivalence is given.

Elementary hypergraphs

We now address the problem of SLOCC classification of n-elementary hypergraph states. The classification depends on the greatest common divisor between the underlying dimension and the hyperedge multiplicity, as show in the following theorem:

Theorem 4.1. Elementary hypergraphs under LU and SLOCC *For a d-dimensional n-partite system, two n-elementary hypergraph states with hyperedge multiplicities k and k' are equivalent under LU, and hence also under SLOCC if and only if $gcd(d, k) = gcd(d, k')$. In case $gcd(d, k) \neq gcd(d, k')$, the states are inequivalent under SLOCC (and LU).*

Proof. If $gcd(d,k) = gcd(d,k')$, we can, according to Proposition 4.1 find a local Clifford transformation with $SZ^kS^\dagger = Z^{k'}$. So we have $S|H\rangle = SZ^k|+\rangle^n = Z^{k'}S|+\rangle^n = Z^{k'}|+\rangle^n = |H'\rangle$ since $S|+\rangle^n = |+\rangle^n$. For the other implication, note that, if $gcd(d,k) \neq gcd(d,k')$, the single-system reduced states have different ranks by Lemma 4.2 and thus the states are not SLOCC equivalent which implies LU inequivalence. □

In other words, the number of different elementary hypergraph SLOCC classes is the number of different values (modulo d) of $gcd(d,k)$, which is obviously the number of divisors of d. It is remarkable that, in this case, SLOCC equivalence is the same as equivalence under Local Clifford operations, by Proposition 4.1. For d being prime, all values $k \in \mathbb{Z}_d$ are obviously coprime with d and hence the following implication is straightforward:

Corollary 4.1. *For d being of prime value, all n-elementary hypergraph states are equivalent under SLOCC.*

In the non-prime case, e.g. dimension $d = 15$, a four-qudit elementary hypergraph of the form $|H\rangle = Z^5_{1234}|+\rangle^{\otimes 4}$ is equivalent to another elementary hypergraph $|H'\rangle$ with $|H'\rangle = Z^{10}_{1234}|+\rangle^{\otimes 4}$: it is $m_e(H) = 5$, $m_e(H') = 10$ and thus $gcd(m_e(H),d) = gcd(5,15) = 5 = gcd(10,15) = gcd(m_e(H'),d)$, see Fig. 4.5.

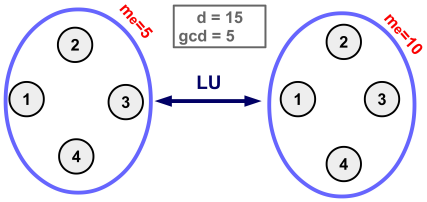

FIGURE 4.5: Elementary hypergraphs in dimension $d = 15$ of $m_e(H) = 5$ (left) and $m_e(H') = 10$ (right) are equivalent under local unitary transformation due to the fact that the multiplicities of their hyperedges are within the same gcd-class. The local unitary conducting the transformation is the symplectic operation $S(\xi,0,0)$ with $\xi^{-1} \cdot 5 \overset{mod\ 15}{\equiv} 10$ and thus $\xi = 8$.

Hypergraphs LU-equivalent to elementary hypergraphs

For elementary hypergraphs, there are also some other hypergraph states belonging to the same equivalence class under local unitary transformations. From Lemma 4.1 and the discussion that followed, one sees that the action of the local gate $X_i^\dagger$ on an n-elementary hypergraph state creates a $n-1$-hyperedge on the neighbourhood of i with equal multiplicity m_e of the n-hyperedge e. Acting k times with this local gate, i.e., application of $(X_i^\dagger)^k$ results in inducing, in the neighbourhood of the qudit i, a $n-1$-hyperedge of multiplicity km_e

$$(X_1^\dagger)^k|H\rangle = (X_1^\dagger)^k Z^{m_e}_{12\ldots n}|+\rangle^{\otimes n} = Z^{m_e}_{12\ldots n} Z^{km_e}_{2\ldots n}|+\rangle^{\otimes n} \tag{4.59}$$

As shown in the proof of Lemma 4.2, the number of different values of the product km_e is given by $d/gcd(d,m_e)$.

$$km_e = (km_e) \bmod d = g[(km'_e) \bmod \frac{d}{g}] \qquad \text{with: } g \equiv gcd(d,m_e),\ m'_e = gm_e \tag{4.60}$$

Hence, only those edges can be created where the multiplicity of the new edge and the multiplicity of the original edge share g as common divisor with d.

Conclusion 4.1. *For a given n-partite elementary hypergraph state of multiplicity m_e with $gcd(d, m_e) = g$, an (n-1)-edge of multiplicity $\tilde{m}_e$ with $gcd(d, \tilde{m}_e) = \tilde{g}$ can be locally created if and only if $\tilde{g} = x \times g$ for $x \in \mathbb{N}$. Therefore for d being of prime value, all hypergraph states with an n-edge are equivalent under LU.*

Thus, the higher the value $g = gcd(d, m_e)$, the smaller the number of possible $n-1$-hyperedges that can be created (or erased) within an elementary hypergraph state.
Following, we give two examples showing local creation of an (n-1)-edge from an n-edge dependent on the gcd-class of the original n-edge. Consider a four-partite elementary hypergraph in dimension $d = 8$. Fig. 4.6 sketches the corresponding LU equivalence classes.

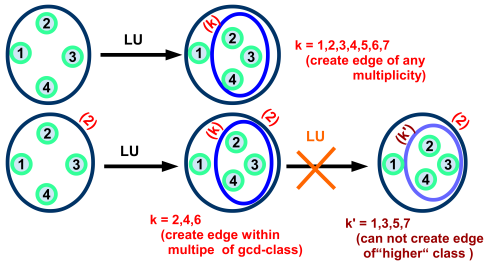

FIGURE 4.6: LU-equivalence classes of four-partite elementary hypergraphs in $d = 8$ with n-edge multiplicity m_e. There are three gcd-classes, $g_1 = gcd(8, m_e) = 1$, $g_2 = gcd(8, m_e) = 2$ and $g_3 = gcd(8, m_e) = 4$. For $gcd(8, m_e) = 1$, (n-1)-edges of arbitrary multiplicity can be created locally by application of the appropriate power of $X_i^\dagger$. If $gcd(8, m_e) = 2$, the options are limited to (n-1)-edges of gcd-classes g_2 and g_3.

4.2.7 Classification of $3 \otimes 3 \otimes 3$

The first example we consider is a tripartite system with dimension $d = 3$. In the following, we give a full classification w.r.t. LU as well as SLOCC equivalence. In the case of a tripartite system of qutrits, there is only one SLOCC equivalence class of hypergraph states and two LU equivalence classes: the GHZ state and the 3-elementary hypergraph state. These two states are inequivalent by LU as they give different values for the geometric measure of entanglement and white noise tolerance (see Table 4.1).

These classes can be derived as follows: Let us first consider the GHZ state. From Appendix B it follows that the GHZ state can be converted to the graph state represented by the local complementation of the GHZ graph via local symplectic unitaries. To see this, consider the transformation from the first graph in Table 4.1 to the second, that is, the creation of an edge Z_{13} in the neighborhood by performing LC on the second qutrit. First, notice that the creation of Z_{13} from the original graph state $|G\rangle = Z_{12}Z_{23}|+\rangle^{\otimes 3}$ can be done by applying X_{12}^2 on $|G\rangle$. Using (4.30), we then have

$$\begin{aligned} X_{12}^2 Z_{23} &= (|0\rangle\langle 0|)_1 \otimes Z_{23} + (|1\rangle\langle 1|)_1 \otimes X_2^2 Z_{23} + (|2\rangle\langle 2|)_1 \otimes X_2 Z_{23} \\ &= (|0\rangle\langle 0|)_1 \otimes Z_{23} + (|1\rangle\langle 1|)_1 \otimes Z_{23} Z_3 X_2^2 + (|2\rangle\langle 2|)_1 \otimes Z_{23} Z_3^2 X_2 \\ &= Z_{23} Z_{13} X_{12} \end{aligned} \tag{4.61}$$

Now, to locally create the necessary controlled X-gate X_{12}, we can use symplectic operations of the form $S(1, 0, \xi)$. From Eq.(4.15), we get $S(1, 0, 2) Z^c S^\dagger(1, 0, 2) = Z^c X^{(2c) \bmod 3} \omega^{(2^{-1} \times 2c) \bmod 3}$

with $2^{-1} = 2$ in dimension three and thus,

$$\begin{aligned} S(1,0,2)_2 Z_{12} S(1,0,2)_2^\dagger &= (|0\rangle\langle 0|)_1 \otimes \mathbb{1}_2 + (|1\rangle\langle 1|)_1 \otimes Z_2 X_2^2 \omega + (|2\rangle\langle 2|)_1 \otimes Z_2^2 X_2 \omega^2 \\ &= Z_{12} Z_1 X_{12}^2. \end{aligned} \tag{4.62}$$

Then, application of $S(1,0,2)_2$ on $|G\rangle$ gives the desired locally complemented graph up to local unitaries Z_1 and Z_3

$$\begin{aligned} S(1,0,2)_2 |G\rangle &= S(1,0,2)_2 Z_{12} S(1,0,2)_2^\dagger S(1,0,2)_2 Z_{23} S(1,0,2)_2^\dagger S(1,0,2)_2 |+\rangle^{\otimes 3} \\ &= Z_{12} Z_1 X_{12}^2 Z_{23} Z_3 X_{23}^2 |+\rangle^{\otimes 3} \\ &= Z_1 Z_3 Z_{12} Z_{23} Z_{13} |+\rangle^{\otimes 3} = Z_1^2 Z_3^2 |G\rangle_{LC} \end{aligned} \tag{4.63}$$

From Proposition 4.1, we see that a hyperedge of arbitrary multiplicity can be converted to an hyperedge of any other multiplicity via local symplectic permutations. Thus, the tripartite GHZ state is equivalent to any other tripartite graph state via local symplectic unitaries.

If we consider the elementary hypergraph state, a 3-hyperdege can be converted to another 3-hyperedge of arbitrary multiplicity via symplectic permutations. In addition, the 3-elementary hypergraph is equivalent to any other 3-hypergraph since edges (2-hyperedges) of arbitrary multiplicities can be created via repeated application of the $X^\dagger$ gate in a neighbouring qutrit. Finally, in order to show the SLOCC equivalence, local invertible operations connecting these two LU subclasses can be achieved by applying A_1 to one of the qutrits of the graph state and $A_{2,3}$ to the other two, where

$$A_1 = \frac{1}{4\sqrt{3}} \begin{pmatrix} -2\sqrt{3}-2i & 4i & 4i \\ -4\sqrt{3}+4i & \sqrt{3}+i & -5\sqrt{3}+7i \\ -6\sqrt{3}-2i & -\sqrt{3}-5i & -\sqrt{3}+7i \end{pmatrix}, \; A_{2,3} = \frac{1}{3} \begin{pmatrix} e^{i2\pi/3} & 1 & 1 \\ \sqrt{3}e^{i\pi/6} & \sqrt{3}e^{i\pi/6} & \sqrt{3}e^{i\pi/6} \\ e^{i2\pi/3} & e^{i2\pi/3} & \frac{5-\sqrt{3}i}{2} \end{pmatrix}. \tag{4.64}$$

These local operations were found with the help of Program 3 (numeric optimization program described in the previous section), which, in this case, gives full product basis for the right subspaces of all states from Table 4.1.

Class	Schmidt ranks	Representatives	Geom. measure/ w-noise tolerance
1	1|23 3 2|13 3 3|12 3	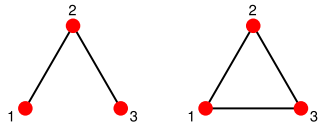	~ 0.66 62.5%
		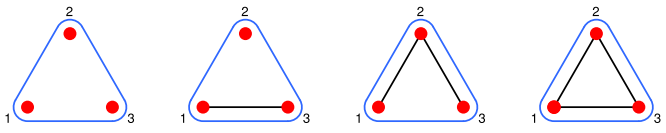	$\sim$ 0.53 $\sim$ 76.0%

TABLE 4.1: Table of SLOCC and LU classes of 3-qutrit hypergraph states. States, which are equivalent to these up to permutations of qutrits, local loops on each qudit and changes of (hyper)edge multiplicities $1 \to 2$, are not shown.

4.2.8 Classification of $4 \otimes 4 \otimes 4$

As a second example, we consider a tripartite system of the smallest non-prime dimension, i.e. $d = 4$. As before, we give a full classification w.r.t. LU as well as SLOCC equivalence. In the case of a tripartite system of ququarts, there are five SLOCC and six LU equivalence classes of hypergraph states. All possible states with respect to permutations and equivalence of edge multiplicities (local Clifford permutation S converts the multiplicity of the 3-hyperedge from 1 to 3 (since $3 = 3^{-1}$ modulo 4, see Proposition 4.1), see also Fig. 4.7b.), are shown in Table 4.2 and the interconversion between representatives within the same class are explained in detail in what follows.

Class 1

Class 1 contains hypergraph states with at least two edges of multiplicity 1 and with either no hyperedges, or with a hyperedge of multiplicity 2. All these states belong to the same LU-equivalence class.

LU-equivalence among the first three state of class 1 (see Table 4.2) is governed by standard local complementation operations, which can be used to create a new edge of multiplicity 1 in the neighborhood of qudit 2, while applying these operations twice generates an edge of multiplicity 2 in the neighborhood of qudit 2. In principle, local complementation works similar to the three qutrit case (see Appendix B for more details). As mentioned in Definition 4.1 and the discussion thereafter, in dimension $d = 4$, the multiplicative inverse 2^{-1} does not exist. By the following argument, it is possible to use $2^{-1} = \frac{1}{2}$: Let $S(1,0,\alpha) = \sum_{m=0}^{3} \omega^{2^{-1}\xi m^2} |m\rangle \langle m|$ with $2^{-1}\xi \equiv \alpha$, $Z^c = \sum_{k=0}^{3} |k \oplus c\rangle \langle k|$ and $X^c = \sum_{i=0}^{3} \omega^{-ic} |i\rangle \langle i|$ be the relevant operations in position basis $\{|p\rangle\}$. For local complementation, controlled $X-$gates X_{12}^c need to be created locally by a local symplectic transformation of the form $S(1,0,\xi) Z S(1,0,\xi)^\dagger = Z X^\xi \omega^{\xi b}$. The calculation for $\xi = 1$ gives

$$\begin{aligned} S(1,0,1) Z S(1,0,1)^\dagger &= \sum_{k=0}^{3} \omega^{-\alpha(2k+1)} |k \oplus 1\rangle \langle k| \\ X Z \omega^b &= \sum_{k=0}^{3} \omega^{-(k+1)+b} |k \oplus 1\rangle \langle k| . \end{aligned} \tag{4.65}$$

Thus, $-\alpha(2k+1) = -(k+1) + b$, i.e. $(2\alpha - 1)k = -\alpha - b + 1$ has to be satisfied for all values of k and we have $\alpha = 2^{-1} \vee \alpha = \frac{1}{2}$. From there, also $b = \frac{1}{2}$ follows. For generation of an edge of multiplicity 1 in the neighborhood, we then can use $S(1,0,3) = \sum_{k=0}^{3} \omega^{-\frac{3}{2}k^2} |k\rangle \langle k|$ and equivalently, for the generation of an edge of multiplicity 2, we apply it twice and have for $|G\rangle = Z_{12} Z_{23} |+\rangle^{\otimes 3}$, $|G\rangle_{LC(1)} = Z_{12} Z_{13} Z_{23} |+\rangle^{\otimes 3}$ and $|G\rangle_{LC(2)} = Z_{12} Z_{13}^2 Z_{23} |+\rangle^{\otimes 3}$

$$\begin{aligned} S_2(1,0,3) |G\rangle &= Z_1^{\frac{3}{2}} Z_3^{\frac{3}{2}} Z_{12} Z_{13} Z_{23} |+\rangle^{\otimes 3} \overset{LU}{=} |G\rangle_{LC(1)} \\ S_2(1,0,3)^2 |G\rangle &= S_2(1,0,3) Z_1^{-\frac{3}{2}} Z_3^{-\frac{3}{2}} |G\rangle_{LC(1)} = |G\rangle_{LC(2)} . \end{aligned} \tag{4.66}$$

The same local complementation is responsible for LU equivalence among the three last states of the first LU class. To prove LU equivalence between these two subgroups of states (with no hyperedge and with a 2-hyperedge) we find the explicit form of their MEBs, which appear to consist of product vectors, using Program 3. It can then be shown that local transformation between these states is unitary. Here, we present such a local unitary for

transformation shown in Figure 4.7e :

$$U_{1,2,3} = \frac{1}{2}\begin{pmatrix} 1+i & 0 & 1-i & 0 \\ 0 & 0 & 0 & -2 \\ 1-i & 0 & 1+i & 0 \\ 0 & -2 & 0 & 0 \end{pmatrix}. \tag{4.67}$$

Class $1'$

Class $1'$ contains all hypergraph states which have a 3-hyperedge of multiplicity 1. LU equivalence of the states within this class is governed by the unitary $(X^\dagger)^m$, which, when applied to some qudit, generates edges of multiplicity m on the neighbourhood of the qudit (see Lemma 4.1).

Class 2

Class 2 consists of two LU equivalence classes. The representative of the first LU-equivalence class are the graph states composed of two and three edges of multiplicity 2, while the representatives of the second LU class are the hypergraph state with a 3-hyperedge of multiplicity 2 with possible edges of multiplicity 2.

We can perform some form of "local complementation" between two states from the first LU class by applying the following unitaries in the basis $\{|p_0\rangle, |p_1\rangle, |p_2\rangle, |p_3\rangle\}$:

$$U_{1,3} = \frac{1}{\sqrt{2}}\begin{pmatrix} 1 & 0 & i & 0 \\ 0 & \sqrt{2} & 0 & 0 \\ -i & 0 & -1 & 0 \\ 0 & 0 & 0 & \sqrt{2} \end{pmatrix}; \quad U_2 = \begin{pmatrix} i & 0 & 0 & 0 \\ 0 & 1 & 0 & 0 \\ 0 & 0 & 1 & 0 \\ 0 & 0 & 0 & 1 \end{pmatrix}. \tag{4.68}$$

Applying the local $(X^\dagger)^m$ unitary to some qudit of the states from the second LU class generates edges of multiplicity $2m$ (i.e., 0 or 2) on the neighbourhood of that qudit.

Using Program 3, one can find the local operation corresponding to SLOCC equivalence between these LU classes. For the representatives shown on the Fig. 4.7d the corresponding LO is

$$A_{1,2,3} = \frac{1}{2}\begin{pmatrix} -i(1+\sqrt[3]{4}) & 0 & (1-\sqrt[3]{4}) & 0 \\ 0 & 2 & 0 & 0 \\ i & 0 & -1 & 0 \\ 0 & 0 & 0 & 2 \end{pmatrix}. \tag{4.69}$$

One can easily check that $A_{1,2,3}$ is invertible but not unitary. To show that there is no local unitary transformation possible, one can look at the entanglement measures for these LU classes (see Table 4.2).

Class 3

The representatives of class 3 are the elementary hypergraph states with a 3-hyperedge of multiplicity 2, one edge of multiplicity 1 and possible edges of multiplicity 2. These three states are in the same LU class and the local transformation between them is $(X^\dagger)$ applied on one of the qudits.

Class 4

The representatives of class 4 are graph states composed of one or two edges of multiplicity 2 and one edge of multiplicity 1. Applying the local unitaries $U_1 = (S(1,1,0))^4$, $U_2 = S(1,0,1)$, $U_3 = S(1,1,0)$ to the first state creates an edge of multiplicity 2 between qudits 2 and 3.

SLOCC-inequivalence of Classes 1-4,1'

To prove the SLOCC-inequivalence of states of most of the classes it is sufficient to look at their Schmidt ranks for each bipartition (see Table 4.2). Exceptions are pairs of classes $1, 1'$ and $3, 4$. To prove that there is no SLOCC transformation between states from classes 3 and 4 let us consider the vectors from the right subspace for bipartition $2|13$ for two representatives from each class. From the Schmidt decomposition of the state from class 3 one finds directly that there is at least one product vector in the right subspace of parties 13, i.e. MEB contains at least one product vector. For the state from class 4, we can prove that in the corresponding subspace there are no product vectors in the MEB using Program 1. Thus, from Lemma 4.3 it follows that these states belong to different SLOCC classes. Unfortunately, we were not able to prove SLOCC-inequivalence of states from classes 1 and $1'$ using the tools presented above. In fact, using Program 3, we found that the states from class 1 have a full product basis in their right subspace for each bipartition and Program showed that for the states from class $1'$ there are states with PPT and full rank in their right subspace. However, the optimal value ϵ of the SDP of Program 2 for the states in class $1'$ had an order magnitude of 10^{-5}. Besides, the direct numerical search for SLOCC transformation bringing a states in class 1 to some state in class $1'$ returned states of fidelity of almost 1, though the numerical search for SLOCC transformation in the opposite direction, from a state in $1'$ to some state in 1, succeed in returning states of fidelity of only 0.875. This difference in fidelities of local transformations in different directions is typical for the three-qubit states of GHZ and W classes, which suggests that classes 1 and $1'$ are inequivalent.

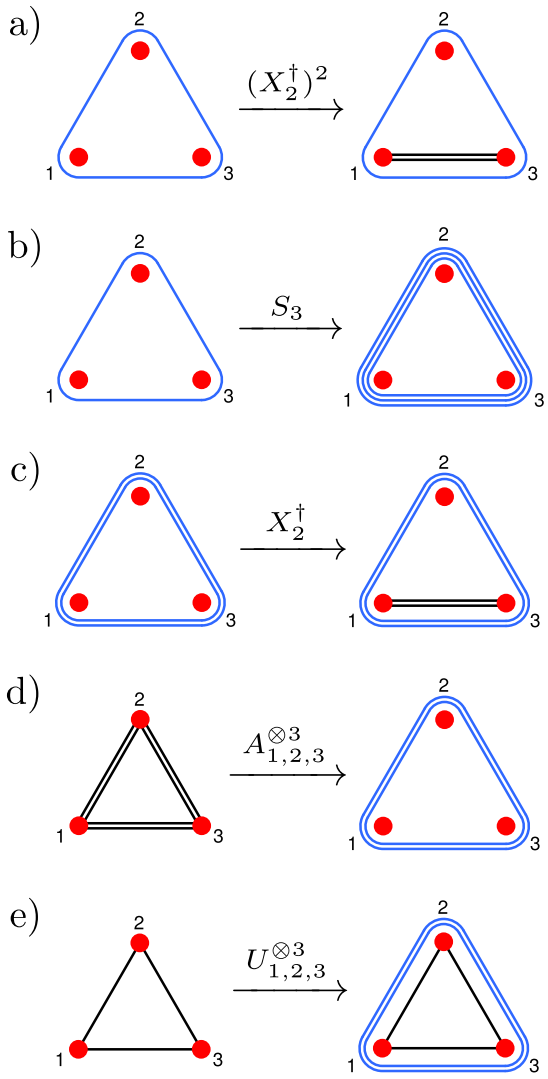

FIGURE 4.7: SLOCC and LU equivalence among representative states of the same SLOCC-class. Picture a): LU-equivalence of two states in SLOCC-class 1' via creation of an (n-1)-edge from an n -edge by the LU $(X_2^\dagger)^2$. Picture b): LU-equivalence between states in SLOCC-class 1' of 3-edges with multiplicity $m_e = 1$ and $m'_e = 3$ as a consequance of Proposition 4.1 and Theorem 4.1, the unitary mediating the transformation, $S_3 = S_3(3, 0, 0)$ is from the symplectic group. Picture c): creation of an (n-1)-edge from an n-edge within SLOCC-class 2 via the LU-operation $X_2^\dagger$. Picture d): SLOCC equivalence between representatives of different LU-classes within SLOCC-class 2 via the invertible, but non-unitary local operation A defined in Eq.(4.69) applied to all ququarts. Picture e): LU-equivalence within SLOCC-class 1 by creation of an 3-edege of multiplicity two from 2-edges of multiplicity one via the local unitaries U as defined in Eq.(4.67).

Class	Schmidt ranks	Representatives	Geom. measure/ w-noise tolerance
1	1|23 4 2|13 4 3|12 4	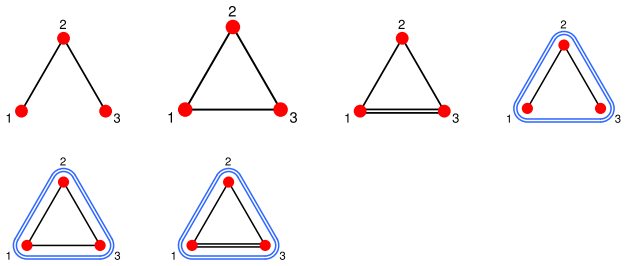	0.75 ∼ 84.2%
1'	1|23 4 2|13 4 3|12 4	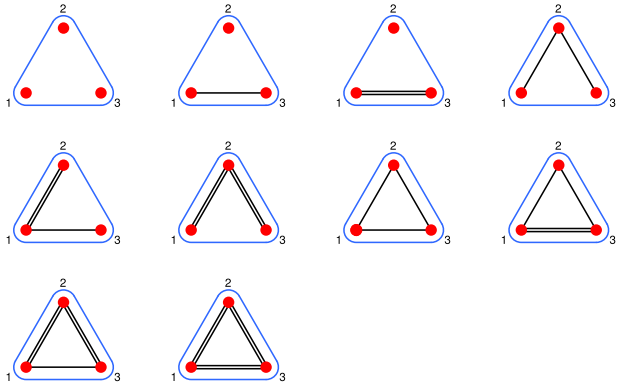	∼ 0.58 ∼ 87.1%
2	1|23 2 2|13 2 3|12 2	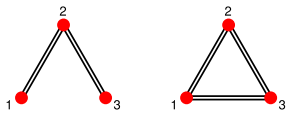	0.50 ∼ 91.4%
		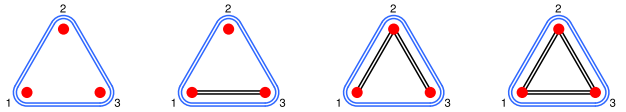	∼ 0.32 ∼ 88.7%
3	1|23 4 2|13 2 3|12 4	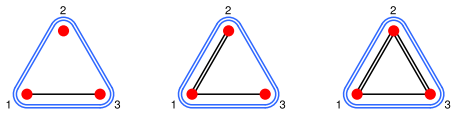	0.75 ∼ 86.1%
4	1|23 4 2|13 2 3|12 4	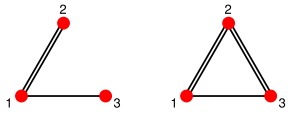	0.75 ∼ 88.8%

TABLE 4.2: Table of SLOCC and LU classes of 3-ququart hypergraph states. States, which are equivalent to these up to permutations of ququarts, local loops on each qudit and changes of (hyper)edge multiplicities $1 \to 3$, are not shown.

4.2.9 Conclusions

In this work, we generalized the class of hypergraph states to systems of arbitrary finite dimensions. For the special class of elementary hypergraph states we obtained the full SLOCC classification in terms of the greatest common divisor, which also governs other properties such as the ranks of reduced states. For tripartite systems of local dimensions 3 and 4, we obtained all SLOCC and LU classes by developing new theoretical and numerical methods based on the original concept of MEBs.

Some open questions are worth mentioning. In the multiqubit case, hypergraph states are a special case of LME states; it would be interesting to generalize the class of LME states to arbitrary dimensions and see if a similar relation holds. Nonlocal properties of qudit hypergraph states were not a part of this work and deserve a separate consideration. Finally, possible applications of these states as a resource for quantum computing should be investigated.

4.2.10 Appendix

Phase-space picture

Infinite-dimensional systems are often described through position and momentum operators Q and P in a phase-space picture. Displacements in this quantum phase-space are performed by unitaries

$$D(q,p) = e^{i(pQ-qP)} \tag{4.70}$$

where q and p are real numbers. These unitaries satisfy

$$D(q,p)D(q',p') = e^{-i(qp'-pq')}D(q',p')D(q,p) \tag{4.71}$$

, characterizing a faithful representation of the Heisenberg-Weyl Lie group. Performing the transformations

$$Q \to \kappa Q + \lambda P; \tag{4.72}$$

$$P \to \mu Q + \nu P, \tag{4.73}$$

subjected to the condition $\kappa\nu - \lambda\mu = 1$, map the Heisenberg-Weyl group onto itself. In other words, unitaries that perform these transformations will generate the normalizer of the Heisenberg-Weyl group. This group constitutes the so-called symplectic group in continuous variables and is related to important concepts in quantum optics such as squeezing.

In finite-dimensional systems it is possible to give an analogous description in terms of a discrete phase-pace, whenever the Hilbert space dimension is a power of a prime number [144]. A general displacement in this discrete phase-space is then performed by an operator $D(m,n) = \omega^{mn2^{-1}}X^nZ^m$; the set of these displacement operators form an unitary representation of the discrete Heisenberg-Weyl group through the multiplication rule

$$D(m,n)D(m',n') = \omega^{(m'n-mn')2^{-1}}D(m+m',n+n').$$

Symplectic transformations in a discrete-phase space act over the Pauli operators in the following fashion

$$SXS^\dagger = \omega^{\kappa\lambda 2^{-1}} X^\kappa Z^\lambda, \tag{4.74}$$
$$SZS^\dagger = \omega^{\mu\nu 2^{-1}} X^\mu Z^\nu, \tag{4.75}$$

subjected to the condition $\kappa\nu - \lambda\mu = 1 \ (mod\ d)$. An arbitrary symplectic operator $S(\kappa, \lambda, \mu)$ can be decomposed as

$$S(\kappa, \lambda, \mu) = S(1, 0, \xi_1) S(1, \xi_2, 0) S(\xi_3, 0, 0) \tag{4.76}$$

where the operators on the right-hand side are given in (4.17), (4.18), (4.19) and

$$\xi_1 = \mu\kappa(1 + \lambda\mu)^{-1}; \tag{4.77}$$
$$\xi_2 = \mu\kappa^{-1}(1 + \lambda\mu); \tag{4.78}$$
$$\xi_3 = \kappa(1 + \lambda\mu)^{-1}. \tag{4.79}$$

The actions of gates (4.18) and (4.19) are given by

$$S(1, \xi, 0) X S(1, -\xi, 0) = \omega^{\xi 2^{-1}} X Z^\xi; \tag{4.80}$$
$$S(1, \xi, 0) Z S(1, -\xi, 0) = Z; \tag{4.81}$$
$$S(1, 0, \xi) Z S(1, 0, -\xi) = \omega^{-\xi 2^{-1}} Z X^\xi; \tag{4.82}$$
$$S(1, 0, \xi) X S(1, 0, -\xi) = X. \tag{4.83}$$

Local complementation of qudit graphs in prime dimension

The graph operation known as local complementation of a graph $G = (V, E)$ at the vertex $a \in V$ consists of the following mapping:

$$G \to G' = (V, E \uplus E_{N_a}) \tag{4.84}$$

where E_{N_a} are the edges in the neighbourhood of a and $\uplus$ denotes the set operation of symmetric sum, i.e., $A \uplus B = \{A \cup B\} \setminus \{A \cap B\}$. The implementation of such an operation for qudit graph states is known in the literature [146] and is restricted to prime-dimensional systems. Here, we give a simpler derivation of this implementation, which is also valid for some special cases in non-prime dimensional systems. Note that we consider only graphs with edges of multiplicity one, which are equivalent to graphs with edges of multiplicity coprime with the underlying dimension d.

From the section on stabilizers of a hypergraph state, we get, as a special case, that the operators

$$K_i = X_i \prod_{e \in E^*} Z_{e \setminus \{i\}} = X_i Z_{N_i}, \quad i \in V \tag{4.85}$$

generate the stabilizer group of the graph state $|G\rangle$ represented by the graph $G = (V, E)$. The graph state $|G\rangle$ is thus the unique $+1$ eigenstate of the operators K_i.

Theorem 4.2. *Given a graph state $|G\rangle$ composed of edges with multiplicity one, let $U_a = S_a(1, 0, -1) S_{N_a}(1, -1, 0)$. Then, $U_a|G\rangle = |G'\rangle$, where G' is the local complementation of G*

at the vertex $a \in V$.

Proof. Let $\{K_i\}_{i\in V}$ denote the set of stabilizer operators of G and let $\mathcal{S}$ be the stabilizer group generated by them. It is clear that $U_a K_i U_a^\dagger = K_i$ if i is not in N_a, while for $c \in N_a$ we have $U_a K_c U_a^\dagger = K_a^{-1} K_c'$, where K_c' is the stabilizer operator for the vertex c of G'. We have then that $U_a \mathcal{S} U_a^\dagger = \mathcal{S}'$, where $\mathcal{S}'$ is the group generated by the stabilizer operators of G'. □

Another way of proving this result is to consider the action of $S_a(1,0,-1)$, which is simply

$$S_a(1,0,-1)|G\rangle = S_{N_a}(1,1,0)|G'\rangle \tag{4.86}$$

Thus, applying $S_{N_a}(1,-1,0)$ on the state above maps G to its local complementation G'.

Proofs of Proposition 4.1

Let us first state the proposition once more:

Propos. 4.1. *Let $k, k' \in \mathbb{Z}_d$ be such that $gcd(d,k) = gcd(d,k') = g$. Then there exists a Clifford operator S defined in Eq. (4.17) such that $S(Z_e)^k S^\dagger = (Z_e)^{k'}$.*

Alternatively to the proof given in the main section, we present two different ways to prove Proposition 4.1:

Proof. Alternative proof 1
We define $k = \alpha g$ and $k' = \beta g$ and consider first a single particle gate Z. Looking at the action of S, $S^\dagger$ and Z on a basis vector $|x\rangle$ one sees that a corresponding S can be found, iff we can find an ξ such that

$$\frac{kx}{\xi} = k'x \mod d \tag{4.87}$$

holds for any x. Dividing by g, this is equivalent to $\alpha x = \beta x \xi \mod (d/g)$. The value of ξ is found by considering first $\xi' = \alpha/\beta \mod (d/g)$. This is well defined, since β and d/g are coprime. It remains to construct a final ξ that is coprime with d. The ξ' fulfills $\beta\xi' = \alpha + y(d/g)$ for some y. It follows that ξ' does not have any prime factors already contained in (d/g) since α and d/g are coprime, but ξ' may still have prime factors present in g (but absent in d/g). If this is the case, we choose $\xi = \xi' + d/g$. This is allowed since ξ' was defined mod (d/g). Now, ξ has no prime factors contained in g (but absent in d/g), and still no prime factors contained in d/g. So, it is coprime to d, and S is unitary.

Finally, if a multiparticle gate Z_e is considered, the proof is the same, starting from the representation in Eq. (4.25). □

Proof. Alternative proof 2
For $gcd(d,k) = 1$, i.e., k is coprime with d, there exists a k^{-1} such that $kk^{-1} = 1$; this multiplicative inverse is given by $k^{-1} = k^{\lambda(d)-1}$, where $\lambda(d)$ is the Carmichael function [159]. The function $f : \mathbb{Z}_d \to \mathbb{Z}_d$ given by $f(q) = qk$ is injective [160], since $qk = q'k$ iff $q = q'$. But it is also surjective since it is a function from $\mathbb{Z}_d$ to itself. Hence, f is a bijection, the unitary $S_k = \sum_{q=0}^{d-1} |q\rangle\langle qk|$ is well-defined and $S_{k-1} Z S_{k-1}^\dagger = Z^k$; notice that this corresponds to the Clifford gate (4.17). Defining the Clifford operator $S = S_{k'-1} S_{k-1}^\dagger$, it follows that $S Z^k S^\dagger = S_{k'-1}(S_{k-1}^\dagger Z^k S_{k-1}) S_{k'-1}^\dagger = S_{k'-1} Z S_{k'-1}^\dagger = Z^{k'}$.

If $gcd(d,k) = g > 1$, then there exists c coprime with d such that $k = gc$. In order to prove this, let us take the prime decomposition of d, i.e., $d = p_1^{n_1} p_2^{n_2} \dots p_N^{n_N}$. Let us consider the decomposition [154, 153] $\mathbb{Z}_d \approx \mathbb{Z}_{d_1} \times \mathbb{Z}_{d_2} \times \dots \mathbb{Z}_{d_N}$, where $d_i = p_i^{n_i}$. Under this

decomposition, any $m \in \mathbb{Z}_d$ is expressed as $m = (m_1, m_2, \ldots, m_N)$, where $m_i = m(mod\ d_i)$. Given c coprime with d, it is straightforward to show that $c = (c_1, c_2, \ldots, c_N)$, where each component c_i is coprime with d_i; indeed, these values c are formed by all possible different combinations of the component values c_i. The only values $k = g\alpha$ which are not already in the form $k = gc$ satisfy $g = p_j^{n_j}$, for some fixed j and $\alpha = p_j^n$, for fixed $1 \leq n \leq n_j$. The decomposition of $k = g\alpha$ is simply $k = (k_1, k_2, \ldots, k_j = 0, \ldots, k_N)$, and the non-zero values k_i, $i \neq j$, are coprime with d_i. Thus, the values c coprime with d for which $c_i = k_i$ for all $i \neq j$ yields $gc = g\alpha = k$.

Let $gcd(d, k) = gcd(d, k') = g$; then there exist c, c' coprime with d such that $k = gc$ and $k' = gc'$ as proved in the discussion above. Let S be the Clifford operator such that $SZ^cS^\dagger = Z^{c'}$. Then, $SZ^kS^\dagger = S(Z^c)^gS^\dagger = (Z^{c'})^g = Z^{k'}$. □

4.3 Local complementation of qudit graph states in arbitrary dimension

Within this section, we derive rules under which local complementation is possible for qudit graph states in arbitrary dimension. Let us start with defining local complementation (LC) within graph states not necessarily of prime dimension. We distinguish between the 'usual' LC and the 'extended' LC which we refer to as ELC. The first allows exclusively for edges of equal multiplicity to be present and created within the graph. The extended version analyzes the case of arbitrary multiplicities which are a unique feature of non-prime dimensional graph states. The aforementioned symplectic operations (SO) with $S = (1, 0, \xi)$ can be used for LC and ELC under the following conditions:

Proposition 4.2. LC und ELC for qudit graph states
Via application of local symplectic operations of the form

$$S(1, 0, \xi) = \sum_{k=0}^{d-1} \omega^{2^{-1}\xi k^2} |k\rangle \langle k| \tag{4.88}$$

we derive the following rules for local complementation

- *LC for prime dimensions.*
  Furthermore, LC for all non-prime dimensions, if and only if the multiplicity m_e of the edges and the system dimension d satisfy

  $$gcd(m_e^2, d) = g \qquad \text{or equivalently} \quad gcd(\frac{d}{g}, g) = 1 \quad \text{with: } g := gcd(d, m_e) \tag{4.89}$$

  The value of ξ associated with the concrete SO is then determined by solving

  $$(-\xi m_e^2) \overset{mod\ d}{=} m_e \tag{4.90}$$

  and in case $m_e = 1$, $\xi = -1$ follows for all dimensions d.

- *ELC for all dimensions. ELC describes the generation of edges of multiplicity $m_e''' = kg\tilde{g}$ with $k \in Rc(\frac{d}{m_e m_e''})$ (where $Rc(\frac{d}{m_e m_e''})$ denotes all values within the modulo-restclass and $\tilde{g} = gcd(\frac{d}{g}, m_e''))$ in the neighborhood of existing edges of multiplicities m_e and m_e''. Here, the concrete SO depends on both, the multiplicity of the new edge to be created*

and the multiplicities of the already present edges. Precisely, to generate an edge of multiplicity m_e''' from edges of multiplicities m_e and m_e'', ξ is determined by solving

$$(-\xi m_e m_e'') \overset{mod\ d}{=} m_e''' \tag{4.91}$$

Following, we will prove the proposition above and give some examples for LC as well as ELC for tripartite systems.

Proof. Let us start with stating the two key points, on which the method of LC and ELC via SO of the form $S(1,0,\xi)$ is based on:

1. We first need the local generation of a controlled $X-$gate on qudits i and j of multiplicity m_e', i.e. $X_{ij}^{m_e'}$, from an existing $Z-$edge connecting qudit i and j of multiplicity m_e, i.e. $Z_{ij}^{m_e}$, while leaving the latter unchanged. The operations performing transformations of this kind are the local symplectic operations $S_i(1,0,\xi)$ on qudit i with:

$$\begin{aligned} S_i(1,0,\xi) Z_i^{m_e} S_i(1,0,\xi)^\dagger &= Z_i^{m_e} X_i^{m_e'} \omega^{-2^{-1} m_e m_e'} \\ S_i(1,0,\xi) Z_{ij}^{m_e} S_i(1,0,\xi)^\dagger &= Z_{ij}^{m_e} X_{ij}^{m_e'} Z_j^{-2^{-1} m_e m_e'} \end{aligned} \tag{4.92}$$

   where $2^{-1} = \frac{1}{2}$ if and only if the system dimension is such that the multiplicative inverse does not exist, that is d is even except for $d = 2$.

2. The generated $X_{ij}^{m_e'}$-gate from 1. then creates a new edge between qudits i and k of multiplicity m_e''', i.e. $Z_{ik}^{m_e'''}$, when applied to an existing edge between qudits i and k of multiplicity m_e'', i.e. $Z_{jk}^{m_e''}$, as

$$X_{ij}^{m_e'} Z_{jk}^{m_e''} = Z_{jk}^{m_e''} Z_{ik}^{m_e'''} X_{ij}^{m e'} \tag{4.93}$$

From 1. it follows that only $X_{ij}^{m_e'}-$gates of multiplicity equal to the multiplicity of the Z-edge they are generated from ,or multiples thereof, can be created.

Lemma 4.5. *Let $S(1,0,\xi)$ be the symplectic operation that acts on a Z-gate as*

$$S(1,0,\xi) Z^{m_e} S(1,0,\xi)^\dagger = Z^{m_e} X^{m_e'} \omega^{2^{-1} m_e m_e'} \tag{4.94}$$

where 2^{-1} is the multiplicative inverse for odd dimension and $d = 2$ and $2^{-1} = \frac{1}{2}$ otherwise. Then $S(1,0,\xi)$ exists if and only if the values of m_e' satisfy $m_e' = n m_e$ with $n \in \mathbb{N}$

Proof. Restrictions on the values of m_e' arise from demanding that

$$S(1,0,\xi) (Z^{me})^{\frac{d}{m_e}} S(1,0,\xi)^\dagger \equiv \mathbb{1} \tag{4.95}$$

needs to be satisfied due to unitarity of $S(1,0,\xi)$ and $Z^d = \mathbb{1}$. Then, for all dimensions, necessity follows from

$$S(1,0,\xi) (Z^{me})^{\frac{d}{m_e}} S(1,0,\xi)^\dagger = (Z^{m_e} X^{m_e'})^{\frac{d}{m_e}} \omega^{2^{-1} d m_e'} \propto X^{d \frac{m_e'}{m_e}} \tag{4.96}$$

with $X^a = \mathbb{1}$ if and only if $a = nd$ with $n \in \mathbb{N}$ and thus, $\frac{m_e'}{m_e} = nd$. To prove that the restriction is sufficient, we have to consider the phases ω^y resulting from the commutation

$X^{m'_e}Z^{m_e} = Z^{m_e}X^{m'_e}\omega^{-m_e m'_e}$. The total number of commutations is calculated using Gauss' sum function

$$(Z^{m_e}X^{m'_e})^{\frac{d}{m_e}} = \underbrace{(Z^{m_e})^{\frac{d}{m_e}}}_{=\mathbb{1}}\underbrace{(X^{m'_e})^{\frac{d}{m_e}}}_{=\mathbb{1}}(\omega^{-m_e m'_e})^{\frac{f(d)}{m_e}} \quad \text{with: } f(d) = \frac{d(d-1)}{2}. \tag{4.97}$$

Combining the phases from the commutation relation and from Eq.(4.96), we have

$$\begin{aligned}\omega^y &= \omega^{2^{-1}dm'_e}(\omega^{-m_e m'_e})^{\frac{d(d-1)}{2m_e}} = \omega^{2^{-1}dm'_e}\omega^{-\frac{m'_e d(d-1)}{2}} \\ &= \begin{cases}\omega^{-\frac{m'_e}{2}d^2} = \omega^{kd} = 1, \quad k \in \mathbb{N} & d: \ even, \ d \neq 2 \\ \omega^{-m'_e(\frac{d-1}{2}+2^{-1})} = \omega^{k'd} = 1, \quad k' \in \mathbb{N} & d: \ odd, \ d = 2.\end{cases}\end{aligned} \tag{4.98}$$

□

Furthermore, from the structure of $S(1,0,\xi)$ given in Eq.(4.80), we identify the value of ξ as

$$\xi \overset{\text{mod } d}{=} \frac{m'_e}{m_e} = \frac{nm_e}{m_e} = n \qquad \text{where: } n \in \mathbb{N}. \tag{4.99}$$

Statement 2. is based on the commutation relation (see also Eq.(4.8))

$$X^{m'_e}Z^{m''_e} = Z^{m''_e}X^{m'_e}\omega^{-m''_e m'_e} = Z^{m''_e}X^{m'_e}\omega^{-nm''_e m_e} \tag{4.100}$$

and its generalization to arbitrary index sets:

$$\begin{aligned}X^{m'_e}_{I'}Z^{m''_e}_{I''} &= Z^{m''_e}_{I''}Z^{d-m'_e m''_e}_{I'''}X^{m'_e}_{I'} \\ \text{where: } I''' &= \begin{cases}\{\} & t(X^{m'_e}_{I'}) \notin \{I''\} \\ (I'' \cup I') - t(X^{m'_e}_{I'}) & t(X^{m'_e}_{I'}) \in \{I''\}\end{cases} \\ \text{and: } t(X^{m'_e}_{I'}) &:= \text{ target index of the set I'.}\end{aligned} \tag{4.101}$$

These rules give clear restrictions as to which edges may or may not be created from existing ones within the original graph. As $m'_e \overset{\text{mod } d}{=} \xi m_e$ (see 1.), because of, 2. the multiplicities m'''_e of the new edge $Z^{m'''_e}_{I'''}$ are restricted to the solutions of

$$\begin{aligned}m'''_e(\xi) &= d - [(\xi m_e m''_e \bmod d] = d - g[(\xi\frac{m_e}{g}m''_e) \bmod (\frac{d}{g})] \\ &= d - g\tilde{g}[(\xi\frac{m_e}{g}\frac{m''_e}{\tilde{g}}) \bmod (\frac{d}{g\tilde{g}})] \\ &\qquad \text{where we used } \tilde{g} = gcd(\frac{d}{g}, m''_e).\end{aligned} \tag{4.102}$$

Let us first consider the consequences of Eq. (4.102) for usual LC. For $m''_e = m'''_e = m_e$, Eq. (4.102) becomes

$$\begin{aligned}m_e(\xi) &= d - (\xi m_e^2 \bmod d) = (-\xi m_e^2 \bmod d) \\ &= g(-\xi x^2 g \bmod y) = gx \\ &\iff \\ &(-\xi x^2 g \bmod y) = x\end{aligned} \tag{4.103}$$

where we used $g = gcd(d, m_e)$ and thus $m_e = xg$ and $d = yg$ with $gcd(x, y) = 1$. Analyzing the term $(-\xi x^2 g \bmod y)$, we need to differ between two possible cases:

- A) $gcd(g, y) = 1$
- B) $gcd(g, y) \neq 1 \quad \longrightarrow \quad g = g'r,\ y = g's \quad \text{with } r, s \in \mathbb{N}$

In case A), for $\xi \in \mathbb{N}$, $D \equiv (-\xi x^2 g \bmod y)$ covers all modulo-restclasses $R_c(y)$ of y, that is $D = Rc(y)$, i.e. $D \in [0, y-1]$. Hence, Eq. (4.103) simplifies to $gD \overset{\text{mod } d}{=} gx$ and obviously, a solution is always possible. For the special case of $m_e = 1$, we have $g = x = 1$ and $y = d$. Hence, Eq.(4.103) takes the form $(-\xi \bmod d) = 1$ and the the value of ξ is $\xi = -1$ for any dimension d.
In case B), Eq. (4.103) takes the form

$$\begin{aligned} m_e(\xi) = gx = g(-\xi x^2 g'r \bmod g's) = gg'(-\xi x^2 r \bmod s) \\ \Longleftrightarrow \\ g'(-\xi x^2 r \bmod s) = x \end{aligned} \tag{4.104}$$

where again $(-\xi x^2 r \bmod s)$ takes values within the modulo-restclass of s, i.e., within the interval $[0, s-1]$. As we know that $gcd(x, y) = 1$, it follows that $gcd(x, g') = gcd(x, \frac{y}{s}) = 1$. Thus, $x \neq g'n$ with $n \in \mathbb{N}$ and Eq.(4.104) has no solution which leaves case A) as the unique possible option for performing LC. Note that from $gcd(\frac{d}{g}, g) = 1$ it readily follows that $gcd(m_e^2, d) = g$ as

$$gcd(m_e^2, d) = gcd(x^2 g^2, yg) = g \cdot gcd(y, g) = g \cdot gcd(\frac{d}{g}, g).$$

This concludes the proof of the first part of the proposition concerning normal LC.
Let us now turn once more to the conditions under which ELC is possible. From Eq. (4.102) it is obvious that only multiplicities $m_e'''(\xi) = g\tilde{g}$ or multiples thereof can be generated. To be precise, $m_e''(\xi) = kg\tilde{g}$ where k may take all values within the modulo-restclass of $\frac{d}{m_e m_e''}$. The value of ξ then follows from solving $(-\xi m_e m_e'') \overset{\text{mod } d}{=} m_e'''$. Finally, notice that for $m_e m_e'' = d$ there is no option of ELC. This can be seen directly from Eq.(4.102), where then $g\tilde{g} = m_e m_e'' = d = m_e'''$. A multiplicity of value d is equal one of value zero and hence no edge is created. □

Following, we will give some examples for LC as well as ELC.

Example 4.2. *: LC, tripartite system,* $d = 6$, $m_e = 3$
From $gcd(d, m_e) = gcd(6, 3) = 3$ and $gcd(m_e^2, d) = gcd(9, 3) = 3 = g$ it follows that LC is possible. The value of ξ is determined by $(-\xi m_e^2) \overset{\text{mod } d}{=} m_e$, i.e., $(-9\xi) \overset{\text{mod } 6}{=} 3$ and therefore $\xi = -1$. The symplectic transformation performing LC is $S(1, 0, \xi = -1) = S(1, 0, 5)$. From the initial graph state $|G\rangle = Z_{12}^3 Z_{23}^3 |+\rangle^{\otimes 3}$, applying $S(1, 0, 5) \equiv S_2$ to qudit two gives:

$$\begin{aligned} S_2 |G\rangle &= (S_2 Z_{12}^3 S_2^\dagger S_2 Z_{23}^3 S_2^\dagger) |+\rangle^{\otimes 3} = (Z_1^{\frac{-3}{2}} Z_3^{\frac{-3}{2}} Z_{12}^3 X_{12}^{-3} Z_{23}^3) |+\rangle^{\otimes 3} \\ &= (Z_1^{\frac{-3}{2}} Z_3^{\frac{-3}{2}} Z_{12}^3 Z_{23}^3 Z_{13}^{(6-3\cdot(-3))} X_{12}^{-3}) |+\rangle^{\otimes 3} = (Z_1^{\frac{-3}{2}} Z_3^{\frac{-3}{2}} Z_{12}^3 Z_{23}^3 Z_{13}^{15} |+\rangle)^{\otimes 3} \end{aligned} \tag{4.105}$$

Where the powers of the local gates $Z_{1|3}^{\frac{-m_e m_e'}{2}}$ are determined by $m_e' \overset{\text{mod } d}{=} \xi m_e$, i.e., $m_e' \overset{\text{mod } 6}{=} -3$ and therefore $\frac{-m_e m_e'}{2} = \frac{9}{2} \overset{\text{mod } 6}{=} \frac{-3}{2}$. Furthermore, in dimension six, $15 \overset{\text{mod } 6}{=} 3$ and

thus, the resulting graph state $S_2 |G\rangle$ is LU-equivalent to the locally complemented graph $|G_{LC}\rangle = Z_{12}^3 Z_{23}^3 Z_{13}^3 |+\rangle^{\otimes 3}$:

$$S_2 |G\rangle = Z_1^{\frac{-3}{2}} Z_3^{\frac{-3}{2}} Z_{12}^3 Z_{23}^3 Z_{13}^3 |+\rangle^{\otimes 3} \overset{LU}{=} |G_{LC}\rangle . \tag{4.106}$$

Example 4.3. *:* **ELC, tripartite system,** $d = 40$**,** $m_e = m_e'' = 12$
From $gcd(d, m_e) = gcd(40, 12) = 4$ and $gcd(m_e^2, d) = gcd(144, 40) = 8 \neq g$ it follows that LC is not possible. Considering ELC, we have $\tilde{g} = gcd(\frac{d}{g}, m_e'') = gcd(10, 12) = 2$. Thus, the generation of edges with multiplicity $m_e''' = kg\tilde{g} = 8k$ with $k \in Rc(\frac{40}{8}) = Rc(5)$, i.e. $0 \leq k \leq 4$, is possible. For $k = 1$, we solve $(-\xi 12^2) \overset{\text{mod } 40}{=} 8$, which results in $\xi = 3$. The symplectic transformation performing ELC is $S(1, 0, \xi = 3)$. From the initial graph state $|G\rangle = Z_{12}^{12} Z_{23}^{12} |+\rangle^{\otimes 3}$, applying $S(1, 0, 3) \equiv S_2$ to qudit two gives:

$$\begin{aligned} S_2 |G\rangle &= (S_2 Z_{12}^{12} S_2^\dagger S_2 Z_{23}^{12} S_2^\dagger) |+\rangle^{\otimes 3} = (Z_1^{24} Z_3^{24} Z_{12}^{12} X_{12}^{36} Z_{23}^{12}) |+\rangle^{\otimes 3} \\ &= (Z_1^{24} Z_3^{24} Z_{12}^{12} Z_{23}^{12} Z_{13}^{(40-12\cdot(36))} X_{12}^{36}) |+\rangle^{\otimes 3} = (Z_1^{24} Z_3^{24} Z_{12}^{12} Z_{23}^{12} Z_{13}^{-392} |+\rangle)^{\otimes 3} \end{aligned} \tag{4.107}$$

Where the powers of the local gates $Z_{1|3}^{\frac{-m_e m_e'}{2}}$ are determined by $m_e' \overset{\text{mod } d}{=} \xi m_e$, i.e., $m_e' \overset{\text{mod } 40}{=} 36$ and therefore $\frac{-m_e m_e'}{2} = -216 \overset{\text{mod } 40}{=} 24$. Furthermore, in dimension $d = 40$, $-392 \overset{\text{mod } 40}{=} 8$ and thus, the resulting graph state $S_2 |G\rangle$ is LU-equivalent to the ELC graph $|G_{LC}\rangle = Z_{12}^{12} Z_{23}^{12} Z_{13}^8 |+\rangle^{\otimes 3}$:

$$S_2 |G\rangle = Z_1^{24} Z_3^{24} Z_{12}^{12} Z_{23}^{12} Z_{13}^8 |+\rangle^{\otimes 3} \overset{LU}{=} |G_{LC}\rangle . \tag{4.108}$$

Example 4.4. *:* **ELC, tripartite system,** $d = 30$**,** $m_e = 2$**,** $m_e'' = 3$
Here, $m_e \neq m_e''$ rules out the option for normal LC. We have $g = gcd(30, 2) = 2$ and $\tilde{g} = gcd(15, 3) = 3$, which allows for the creation of a new edge of multiplicities $m_e''' = k\tilde{g}g = 6k$ with $0 \leq k \leq 4$. For $k = 3$, we solve $(\xi 6^2) \overset{\text{mod } 30}{=} 18$ and find $\xi = 2$. The symplectic transformation performing ELC is $S(1, 0, \xi = 2)$. Furthermore, $m_e' = 4$ and $\frac{-m_e m_e'}{2} = -4$ From the initial graph state $|G\rangle = Z_{12}^2 Z_{23}^3 |+\rangle^{\otimes 3}$, applying $S(1, 0, 2) \equiv S_2$ to qudit two gives:

$$\begin{aligned} S_2 |G\rangle &= (S_2 Z_{12}^2 S_2^\dagger S_2 Z_{23}^3 S_2^\dagger) |+\rangle^{\otimes 3} = (Z_1^{-4} Z_3^{-4} Z_{12}^2 X_{12}^4 Z_{23}^3) |+\rangle^{\otimes 3} \\ &= (Z_1^{-4} Z_3^{-4} Z_{12}^2 Z_{23}^3 Z_{13}^{(30-3\cdot(4))} X_{12}^4) |+\rangle^{\otimes 3} = (Z_1^{-4} Z_3^{-4} Z_{12}^2 Z_{23}^3 Z_{13}^{18} |+\rangle)^{\otimes 3}. \end{aligned} \tag{4.109}$$

The resulting graph state $S_2 |G\rangle$ is LU-equivalent to the ELC graph $|G_{LC}\rangle = Z_{12}^2 Z_{23}^3 Z_{13}^{18} |+\rangle^{\otimes 3}$:

$$S_2 |G\rangle = Z_1^{-4} Z_3^{-4} Z_{12}^2 Z_{23}^3 Z_{13}^{18} |+\rangle^{\otimes 3} \overset{LU}{=} |G_{LC}\rangle . \tag{4.110}$$

With these examples, we conclude the section, having found conditions under which, for a given graph state in arbitrary dimension, LC and a broadened version, ELC, is possible. Here, it is important to stress that for cases which do not allow for LC or ELC under the conditions according to Proposition 4.2, there might still be an option to locally create edges. This is due to the fact that the argumentation within this section is based on LC (or ELC) to be generated by application of local symplectic operations of the form $S(1, 0, \xi)$. This still leaves the option for other local operations to create edges, even though it might not be possible for $S(1, 0, \xi)$. Although we do not have a general way to determine those operations, or make a general statement about their existence, we can give an example in dimension $d = 4$.
Consider the initial graph state with $m_e = m_e'' 2$, $|G\rangle = Z_{12}^2 Z_{23}^2 |+\rangle^{\otimes 3}$. As $g = gcd(4, 2) = 2$ and $gcd(m_e^2, d) = 4 \neq g$, there is no option for LC via $S(1, 0, \xi)$. Furthermore, for ELC, edges

with $m_e''' = kg\tilde{g} = 4k$ could be created with $0 \leq k \leq 1$. Thus, m_e''' is limited to multiples of d and as $Z^d = \mathbb{1}$ this corresponds to no edge at all. Despite this, we found local unitaries U_1 and U_3 of the form given in Eq. (4.68) generating an edge of multiplicity $m_e''' = m_e = 2$.

4.4 Weighted hypergraphs

Within this section, we extend the family of (hyper-)graph states by exchanging the generalized Pauli-Z-gate for the *Z-phase gate*, Z^φ. The phase gate depends on weights in form of complex phases $e^{i\varphi}$ with arbitrary, real valued φ and is defined as

$$Z^\varphi = \mathrm{diag}(1, e^{i\varphi}, e^{2i\varphi}, ..., e^{(d-1)i\varphi}) \qquad \text{with: } \varphi \in \mathbb{R} \tag{4.111}$$

where $Z^\varphi [Z^\varphi]^\dagger = \mathbb{1}$ as $[Z^\varphi]^{-1} = [Z^\varphi]^\dagger = \mathrm{diag}(1, e^{i\varphi}, e^{-2i\varphi}, ..., e^{-(d-1)i\varphi})$. Consequently, a *weighted* (hyper-)graph state, $|H_\varphi\rangle$ can be written as

$$|H_\varphi\rangle = \prod_{I \in E} Z_I^{\varphi_I} |+\rangle^{\otimes V} \tag{4.112}$$

where, as before, E denotes the set of (hyper-)edges, V the set of vertices and I all sets of vertices connected by an (hyper-)edge. Alternatively, we can in analogy to Eq. (4.28), write the state in computational basis

$$|H_\varphi\rangle = \prod_{a=1}^{k} Z_{I_a}^{\varphi_a} |+\rangle^{\otimes n} = \sum_{c_i=0,\ i\in[1,...,n]}^{d-1} \prod_{a=1}^{k} e^{(i\varphi \prod_{i\in I_a} c_i)} \bigotimes_{i=1}^{n} |c_i\rangle \tag{4.113}$$

In analogy to the unweighted graph states, we can describe weighted graph states within the stabilizer formalism. Using the commutation relation $X_i Z_{ij}^\varphi = Z_j^\varphi Z_{ij}^{-\varphi}$, the $n-$th element K_n within the set of stabilizers $\{K_n\}$ of an n-partite weighted qubit graph state is constructed by

$$K_n = \prod_i Z_n^{\varphi_i} X_n \prod_{\bar{m}} X_{\bar{m}} Z_m^{\varphi_{\bar{m}}} \qquad \text{with: } \bar{m} := \forall\ m \neq n \text{ in neighborhood of } n. \tag{4.114}$$

Thus, in case of a three qubit weighted graph with not necessarily equal weights φ, φ' and φ'', the operators stabilizing the corresponding state

$$|G\rangle = Z_{12}^\varphi Z_{13}^{\varphi'} Z_{23}^{\varphi''} |+\rangle^{\otimes 3} = \sum_{ijk=0}^{1} (e^{i\varphi})^{ij} (e^{i\varphi'})^{ik} (e^{i\varphi''})^{jk} \tag{4.115}$$

have the following form:

$$\begin{aligned} K_1 &= Z_1^\varphi Z_1^{\varphi'} X_1 X_2 Z_2^{-\varphi} X_3 Z_3^{-\varphi'}, \\ K_2 &= X_1 Z_1^{-\varphi} Z_2^\varphi Z_2^{\varphi''} X_2 X_3 Z_3^{-\varphi''}, \\ K_3 &= Z_1^{\varphi'} X_2 Z_2^{-\varphi''} Z_3^{\varphi'} Z_3^{\varphi''} X_3. \end{aligned} \tag{4.116}$$

Straightforward calculation gives $K_n |G\rangle = |G\rangle$ for $n = (1, 2, 3)$. For instance, applying K_1 to $|G\rangle$ gives

$$\begin{aligned} K_1 |G\rangle &= Z_1^{\varphi} Z_1^{\varphi'} X_1 X_2 Z_2^{-\varphi} X_3 Z_3^{-\varphi'} Z_{12}^{\varphi} Z_{13}^{\varphi'} Z_{23}^{\varphi''} |+\rangle^{\otimes 3} \\ &= Z_1^{\varphi} Z_1^{\varphi'} X_2 Z_2^{-\varphi} X_3 Z_3^{-\varphi'} Z_2^{\varphi} Z_3^{\varphi'} Z_{12}^{-\varphi} Z_{13}^{-\varphi'} Z_{23}^{\varphi''} |+\rangle^{\otimes 3} \\ &= Z_1^{\varphi} Z_1^{\varphi'} Z_1^{-\varphi} Z_1^{-\varphi'} Z_{12}^{\varphi} Z_{13}^{\varphi'} Z_{23}^{\varphi''} |+\rangle^{\otimes 3} = |G\rangle . \end{aligned} \tag{4.117}$$

Since this introduced generalization gives rise to a significantly bigger family of states, classification of equivalence classes becomes complex even for small dimensions. This is mainly because Z^{φ}, in contrary to the 'normal' Z-gate, has lost the property of the $d-$th power to equal identity, i.e. $[Z^{\varphi}]^d \neq \mathbb{1}$. Thus, there exists no commutation relation of the form $XZ^{\varphi} = Z^{\varphi}Xc$ with $c \in \mathbb{C}$ on which many rules regarding locally generating or deleting edges are based on. Nonetheless, it is possible to make some statements about SLOCC-equivalent (hyper-)graphs as well as the creation of edges from existing ones by using a slight variation of the $X-$gate. Following, we will start with the latter and then move on to special cases, for which we can prove SLOCC-equivalence.

4.4.1 Elementary weighted hypergraphs

In analogy to the class of unweighted hypergraphs, we define an n-partite elementary weighted hypergraph, that is, a hypergraph $|H_{\varphi}\rangle^{elem}$ within which the set of hyperedges has only one element: an hyperedge of some weight φ that connects all vertices

$$|H_{\varphi}\rangle^{elem} = Z_{12\ldots n}^{\varphi} |+\rangle^{\otimes n} . \tag{4.118}$$

Then we can define a class of states LU-equivalent to $|H_{\varphi}\rangle^{elem}$. For dimension d and n qudits, this class is defined by the fact that it is possible to create an edge of a defined weight $(d-1)\varphi$ connecting (n-1) vertices from the existing n-hyperedge of weight φ. The main difference to the unweighted case is that simultaneously, the weight of the original hyperedge is changed to $-\varphi$.

Theorem 4.3. LU-equivalence of elementary weighted hypergraphs
Let $|H_{\varphi}\rangle = Z_{(1\ldots n):=I}^{\varphi} |+\rangle^{\otimes n}$ be an n-partite , d-dimensional elementary weighted hypergraph. Then, the class of weighted hypergraph states defined by

$$|H'_{\varphi}\rangle = Z_{I\setminus\{k\}}^{(d-1)\varphi} Z_I^{-\varphi} |+\rangle^{\otimes n} \qquad k \in I \tag{4.119}$$

is LU-equivalent to $|H_{\varphi}\rangle$.

Proof. We give the proof in detail for d=3, the generalization to arbitrary dimensions is then straightforward. Let $\widetilde{X}$ be a variation of the X-gate, i.e.

$$\widetilde{X} \overset{d=3}{=} |0\rangle\langle 2| + |1\rangle\langle 1| + |2\rangle\langle 0| = \begin{pmatrix} 0 & 0 & 1 \\ 0 & 1 & 0 \\ 1 & 0 & 0 \end{pmatrix} \quad \text{and in general: } \widetilde{X} = \sum_{j=0}^{d-1} |j\rangle\langle (d-1)-j| \tag{4.120}$$

with $\widetilde{X}^{-1} = \widetilde{X}^{\dagger} = \widetilde{X}$, that is, $\tilde{X}$ is unitary and selfadjoint, thus $\widetilde{X}^2 = \mathbb{1}$. Furthermore, with $\widetilde{X}|+\rangle = |+\rangle$, $\widetilde{X}$ inhibits a property that is crucial for staying within the class of weighted

hypergraph states. We then have

$$\widetilde{X} Z^{\varphi} \widetilde{X}^{\dagger} = e^{2i\varphi} \begin{pmatrix} 1 & 0 & 0 \\ 0 & e^{-i\varphi} & 0 \\ 0 & 0 & e^{-2i\varphi} \end{pmatrix} = e^{2i\varphi} Z^{-\varphi} \tag{4.121}$$

The phase $e^{2i\varphi}$ generates the new hyperedge in case $\widetilde{X}$ is applied to a controlled Z-phase gate. To see this, consider the action of $\widetilde{X}$ on Z_{12}^{φ}:

$$\begin{aligned} \widetilde{X}_1 Z_{12}^{\varphi} \tilde{X}^{\dagger} &= (|0\rangle\langle 0|)_1 \otimes Z_2^{2\varphi} + (|1\rangle\langle 1|)_1 \otimes Z_2^{\varphi} + (|2\rangle\langle 2|)_1 \otimes \mathbb{1}_2 \\ &= Z_2^{2\varphi}[(|0\rangle\langle 0|)_1 \otimes \mathbb{1} + (|1\rangle\langle 1|)_1 \otimes Z_2^{-\varphi} + (|2\rangle\langle 2|)_1 \otimes Z_2^{-2\varphi} \\ &= Z_2^{2\varphi} Z_{12}^{-\varphi}. \end{aligned} \tag{4.122}$$

The recursive definition of the controlled Z-phase gate acting on an arbitrary index set I then directly allows for the following rule

$$\widetilde{X}_k Z_I^{\varphi} \widetilde{X}^{\dagger} = Z_{I\setminus\{k\}}^{(d-1)\varphi} Z_I^{-\varphi} \tag{4.123}$$

and thus, applying $\widetilde{X}$ on the $k-$th qudit of an elementary weighted hypergraph leads to

$$\begin{aligned} \widetilde{X}_k |H_{\varphi}\rangle &= \widetilde{X} Z_I^{\varphi} \widetilde{X}^{\dagger} \widetilde{X} |+\rangle^{\otimes n} \\ &= Z_{I\setminus\{k\}}^{(d-1)\varphi} Z_I^{-\varphi} |+\rangle^{\otimes n} \overset{LU}{=} |H_{\varphi}\rangle \end{aligned} \tag{4.124}$$

which hereby proves Theorem 4.3. □

4.4.2 SLOCC equivalence of weighted hypergraphs

Here, we show SLOCC equivalence of all elementary qubit weighted hypergraph states for different weights φ. Additionally, we prove SLOCC equivalence for some chosen tripartite qubit weighted graph-and hypergraph states via a method denoted as 'basis mapping'.

SLOCC equivalence of elementary weighted hypergraphs with different weights

Following, the key points of the used method will be presented in detail for the case of three qubits. The generalization to an arbitrary number of qubits will be motivated by showing that the crucial structure of the proof remains unchanged when the number of qubits increases.

Theorem 4.4. SLOCC equivalence of elementary weighted hypergraphs
Let $|H\rangle$ be an n-qubit elementary hypergraph state of weight φ and let $|H'\rangle$ be an n-qubit elementary hypergraph state of weight φ'. Then,

$$\begin{aligned} |H\rangle = Z_{123}^{\varphi} |+\rangle^{\otimes 3} \quad &\overset{SLOCC}{=} \quad Z_{123}^{\varphi'} |+\rangle^{\otimes 3} \\ &\forall\ \varphi, \varphi' \in \mathbb{R} \ \setminus\ \{(\varphi = n\pi \wedge \varphi' \neq n\pi)\ \vee\ (\varphi' = n\pi \wedge \varphi \neq n\pi),\ n := \text{even}\}. \end{aligned} \tag{4.125}$$

Proof. Consider $|H\rangle = Z_{123}^{\varphi} |+\rangle^{\otimes 3}$ in dimension $d = 2$. Then, the coefficient matrix in the split $(1|23)$ describing $|H\rangle$ is given by

$$C_H = \begin{pmatrix} 1 & 1 & 1 & 1 \\ 1 & 1 & 1 & e^{i\varphi} \end{pmatrix} \qquad \text{and:} \quad C_H^\dagger = \begin{pmatrix} 1 & 1 \\ 1 & 1 \\ 1 & 1 \\ 1 & e^{i\varphi} \end{pmatrix}. \tag{4.126}$$

We prove SLOCC equivalence by showing that the right subspace of C_H, i.e. the matrix $V^\dagger$ within the singular value decomposition of C_H, $C_H = U\Sigma V^\dagger$, is spanned by two product vectors for any weight φ. The singular values σ_i are the roots of the eigenvalues λ_i of $C_H C_H^\dagger$. Solving $\det(C_H C_H^\dagger - \lambda \mathbb{1}) = 0$ gives $\lambda_{1|2} = 4 \pm \sqrt{10 + 6cos(\varphi)}$, and hence, the eigenvectors are $\vec{u_{1|2}} = (\pm \frac{\sqrt{10+6cos(\varphi)}}{3+e^{i\varphi}}, 1)^T$. The vectors $\vec{v_{1|2}}$ spanning the right subspace read:

$$\vec{v_{1|2}} = \frac{1}{\sigma_{1|2}} C_H^\dagger \vec{u_{1|2}} = \frac{1}{\sigma_{1|2}} \begin{pmatrix} \pm\gamma(\varphi) + 1 \\ \pm\gamma(\varphi + 1) \\ \pm\gamma(\varphi) + 1 \\ \pm\gamma(\varphi) + e^{-i\varphi} \end{pmatrix} \qquad \text{where: } \gamma(\varphi) = \frac{\sqrt{10 + 6cos(\varphi)}}{3 + e^{i\varphi}}. \tag{4.127}$$

Performing a basis transformation such that $\vec{v'_{1|2}} = \sigma_1 \vec{v_1} \pm \sigma_2 \vec{v_2}$ and a second one, we get

$$\begin{aligned} \vec{v_1''} &= 0 \times \vec{v_1'} + \frac{1}{2\gamma} \vec{v_2'} = (1, 1, 1, 1)^T \\ \vec{v_2''} &= \gamma(\varphi) \vec{v_1'} - \vec{v_2'} = (0, 0, 0, 2\gamma(\varphi)(e^{i\varphi} - 1))^T \end{aligned} \tag{4.128}$$

which are obviously both product vectors, that is $\vec{v_1} = (|0\rangle + |1\rangle)_2 \otimes (|0\rangle + |1\rangle)_3$ and $\vec{v_2} = 2\gamma(\varphi)(e^{i\varphi} - 1) |11\rangle_{23}$. As this is valid for arbitrary φ, using Lemma 4.4, SLOCC equivalence follows readily. Thus, in case of three qubits, all elementary weighted hypergraph states are within the GHZ-class. Naturally, if $\varphi = n\pi$ with even valued n, it follows that $\sigma_2 = 0$ and hence, the right subspace is spanned by a single product vector, i.e., the state is fully separable $(1|2|3)$.
Increasing the number of qubits does not change the structure of $C_H C_H^\dagger$, i.e., for n parties $\dim(C_H C_H^\dagger) = (2 \times 2^{n-1}) \cdot (2^{n-1} \times 2)$. Thus,

$$C_H C_H^\dagger = \begin{pmatrix} 2^{n-1} & (2^{n-1} - 1) + e^{-i\varphi} \\ (2^{n-1} - 1) + e^{-i\varphi} & 2^{n-1} \end{pmatrix} \tag{4.129}$$

A calculation analogous to the $n = 3$ case gives a full product basis for arbitrary weights φ, thus, all elementary weighted hypergraphs are SLOCC-equivalent to the generalized n-qubit GHZ-state $|GHZ_n\rangle = \bigotimes_{i=1}^n |0\rangle_i + \bigotimes_{i=1}^n |1\rangle_i$ □

Note that this also proves that the structure of the vectors spanning the right subspace can be read out easily by recognizing that $C_H = (\frac{1}{2}\vec{v_1'}, \frac{1}{2\gamma(\varphi)} v_2')$. This property is very useful. To determine their product structure of the basis vectors, one can use C_H directly.

SLOCC-equivalence via basis mapping

Another way of proving SLOCC equivalence, which additionally gives the local operation realizing the transformation from a φ-edge to a φ'-edge, we denote by basis mapping. The

term becomes clear when looking at the most simple example of two qubits.

Lemma 4.6. *Let $|G\rangle$, $|G'\rangle$ be bipartite weighted qubit graph states with corresponding weights φ and φ'. Then, there exist invertible local operations (ILOs) M_1, M_2 such that:*

$$(M_1 \otimes M_2)\,|G\rangle = (M_1 \otimes M_2) Z_{12}^{\varphi}\,|{+}{+}\rangle = Z_{12}^{\varphi'}\,|{+}{+}\rangle = |G'\rangle \\ \forall\ \varphi, \varphi' \in \mathbb{R}\ \setminus\ \{(\varphi = n\pi \wedge \varphi' \neq n\pi)\ \vee\ (\varphi' = n\pi \wedge \varphi \neq n\pi),\ n := \text{even}\}. \tag{4.130}$$

Proof. W.l.o.g, let $\varphi' = \pi$. Then, $Z^{\pi} = Z$ corresponds to the Pauli Z-gate. Now consider the associated graph states

$$\begin{aligned} |G_\pi\rangle &= Z_{12}^{\pi}\,|{+}{+}\rangle = Z_{12}\,|{+}{+}\rangle = |0{+}\rangle + |1{-}\rangle \\ |G_\varphi\rangle &= Z_{12}^{\varphi}\,|{+}{+}\rangle = |0{+}\rangle + |1\rangle\, Z_2^{\varphi}\,|{+}\rangle = |0{+}\rangle + |1\varphi\rangle \qquad \text{with: } |\varphi\rangle = |0\rangle + e^{i\varphi}\,|1\rangle \end{aligned} \tag{4.131}$$

Comparing $|G_\pi\rangle$ and $|G_\varphi\rangle$ in Eq. (4.131), we have to solve the following pair of equations to find the ILOs M_1, M_2 such that Eq. (4.130) is satisfied:

$$\begin{aligned} M\,|{+}\rangle = |{+}\rangle \qquad &\longleftrightarrow \qquad M^{-1}\,|{+}\rangle = |{+}\rangle \\ M\,|\varphi\rangle = |{-}\rangle \qquad &\longleftrightarrow \qquad M^{-1}\,|{-}\rangle = |\varphi\rangle\,. \end{aligned} \tag{4.132}$$

The solution to Eq. (4.132) is given by

$$M = \begin{pmatrix} 1 & 0 \\ -\frac{1+e^{i\varphi}}{1-e^{i\varphi}} & \frac{2}{1-e^{i\varphi}} \end{pmatrix} \qquad \text{and thus:} \quad M^{-1} = \begin{pmatrix} 1 & 0 \\ \frac{1+e^{i\varphi}}{2} & \frac{1-e^{i\varphi}}{2} \end{pmatrix}. \tag{4.133}$$

This proves Lemma 4.6 for $M_1 = \mathbb{1}$ and $M_2 = M$. □

We can now use this result to show SLOCC equivalence between all three qubit weighted graph states with all existing edges of same weight and accordingly for hypergraph states. The argument goes as follows: via basis mapping (or Theorem 4.4) we show that all three qubit weighted hypergraph states are SLOCC equivalent to $|H\rangle = Z_{123}\,|{+}{+}{+}\rangle$ which, in turn, is SLOCC-equivalent to the graph state $|G\rangle = Z_{12}Z_{13}Z_{23}\,|{+}{+}{+}\rangle$. E.g., the locally complemented graph $|G_{LC_2}\rangle = Z_{12}Z_{13}\,|{+}{+}{+}\rangle$, which can be shown to be SLOCC-equivalent to $|G^2_{\varphi,\varphi'}\rangle = Z_{12}^{\varphi}Z_{13}^{\varphi'}\,|{+}{+}{+}\rangle$. Then, we are left with proving SLOCC equivalence between $|G^3_{\varphi,\varphi',\varphi''}\rangle = Z_{12}^{\varphi}Z_{13}^{\varphi'}Z_{23}^{\varphi''}\,|{+}{+}{+}\rangle$ and $|G\rangle$.

Proposition 4.3. *All weighted three qubit (hyper-)graph states are SLOCC equivalent to the GHZ-state*

Proof. The first part of the argument is in principal already covered by Theorem 4.4. Nonetheless, via basis mapping, we can determine the concrete ILO: Consider

$$\begin{aligned} |H_\pi\rangle &= Z_{123}\,|{+}{+}{+}\rangle = |0\rangle\,|{+}{+}\rangle + |1\rangle\, Z_{23}\,|{+}{+}\rangle = |0\rangle\,|{+}{+}\rangle + |1\rangle\,|G_\pi\rangle \\ |H_\varphi\rangle &= Z_{123}^{\varphi}\,|{+}{+}{+}\rangle = |0\rangle\,|{+}{+}\rangle + |1\rangle\, Z_{23}^{\varphi}\,|{+}{+}\rangle = |0\rangle\,|{+}{+}\rangle + |1\rangle\,|G_\varphi\rangle \end{aligned} \tag{4.134}$$

We know from Eq. (4.133) that $(\mathbb{1}\otimes M^{-1})\,|G_\pi\rangle = M_{23}^{-1}\,|G_\pi\rangle = |G_\varphi\rangle$. Furthermore, this ILO leaves $|{+}{+}\rangle$ unchanged,i.e., $M_{23}\,|{+}{+}\rangle = |{+}{+}\rangle$ and thus,

$$\begin{aligned} M_{23}^{-1}\,|H_\pi\rangle &= (\mathbb{1}_{12}\otimes M_3^{-1})\,|H_\pi\rangle = |0{+}{+}\rangle + |1\rangle\,(\mathbb{1}\otimes M^{-1}\,|G_\pi\rangle \\ &= |0{+}{+}\rangle + |1\rangle\,|G_\varphi\rangle = |H_\varphi\rangle\,. \end{aligned} \tag{4.135}$$

For the SLOCC equivalence of $|G_{LC_2}\rangle$ and $|G_\varphi^2\rangle$ consider

$$\begin{aligned} |G_{LC_2}\rangle &= |0{+}{+}\rangle + |1\rangle\,(Z_2\otimes Z_3)\,|{+}{+}\rangle = |0{+}{+}\rangle + |1{-}{-}\rangle \\ |G_\varphi^2\rangle &= |0{+}{+}\rangle + |1\rangle\,(Z_2^\varphi\otimes Z_3^{\varphi'})\,|{+}{+}\rangle = |0{+}{+}\rangle + |1\varphi\varphi'\rangle\,. \end{aligned} \tag{4.136}$$

Therefore, we can use the same ILOs $M_2^{-1}(\varphi)$, $M_3^{-1}(\varphi')$ of the form given in Eq.(4.132) to transform $|G_{LC_2}\rangle$ to $|G_\varphi^2\rangle$

$$(\mathbb{1}_1\otimes M_2^{-1}(\varphi)\otimes M_3^{-1}(\varphi'))\,|G_{LC_2}\rangle = |0{+}{+}\rangle + |1\rangle\,(M_2^{-1}(\varphi)\otimes m_3^{-1}(\varphi')\,|{-}{-}\rangle = |G_\varphi^2\rangle\,. \tag{4.137}$$

The last part, showing SLOCC equivalence between an unweighted three-edge graph state and a weighted graph with arbitrary weights for each edge Z_{ij} is more complex and not easily seen by basis mapping. Thus, we make use of the fact that $|G\rangle = Z_{12}Z_{13}Z_{23}$ is SLOCC equivalent to $|GHZ\rangle$ for three qubits. Then, any state is within the GHZ- class if and only if the minimally entangled basis spanning the right subspace of the coefficient matrix is a full product basis (see Lemma 4.4). The coefficient matrix of $|G^3_{\varphi,\varphi',\varphi''}\rangle$ within the split $(1|23)$ is given by

$$C_H(|G^3_{\varphi,\varphi',\varphi''}\rangle) = \begin{pmatrix} 1 & 1 & 1 & e^{i\varphi} \\ 1 & e^{i\varphi'} & e^{i\varphi''} & e^{i(\varphi+\varphi'+\varphi'')} \end{pmatrix} \qquad \text{with:}\quad \varphi,\varphi',\varphi''\in\mathbb{R}. \tag{4.138}$$

Hence, a basis transformation on systems (23), realizable by an ILO $A = \begin{pmatrix} a & b \\ c & d \end{pmatrix}$ on system (1), gives the new basis vectors

$$\begin{aligned} |v_1'\rangle &= a\,|v_1\rangle + c\,|v_2\rangle = (a+c, a+e^{i\varphi'}c, a+e^{i\varphi''}c, ae^{i\varphi}+e^{i(\varphi+\varphi'+\varphi'')}c)^T \\ |v_2'\rangle &= b\,|v_1\rangle + c\,|v_2\rangle = (b+d, b+e^{i\varphi'}d, b+e^{i\varphi''}d, be^{i\varphi}+e^{i(\varphi+\varphi'+\varphi'')}d)^T \end{aligned} \tag{4.139}$$

where $|v_1\rangle = (1,1,1,e^{i\varphi})^T$ and $|v_2\rangle = (1,e^{i\varphi'},e^{i\varphi''},e^{i(\varphi+\varphi'+\varphi'')})^T$. To guarantee product structure of $|v_1'\rangle$ and $|v_2'\rangle$, there have to exist a,b,c,d in $\mathbb{C}$, such that

$$\begin{aligned} \det(V_1) &= \det\begin{pmatrix} a+c & a+e^{i\varphi'}c \\ a+e^{i\varphi''}c & ae^{i\varphi}+e^{i(\varphi+\varphi'+\varphi'')}c \end{pmatrix} \equiv 0 \\ \det(V_2) &= \det\begin{pmatrix} b+d & b+e^{i\varphi'}d \\ b+e^{i\varphi''}d & be^{i\varphi}+e^{i(\varphi+\varphi'+\varphi'')}d \end{pmatrix} \equiv 0 \end{aligned} \tag{4.140}$$

and, as A has to be invertible, $\det(A) = ab-ac \neq 0$ has to hold. From Eq. (4.140) we derive the following quadratic equation for a,c and, due to the equivalent structure, the same for b,d. This in turn demands two inequivalent solutions, such that $\det(A) = 0$. From Eq. (4.140) we get:

$$a^2(e^{i\varphi}-1) + ac(e^{i(\varphi+\varphi'+\varphi'')} - e^{i\varphi'}) + c^2(e^{i(\varphi+\varphi'+\varphi'')} - e^{i(\varphi+\varphi')}) \equiv 0. \tag{4.141}$$

The solutions exist and are of the form

$$a_{1|2} = -\frac{c}{2(e^{i\varphi}-1)}[(e^{i(\varphi+\varphi'+\varphi'')} - e^{i\varphi'}) \pm \sqrt{e^{i(\varphi+\varphi'+\varphi'')} - e^{i\varphi'})^2 - 4(e^{i(\varphi+\varphi'+\varphi'')} - e^{i(\varphi+\varphi')})(e^{i\varphi}-1)}] \tag{4.142}$$

where we can use $a_1 = a$ and $a_2 = b$ for $c \Leftrightarrow d$. Note that for $\varphi = \varphi' = \varphi'' = \pi$, i.e. $C_H = \begin{pmatrix} 1 & 1 & 1 & -1 \\ 1 & -1 & -1 & -1 \end{pmatrix}$, Eq. (4.142) takes the form $a_{1|2} = \pm ic$. Then, for $c = d = 1$, $A = \begin{pmatrix} i & -i \\ 1 & 1 \end{pmatrix}$. The basis transformed vectors of the right subspace thus read

$$\begin{aligned} |v_1'\rangle &= a\,|v_1\rangle + c\,|v_2\rangle = -\frac{2}{i-1}(1,i,i,-1) \propto (|0\rangle + i\,|1\rangle) \otimes (|0\rangle + i\,|1\rangle) \\ |v_2'\rangle &= b\,|v_1\rangle + c\,|v_2\rangle = -\frac{2}{i+1}(-1,i,i,1) \propto (i\,|0\rangle + |1\rangle) \otimes (i\,|0\rangle + |1\rangle). \end{aligned} \tag{4.143}$$

With this, we have proven that all three qubit graph and hypergraph states, even when allowing for arbitrary weighted edges, are within the same SLOCC class with representative state $|GHZ\rangle$. □

Within the final observation in the field of SLOCC-equivalence classes, we turn the focus on systems of arbitrary dimension $d > 2$. The method of basis mapping, presented in detail in the forgoing part of this section, also proves to be useful when considering two qudit weighted graphs as well as three qudit weighted graphs occupying two edges of not necessarily the same weight.

Proposition 4.4. SLOCC equivalence of bipartite weighted qudit graphs
All two qudit graph states of dimension $d > 2$ with an edge of weight φ are SLOCC equivalent to the corresponding unweighted, i.e. $\varphi = \pi$, graph state

$$|G_\varphi\rangle = Z_{12}^{\varphi}\,|+_0+_0\rangle \overset{SLOCC}{=} Z_{12}\,|+_0+_0\rangle = |G_\pi\rangle \tag{4.144}$$

where $|+_0\rangle = \sum_{n=0}^{d-1} |n\rangle$.

Proof. Consider $|G_\varphi\rangle$ and $|G_\pi\rangle$ in some dimension $d > 2$

$$\begin{aligned} |G_\varphi\rangle &= Z_{12}^{\varphi}\,|+_0+_0\rangle = |0+_0\rangle + |1\varphi\rangle \\ |G_\pi\rangle &= Z_{12}\,|+_0+_0\rangle = |0+_0\rangle + |1+_1\rangle \end{aligned} \tag{4.145}$$

where $|+_1\rangle = Z\,|+_0\rangle = \sum_{n=0}^{d-1} \omega^n\,|n\rangle$ with $\omega = e^{\frac{2\pi i}{d}}$ and $|\varphi\rangle = Z^{\varphi}\,|+_0\rangle = \sum_{n=0}^{d-1}(e^{i\varphi})^n\,|n\rangle$. Then, we need to find 3×3 ILOs $M = \sum_{ij} m_{ij}\,|i\rangle\langle j|$ such that

$$\text{I) } M\,|+_0\rangle = |+_0\rangle \qquad \text{and: II) } M\,|+_1\rangle = |\varphi\rangle \tag{4.146}$$

From I) we get the linear equations $\sum_{j=0}^{d-1} m_{kj} = 1$ for all $k \in [0, d-1]$. II) yields $\sum_{j=0}^{d-1} m_{kj} e^{ij\varphi} = \omega^j$ for all $k \in [0, d-1]$. Solving the system of linear equations gives

$$\begin{aligned} m_{00} = 1,\ m_{0j} = 0 \ \text{ for } \ 1 \le j \le d-1 \\ -m_{i0} = m_{i(d-1)} \ \text{ for } \ 1 \le i \le d-1 \\ m_{il} = \frac{1}{d-2} \ \text{ for } \ 1 \le i \le d-1, \ \ 1 \le l \le d-2 \end{aligned} \tag{4.147}$$

where the matrix elements $m_{i(d-1)}$, for $1 \leq i \leq d-1$ are determined by

$$m_{i(d-1)} = \frac{1}{(1-e^{(d-1)i\varphi})}\left(1-\omega^i+\sum_{n=0}^{d-2}\frac{1}{d-2}(e^{in\varphi}-1)\right). \tag{4.148}$$

As this solution exists for all values of φ and all dimensions $d > 2$, this proves Proposition 4.4:

$$\begin{aligned}(\mathbb{1}_1 \otimes M_2)\,|G_\pi\rangle &= |0\rangle \otimes M_2\,|+_0\rangle + |1\rangle \otimes M_2\,|+_1\rangle \\ &= |0+_0\rangle + |1\varphi\rangle = |G_\varphi\rangle\end{aligned} \tag{4.149}$$

□

From Proposition 4.4 we can directly conclude SLOCC equivalence of all three qudit graph states with weighted edges φ and φ'. This can be seen as follows: consider $|G_{\varphi,\varphi'}\rangle$ and $|G^2_\pi\rangle$ with

$$\begin{aligned}|G_{\varphi,\varphi'}\rangle &= Z^{\varphi}_{12}Z^{\varphi'}_{13}\,|+_0+_0+_0\rangle = |0+_0+_0\rangle + |1\varphi\varphi'\rangle \\ |G^2_\pi\rangle &= Z_{12}Z_{13}\,|+_0+_0+_0\rangle = |0+_0+_0\rangle + |1+_1+_1\rangle\end{aligned} \tag{4.150}$$

Then, via the invertible local matrices $M(\varphi)$ on qudit 2 and $M(\varphi')$ on qudit 3 with matrix elements satisfying Eq. (4.147) and Eq. (4.148), we can perform the transformation from $|G^2_\pi\rangle$ to $|G_{\varphi,\varphi'}\rangle$ for any value of φ and φ' and dimensions three or higher:

$$(\mathbb{1}_1 \otimes M_2(\varphi) \otimes M_3(\varphi')\,|G^2_\pi\rangle = |G_{\varphi,\varphi'}\rangle\,. \tag{4.151}$$

Let us conclude this section with an observation, which is a direct consequence of Proposition 4.4 and its generalization to n-partite qudit systems.

Observation 4.1. SLOCC equivalence of qudit star-graphs
All n-partite qudit star-graph states with not necessarily equivalent weighted edges $Z^{\varphi_j}_{ij}$ with $\{ij\}$ in the set of edges E are SLOCC equivalent to the associated unweighted star-graph:

$$\prod_{j=1}^{n-1} Z^{\varphi_j}_{ij}\,|+\rangle^{\otimes n} \overset{SLOCC}{=} \prod_{j=1}^{n-1} Z_{ij}\,|+\rangle^{\otimes n} \tag{4.152}$$

The term 'star-graph' denotes a graph within which one vertex i is connected to all others and there are no edges apart from those. Furthermore, the ILOs for the SLOCC transformation are of the form given in Eq. (4.147) and Eq. (4.148).

Chapter 5

Characterizing genuine multilevel entanglement

This chapter is dedicated to a novel definition of entanglement within multilevel quantum systems. Whereas high dimensional entanglement hierarchy was up to now mostly characterized by the ability of the state to violate certain inequalities or maximize entanglement monotones, e.g. the entropy of entanglement, it turns out that this definition conducts contradictions when focusing on experimental realization. That is, some of the states classified as highly entangled with respect to the system dimension, are in fact realizable through lower dimensional systems. This poses the question, why one should denote such states as d-level entangled, if there is no need to have access to any d-level system to correctly reproduce all correlations characterizing the state. Based on this, we aim to find a way to define *genuine* multilevel entanglement, such that it is in accordance to an experimental context. I.e., to generate genuine d-level entangled states, it should be necessary to have access to d-level systems. The chapter is organized as follows: Section 5.1 covers the work published in the paper [186], that is, the general theory of defining and characterizing genuine multilevel entangled states in bipartite as well as multipartite scenarios. The following Section 5.2 presents an unpublished analytical method, which allows for a necessary but not sufficient criterion to differ between decomposable and multilevel entangled states. Furthermore, in Section 5.3, we present a generic way to find the lower dimensional representation of qudit-graph states of dimension $d = d_i^k$. Within the last part of this chapter (Section 5.4), an alternative configuration of distributing the lower dimensional qudits is shown. We denote this as network configuration.

5.1 Genuine multilevel entanglement

Entanglement of high-dimensional quantum systems has become increasingly important for quantum communication and experimental tests of nonlocality. However, many effects of high-dimensional entanglement can be simulated by using multiple copies of low-dimensional systems. We present a general theory to characterize those high-dimensional quantum states, for which the correlations cannot simply be simulated by low-dimensional systems. Our approach leads to general criteria for detecting multi-level entanglement in multiparticle quantum states, which can be used to verify these phenomena experimentally.

5.1.1 Introduction

Entangled quantum systems are now routinely prepared and manipulated in labs all around the world, using all sorts of physical platforms. In particular, there has been tremendous progress for creating high-dimensional entangled systems, which can in principle contain a very large amount of entanglement [162, 163, 164]. This makes such systems extremely interesting from the perspective of quantum information science, as they can enhance certain protocols in particular in quantum communications [165, 166]. At first sight, it seems that the tools of entanglement theory can readily be applied to experiments generating high-dimensional entangled states. After a closer look, however, one realizes that this is not the case in general. Let us illustrate our argument via a simple example.

Imagine an experimentalist who wants to demonstrate his ability to entangle two high-dimensional quantum systems. He decides to prepare the optimal resource state, the maximally entangled state, in increasingly large dimensions. First, he successfully entangles two qubits in the state $|\psi_2\rangle = (|00\rangle + |11\rangle)/\sqrt{2}$ and two qutrits in the state $|\psi_3\rangle = (|00\rangle + |11\rangle + |22\rangle)/\sqrt{3}$. While preparing the two ququart maximally entangled state $|\psi_4\rangle = (|00\rangle + |11\rangle + |22\rangle + |33\rangle)/2$ he realizes that he could also prepare the two-qubit Bell state $|\psi_2\rangle$ twice, see Fig. 5.1(a). Clearly, the two copies are equivalent to the maximally entangled state of two ququarts when identifying $|00\rangle_{A_1A_2} \mapsto |0\rangle_A$, $|01\rangle_{A_1A_2} \mapsto |1\rangle_A$, $|10\rangle_{A_1A_2} \mapsto |2\rangle_A$ and $|11\rangle_{A_1A_2} \mapsto |3\rangle_A$. Furthermore, using the source n times, the experimentalist prepares the state $|\psi_2\rangle^{\otimes n}$, which is equivalent to a maximally entangled state in dimension $2^n \times 2^n$. The experimentalist is thus enthusiastic, as he now has access to essentially any entangled state with an entanglement cost of at most n ebits. In particular this should allow him to implement enhanced quantum information protocols based on high-dimensional entangled states, which are proven to boost the performance of certain protocols.

Clearly, the view of the experimentalist is too simplistic and key aspects have been put under the carpet. In order to use the full potential of the state, and thus really claim to have access to high-dimensional entanglement, the experimentalist should be able to perform arbitrary local measurements, including joint measurements between the two subspaces (e.g. photons), which can be non-trivial to implement in certain experimental setups. Ideally, the experimentalist should be able to implement arbitrary local transformations on the local four-dimensional space.

If one focuses on the generated state, however, the known methods of entanglement verification support the naive view of the experimentalist. For instance, there are tools to certify the Schmidt rank of the state [167, 168], but these do not distinguish between many copies of a Bell state and a genuine high-dimensional state. Bell inequalities have been proposed as dimension witnesses for quantum systems [169], but recently it has turned out that these do not recognize the key feature, as independent measurements on two Bell pairs can mimic the statistics of a high-dimensional system [170, 171]. So they just characterize the Schmidt rank in a device-independent manner.

In this work, we characterize the high-dimensional quantum states which give rise to correlations that can not be simulated many copies of small-dimensional systems. This leads to the notion of genuine multi-level entanglement and we show how this can be created and certified. Then we extend this idea to the multiparticle case. Our results imply that many of the prominent entangled states in high dimensions can directly be simulated with small-dimensional systems.

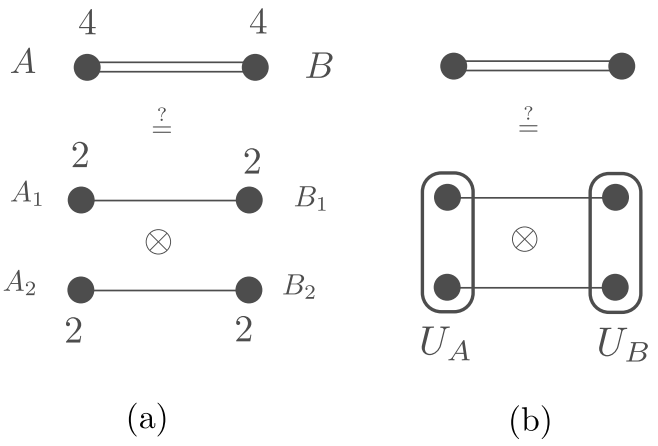

FIGURE 5.1: Left: The four-dimensional maximally entangled state $|\psi_4\rangle$ shared by the parties A and B directly decomposes in two entangled pairs of qubits shared by A_1B_1 and A_2B_2. Right: More generally, we ask whether a high-dimensional entangled state can be decomposed into pairs of entangled systems of smaller dimension, up to some local unitary operations. We show that this is not always possible and characterize those states carrying genuine multi-level entanglement.

5.1.2 The scenario

To explain the scenario, we discuss two entangled four-level systems, also called ququarts. A general two-ququart entangled state can be written in the Schmidt decomposition as

$$|\psi\rangle = s_0 |00\rangle_{AB} + s_1 |11\rangle_{AB} + s_2 |22\rangle_{AB} + s_3 |33\rangle_{AB} , \tag{5.1}$$

where we assume here and in the following the Schmidt coefficients to be ordered, i.e., $s_0 \geq s_1 \geq s_2 \geq s_3 \geq 0$ and $\sum_i s_i^2 = 1$. One can replace each ququart with two qubits, so the total state may also be considered as a four-qubit state. The question we ask is whether it is possible to reproduce any correlations in the two-ququart state by preparing two entangled pairs of qubits only (see Fig. 5.1).

A first approach is to replace on Alice's side $|0\rangle \mapsto |00\rangle$, $|1\rangle \mapsto |01\rangle$, $|2\rangle \mapsto |10\rangle$, and $|3\rangle \mapsto |11\rangle$ and similarly for Bob. Note that this is, so far, not guaranteed to be the optimal assignment of basis states on two qubits to the basis states $\{|0\rangle , |1\rangle , |2\rangle , |3\rangle\}$. This replacement leaves us, after a reordering, with the four-qubit state

$$\begin{aligned} |\psi\rangle &= s_0 |00\rangle_{A_1B_1} |00\rangle_{A_2B_2} + s_1 |00\rangle_{A_1B_1} |11\rangle_{A_2B_2} \\ &+ s_2 |11\rangle_{A_1B_1} |00\rangle_{A_2B_2} + s_3 |11\rangle_{A_1B_1} |11\rangle_{A_2B_2} . \end{aligned} \tag{5.2}$$

Now we ask under which conditions on the Schmidt coefficients this state can be decomposed in the form

$$\begin{aligned} |\varphi\rangle &= (\alpha_0 |00\rangle_{A_1B_1} + \alpha_1 |11\rangle_{A_1B_1}) \\ &\otimes (\beta_0 |00\rangle_{A_2B_2} + \beta_1 |11\rangle_{A_2B_2}). \end{aligned} \tag{5.3}$$

For the coefficients it must hold that $s_0 = \alpha_0\beta_0$, $s_1 = \alpha_0\beta_1$, $s_2 = \alpha_1\beta_0$ and $s_3 = \alpha_1\beta_1$. If $|\psi\rangle$ can be written in this form, we call $|\psi\rangle$ decomposable and otherwise genuinely four-level entangled.

An interesting example is the maximally entangled state of two ququarts, $|\psi_4\rangle = (|00\rangle_{AB} + |11\rangle_{AB} + |22\rangle_{AB} + |33\rangle_{AB})/2$. Here $s_i = 1/2$ and for $\alpha_0 = \alpha_1 = \beta_0 = \beta_1 = 1/\sqrt{2}$ we have $|\psi\rangle = |\varphi\rangle$. Thus the maximally entangled state is decomposable, its correlations are reproducible by two pairs of entangled qubits, and the state is not sufficient to certify genuine four-level entanglement.

In order to decide decomposability for a general $|\psi\rangle$ we compute the maximal overlap between $|\psi\rangle$ and all decomposable states $|\varphi\rangle$:

$$\begin{aligned}\max_{|\phi\rangle} |\langle\psi|\,\varphi|\rangle &= \max_{\alpha_i,\beta_i} \{s_0\alpha_0\beta_0 + s_1\alpha_0\beta_1 + s_2\alpha_1\beta_0 + s_3\alpha_1\beta_1\} \\ &= \max_{\alpha,\beta} \langle\beta|\, S\,|\alpha\rangle = \max \text{singval}(S),\end{aligned} \tag{5.4}$$

where $|\alpha\rangle = (\alpha_0, \alpha_1)^T$, $|\beta\rangle = (\beta_0, \beta_1)^T$ and

$$S = \begin{bmatrix} s_0 & s_1 \\ s_2 & s_3 \end{bmatrix}, \tag{5.5}$$

and $\text{singval}(S)$ denotes the singular values.

Note that up to now, we have not determined the optimal choice for the basis assignment, that is, we used the simple assignment $|0\rangle \mapsto |00\rangle$ etc. introduced above. The optimal assignment can be determined by optimizing over local unitaries on the ququarts. In Appendix A [172] we show that the maximal singular value is obtained if the states $|\psi\rangle$ and $|\varphi\rangle$ have the same Schmidt basis and the remaining freedom encompasses permutations in the assignment of basis elements. As it turns out, the choice of basis we made in the beginning is already optimal. From this we can make the following observation:

Observation 1. *The two-ququart state $|\psi\rangle$ is decomposable if and only if* $\max \text{singval}(S) = 1$. *This is equivalent to* $\det(S) = 0$. *The proof is given in Appendix A [172].*

The extension of decomposability to mixed states is straightforward. We define a mixed state to be decomposable, if it can be written as $\varrho = \sum_i p_i\,|\psi_i\rangle\langle\psi|$ where the $|\psi_i\rangle$ are decomposable, and genuine four-level entangled otherwise. The set of decomposable states $\mathcal{D}$ is convex by definition. This allows to construct witnesses for four-level entanglement. Recall that an operator $\mathcal{W}$ is called an entanglement witness, iff $\text{tr}(\sigma\mathcal{W}) \geq 0$ for all separable states σ and $\text{tr}(\varrho\mathcal{W}) < 0$ for at least one entangled state ϱ [173]. Special types of witnesses are the projector-based witnesses which are of the form $\mathcal{W} = \alpha\mathbb{1} - |\xi\rangle\langle\xi|$, where α is the maximal squared overlap between $|\xi\rangle$ and the decomposable states [174]. In order to detect as many states as possible, we chose $|\xi\rangle$ to be the state with the largest distance to $\mathcal{D}$, meaning that α is as small as possible. The state $|\xi\rangle$ can be determined by minimizing the maximal singular value of S according to Eq. (5.4). According to the derivation of Observation 1 the maximal overlap is a function of the squared determinant. Thus we have to distinguish between positive and negative values of the determinant, giving two interesting states $|\xi_i\rangle$, see Appendix B [172] for details:

Observation 2. *The following two states locally maximize the distance to the decomposable states: For* $\det(S) < 0$ *the Schmidt-rank three state*

$$|\xi_1\rangle = \frac{1}{\sqrt{3}}(|00\rangle + |11\rangle + |22\rangle) \tag{5.6}$$

has the largest distance with $\alpha = [(3+\sqrt{5})/6]^{\frac{1}{2}} \simeq 0.934$ *to the set of decomposable states. For* $\det(S) > 0$ *the Schmidt-rank four state*

$$|\xi_2\rangle = \sqrt{\frac{3}{4}}\,|00\rangle + \frac{1}{2\sqrt{3}}(|11\rangle + |22\rangle + |33\rangle) \tag{5.7}$$

maximizes the distance with a value of $\alpha = [(3+2\sqrt{2})/6]^{\frac{1}{2}} \simeq 0.986$ *to the set of decomposable states.*

5.1.3 General theory for bipartite systems

Let us start by considering only decompositions in two lower-dimensional states. In this case the results from the previous section still hold, only the matrix S increases according to the dimensions of the subsystems. This leaves us with the problem that the maximal singular value depends on the encoding, which defines the arrangement of Schmidt coefficients in the matrix S.

As an example we consider the embedding of the rank-four state from Eq. (5.1) in a 6×6 dimensional system, that is, each party has a qubit and a qutrit. Using the encoding $|0\rangle \mapsto |00\rangle, |1\rangle \mapsto |01\rangle, |2\rangle \mapsto 02, |3\rangle \mapsto |10\rangle, |4\rangle \mapsto |11\rangle, |5\rangle \mapsto |12\rangle$ we obtain the matrix S_1 whereas using $|0\rangle \mapsto |00\rangle, |1\rangle \mapsto |01\rangle, |2\rangle \mapsto 10, |3\rangle \mapsto |11\rangle, |4\rangle \mapsto |02\rangle, |5\rangle \mapsto |12\rangle$ we obtain a different matrix S_2. The matrices are given by

$$S_1 = \begin{bmatrix} s_0 & s_1 & s_2 \\ s_3 & s_4 & s_5 \end{bmatrix}, \qquad S_2 = \begin{bmatrix} s_0 & s_1 & s_4 \\ s_2 & s_3 & s_5 \end{bmatrix} \tag{5.8}$$

and can lead to different singular values. For instance, if we embed the two-ququart state $|\psi_4\rangle$ in this configuration, i.e., $s_0 = s_1 = s_2 = s_3 = 1/2$ and $s_4 = s_5 = 0$, we find that $\max \operatorname{singval}(S_1) \neq 1$, whereas $\max \operatorname{singval}(S_2) = 1$. Consequently, when deciding decomposability, it is crucial to optimize over all possible permutations of entries in S. As the number of permutations grows super-exponentially, it is in general hard to compute this for increasing dimensions.

Nevertheless, the complexity can be reduced, as we have to consider only those permutations, which lead to different maximal singular values. First, note that given two probability distributions $\{p_i\}$ and $\{q_i\}$ the sum over the products $\sum_i \sqrt{p_i q_i}$ is maximal iff both are ordered in the same way. We can further assume in Eq. (5.4) that $\alpha_0 \geq \alpha_1$ and similarly for β_i, since exchanging the components of α and β correspond to exchanging rows or columns of S, which does not change its singular values. This implies that the entries of $|\alpha\rangle\langle\beta|$ decrease in each row and column. Different values for α_i and β_i thus lead to different arrangements. Consequently, we have to optimize S under the constraints that the entries of S must be non-increasing in each row from left to right and in each column from top to bottom. From the theory of Young tableaux [175] it follows that under these constraints for a decomposition into $d = d_1 \times d_2$ there are at most

$$\mathcal{N} = \frac{(d_1 \times d_2)!}{\prod_{i=1}^{d_1}\prod_{j=1}^{d_2}(i+j-1)} \tag{5.9}$$

different matrices that could lead to different singular values (see Appendix C [172]). Furthermore, the Master thesis of Tristan Kraft gives a more detailed discussion regarding Young tableaux and the connection to the rank of the Schmidt matrix. Examples of this approach

for maximally entangled states embedded in higher dimensions can be found in Appendix B [172].

Furthermore, if one is only interested in decomposability, it suffices to check whether there exists an arrangement such that S has rank one. This adds further restrictions since the rows and columns must be linearly dependent. The number of possible arrangements reduces to at most (see Appendix C [172])

$$\mathcal{N}' = \frac{(d_1 + d_2 - 2)!}{(d_1 - 1)! \times (d_2 - 1)!}. \tag{5.10}$$

It should be noted that an equivalent problem and solution has been considered in quantum thermodynamics, where one may ask whether the correlations in a bipartite system can drop to zero under global unitaries [176].

To complete the discussion, one may also take into account a decomposition of the system into more than two lower-dimensional subsystems. In this case, the matrix S becomes a tensor and thus deriving an analytical expression, equivalent to the singular value decomposition, is difficult. However, there is an iterative algorithm ,which can be used to calculate the maximal overlap between the original state and a given set of decomposable states (see Appendix E [172]).

5.1.4 Multiparticle systems

We call an N-partite pure state $|\psi\rangle$ in $(\mathbb{C}^D)^{\otimes N}$ fully decomposable iff there exist N-partite states $|\varphi\rangle$, $|\varphi'\rangle$ of dimension d, d' such that:

$$|\psi\rangle = U_1 \otimes \cdots \otimes U_N \, |\varphi\rangle \otimes |\varphi'\rangle \,, \tag{5.11}$$

for some $d \times d' = D$. Here, the U_i denote the unitaries each party applies to their local subsystems. This definition is in analogy to full separability in entanglement theory [174]. A state that is not fully decomposable is multipartite multi-level entangled (MME).

If a state is non-decomposable according to Eq. (5.11), there might exist partitions under which such states are decomposable. For instance, a state may be decomposable, if the unitary on the first two particles is allowed to be nonlocal, i.e., we may set $U_1 \otimes U_2 \mapsto U_{12}^{\mathrm{nl}}$. More generally, there may be a bipartition of the N particles for which the state is decomposable.

Observation 3. *Consider an N-particle state $|\psi\rangle$. If there exists a bipartition $M|M'$ of the N particles for which the state is decomposable, the state is called bidecomposable. Otherwise the state is genuinely multipartite multi-level entangled (GMME). Verifying GMME for pure states can be done by applying the methods for bipartite systems to all bipartitions.*

To show that a pure multiparticle state is not fully decomposable is, however, not straightforward, as there is in general no Schmidt decomposition for systems consisting of more than two parties [177]. Nevertheless, an iterative algorithm can be utilized, which we explain in Appendix E [172]. Note that within the optimally decomposed state, the largest block that cannot be decomposed any further identifies the minimal number of parties and dimensions needed to reproduce the correlations in the original state. Also, the definitions above can be readily generalized to mixed states by considering convex combinations. In the following sections, we discuss examples, which are relevant for current experiments.

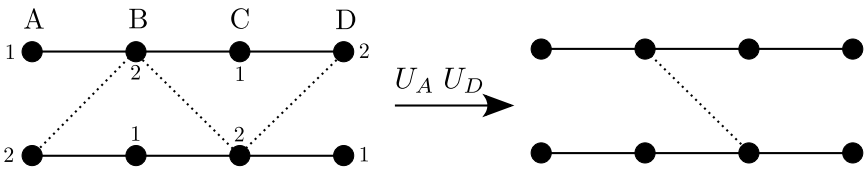

FIGURE 5.2: Examples of weighted graph states. Left: The four-ququart chain-graph state from Eq. (5.14) can be encoded into a weighted graph state of eight qubits, see Eq. (5.16). Right: After application of the unitaries $U_{A_1A_2}$ and $U_{D_2D_1}$ the state exhibits decomposability with respect to the bipartitions $A|BCD$, $D|ABC$ and $AD|BC$ [see Eq. (5.17)] and thus the original ququart state is bidecomposable and not GMME.

Example 1: Generalized GHZ states.— Motivated by our result from the bipartite case that the maximally entangled state is decomposable, we start with studying Greenberger-Horne-Zeilinger (GHZ) states, $|GHZ^{(D)}\rangle = \frac{1}{\sqrt{D}}(|0\cdots0\rangle + |1\cdots1\rangle + \cdots + |(D-1)\cdots(D-1)\rangle)$ for N particles with local dimension D.

First, we observe that the GHZ state is fully decomposable. In fact, it is decomposable with respect to the finest factorization of the local dimension D, given by the prime decomposition $D = \prod_{j=1}^{k} d_j$ of D, as we can write:

$$|GHZ^{(D)}\rangle \overset{enc.}{=} \bigotimes_{j=1}^{k} |GHZ^{(d_j)}\rangle\,, \tag{5.12}$$

where $|\varphi_j\rangle$ represents the N-partite state of the subsystem with dimension d_j.

The proof of Eq. (5.12) is straightforward. We just have to replace each level $|i\rangle$ (with $i \in [0, D-1]$) of the original state with its respective encoding into the lower levels $|i_1, \ldots, i_k\rangle$ where each i_j has dimension d_j and as such values $\in [0, d_j - 1]$ for all j. The ordering of the encoding is chosen such that the value within the respective number system is increasing, that is it corresponds to a binary encoding for qubits ($d_j = 2$), ternary for qutrits ($d_j = 3$), and similarly for higher dimensions. This leads to $|0\rangle \mapsto |0\ldots0\rangle, ..., |D-1\rangle \mapsto |\bigotimes_j(d_j-1), \ldots, \bigotimes_j(d_j-1)\rangle$. Following this encoding process, a reordering, that is

$$(A_1 \ldots A_n, B_1 \ldots B_n, \ldots) \mapsto (A_1B_1 \ldots, \ldots, A_nB_n \ldots),$$

directly reveals the tensor structure of the encoded state with respect to every factor d_j. In Appendix D [172] we give the calculation for a six-dimensional GHZ state. Furthermore we show there that the absolutely maximally entangled state of six qubits represents a decomposable three-ququart state in the GHZ class.

This example shows that all the correlations of a GHZ state in high dimensions, although having a high Schmidt-rank for the bipartitions, can be simulated by low-dimensional systems. This is distinct from other approaches that have been made, such as the Schmidt number vectors from Ref. [178] or the criterion in Ref. [179], where the GHZ state was used to detect higher-order entanglement. For completeness, a proof of the LU-equivalence between GHZ- and the star-type graph states used in Ref. [179] is given in Appendix D [172].

Example 2. Graph states.— A D-dimensional weighted graph state can be written as [180, 181]

$$|G\rangle = \prod_{\{ij\}\in E} Z^{\alpha}_{\{ij\}}\, |+^D\rangle^{\otimes V}\,, \tag{5.13}$$

where V denotes the set of vertices, E the set of edges connecting two vertices i and j and $|+^D\rangle$ is given by $|+^D\rangle \propto |0\rangle + |1\rangle + ... + |D-1\rangle$. Entanglement is created by the controlled Z-gates $Z^{\alpha}_{\{ij\}} = \sum_{g=0}^{d-1} (|g\rangle\langle g|)_i \otimes Z_j^{g\alpha}$, where $Z_q = \sum_{q=0}^{D-1} \omega^q |q\rangle\langle q|$ (with $\omega = e^{2\pi i/D}$) defines the single-qudit Z-gate. For $\alpha = 1$ the structure reduces to non-weighted graph states, for $\alpha = \frac{1}{2}$ the weighted edges can be graphically represented by dashed lines.

As an example for a state which is MME but not GMME, let us consider the chain graph state of four ququarts:

$$|G^{(4)}\rangle = Z_{AB} Z_{BC} Z_{CD} |+^4\rangle^{\otimes 4}. \tag{5.14}$$

Encoding to eight qubits gives us the state (see Fig. 5.2, detailed calculations can be found in Appendix D [172]):

$$\begin{aligned} |G^{(2)}\rangle = {} & Z_{A_1B_1} Z_{B_1C_1} Z_{C_1D_1} Z_{A_2B_2} Z_{B_2C_2} Z_{C_2D_2} \\ & \times Z^{\frac{1}{2}}_{A_2B_1} Z^{\frac{1}{2}}_{B_1C_2} Z^{\frac{1}{2}}_{C_2D_1} |+^2\rangle^{\otimes 8}. \end{aligned} \tag{5.15}$$

Now we apply two-qubit unitaries of the form $U_{ij} = |+\rangle\langle+|_i \otimes \mathbb{1}_j + |-\rangle\langle-|_i \otimes Z_j^{3/2}$ with $|\pm\rangle = (|0\rangle \pm |1\rangle)/\sqrt{2}$ on the two qubits of system A and D respectively and end up with

$$U_{A_1A_2} U_{D_2D_1} |G^{(2)}\rangle = Z^{\frac{1}{2}}_{B_1C_2} |G^{(2)}_{\mathcal{D}}\rangle, \tag{5.16}$$

where

$$|G^{(2)}_{\mathcal{D}}\rangle = Z_{A_1B_1} Z_{B_1C_1} Z_{C_1D_1} Z_{A_2B_2} Z_{B_2C_2} Z_{C_2D_2} |+^2\rangle^{\otimes 8} \tag{5.17}$$

is a fully decomposable state with no diagonal edges.

Thus for the bipartitions $A|BCD$ or $D|ABC$ the state is decomposable and thereby not GMME. In fact, for the given state we find decomposability with respect to every possible bipartition (see Appendix D [172]). For claiming multi-level entanglement, we still have to exclude full decomposability. As mentioned before, this is a difficult task. We applied a numerical algorithm (Appendix E [172]) which strongly indicates non-decomposability with an maximal overlap of 0.8536 with the set of fully decomposable states.

Example 3. A genuine multilevel entangled state.— As a final example, consider the three ququart state

$$|\psi^{(4)}\rangle = \sum_{j=0}^{3} |u_j\rangle |j\rangle |u_j\rangle - 2 |3\rangle |3\rangle |3\rangle, \tag{5.18}$$

where $|u_0\rangle = |0\rangle + |1\rangle + |2\rangle + |3\rangle$, $|u_1\rangle = |0\rangle - |1\rangle + |2\rangle - |3\rangle$, $|u_2\rangle = |0\rangle + |1\rangle - |2\rangle - |3\rangle$, $|u_3\rangle = |0\rangle - |1\rangle - |2\rangle + |3\rangle$. This state corresponds to the six-qubit state $|\psi^{(2)}\rangle = Z_{123456} Z_{13} Z_{35} Z_{24} Z_{46} |+^{(2)}\rangle$, a graph state with an additional hyperedge connecting all vertices [182]. For this state we found for all bipartitions the Schmidt coefficients to be $s_0 = 0.551$, $s_1 = s_2 = 0.5$, $s_3 = 0.443$ which leads to a non-zero determinant of $\det(S) = -0.0059$. Hence, $\mathrm{rank}(S) \neq 1$ for all bipartitions and the state is non-decomposable for any bipartition. Conclusively this state is GMME, to be exact, genuine 3-partite 4-level entangled.

5.1.5 Conclusion

In conclusion, we have introduced the notion of genuine multi-level entanglement. This formalizes the notion of high-dimensional entanglement that cannot be simulated directly with low-dimensional systems. We have provided methods to characterize those states for the bipartite and multipartite case, including the construction of witnesses for an experimental

test. The results can be interpreted as a cautionary tale with regards to naively employing standard entanglement characterization tools. Whereas under general local operations and classical communication, multiple copies of small dimensional systems are universal, this is not the case anymore in restricted scenarios, even having access to all possible local unitaries. This suggests that in practice, high-dimensional quantum systems do present a fundamentally different resource under realistic conditions.

For future research there are different topics to address. First, one may consider network scenarios, where a high-dimensional quantum state is distributed between several parties, and the correlations should be explained by low-dimensional states shared between subsets of the parties. Second, it would be desirable to develop a resource theory of high-dimensional entanglement, where not only the state preparation, but also the local operations (like filters) of the parties are considered. This may finally lead to a full understanding of quantum information processing with high-dimensional systems.

5.1.6 Appendix

A: Proof of Observation 1

Here we prove Observation 1, which states that a two ququart state is decomposable iff $\max \operatorname{sinval}(S) = 1$, where

$$S = \begin{bmatrix} s_0 & s_1 \\ s_2 & s_3 \end{bmatrix}. \tag{5.19}$$

First, let us consider two bipartite ququart states $|\psi\rangle$ and $|\varphi\rangle$. We prove that the maximal overlap between $|\psi\rangle$ and $|\varphi\rangle$, where each party is allowed to perform local unitary operations, is given by:

$$F_{max} = \max_{U_A, U_B} |\langle\psi| U_A \otimes U_B |\varphi\rangle| = \sum_{i=0}^{D-1} \eta_i \sigma_i \tag{5.20}$$

where $\eta_0 \geq \cdots \geq \eta_3 \geq 0$ are the Schmidt coefficients of the state $|\psi\rangle$ and $\sigma_0 \geq \cdots \geq \sigma_3 \geq 0$ are the Schmidt coefficients of the state $|\varphi\rangle$. This was already shown in Ref. [183], but we add this here for completeness. We start by writing the overlap in terms of coefficient matrices of the states $|\psi\rangle$ and $|\varphi\rangle$, that is, we write $|\psi\rangle = \sum_{i,j} C_\psi^{ij} |ij\rangle$ as $C_\psi = \sum_{ij} C_\psi^{ij} |i\rangle \langle j|$, and similarly for $|\varphi\rangle$. We have

$$\begin{aligned} F_{max} &= \max_{U_A, U_B} |\langle\psi| U_A \otimes U_B |\varphi\rangle| \\ &= \max_{U_A, U_B} |\mathrm{tr}(C_\psi^\dagger U_A C_\varphi U_B^T)| \\ &= \sum_{i=0}^{D-1} s_i(C_\psi) s_i(C_\varphi). \end{aligned} \tag{5.21}$$

In the last step of Eq. (5.21) we used von Neumann's trace inequality:

$$|\mathrm{tr}(\Lambda\Gamma)| \leq \sum_i \lambda_i \gamma_i \tag{5.22}$$

which holds for all complex $n \times n$ matrices Λ and Γ with ordered singular values $\lambda_i \leq \lambda_{i-1}$ and $\gamma_i \leq \gamma_{i-1}$. It was proven in Ref. [184] that equality in Eq. (5.22) can only be reached when Λ and Γ are simultaneously unitarily diagonalizable and hence both states need to have

the same Schmidt basis. Therefore it is optimal to choose the encoding between the four-dimensional systems and the qubits in the Schmidt basis. Furthermore note that the singular values of the coefficient matrices are nothing but the Schmidt coefficients of the state. For the 2×2 matrix S the maximal singular value is given by

$$\alpha = \sqrt{\frac{1}{2}(1 + \sqrt{1 - 4\det(S)^2})}. \tag{5.23}$$

Hence, we find that $\max \text{singval}(S) = 1$ iff $\det(S) = 0$, which finishes the proof of Observation 1. Other encodings lead to the same result since changing the encoding, can, for the special case of two qubits, be described by swapping rows or columns of S, which does not change its singular values. Note that for higher-dimensional systems (e.g., a qubit and a qutrit) the last point is not true, and this is the reason, why we have to consider different matrices S there [see Eq. (5.8) in the main text].

B: Witnesses for the bipartite case

Here we show how to construct a witness operator for four-level entanglement. We are seeking for the state $|\xi\rangle$ which has the largest distance to the set of decomposable states and the smallest coefficient α such that the witness $\mathcal{W} = \alpha \mathbb{1} - |\psi\rangle\langle\psi|$ is positive on all decomposable states. Note that since $\mathcal{D}$ is a convex set, it is sufficient to optimize over all pure decomposable states. In order to find $|\xi\rangle$ we compute

$$\begin{aligned} \alpha = \min_S & [\max \text{singval}(S)] \\ \text{s. t.:} \quad & \det(S) \neq 0, \\ & s_0^2 + s_1^2 + s_2^2 + s_3^2 = 1, \\ & s_0 \geq s_1 \geq s_2 \geq s_3 \geq 0. \end{aligned} \tag{5.24}$$

First note that the maximal singular value of a 2×2 matrix is of the form of Eq. (5.23). In the following we separately analyse the cases $\det(S) < 0$ and $\det(S) > 0$.

For $\det(S) < 0$ we have to minimize $\det(S) = s_0 s_3 - s_1 s_2$. Since s_3 is by definition the smallest coefficient we choose $s_3 = 0$. Then we are left with $\max s_1 \cdot s_2$. For fixed s_0, we have that

$$s_1^2 + s_2^2 = const. \tag{5.25}$$

which is the equation of a circle. Therefore the problem is equivalent to maximizing the area of a rectangle with one corner at the origin and the other one on the circle defined by Eq. (5.25). The obvious solution is therefore $s_1 = s_2$. Since $s_0 \geq s_1$ the maximum is obtained at $s_0 = s_1 = s_2 = \frac{1}{\sqrt{3}}$.

For $\det(S) > 0$ we have to maximize $\det(S) = s_0 s_3 - s_1 s_2$. Therefore we have for any given s_0, s_3 to minimize $f(s_1) = s_1 \cdot s_2 = s_1\sqrt{C - s_1^2}$ such that $s_0 \geq s_1 \geq s_2 \geq s_3 \geq 0$ and $C = 1 - s_0^2 - s_3^2$. The minimum of the function $f(s_1)$ is obtained at the boundary for $s_1 = s_3$, which implies $s_2 = s_3$. Therefore the maximum of the determinant is obtained at $s_1 = s_2 = s_3 = \frac{1}{2\sqrt{3}}$ and $s_0 = \sqrt{3/4}$.

We see that for dimension four the state with the largest distance to the set of decomposable states is the maximally entangled state of two qutrits. We observe that for increasing dimensions the distance between the maximally entangled states with lower dimension and the set of decomposable states decreases. Some analytical and numerical values are shown in

Source	rank	overlap
$2 \times 2\,(\mathbf{4})$	3	$\sqrt{\frac{1}{6}(3+\sqrt{5})} \simeq 0.934$
$2 \times 3\,(\mathbf{6})$	5	$\sqrt{\frac{1}{10}(5+\sqrt{17})} \simeq 0.955$
$2 \times 4\,(\mathbf{8})$	5	$\sqrt{\frac{1}{10}(5+\sqrt{17})} \simeq 0.955$
	7	$\sqrt{\frac{1}{14}(7+\sqrt{37})} \simeq 0.966$
$3 \times 3\,(\mathbf{9})$	5	$\sqrt{\frac{1}{10}(5+\sqrt{17})} \simeq 0.955$
	7	$\sqrt{\frac{1}{14}(7+\sqrt{33})} \simeq 0.954$
	8	$\sqrt{\frac{1}{16}(7+\sqrt{48})} \simeq 0.965$
$2 \times 4\,(\mathbf{10})$	7	$\sqrt{\frac{1}{14}(7+\sqrt{37})} \simeq 0.966$
	9	$\sqrt{\frac{1}{18}(9+\sqrt{65})} \simeq 0.973$
$2 \times 6\,(\mathbf{12})$	7	$\sqrt{\frac{1}{14}(7+\sqrt{37})} \simeq 0.966$
	9	$\sqrt{\frac{1}{18}(9+\sqrt{65})} \simeq 0.973$
$7 \times 7\,(\mathbf{49})$	11	$\sqrt{\frac{1}{22}(11+\sqrt{101})} \simeq 0.9781$

TABLE 5.1: This table shows the analytical and numerical fidelities of the maximally entangled state $|\psi\rangle = 1/\sqrt{D}\sum_{i=0}^{D-1}|ii\rangle$ with all decomposable states for a given dimension of the source.

Table 5.1. This might lead to the conclusion that the multi-level entangled states get closer to the set of decomposable states for larger dimensions. However, a proof that the maximally entangled states are the ones having the largest distance to the set of decomposable states is still missing.

C: Connection to the theory of Young tableaux

In this section we want to discuss the relation between the number of arrangements of Schmidt coefficients in the matrix S and the number of standard Young tableaux. First let us recall the definition of a Young diagram. Given some number $N \in \mathbb{N}$ we call $\lambda = (\lambda_1, \lambda_2 \cdots, \lambda_n)$ a partitioning of the number N, that is $\sum_k \lambda_k = N$, $\lambda_1 \geq \lambda_2 \geq \cdots \geq \lambda_n$, and $\lambda_i \in \mathbb{N}$. Then a Young diagram is an arrangement of left-justified rows, where the number of boxes in the k-th row is given by λ_k (see Fig. 5.3).

A Young tableau of shape λ is a filling of the numbers $1, 2, \cdots, n$ into the boxes of the Young diagram such that every number appears exactly once. A Young tableau is called standard if the numbers are increasing in each row and each column. From here it is straightforward to see that this problem is equivalent to the problem of finding the number of possible arrangements of the Schmidt coefficients in the matrix S under the constraints that we discussed in the main text. The number of possible arrangements that could lead to different maximal singular values is simply given by the number of standard Young tableaux consisting of $d_1 \times d_2$ boxes, arranged in a single block. This number is given by the so-called hook-length formula [175]

$$\mathcal{N} = \frac{n!}{\prod_{(i,j)} h_{i,j}}, \tag{5.26}$$

where $h_{i,j}$ is called a hook-length of the box (i, j). For a given box (i', j'), its hook consists of all boxes with either $(i = i', j > j')$ or $(i > i', j = j')$ and the box itself. The length of the hook is then given by the number of boxes in the hook. For a Young tableau of $d_1 \times d_2$ boxes

$$N = 8 \qquad \lambda = (4, 3, 1)$$

1	2	6	7
3	5	8	
4			

FIGURE 5.3: This figure shows an example of a standard Young tableau for $N = 8$ and a partitioning $\lambda = (4, 3, 1)$. The numbers $1, \ldots, 8$ are arranged in such a way that their values increase in each row and each column.

this simplifies to

$$\mathcal{N} = \frac{(d_1 \times d_2)!}{\prod_{i=1}^{d_1} \prod_{j=1}^{d_2} (i + j - 1)}. \tag{5.27}$$

In case one is only interested whether or not a state is decomposable, the number of different matrices that lead to a maximal singular value of one can be further reduced. This is due to the additional constraint that, if the matrix S has rank one, all the rows as well as the columns must me mutually linearly dependent. Then, it is easy to see that the following algorithm can solve the problem. We start again by filling the Schmidt coefficients in an array such that their values are non-increasing in each row and each column. We can fix the upper left entry to be the largest element. Whenever we get in a situation, in which we fix the constant between two rows or columns we check whether there are some remaining Schmidt coefficients which lead to linearly dependent rows or columns. If this is the case, we fill the array with the appropriate number and continue. If these numbers do not exist, we abort and have to start all over again with a different arrangement. It is obvious that, if there exists an arrangement which leads to a matrix with rank one, then the algorithm will find it. Using the formalism of Young tableaux we can again calculate the maximum number of different matrices that we need to check. First note that when we apply the algorithm, we always fix the values of the entries in the first row and the first column. The only thing that changes is the order in which we fill the entries. The number of all possible ways to do this is again given by a number of standard Young tableaux consisting of a single row and a single column. By applying the hook length formula we obtain

$$\begin{aligned} \mathcal{N}' &= \frac{(d_1 + d_2 - 1)!}{(d_1 + d_2 - 1) \times (d_1 - 1)! \times (d_2 - 1)!} \\ &= \frac{(d_1 + d_2 - 2)!}{(d_1 - 1)! \times (d_2 - 1)!}. \end{aligned} \tag{5.28}$$

D: Examples

In this section, we provide some notes on Example 1 (fully decomposable state) as well as a detailed proof for Example 2 (MME state) for the multipartite exemplary states given in the main text. Furthermore we present another interesting fully decomposable state of six qubits.

Example 1. GHZ States

LU-equivalence of GHZ- and star-type graph states. Here we show the equivalence of star-type graph states and GHZ states in arbitrary dimension and system size under local unitary (LU) operations. Decomposability is a property of a state, which does not change

under LU-operations on the original state, therefore it is sufficient to show that $|G_{star}\rangle \overset{LU}{=} |GHZ^{(D)}\rangle$ for any dimension D and any number of qudits N.

Star-type graphs are graphs where one central vertex is connected to any other vertex by an edge, and no other edges are present. For the corresponding quantum state we have according to Eq. (5.13) in the main text $|G_{star}\rangle = \prod_{q=2}^{N} Z_{1q} |+\rangle^{\otimes N}$. This can be simplified to:

$$\begin{aligned} |G_{star}\rangle &= \sum_{p=0}^{N-1} |p\rangle_1 \bigotimes_{q=2}^{N} |+_p\rangle_q \\ &\propto |0\rangle_1 |+_0\rangle_2 \dots |+_0\rangle_N + |1\rangle_1 |+_1\rangle_2 \dots |+_1\rangle_N \\ &\quad + \dots + |D-1\rangle_1 |+_{D-1}\rangle_2 \dots |+_{D-1}\rangle_N . \end{aligned} \tag{5.29}$$

Here we use the (D-dimensional) single qudit states $|+_i\rangle = \frac{1}{\sqrt{D}} \sum_{k=0}^{D-1} \omega^{ki} |k\rangle$ with $\omega = e^{2\pi i/D}$, note that $|+_0\rangle = |+^D\rangle$ in our previous notation. Since $\langle +_i|+_j\rangle = \delta_{ij}$, the set $\{|+_i\rangle\}$ forms a basis of $\mathbb{C}^D$. Eq. (5.29) is, up to local rotations on all subsystems except the first, equal to $|GHZ^{(D)}\rangle$.

Full decomposability of a $6 \times 6 \times 6$ system To clarify the proof of Eq. (5.12) in the main text, we exemplary do the complete calculation for a system of three parties each of which has dimension six, such that the prime decomposition $D = 2 \times 3$ equals access to a qubit and a qutrit. The state, up to normalization, reads $|GHZ^{(6)}\rangle = \sum_{\ell=0}^{5} |\ell\ell\ell\rangle$. The encoding and resorting of the order, which groups the subsystems of the qubits and qutrits respectively, then gives the six-partite state

$$\begin{aligned} |GHZ^{(6)}\rangle &\overset{enc.}{=} |000000\rangle + |010101\rangle + |020202\rangle \\ &\quad + |101010\rangle + |111111\rangle + |121212\rangle \\ &\overset{res.}{=} |000000\rangle + |000111\rangle + |000222\rangle \\ &\quad + |111000\rangle + |111111\rangle + |111222\rangle \\ &= (|000\rangle + |111\rangle) \otimes (|000\rangle + |111\rangle + |222\rangle), \end{aligned} \tag{5.30}$$

which shows decomposability into $|GHZ^{(2)}\rangle$ and $|GHZ^{(3)}\rangle$. The generalization to an arbitrary number of systems N and arbitrary dimension D follows straightforward.

Example 2: Graph states

Here we present the calculation for the four-ququart graph states, see also Fig. 5.4 and Fig. 5.2 in the main text. To start, the chain graph state of $N = 4$ ququarts is given by

$$\begin{aligned} |G^{(4)}\rangle &= \tilde{Z}_{AB} \tilde{Z}_{BC} \tilde{Z}_{CD} |+^4\rangle^{\otimes 4} \\ &= \sum_{ABCD=0}^{3} \omega_{(4)}^{AB} \omega_{(4)}^{BC} \omega_{(4)}^{CD} |ABCD\rangle . \end{aligned} \tag{5.31}$$

Here $\tilde{Z}_{ij} = \mathrm{diag}(1, i, -1, -i)$ is the ququart controlled Z-gate and $\omega_{(4)} = e^{2\pi i/4} = i$. We use the computational basis $|ABCD\rangle$ to simplify the encoding process. The ququarts corresponding to (A, B, C, D) are decomposed into two qubits each with the following labels $(A_1, A_2, B_1, B_2, C_1, C_2, D_1, D_2) = (1, 2, 4, 3, 5, 6, 8, 7)$, see Fig. 5.4(a).

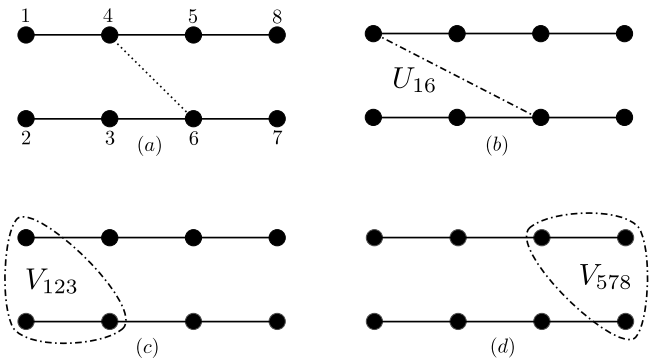

FIGURE 5.4: Example of a state that is MME but not genuine MME. The four-ququart chain-type graph is encoded into LU-equivalent eight-qubit states. (a): The equivalence to this state has already been shown in the main text, see Fig. 5.2. (b): The state is also equivalent to this configuration, see Eq. (5.37). (c) and (d): These equivalences follow from Eq. (5.35). In summary, the state is decomposable with respect to all possible bipartitions.

To represent the ququart state, we make the replacements: $A \to 2A_1 + A_2$, $B \to 2B_2 + B_1$, $C \to 2C_1 + C_2$ and $D \to 2D_2 + D_1$, as this reproduces for an additional replacement of the $\sum_{A,B,C,D=0}^{3} \to \sum_{A_1 \ldots D_2=0}^{1}$ the same exponents as in Eq. (5.31). Then we have:

$$\begin{aligned} |G^{(4)}\rangle &\overset{enc.}{=} |G^{(2)}\rangle \\ &= \sum_{A_1 \ldots D_2=0}^{1} \omega_{(4)}^{(2A_1+A_2)(2B_2+B_1)} \omega_{(4)}^{(2B_2+B_1)(2C_1+C_2)} \\ &\qquad \omega_{(4)}^{(2C_1+C_2)(2D_2+D_1)} |A_1 A_2 B_1 B_2 C_1 C_2 D_1 D_2\rangle \,. \end{aligned} \tag{5.32}$$

We furthermore use $\omega_{(4)} = e^{\frac{i\pi}{2}} = \omega_{(2)}^{\frac{1}{2}}$ and $\omega_{(2)}^{2c} = 1,\ c \in \mathbb{N}$ and can simplify Eq. (5.32)

$$\begin{aligned} |G^{(2)}\rangle &= \sum_{A_1 \ldots D_2=0}^{2} \omega_{(2)}^{A_1 B_1} \omega_{(2)}^{A_2 B_2} \omega_{(2)}^{B_2 C_2} \omega_{(2)}^{B_1 C_1} \omega_{(2)}^{C_1 D_1} \omega_{(2)}^{C_2 D_2} \\ &\qquad \omega_{(2)}^{\frac{A_2 B_1}{2}} \omega_{(2)}^{\frac{B_1 C_2}{2}} \omega_{(2)}^{\frac{C_2 D_1}{2}} |A_1 A_2 B_1 B_2 C_1 C_2 D_1 D_2\rangle \\ &= Z_{A_1 B_1} Z_{A_2 B_2} Z_{B_2 C_2} Z_{B_1 C_1} Z_{C_1 D_1} Z_{C_2 D_2} \\ &\quad Z_{A_2 B_1}^{\frac{1}{2}} Z_{B_1 C_2}^{\frac{1}{2}} Z_{C_2 D_1}^{\frac{1}{2}} |+^2\rangle^{\otimes 8} \,. \end{aligned} \tag{5.33}$$

Here, $Z_{ij} = \mathrm{diag}(1, -1)$ is the qubit-controlled Z-gate, this state is shown in left side of Fig. 5.2 in the main text. We then apply $V_{A_1 A_2}$, $V_{B_1 B_2}^{\frac{3}{2}}$ and $V_{D_1 D_2}^{\frac{3}{2}}$ to $|G^{(2)}\rangle$. Those are for the further analysis in this example defined as

$$V_{X_1 X_2} = (|+\rangle\langle+|)_{X_1} \otimes \mathbb{1}_{X_2} + (|-\rangle\langle-|)_{X_1} \otimes Z_{X_2}, \tag{5.34}$$

where for $X = A, B, C, D$ all $V_{X_1 X_2}$ are included in the set of vertical unitaries $\{U_{\mathrm{Vert}}\}$. By straightforward calculation, one verifies:

$$\begin{aligned} (V_{A_1 A_2} V_{B_1 B_2}^{\frac{3}{2}} V_{D_1 D_2}^{\frac{3}{2}}) |G^{(2)}\rangle &= V_{A_1 A_2 B_2} |G_{\mathcal{D}}^{(2)}\rangle \,, \\ (V_{D_1 D_2} V_{C_1 C_2}^{\frac{3}{2}} V_{A_1 A_2}^{\frac{3}{2}}) |G^{(2)}\rangle &= V_{C_1 D_1 D_2} |G_{\mathcal{D}}^{(2)}\rangle \,. \end{aligned} \tag{5.35}$$

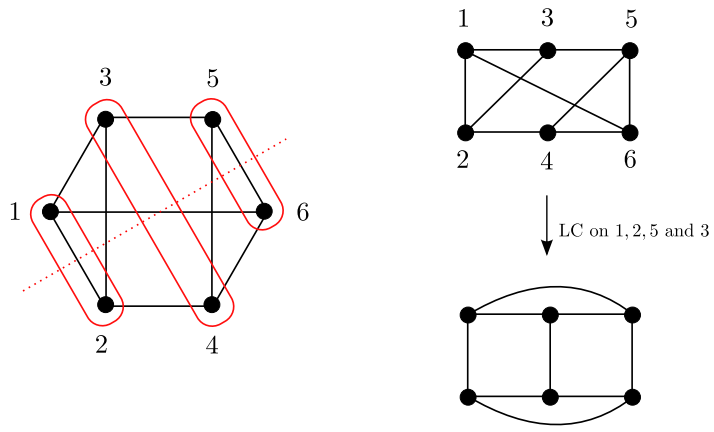

FIGURE 5.5: The maximally entangled state on six qubits represents a decomposable three ququart state.

This means that for the question of decomposability the weighted diagonal edges have the same effect on the decomposable state $|G_{\mathcal{D}}^{(2)}\rangle$ as one hyper-edge connecting three qubits either one or the other end of the chain, see Fig. 5.4(c) and Fig. 5.4(d). The mentioned hyper-edge is formally a three-qubit unitary of the form

$$V_{X_1X_2Y_1} = (|+\rangle\langle+|)_{X_1} \otimes \mathbb{1}_{X_2Y_1} + (|-\rangle\langle-|)_{X_1} \otimes V_{X_2Y_1} \tag{5.36}$$

with $V_{X_2Y_1}$ as defined in Eq. (5.34) and $|G_{\mathcal{D}}^{(2)}\rangle$ is a decomposable state, defined in Eq. (5.17) in the main text.

Furthermore, one can directly check that we can replace the three weighted Z-gates ($Z_{ij}^{\frac{1}{2}}$) in Eq. (5.33) by one weighted edge acting on qubits A_1 and C_2

$$|G^{(2)}\rangle = U_{A_1A_2}^{\frac{3}{2}} U_{B_1B_2}^{\frac{3}{2}} U_{A_1C_2} |G_{\mathcal{D}}^{(2)}\rangle \tag{5.37}$$

with $U_{A_1C_2} = (|+\rangle\langle+|)_{A_1} \otimes \mathbb{1}_{C_2} + (|-\rangle\langle-|)_{A_1} \otimes Z_{C_2}$ and two vertical unitaries $U_{A_1A_2}^{\frac{3}{2}}$ and $U_{B_1B_2}^{\frac{3}{2}}$ [see Fig. 5.4(b)].

From Eq. (5.35) and Eq. (5.37) we see that, whereas this state is not decomposable, there exists for every bipartition a representation of this state, for which the S-matrix has rank one. In Fig. 5.4, the different equivalent representations of the state are shown graphically. Each option presents decomposability with respect to another bipartite split, such that all possible ones are covered. However, to exclude genuine MME, let us once again stress that the existence of one split exhibiting decomposability is enough.

The maximally entangled state of six qubits

We have already seen that the highly entangled GHZ states are not necessarily multi-level entangled. Therefore one might ask the following question: Are there other highly entangled states which are not multi-level entangled? One example is the three-ququart state that corresponds to the absolutely maximally entangled state of six qubits (see Fig. 5.5). The six-qubit state is given by

$$|G^{(2)}\rangle = Z_{12}Z_{34}Z_{56}Z_{23}Z_{36}Z_{45}Z_{24}Z_{35}Z_{16} |+\rangle^{\otimes 6} \tag{5.38}$$

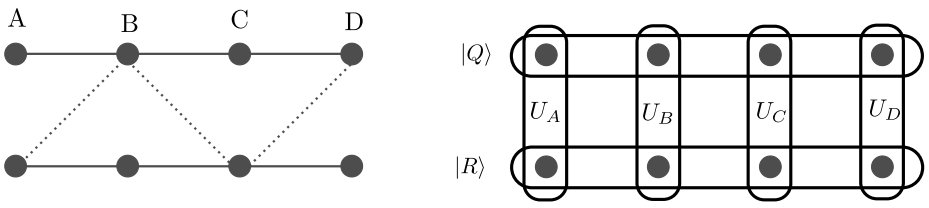

FIGURE 5.6: We ask whether the state on the left can be constructed by first preparing states $|Q\rangle$ and $|R\rangle$ and then applying local unitary operations $U_A, \ldots, U_D$. Since this is not possible the state is not decomposable, it is MME.

and corresponds to a graph state. Nevertheless, this state is fully decomposable. To prove this, we first mention that via local complementation [181] (LC), we can obtain:

$$|G^{(2)}\rangle \xrightarrow[\text{on } 1,2,5,3]{\text{LC}} Z_{12}Z_{56}Z_{14}Z_{23}Z_{36}Z_{45}Z_{15}Z_{26}\,|+\rangle^{\otimes 6} \tag{5.39}$$

Comparing Eq. (5.38) and Eq. (5.39), the difference between those is depicted in Fig. 5.5 on the right side. Whereas the first equation contains diagonal connections (which contradicts a direct decomposition), the second form shows that these can be replaced by vertical and horizontal ones. Therefore we can reach the original state by starting from a decomposable state.

E: Algorithm for testing full decomposability

In this section we explain the algorithm that we used to test whether or not the four ququart chain-graph state $|\psi\rangle$ in Eq. 5.14 in the main text. The aim is to test whether or not the state $|\psi\rangle$ can be written as $|\psi\rangle \stackrel{?}{=} U_A \otimes U_B \otimes U_C \otimes U_D\,|Q\rangle \otimes |R\rangle$, see also Fig. 5.6. Thus, we want to compute

$$\max_{\substack{U_A \cdots U_D \\ |Q\rangle|R\rangle}} |\langle Q|\,\langle R|\,U_A \otimes U_B \otimes U_C \otimes U_D\,|\psi\rangle|. \tag{5.40}$$

The idea is to choose initial states $|Q\rangle$ and $|R\rangle$, as well as unitaries $U_A, \ldots, U_D$ at random and then optimize the states and unitaries iteratively, until a fix-point is reached. The point is that any of the iteration steps can be performed analytically. In order to optimize the state $|Q\rangle$, we fix the unitaries $U_A, \ldots, U_D$ and the state $|R\rangle$. We obtain the optimal choice of $|Q\rangle$ by computing $\max_Q |\langle Q|\,(\langle R|\,U_A \otimes U_B \otimes U_C \otimes U_D\,|\psi\rangle)| = \max_Q |\,\langle Q\rangle\,\tilde{\psi}|$. We have that $|Q\rangle \propto |\tilde{\psi}\rangle$ is optimal up to normalization. The similar argument holds for $|R\rangle$. For optimizing the local unitaries we fix any unitary, but the one we want to optimize, say U_A. Then, we have

$$\begin{aligned} & \max_{U_A} |\langle Q|\,\langle R|\,U_A \otimes U_B \otimes U_C \otimes U_D\,|\psi\rangle| \\ = & \max_{U_A} |\langle Q|\,\langle R|\,U_A|\tilde{\psi}\rangle| \\ = & \max_{U_A} |\mathrm{tr}(U_A|\tilde{\psi}\rangle\,\langle Q|\,\langle R|)| \\ = & \max_{U_A} |\mathrm{tr}_A(U_A\varrho_A)| = \sum_i s_i(\varrho_A) \end{aligned} \tag{5.41}$$

where $\varrho_A = \mathrm{tr}_{BCD}(|\tilde{\psi}\rangle\langle Q|\langle R|)$. We write ϱ_A in the singular value decomposition and we get $\varrho_A = UDV^\dagger$. Then we choose $U_A = VU^\dagger$ and hence

$$|\mathrm{tr}_A(U_A\varrho_A)| = |\mathrm{tr}(D)| = \sum_i s_i(\varrho_A). \tag{5.42}$$

5.2 Distinguishing MME from DEC

Within this section, we present a method to analytically decide whether for a given multipartite state of dimension $d = \prod_i d_i$ it is possible to be within the set of decomposable states. Note that this criterion is only necessary but not sufficient. Nonetheless, it has proven to be useful, e.g. for the state from Example 2 in the foregoing Section 5.1 (see Eq.(5.14)) decomposability can be excluded.

The idea behind the method to be presented in the following is based on the rank of the coefficient matrix, $\mathrm{rank}(C)$ (Eq.(2.12)). Remember that $\mathrm{rank}(C)$ is invariant under SLOCC operations, which is a crucial property for this method to work.
Whereas in general for a d-dimensional state $|\psi\rangle$, the rank can take all values between $\mathrm{rank}(C) = 1$ and $\mathrm{rank}(C) = d$, this is not the case for the DEC-class when switching to a representation by lower dimensional systems. We show that the possible ranks of the state $|\psi_{dec}\rangle$ are dependent on the factors d_i within the chosen division of subsystems. That is, the rank values are limited to the product of the subsystem dimensions and we can formulate the following theorem:

Theorem 5.1. Rank values of the coefficient matrix
If the rank of the coefficient matrix of a state is not equal to the product of the $0-th$ *or* $1-th$ *power of the subsystem dimensions in the chosen split, then the state is not decomposable.*

Proving Theorem 5.1 reduces to proving the following Lemma 5.1:

Lemma 5.1. *Let* $|\psi\rangle$ *be an n-partite pure state of dimension* $d = \prod_i d_i$*. Furthermore, let* $d = \prod_k d_k$ *be an arbitrary, k-partite split of each qudit into lower dimensional systems of dimension* d_k *with* $|\psi_k\rangle$ *being the encoded state associated with the chosen split. If* $|\psi_k\rangle$ *is within the set of decomposable states* $\{|\psi_{dec}\rangle\}$*, i.e.* $|\psi_k\rangle = \bigotimes_{j=0}^{k-1} |\psi_j\rangle(d_j) \equiv |\psi_{dec}\rangle$ *with* $|\psi_j\rangle(d_j)$ *denoting the n-partite state of dimension* d_j*, then the rank of the corresponding coefficient matrix* C_{dec} *can take the values*

$$\mathrm{rank}(C_{dec}) = \{\prod_{k=1}^{n} d_k^{x_k}\}, \quad \text{where: } x_k \in [0,1] \tag{5.43}$$

Proof. For better readability, let us start with proving Lemma 5.1 for the most simple system of two ququarts. Let A and B denote the parties of the ququart system and $A \mapsto A_1A_2$, $B \mapsto B_1B_2$ represents the only possible split of the original system is into two qubits each. Any pure ququart state can be written in Schmidt decomposition: $|\psi\rangle = \sum_{i=0}^{3} s_i |ii\rangle_{AB}$. The rank $r(C_{A|B})$ of the coefficient matrix then can take all values within $[1,2,3,4]$. In the bipartite case, the rank equals the number of non-zero Schmidt coefficients s_i. Now consider a state out of the set of decomposable states, that is $|\psi_{dec}\rangle = |\psi\rangle_{A1B1} \otimes |\psi\rangle_{A2B2}$ with $|\psi\rangle \overset{enc.}{=} |\psi_{dec}\rangle$. Both again can be written in Schmidt decomposition: $|\psi_{A1B1}\rangle = \sum_{j=0}^{1} t_j |jj\rangle$ and $|\psi_{A1B1}\rangle = \sum_{k=0}^{1} r_j |kk\rangle$. The corresponding coefficient matrices $C_{A1|B1}$ and $C_{A2|B2}$ can both be of either rank one or rank two as $d_1 = d_2 = 2$ and thus the rank of the coefficient

matrix representing the complete system $C_{A1B1|A2B2}$ can take the values

$$\operatorname{rank}(C_{A1B1|A2B2}) = \prod_{k=1}^{2} d_k^{x_k} = \begin{cases} d_1^0 \cdot d_2^0 = 1 & x_1 = x_2 = 0 \\ d_1^0 \cdot d_2 = 2 & x_1 = 0,\ x_2 = 1 \\ d_1 \cdot d_2^0 = 2 & x_1 = 1,\ x_2 = 0 \\ d_1 \cdot d_2 = 4 & x_1 = x_2 = 1 \end{cases} \tag{5.44}$$

this can be seen when considering $|\psi_{dec}\rangle$ as tensor product of $|\psi\rangle_{A1B1} \otimes |\psi\rangle_{A2B2}$ in Schmidt decomposition. Then

$$|\psi_{dec}\rangle = \sum_{jk=0}^{1} t_j r_k \, |jkjk\rangle_{A1B1A2C2}$$

$$\text{and therefore: } C_{dec} = C_{A1B1|A2B2} = \begin{pmatrix} t_0 r_0 & 0 & 0 & 0 \\ 0 & t_0 r_1 & 0 & 0 \\ 0 & 0 & t_1 r_0 & 0 \\ 0 & 0 & 0 & t_1 r_1 \end{pmatrix} \tag{5.45}$$

From this, it is obvious that if $t_j = 0$ the rank is reduced by two as all diagonal elements having t_i as factor go to zero. Same is true for r_k. Thus we infer $\operatorname{rank}(C_{dec}) \neq 3$. □

Lemma 5.1 directly proves Theorem 5.1, as a rank of three, i.e. $\operatorname{rank}(C_{A|B}) = 3$, of the original ququart state excludes decomposability with respect to the split $(A1B1|A2B2)$. Generalizing this proof to arbitrary system size and number of participating particles is straightforward. To see this, take into consideration that the coefficient matrix always represents some bipartite split within the system and as such the argumentation based on the Schmidt decomposition is valid for the multipartite case. Moreover, the restriction on the ranks has to be satisfied for any possible bipartite split $A_iB_i|A_IB_I$ with $I = \{1, ..., n \ \setminus \{i\}\}$. Regarding a higher dimension and thus more options for a k-partite split changes the number of non-zero t_j and r_k as well as their possible values. The argumentation from above still works, as full rank equals to all t_j and r_k non-zero. One coefficient equal to zero reduced the number of non-zero diagonal components of C_{dec} to $\frac{d}{d_i}$, which directly corresponds to possible rank values determined by Eq. (5.43)

5.3 Lower dimensional representation of qudit graph states

Within this section, we give a general method how to generate from a given qudit graph state the associated (weighted) graph state within a lower dimensional encoding. The structure of graph states hereby restricts the possible values of the original systems dimension to $D = d^k$. Otherwise, the encoded graph would consist of qudits with different dimensions and thus fall out of the classical definition of graph states as well as their extension to weighted graphs.
Let us first clarify that the encoding of a D-dimensional system into k d-dimensional parties in done by using d-ary ordering, i.e. $|0\rangle_D \mapsto \underbrace{|0...0\rangle_d}_{k-times}$, $|d-1\rangle_D \mapsto |0...0d-1\rangle_d$, $|d\rangle_D \mapsto |0...10\rangle_d$ and $|D-1\rangle_D \mapsto |d-1...d-1\rangle_d$. The main statement of this section is formulated in the following theorem:

Theorem 5.2. Encoding of graph states into lower dimensions
Let $|G_D\rangle$ be an N-partite qudit graph state of dimension $D = d^k$, i.e.

$$|G_D\rangle = \prod_{(ij)\in E} Z_{ij}(D)\,|+_D\rangle^{\otimes N}, \qquad \text{with: } Z_{ij}(D) = \sum_{a=0}^{D-1} |a\rangle\langle a|_i \otimes Z_j(D)^a \tag{5.46}$$

and the D-dimensional single qudit $Z-$gate $Z_j(D) = \sum_{\alpha=0}^{D-1} \omega_D^\alpha |\alpha\rangle\langle\alpha|$. Then, the $n = k\cdot N$-partite weighted graph state of dimension d associated with the $k-$partite split of each D-dimensional qudit into k d-dimensional qudits is of the form

$$|G_d\rangle = \prod_{(i_l j_m)\in E_k;(l,m)\in[1,k]} Z_{i_l j_m}^{f(l,m)}(d)\,|+_d\rangle^{\otimes n} \qquad \text{with: } Z_{i_l j_m}(d) = \sum_{b=0}^{d-1} |b\rangle\langle b|_{i_l} \otimes Z_{j_m}(d)^b \tag{5.47}$$

where $Z_{j_m}(d) = \sum_{\beta=0}^{d-1} (\omega_d^{f(l,m)})^\beta |\beta\rangle\langle\beta|$. The phases are related by $\omega_D^{d^{k-1}} = \omega_d$ and the mapping $f(l,m)$ is defined as

$$f(l,m) = \left\{ \begin{array}{cc} \frac{1}{d^0} & l > k-m,\ l+m = k+1 \\ \frac{1}{d^1} & l > k-m,\ l+m = k+2 \\ \vdots & \vdots \\ \frac{1}{d^{k-1}} & l > k-m,\ l+m = 2k \\ 0 & l \le k-m \end{array} \right\} \equiv \left\{ \begin{array}{cc} \frac{1}{d^{l+m-k-1}} & l > k-m \\ 0 & l \le k-m \end{array} \right. \tag{5.48}$$

Proof. We will give proof by considering the action of one controlled Z-gate $Z_{ij}(D)$ on the relevant qudits $|++\rangle_{ij}$, using Eq. (2.112) we have

$$Z_{ij}(D)\,|++\rangle_{ij} = \sum_{ij=0}^{D-1} \omega_D^{ij} |ij\rangle \tag{5.49}$$

We now seek to find a function $f(l,m)$ that reproduces the same phases, such that the states correlations remain unchanged after the encoding process, i.e. $\omega_D^{ij} = \omega_D^{f(l,m)}$. The structure of the chosen encoding directly gives for a two-partite split, i.e. $k = 2$, the partioning of the form $i = di_1 + i_2$ and $j = dj_1 + j_2$. The generalization to arbitrary k then is found to be

$$i = \sum_{l=1}^{k} d^{k-l} i_l \qquad \text{and:} \qquad j = \sum_{m=1}^{k} d_{k-m} j_m \tag{5.50}$$

Exemplary this is shown in Table 5.2 for $k = 4$ and $d = 3$.

i	i_1	i_2	i_3	i_4	$27i_1 + 9i_2 + 3i_3 + i_4$
0	0	0	0	0	0
1	0	0	0	1	1
2	0	0	0	2	2
3	0	0	1	0	3
⋮	⋮	⋮	⋮	⋮	⋮
8	0	0	2	2	8
9	0	1	0	0	9
⋮	⋮	⋮	⋮	⋮	⋮
25	0	2	2	1	25
26	0	2	2	2	26
⋮	⋮	⋮	⋮	⋮	⋮
79	2	2	2	1	79
80	2	2	2	2	80

TABLE 5.2: Encoding of one qudit of D=81 into four qudits with d=3 and mapping $f(l,m)$: $i \mapsto \sum_{l=1}^{4} d^{4-l} i_l$ which gives the correct values for i, analogously, this can be done for the index j. The equivalent values of the first and last column show that $f(l,m)$ leaves the phases unchanged, i.e. $\omega_{81}^{ij} = \omega_{81}^{f(l,m)}$.

Next, we replace the $D-$dimensional phase ω_D by ω_d to find the $d-$dimensional controlled Z-gates and plug in $f(l,m)$, i.e. make the replacements for i and j according to Eq.(5.50)

$$\begin{aligned} \omega_D^{ij} = \omega_D^{f(l,m)} &= \omega_D^{(\sum_{l=1}^{k} d^{k-l} i_l)(\sum_{m=1}^{k} d^{k-m} j_m)} \\ = \omega_D^{\sum_{l,m=1}^{k} d^{k-l} d^{k-m} i_l j_m} &= (\omega_d^{\sum_{l,m=1}^{k} d^{k-l} d^{k-m} i_l j_m})^{\frac{1}{d^{k-1}}} \end{aligned} \tag{5.51}$$

Keeping in mind that $d^{k-l} \in [d^0, d^{k-1}]$ and likewise $d^{k-m} \in [d^0, d^{k-1}]$ we can, by noticing that

$$\omega_D^{d^{k+c}} = \omega_d^{\frac{d^{k+c}}{d^{k-1}}} = \omega_d^{d^{c+1}} \overset{\text{mod } d}{=} \begin{cases} \omega_d^0 = 1 & c \geq 0 \\ \omega_d^{\frac{1}{d^{-(c+1)}}} = \sqrt[d^{-(c+1)}]{\omega_d} & c < 0, \end{cases} \tag{5.52}$$

identify the surviving terms in the product of sums in Eq.(5.51), i.e. all (l,m)-tupels with $l > k - m$ and thereby simplifying it further. The following table (Table 5.3) shows those terms and the associated d-dimensional controlled Z-gates.

That is, for each $(l,m)-$ tupel, a Z(d)-gate of power $s = \frac{1}{l+m-k-1}$ emerges:

$$(l,m) \quad \mapsto \quad Z(d)_{i_l j_m}^{\frac{1}{l+m-k-1}} \qquad \forall\, l > k-m,\ l,m \in [1,k]. \tag{5.53}$$

which proves the Theorem.

For the example above with $D = 81$, $k = 4$, $d = 3$ the $n = 4$-partite chain graph state

(l,m)-tupel	related powers of $\omega_D = \omega_d^{\frac{1}{d^{k-1}}}$	associated $Z^s_{i_l j_m}(d)$-gate
(1,k)	$\omega_D^{d^{k-1}d^0 i_1 j_k}$	$Z_{i_1 j_k}(d)$
(2,k)	$\omega_D^{d^{k-2}d^0 i_1 j_k}$	$Z_{i_2 j_k}(d)^{\frac{1}{d}}$
(2,k-1)	$\omega_D^{d^{k-2}d^1 i_2 j_{k-1}}$	$Z_{i_2 j_{k-1}}(d)^1$
(3,k)	$\omega_D^{d^{k-3}d^0 i_3 j_k}$	$Z_{i_3 j_k}(d)^{\frac{1}{d^2}}$
(3,k-1)	$\omega_D^{d^{k-3}d^1 i_2 j_{k-1}}$	$Z_{i_3 j_{k-1}}(d)^{\frac{1}{d}}$
(3,k-2)	$\omega_D^{d^{k-3}d^2 i_2 j_{k-2}}$	$Z_{i_3 j_{k-2}}(d)$
$\vdots$	$\vdots$	$\vdots$
(k,k)	$\omega_D^{d^0 d^0 i_k j_k}$	$Z_{i_k j_k}(d)^{\frac{1}{d^{k-1}}}$
(k,k-1)	$\omega_d^{d^0 d^1 i_k j_{k-1}}$	$Z_{i_k j_{k-1}}(d)^{\frac{1}{d^{k-2}}}$
$\vdots$	$\vdots$	$\vdots$
(k,1)	$\omega_D^{d^0 d^{k-1} i_k j_1}$	$Z_{i_k j_1}(d)$

TABLE 5.3: For each tupel (l,m) the phases $\omega_D^{f(l,m)} \neq 0$ and associated controlled Z-gates Z_d in the lower dimensional representation of a $k-$partite split are assigned.

$|G_D\rangle = Z(D)_{12}Z(D)_{23}Z(D)_{34}\,|+\rangle_D^{\otimes 4}$ gives for each $Z(d)_{xy}$ with $(xy) = [(12),(23),(34)]$

$$\begin{aligned} Z(D)_{xy} \;\mapsto\; & Z(d)_{x_1y_4}Z(d)_{x_2y_3}Z(d)_{x_3y_2}Z(d)_{x_4y_1} \\ & Z(d)^{\frac{1}{3}}_{x_2y_4}Z(d)^{\frac{1}{3}}_{x_3y_3}Z(d)^{\frac{1}{3}}_{x_4y_2} \\ & Z(d)^{\frac{1}{9}}_{x_3y_4}Z(d)^{\frac{1}{9}}_{x_4y_3}Z(d)^{\frac{1}{27}}_{x_4y_4} \end{aligned} \tag{5.54}$$

The graphical representation of the encoded state is shown in Fig. 5.7

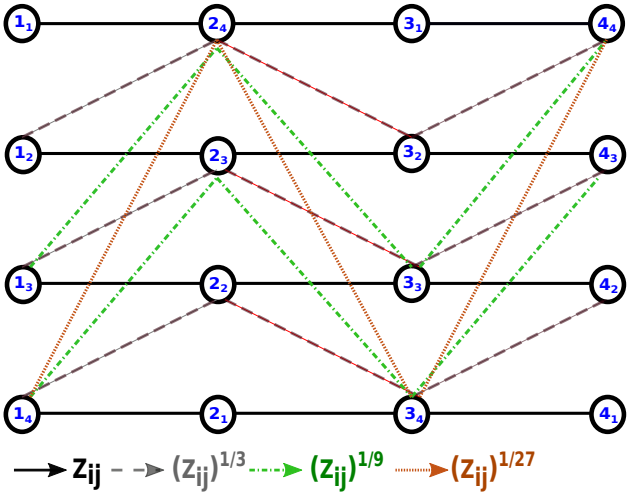

FIGURE 5.7: The encoded state $|G_d\rangle$ associated to the chain graph state of four qudits, $|G_D\rangle$ in $D = 81$ w.r.t the 4-partite split of each 81-dimensional qudit into four 3-dimensional qudits.

□

5.4 Network configuration

Within this section, we indroduce an alternative way of distributing the subsystems when splitting the original systems into a set of lower dimensional qudits. Here, each system, i.e. its split into k parts, can be seen as a node of a quantum network. Entanglement is then created by sources in between two nodes such that one part of each node is connected to another part of the second node. We call this connection a (quantum) link. Spreading the entanglement initially generated on the links over the whole network can then be done by making non-local measurements on the nodes. In this way, a strongly correlated multipartite entangled state is generated. Note, that for a network of N nodes, each having k subsystems, at most *genuine* $k-$partite entangled states can be generated as the entanglement generating operations on the nodes act on no more than k parties and the sources are taken to be independent or - as an extension to the model - classical communication could be possible. Applications for quantum networks exist i.e. in quantum processors, where information and entanglement is exchanged between parties (nodes) via a quantum link, i.e., the entangled source state. Furthermore, network states could be useful for long distance communications, where quantum repeaters based on entangled photon sources and quantum memories are used. This motivates to take a closer look at the properties of those network states. That is, from the theoretical point of view, a first step is to characterize the set of states which can be generated in such a network scenario.
As this field is ongoing work, we want to give an introduction to the framework and, based on some interesting properties within a triangular network, motivate further investigation.

5.4.1 Triangular network configuration

As in the bipartite case ($N = 2$) the network configuration coincides with the original configuration proposed in Sec. 5.1, the triangular network configuration is the most simple realization of a quantum network. Here, we have three nodes, denoted by A, B and C which, dependent on the dimension of the respective systems, are divided into two lower dimensional subsystems. Furthermore, there are three independent sources $\tilde{A}$, $\tilde{B}$ and $\tilde{C}$ creating entangled two-qudit states $|\alpha\rangle$, $|\beta\rangle$ and $|\gamma\rangle$ between the nodes subsystems. The entanglement propagation, i.e. generating multipartite correlations, is then realized by allowing unitaries U_A, U_B and U_C to be performed by each party on their own node. These unitaries are local with respect to each party but nonlocal with respect to their action on all subsystems of each node. The graphical representation of such triangular network states with independent sources or classically correlated sources is shown in Fig. 5.8.

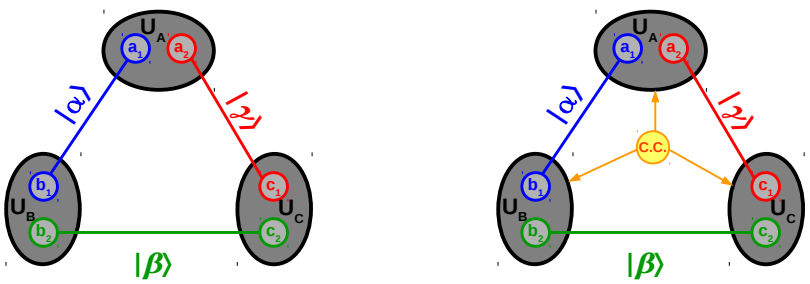

FIGURE 5.8: (Left) Triangular quantum network consisting of three indpendent sources $|\alpha\rangle$, $|\beta\rangle$ and $|\gamma\rangle$. (Right) Triangular quantum network where classical communication (c.c) between the sources is allowed.

A general six-partite state $|\psi\rangle$ written in network notation, i.e. denoting the partites with respect to their relation to being subsystems of a node, then is of the form

$$|\psi\rangle = \sum_{a_1a_2b_1b_2c_1c_2=0}^{d-1} T_{a_1a_2b_1b_2c_1c_2} |a_1a_2b_1b_2c_1c_2\rangle . \tag{5.55}$$

On the other hand, all states $|\psi_N\rangle$ possible to be generated within the triangular network configuration can be written as

$$\begin{aligned} |\psi_N\rangle &= (U_A \otimes U_B \otimes U_C) |\alpha\rangle_{a_1b_1} |\beta\rangle_{b_2c_2} |\gamma\rangle_{c_1a_2} \\ &= (U_A \otimes U_B \otimes U_C) \sum_{a_1a_2b_1b_2c_1c_2=0}^{d-1} \alpha_{a_1b_2}\beta_{b_2c_2}\gamma_{c_1a_2} |a_1a_2b_1b_2c_1c_2\rangle . \end{aligned} \tag{5.56}$$

Whether a given state $|\psi\rangle$ can be generated within a triangular quantum network, is then answered by the question whether there exist source states $|\alpha\rangle_{a_1b_1}$, $|\beta\rangle_{b_2c_2}$, $|\gamma\rangle_{c1a2}$ and unitaries U_A, U_B, U_C such that $|\psi\rangle = |\psi_N\rangle$.
To decide this, we employ a numerical algorithm similar to the one used for distinguishing between DEC and MME, see 5.1.6. Choosing random source states $|\alpha\rangle$, $|\beta\rangle$, $|\gamma\rangle$, we start the optimization process by optimizing over each source state, i.e., for the finding the optimal $|\alpha\rangle$, we need to compute

$$\begin{aligned} \max_{\alpha} \langle\alpha\beta\gamma|\psi\rangle &= \max_{\alpha} \left(\langle\alpha| \sum_{a_1a_2b_1b_2c_1c_2=0}^{d-1} \beta^*_{b_2c_2}\gamma^*_{c_1a_2} \langle a_2b_2c_1c_2| T_{a_1a_2b_1b_2c_1c_2} |a_1a_2b_1b_2c_1c_2\rangle \right) \\ &= \max_{\alpha^*_{a_1b_1}} \left(\sum_{a_1b_1} \langle a_1b_1| \alpha^*_{a_1b_1} \sum_{a_2b_2c_1c_2} T_{a_1a_2b_1b_2c_1c_2}\beta^*_{b_2c_2}\gamma^*_{c_1a_2} |a_1b_1\rangle \right) . \end{aligned} \tag{5.57}$$

Then the optimal choice for each $\alpha_{a_1b_1}$ is found by:

$$\alpha^*_{a_1b_1} = \sum_{a_2b_2c_1c_2} \beta^*_{b_2c_2}\gamma^*_{c_1a_2} T_{a_1a_2b_1b_2c_1c_2} \tag{5.58}$$

and therefore the corresponding optimal state $|\alpha\rangle_{a_1b_1}$ is given by $|\alpha\rangle_{a_1b_1} \propto |\bar{\psi}\rangle$ up to normalization and with $|\bar{\psi}\rangle = \langle\beta|_{b_2c_2} \langle\gamma|_{c_1a_2} |\psi\rangle$. The optimization over $|\beta\rangle_{b_2c_2}$ and $|\gamma\rangle_{c_1a_2}$ is done in analogous fashion. Following, the optimization process moves on to the unitaries. For a given resource state $|\alpha_{a_1b_1}\beta_{b_2c_2}\gamma_{c_1a_2}\rangle \equiv |\alpha\beta\gamma\rangle$, we optimize over each unitary separately, starting with U_A for fixed, randomly chosen U_B, U_C

$$\begin{aligned} &\max_{U_A} |\langle\alpha\beta\gamma|(U_A \otimes U_B \otimes U_C)\tilde{\psi}\rangle| \\ &= \max_{U_A} |\mathrm{tr}(U_A |\tilde{\psi}\rangle \langle\alpha\beta\gamma|)| \\ &= \max_{U_A} |\mathrm{tr}_A(U_A\rho_A)| \end{aligned} \tag{5.59}$$

where $|\tilde{\psi}\rangle = U_B \otimes U_C |\psi\rangle$ and the reduced density matrix $\rho_A = \mathrm{tr}_{BC}(|\tilde{\psi}\rangle \langle\alpha\beta\gamma|)$. Furthermore, we can use the singular value decomposition of $\rho_A = VDW^\dagger$ to rewrite Eq. (5.59) as

$$\max_{U_A} |\mathrm{tr}_A(U_A\rho_A)| = \max_{U_A} |\mathrm{tr}_A(U_AV_AD_AW_A^\dagger| \tag{5.60}$$

which gives an optimal unitary $U_A = W_A V_A^\dagger$ and finally can express the maximization over U_A in terms of the singular values $\{s_i\}$ of ρ_A

$$\max_{U_A} |\mathrm{tr}_A(U_A \rho_A)| = \sum_i d_i(\rho_A) \tag{5.61}$$

Equivalently, we proceed for U_B and U_C which concludes the first optimization round. We go on by repeating those rounds until a fixpoint is reached. Running this numerical optimization algorithm over sufficiently many randomly chosen source states, there is a high probability for obtaining the maximal overlap between a given state $|\psi\rangle$ and any state $|\psi_N\rangle$ that can be generated within the triangular network configuration.

Examples: GHZ-states and the network configuration

Let us now use the presented algorithm for calculating the maximal overlap for two concrete given states within the GHZ class. As GHZ-states inhibit genuine multilevel entanglement, it is clear that it can not be generated within the network scenario. Thus the maximal overlap has to be smaller than one. In some cases, from the decomposition, we can directly derive a lower bound on the overlap, which can then be a useful starting point for our algorithm. As a first example state consider the tripartite GHZ state in dimension $d = 2$. The binary encoding then gives

$$\begin{aligned} |GHZ_2\rangle_{ABC} &= \frac{1}{\sqrt{2}}(|000\rangle + |111\rangle)_{ABC} \overset{enc.}{=} \frac{1}{\sqrt{2}}(|000000\rangle + |010101\rangle)_{a_1a_2b_1b_2c_1c_2} \\ &= |000\rangle_{a_1b_1c_1} \otimes (|000\rangle + |111\rangle)_{a_2b_2c_2} = |000\rangle_{a_1b_1c_1} \otimes |GHZ_2\rangle_{a_2b_2c_2} \\ &\equiv |ghz_2\rangle \end{aligned} \tag{5.62}$$

From Eq. (5.62), we can infer that the maximal overlap has to be lower bounded by the maximal overlap of a three-qubit GHZ-state and the set of biseparable states. To see this, notice that the state $|000\rangle$ on systems $(a_1b_1c_1)$ is a product state and thus can always be generated by the source states and therefore gives an overlap of one. Then the total overlap is dependent only on $\langle GHZ_2|\beta \otimes |0\rangle\rangle$. Applying the algorithm then gives a maximal overlap with the set of network states $\{|\psi_N\rangle\}$

$$\max_{\substack{\alpha\beta\gamma \\ U_A,U_B,U_C}} |\langle \psi_N | ghz_2 \rangle| = \frac{1}{2} \tag{5.63}$$

which is equal to the overlap between the three qubit GHZ-state and the set of biseparable states. Considering that in the network configuration the subspace of systems a_2 b_2 and c_2 produces biseparable states with respect to the split $(b_2c_2|a_2)$, this result is to be expected. As another example, we take the three-dimensional GHZ-state of two parties, i.e.

$$\begin{aligned} |GHZ_3\rangle &= \frac{1}{\sqrt{3}}(|00\rangle + |11\rangle + |22\rangle)_{AB} \\ &\overset{enc.}{=} \frac{1}{\sqrt{3}}(|0000\rangle + |0101\rangle + |1010\rangle)_{a_1a_2b_1b_2}. \end{aligned} \tag{5.64}$$

Applying the numerical algorithm, we reach a maximal overlap of $\frac{4}{9}$ for the source states and unitaries given as

$$\begin{aligned}\max_{\substack{\alpha\beta\gamma,\\ U_A U_B U_C}} |\langle GHZ_3|\psi_N\rangle| = \frac{4}{9} \quad \text{for:} \quad |\alpha\rangle = |\beta\rangle = |\gamma\rangle = \sqrt{\frac{2}{3}}|00\rangle + \sqrt{\frac{1}{3}}|11\rangle \\ U_A = U_C = -i(|0\rangle\langle 0|)_{a_1} \otimes (\sigma_y)_{a_2} + (|1\rangle\langle 1|)_{a_1} \otimes \mathbb{1}_{a_2}, \\ U_B = \mathbb{1}_{b_1 b_2}\end{aligned} \tag{5.65}$$

Lastly, we consider the bipartite GHZ-state in dimension four, which we know from Section 5.1.2 to be reproducible by preparing qubit-GHZ-states on $(a_1 b_1)$ and $(a_2 b_2)$ respectively

$$\begin{aligned}|GHZ_4\rangle &= \frac{1}{2}(|00\rangle + |11\rangle + |22\rangle + |33\rangle)_{AB} \\ &\overset{enc.}{=} \frac{1}{2}(|GHZ_2\rangle_{a_1 b_1} \otimes |GHZ_2\rangle_{a_2 b_2})\end{aligned} \tag{5.66}$$

The maximal overlap of $|GHZ_4\rangle$ and the set of triangular network states is now lower bounded by the product of the maximal overlaps for each $|GHZ_2\rangle$. This would give a value of $\frac{1}{2}\cdot\frac{1}{2} = \frac{1}{4}$, as we know from Eq. (5.63). Using the algorithm, it turns out that the reachable overlap is significant higher then the lower bound, i.e. we were able to determine a maximal overlap of $\frac{1}{2}$ for Bell states generated by each source, such that:

$$\begin{aligned}\max_{\substack{\alpha\beta\gamma,\\ U_A U_B U_C}} |\langle GHZ_4|\psi_N\rangle| = \frac{1}{2} \qquad \text{for:} \quad |\alpha\rangle = |\beta\rangle = |\gamma\rangle = \sqrt{\frac{1}{2}}(|00\rangle + |11\rangle) \\ U_A = U_C = -i(|0\rangle\langle 0|)_{a_1} \otimes (\mathbb{1} - \sigma_y)_{a_2} \\ + (|1\rangle\langle 1|)_{a_1} \otimes (\mathbb{1} + \sigma_y)_{a_2}, \\ U_B = \mathbb{1}_{b_1 b_2}\end{aligned} \tag{5.67}$$

Chapter 6

Summary and Outlook

Within this thesis, the structure and detection of entanglement within multipartite and high-dimensional systems was investigated.

For the general scenario of arbitrary system size and dimensionality, a one-to-one connection between SLOCC witnesses and entanglement witnesses within a two-copy Hilbert space was established. This connection can be exploited both ways, that is, solving one problem directly provides a solution to the related one. Thus, it is possible to get insight in the entanglement properties and structure of complex systems, which can not be characterized directly.

Furthermore, a new class of multipartite quantum states was defined, arising from the generalization of qubit hypergraphs to arbitrary dimension. In this context, methods were found, which allow for classification of qudit hypergraph states with respect to LU and SLOCC equivalence. For tripartite systems of dimension three and four, a full LU- and SLOCC classification is given, moreover, general criteria valid for arbitrary dimension and system size were developed.
Beyond that, qudit hypergraphs were extended even further by introducing weighted hyperedges. This could be an interesting topic for further research. Combining the richer structure arising from the weighted edges with applicable characterizing methods, derived for the unweighted case, could lead to a better understanding of a larger class of multiparite, high-dimensional entangled states. Furthermore, it could be interesting to investigate the connection of weighted hypergraphs to LME states for higher dimensions. In addition, a method was developed that identifies LU-equivalent graph states of arbitrary dimension by using a method similar to LC of graph states in prime dimensions.

Finally, an experimentally consistent definition of multilevel entanglement was introduced. This new method to identify genuine multilevel entangled states provides clear guidelines for using high-dimensional entanglement as a resource. Hence, developing a resource theory of multilevel entanglement poses a natural continuation of this work. Furthermore, in the context of multilevel entanglement, a different distribution of subsystem was discussed. This distribution is closely related to quantum network scenarios, which is a promising field to investigate in more detail for future research.

Acknowledgements

First and foremost I want to thank my supervisor Prof. Dr. Otfried Gühne for giving me the opportunity to do my doctoral studies within his group. For his constant support, his patience and guidance and for the chance to work on several interesting and challenging problems.

During my time as Ph.D. student, I had the honor to work with several bright people. Special thanks go to Frank Steinhoff for the great time working on the Hypergraph project, the many hours spent juggling with numbers, for sharing the enthusiasm and passion working on this topic. In this context, my thanks also go to Nikolai Miklin for contributing his programming skills to our project, which gave essential insights. I also want to thank Tristan Kraft for the great collaboration on the GMME project, for complementing each other on the many facades of this topic, for the productive way of working together and for the humor, which was never far. I want to thank Cornelia Spee for the collaboration on the Tensor witness project. For her guidance and many indispensable ideas and persistence until a solution was found. My thanks go to Matthias Kleinmann, for countless inspiring discussions that explored (quantum) physics in an beyond-the-horizon way.

Furthermore, my thanks go to the whole TQO-group of the University of Siegen, including all former members of the last years, for many interesting and fruitful discussions and an overall great time. Special thanks go to Tristan Kraft, Fabian Bernards, Nikolai Wyderka and Timo Simnacher for taking the time to proofread this thesis.

Finally, I want to thank my parents for their unshakable support, for listening to my ideas and asking questions from an outside perspective that really got me thinking outside the box on many occasions. I thank my family and friends for always being there, especially in busy times with no time. Thanks go to my jujutsu training group, there is nothing like a good sparring to reset the mind and have a fresh start when scientific thoughts get stuck in circles. Lastly, I thank you, B., for your trust, for your inspiration and energy. For reminding me to be myself, to keep on walking no matter what, to never stop being persistent. For not talking, but always saying the right thing.

Appendix A

SLOCC classification of 233 systems

Within this section, we give an alternative way to classify 233 systems regarding the equivalence under SLOCC. We analyze the stochastic local quantum transformations (SLOCC) of states of tripartite quantum systems composed form one two-level system and two three-level systems. We find that there are 17 inequivalent SLOCC classes of which six are genuine 233-entangled. In the SLOCC-hierarchy, only three of the six classes can converted to any of the SLOCC classes which are not genuine 233-entangled.

1. **INTRODUCTION**

   The most widely used classification of entanglement in multipartite quantum states is based on the equivalence under stochastic local operations and classical communication (SLOCC) [187]. Two states are SLOCC-equivalent if they can be converted to each other with a nonzero probability by means of local quantum operations such as unitary operations and partial measurements. A landmark result in understanding multipartite entanglement was the discovery [188] that three qubits have two different SLOCC classes of genuine multipartite entanglement, the representatives of which are the Greenberger–Horne–Zeilinger state (GHZ-state) [189] and the W-state [188]. The SLOCC classification of other systems has attracted less attention, with the most notably exception of the case where two parties hold a qubit and a third party holds an arbitrary quantum system [190]. In such $22N$-systems there are six SLOCC classes for $N = 2$, nine for $N = 3$ and ten for $N \geq 4$ [190]. In contrast, for the case of four qubits it has been found that the number of SLOCC classes in uncountably infinite [191] and hence the SLOCC classification of larger systems is less significant.

   An SLOCC transformation from a pure tripartite states $|\psi\rangle\langle\psi|$ to another pure tripartite state $|\psi'\rangle\langle\psi'|$ is possible if and only if there exist local operators α, β, and γ, such that $|\psi'\rangle = (\alpha \otimes \beta \otimes \gamma)\,|\psi\rangle$. This follows from the fact that any stochastic local operation is necessarily of the form $\Lambda\colon \varrho \mapsto \sum_k A_k \varrho A_k^\dagger$, where $A_k = \alpha_k \otimes \beta_k \otimes \gamma_k$ and $\sum A_k^\dagger A_k \leq \mathbb{1}$ and from the fact that any term k can be implemented—up to a factor $0 < p \leq 1$—as a unitary and a postselected measurement. Consequently, if the local operators are invertible (invertible local operators, ILOs), then the two states are SLOCC-equivalent as also the backwards transformation can be achieved by SLOCC. This way, the set of pure states decomposes into SLOCC-equivalent classes and each class can be represented by a canonical vector $|\psi\rangle$, e.g., for the $|001\rangle + |010\rangle + |100\rangle$ for the W-class and $|000\rangle + |111\rangle$ for the GHZ-class. For an SLOCC classification it is then possible to ask for SLOCC transformations which are only possible in one direction. In this case, the

k	Ω	Ψ_A	Ξ_A	type	k	Ω	Ψ_A	Ξ_A	type
1	(1,1,1)	(0,1)	1	separable	10	(2,3,3)	(1,2)	3	Md
2	(1,2,2)	(0,2)	2	biseparable	11	(2,2,3)	(2,2)	2	A4
3	(1,3,3)	(0,3)	3	biseparable	12	(2,3,2)	(2,2)	2	A4
4	(2,1,2)	(1,1)	1	biseparable	13	(2,3,3)	(2,2)	3	Mc
5	(2,2,1)	(1,1)	1	biseparable	14	(2,3,3)	(2,2)	2	C
6	(2,2,2)	(1,1)	2	GHZ	15	(2,3,3)	(2,2)	3	Me
7	(2,2,2)	(1,2)	2	W	16	(2,3,3)	(1,3)	3	Mb
8	(2,2,3)	(1,2)	2	A3	17	(2,3,3)	(2,3)	3	Ma
9	(2,3,2)	(1,2)	2	A3					

TABLE A.1: Properties of the 17 SLOCC classes for 233. For each class k and its representative vector $|\psi_k\rangle$ from Eq. (A.1) the Schmidt-rank characteristics Ω, Ψ_A, and Ξ_A are provided, cf. Sec. 3. The column "type" refers to prior classifications, cf. discussion below Eq. (A.1).

target is arguably less entangled than the original state and it emerges the hierarchy of SLOCC classes.

Here we study the SLOCC classification of $2NM$-systems. In Sec. 2, Sec. 3 and Sec. 4 we give a full classification of 233-systems and we provide the corresponding SLOCC-hierarchy in Sec. 5. For 244-systems, the number of SLOCC classes is already uncountably infinite, as we prove in Sec. 6 before we conclude in Sec. 7.

2. **SLOCC classification of 233-systems**

In this section we show that there are 17 SLOCC classes for 233-systems. Representative vectors for these classes are given by

$$
\begin{aligned}
|\psi_1\rangle &= |000\rangle\,,\\
|\psi_2\rangle &= |000\rangle + |011\rangle\,,\\
|\psi_3\rangle &= |000\rangle + |011\rangle + |022\rangle\,,\\
|\psi_4\rangle &= |000\rangle + |101\rangle\,,\\
|\psi_5\rangle &= |000\rangle + |110\rangle\,,\\
|\psi_6\rangle &= |000\rangle + |111\rangle\,,\\
|\psi_7\rangle &= |000\rangle + |011\rangle + |101\rangle\,,\\
|\psi_8\rangle &= |000\rangle + |011\rangle + |102\rangle\,,\\
|\psi_9\rangle &= |000\rangle + |011\rangle + |120\rangle\,,\\
|\psi_{10}\rangle &= |000\rangle + |011\rangle + |122\rangle\,,\\
|\psi_{11}\rangle &= |000\rangle + |011\rangle + |101\rangle + |112\rangle\,,\\
|\psi_{12}\rangle &= |000\rangle + |011\rangle + |110\rangle + |121\rangle\,,\\
|\psi_{13}\rangle &= |000\rangle + |011\rangle + |102\rangle + |120\rangle\,,\\
|\psi_{14}\rangle &= |000\rangle + |011\rangle + |112\rangle + |120\rangle\,,\\
|\psi_{15}\rangle &= |000\rangle + |011\rangle + |100\rangle + |122\rangle\,,\\
|\psi_{16}\rangle &= |000\rangle + |011\rangle + |022\rangle + |101\rangle\,,\ \text{and}\\
|\psi_{17}\rangle &= |000\rangle + |011\rangle + |022\rangle + |101\rangle + |112\rangle\,.
\end{aligned}
\tag{A.1}
$$

Clearly, class 1 are all product states and the states in the classes 2–5 are merely bipartite entangled. Classes 1, 2, and 4–7 are the SLOCC classes for three qubits

with class 6 the GHZ-class and class 7 the W-class. The case 322 has been studied in Ref. [192] finding two additional classes represented by $|\mathrm{A3}\rangle = |000\rangle + |101\rangle + |211\rangle$ and $|\mathrm{A4}\rangle = |000\rangle + |101\rangle + |110\rangle + |211\rangle$. For 223-systems, class 8 corresponds to the A3-class and class 11 to the A4-class. Similarly, for 232-systems, class 9 corresponds to the A3-class and class 12 to the A4-class. In Ref. [193] Sec. IIB, five inequivalent classes for 233-systems have been introduced, Ma–Me, represented by vectors $|\psi_a\rangle$ to $|\psi_e\rangle$. We mention that for 233-systems, 18 representative vectors have been found in Ref. [194], which happen to be equivalent under ILOs to the vectors in Eq. (A.1), but three of the vectors are equivalent to $|\psi_{17}\rangle$ while representative vector of class 15 is missing. In the column "type" of Table A.1 we summarize the different types outlined in this paragraph.

The proof of the classification is split into two parts. Within Sec. 3, we show that the 17 representative vectors are not interconvertible via ILOs and hence represent distinct SLOCC classes. Then, within Sec. 4, we prove that for any 233-state $|\psi\rangle\langle\psi|$ there are ILOs transforming $|\psi\rangle$ to at least one of the 17 representative vectors and hence the 17 classes are exhaustive.

3. **Schmidt-rank classifications**

Before proving that none of the 17 representative vectors can be interconverted by ILOs, we introduce three criteria that allow a coarse-grained classification. Either criterion is based on the Schmidt-rank of a vector $|\varphi\rangle$, i.e., on the rank r_φ of the matrix $[\langle ij|\varphi\rangle]_{ij}$. The Schmidt-rank is independent of the choice of the local bases $|i\rangle$ and $|j\rangle$, even if the basis vectors are not orthonormal. Consequently, r_φ does not change under ILOs. For tripartite states, there are three bipartite splits, $A|BC$, $B|AC$, and $C|AB$, giving rise to the triple $\mathbf{\Omega}$ [195, 196] of Schmidt-ranks which then is invariant under ILOs.

We introduce two additional Schmidt-rank classifications. For that we consider all possible decompositions $|\psi\rangle_{ABC} = |\xi\rangle_A |\eta\rangle_{BC} + |o\rangle_A |\theta\rangle_{BC}$. The pair (r_η, r_θ) which is smallest in the lexicographic order is denoted by $\mathbf{\Psi}_A(\psi)$. Similarly, we consider the maximal rank Ξ_A that can be achieved for r_η. Both classifications are invariant under ILOs, since the set of pairs $(|\eta\rangle, |\theta\rangle)$ does not change under ILOs on the first party and r_η and r_θ do not change under ILOs on the other parties.

In Table A.1 we list the Schmidt-rank triple $\mathbf{\Omega}$, the pair $\mathbf{\Psi}_A$ and the index Ξ_A for all representative vectors. Note, that all these values are evident from Eq. (A.1). This proves already large parts of the following.

Proposition A.1. *Let $|\psi_i\rangle$ and $|\psi_j\rangle$ be two different representative vectors from Eq. (A.1). Then there exist no ILOs α, β, and γ such that $|\psi_i\rangle = (\alpha \otimes \beta \otimes \gamma)\,|\psi_j\rangle$.*

Proof. Due to the Schmidt-rank classifications in Table A.1, it remains to consider the case with $i = 13$ and $j = 15$. For this we define $\mathbf{\Psi}_B$ analogously to $\mathbf{\Psi}_A$ and from mere inspection one finds that $\mathbf{\Psi}_B(\psi_{13}) = (1, 1, 2)$, while $\mathbf{\Psi}_B(\psi_{15}) = (1, 1, 1)$, and hence both vectors cannot be interconverted by ILOs. □

4. **SLOCC transformation to the 17 classes**

In order to show that the 17 classes are sufficient, we start with an arbitrary pure 233-state $|\psi\rangle\langle\psi|$. If $\mathbf{\Omega}(\psi) = (1, 3, 3)$, then the state is only bipartite entangled, has Schmidt-rank 3, and therefore is in class 3. Otherwise, unless $\mathbf{\Omega}(\psi) = (2, 3, 3)$, the state can be interconverted according to the analysis of the 322-states provided in Ref. [192].

In Ref. [193] the classes 10, 13, 15, 16, and 17 have been found to be sufficient if $\Omega(\psi) = (2,3,3)$ and $\Xi_A(\psi) = 3$. For completeness, we show this using a simplified argument in Appendix 8. The remaining cases can be interconverted to class 14.

Proposition A.2. *Any 233-state $|\psi\rangle\langle\psi|$ with $\Omega(\psi) = (2,3,3)$ and $\Xi_A(\psi) \leq 2$ is of class 14.*

Proof. We write $|\psi\rangle = \sum_{ij} A_{ij} |0ij\rangle + \sum_{ij} B_{ij} |1ij\rangle$, which defines the 3×3 matrices A and B. Since $\Xi_A(\psi) \leq 2$, the rank of $\lambda A + \mu B$ is at most 2 for any $\lambda, \mu \in \mathbb{C}$. In addition, $\Omega(\psi) = (2,3,3)$ excludes the existence of any nontrivial vector v with $Av = 0 = Bv$ or $A^T v = 0 = B^T v$. We can therefore apply Lemma A.1 and obtain the matrices Y and Z. These define the ILOs $\beta = \sum_{ij} Y_{ij} |i\rangle\langle j|$ and $\gamma = \sum_{ij} Z_{ij} |i\rangle\langle j|$ which then achieve $(\mathbb{1}_2 \otimes \beta \otimes \gamma) |\psi\rangle = |\psi_{14}\rangle$. □

Lemma A.1. *Let A and B be complex 3×3 matrices, such that for all $\lambda, \mu \in \mathbb{C}$, the matrix $\lambda A + \mu B$ has at most rank 2. If $Av = 0 = Bv$ and $A^T w = 0 = B^T w$ implies $v = 0$ and $w = 0$ for $v, w \in \mathbb{C}^3$, then there exist invertible matrices Y and Z, such that*

$$YAZ^T = \begin{pmatrix} 1 & 0 & 0 \\ 0 & 1 & 0 \\ 0 & 0 & 0 \end{pmatrix} \text{ and } YBZ^T = \begin{pmatrix} 0 & 0 & 0 \\ 0 & 0 & 1 \\ 1 & 0 & 0 \end{pmatrix}. \tag{A.2}$$

The proof of this Lemma is provided in Appendix 9.

5. **SLOCC-Hierarchy**

Within this section, we present the hierarchic order of the 17 classes that we derived within the foregoing analysis. The hierarchy is defined by convertibility under noninvertible SLOCC and summarized in Fig. A.1. There exists an SLOCC transformation form class i to class j if and only if there is a path from vertex i to vertex j in the directed graph (no interconvertion between classes 8, 9, 11, and 12 is possible). Out of the six genuine 233-entangled classes, cf. the top row in Fig. A.1, only the classes 13, 15, and 17 are sufficiently entangled in order to reach all states which are not genuine 233-entangled. We note, that from a preliminary numerical analysis, it seems that basically all pure states (with respect to the Haar measure) are of class 15. The proof odf the hierarchy goes as follows: In order to prove the allowed and forbidden transformations as depicted in Fig. A.1, first note that the hierarchy for the classes 1,2, 4–9, 11, and 12 has already been established in Ref. [192], while clearly class 3 can only be converted to class 2 and class 1. Using, that noninvertible SLOCC transformations lower the Schmidt-rank of at least one subsystem as well as the constraints due to the fact that any SLOCC operation may increase neither the first entry on Ψ_A nor Ξ_A, we can already exclude many transitions. In particular, it is clear that no transition between any of the classes in the top row of Fig A.1 (10 and 13–17) is admissible and that all relations not shown between the top row and the second top row (3, 8, 9, 11, and 12) are impossible, except for the following special case.

Proposition A.3. *There is no SLOCC transformation from class 14 to class 11 or class 12.*

Proof. Since class 14 is invariant under exchange of the qutrit-systems while class 11 and class 12 interchange places, it is enough to consider $14 \to 11$. We assume the

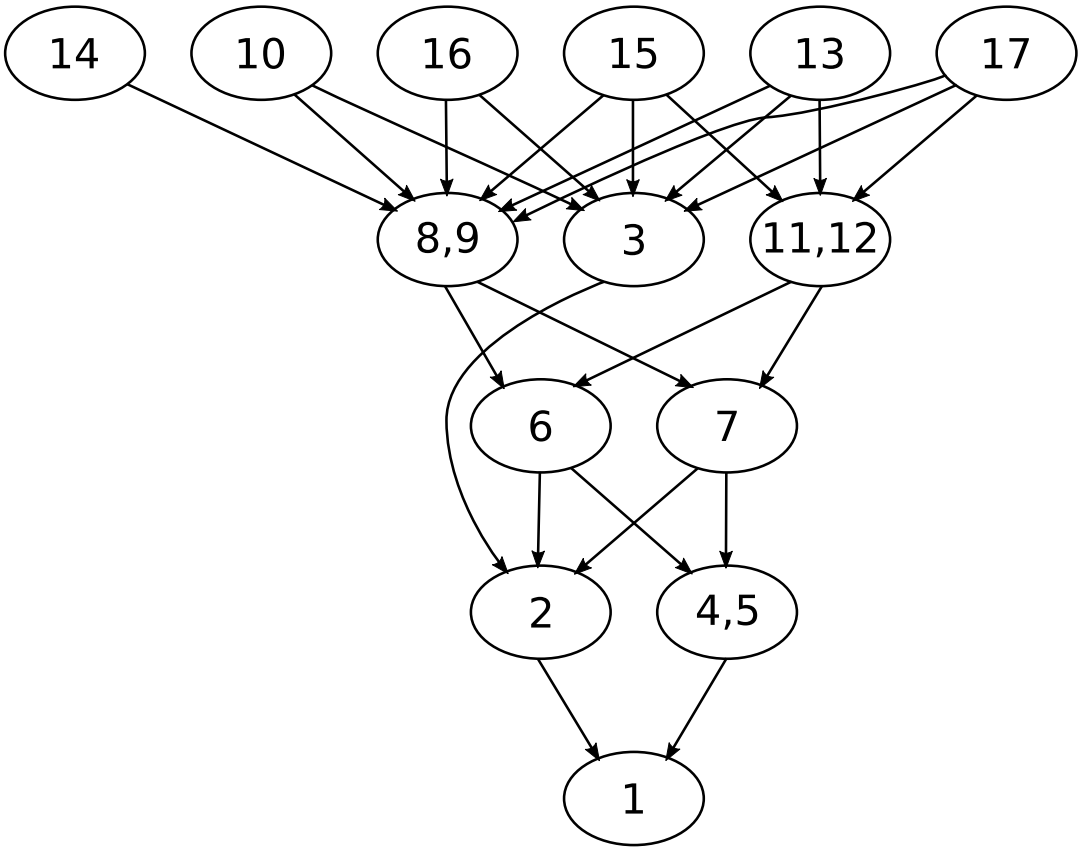

FIGURE A.1: SLOCC-hierarchy of 233-systems. Class k can be transformed to class ℓ if and only if there is a path from vertex k to ℓ. Representative vectors for the 17 classes are given in Eq. (A.1). The classes 8 and 9 exchange places under exchange of the qutrit-systems, and so the classes 11 and 12, while all other classes are invariant under this exchange.

contrary, that there are local operators $\tilde{\alpha}$, $\tilde{\beta}$, and $\tilde{\gamma}$, such that $(\tilde{\alpha}\otimes\tilde{\beta}\otimes\tilde{\gamma})\,|\psi_{15}\rangle = |\psi_{11}\rangle$. Since $\Omega(\psi_{15}) = (2,3,3)$, $\Omega(\psi_{11}) = (2,2,3)$, and $\langle i2j|\psi_{11}\rangle = 0$ for any i and j, there is an ILO β with $\tilde{\beta} = (|0\rangle\langle 0| + |1\rangle\langle 1|)\beta$, while $\tilde{\alpha}$ and $\tilde{\gamma}$ must be invertible. Therefore, there is a representative vector $|\phi\rangle$ of class 15 such that $|\phi\rangle = |\psi_{11}\rangle + |\eta\rangle$ for some $|\eta\rangle = \sum_{ij} x_{ij}\,|i2j\rangle$. It is now straightforward to show that $\Xi(\phi) \leq 2$ holds for any η, which is in contradiction to $|\phi\rangle$ being a representative vector of class 15. □

To demonstrate the allowed transitions between the two top rows in Fig A.1, we establish convertibility by applying local operators $\tilde{\alpha}$, $\tilde{\beta}$, and $\tilde{\gamma}$ to the representative vectors of each pair of classes. In Appendix 10 we explicitly provide all of those 14 triples of operators. This concludes the proof of the SLOCC-hierarchy.

6. **SLOCC classification in higher dimensions**

The number of SLOCC classes for LMN-systems with $L, M, N \geq 3$ is uncountably infinite, as can be seen by comparing the number of parameters of the representative vector and of the ILOs [188]. In addition, also the number of SLOCC classes for $2MN$-systems with $M, N \geq 4$ is uncountably infinite as it follows from the following result.

Proposition A.4. *There is no countable set of 244-states from which all pure 244-states can be generated by means of SLOCC.*

Proof. We consider the family of vectors $|\psi_p\rangle = |0\rangle_A\,|v\rangle_{BC} + |1\rangle_A\,|w_p\rangle_{BC}$ with parameter $p \geq 1$, where

$$|v\rangle = |00\rangle + |11\rangle + |22\rangle + |33\rangle\,, \text{ and} \tag{A.3}$$

$$|w_p\rangle = |00\rangle - |11\rangle + p\,|22\rangle\,. \tag{A.4}$$

Since $\Omega(\psi_p) = (2,4,4)$ for all p, none of the vectors $|\psi_p\rangle$ can be generated by local operators from any other 244-vector. Also, as we show next, there are no ILOs α, β, and γ, such that

$$(\alpha\otimes\beta\otimes\gamma)\,|\psi_p\rangle = |\psi_q\rangle\,, \text{ where } p \neq q, \tag{A.5}$$

and hence the assertion of the proposition holds.

We define the 3×3-matrices $V = [\langle ij|v\rangle]_{ij}$, $W_p = [\langle ij|w_p\rangle]_{ij}$, $Y = [\langle i|\beta|j\rangle]_{ij}$, and $Z = [\langle i|\gamma|j\rangle]_{ij}$. With $\alpha = a|0\rangle\langle 0| + b|1\rangle\langle 0| + c|0\rangle\langle 1| + d|1\rangle\langle 1|$, Eq. (A.5) is equivalent to the conditions

$$Y(aV + cW_p)Z^T = V, \text{ and} \tag{A.6}$$

$$Y(bV + dW_p)Z^T = W_q. \tag{A.7}$$

Writing $D \equiv aV + cW_p$ and noting that $V = \mathbb{1}_4$, Eq. (A.6) implies $Y = (Z^T)^{-1}D^{-1}$. Applying this to Eq. (A.7), we get that $D^{-1}(bV + dW_p)$ has to be similar to W_q. (Two matrices A and B are similar if there exists an invertible matrix R, such that $RA = BR$). This is the case only if the eigenvalues of both matrices coincide (cf., e.g., Corollary 1.3.4 in Ref. [197]). Since all matrices are already diagonal, Eq. (A.5) can be satisfied, if and only if

$$\left(\tfrac{b+d}{a+c}, \tfrac{b-d}{a-c}, \tfrac{b+pd}{a+pc}, \tfrac{b}{a}\right) = \pi[(1,-1,q,0)] \tag{A.8}$$

can be solved for some permutation π of the 4 entries. In a lengthy, but straightforward calculation, one finds that for $p \geq 1$ and $q \geq 1$ this implies $p = q$. □

The remaining cases which may have a finite number of SLOCC classes are hence $23N$ for $N > 3$. Note, that for $N > 6$, no new SLOCC classes can appear, since clearly at most $\Omega = (2, 3, 6)$ can hold. A representative vector of such a state is $|\psi\rangle = |000\rangle + |011\rangle + |022\rangle + |103\rangle + |114\rangle + |125\rangle$. In a case study, we were not able to find an example demonstrating that in this case the number of SLOCC classes is infinite and hence the cases $23N$ with $N = 4, 5, 6$ remain open.

7. **Conclusions**

We studied the entanglement classification of pure $2NM$ quantum states under stochastic local quantum operations (SLOCC). We provided a full classification for the case 233, yielding 17 entanglement classes, 12 of which are genuine multipartite entangled and six begin genuine 233-entangled. Out of these six classes, states $|\psi\rangle\langle\psi|$ from class 14 are special as in any decomposition $|\psi\rangle = |\xi\rangle_A |\eta\rangle_{BC} + |o\rangle_A |\theta\rangle_{BC}$, the vectors $|\eta\rangle$ and $|\theta\rangle$ are exactly 2×2-entangled. The other extreme case is class 17, where in any such decomposition at least one of the vectors is 3×3-entangled. We calculated the SLOCC-hierarchy for 233-systems, finding 23 new allowed and seven new forbidden transformations. We also showed that for 244-systems the number of SLOCC classes is uncountably infinite, while for $23N$-systems the SLOCC classification remains open.

Recently, it has become possible to prepare genuine 233-entangled states, using the orbital angular momentum of three photons [198]. The target state in this case was of class 10. It would be interesting to aim for the exotic classes 14 and 17. Also, since numerical evidence suggests that most states are in class 15, those will also be interesting target states.

8. **Appendix A: SLOCC classification of all 233-states with and $\Xi_A = 3$**

In this section we prove that any 233-state $|\psi\rangle\langle\psi|$ with $\Xi_A(\psi) = 3$ can be transformed by means of SLOCC to some of the classes 3, 10, 13, 15, 16, or 17. That is, we show that there exist ILOs α, β, and γ such that $(\alpha \otimes \beta \otimes \gamma) |\psi\rangle = |\psi_k\rangle$ for some corresponding representative vector $|\psi_k\rangle$ from Eq. (A.1). We now proceed along the lines of Ref. [193].

Since $\Xi_A(\psi) = 3$, there exists some vectors $|\xi\rangle_A$ and $|o\rangle_B$, such that $|\psi\rangle = \sum_{ij} A_{ij} |\xi\rangle_A |ij\rangle + \sum_{ij} B_{ij} |o\rangle_A |ij\rangle$ where the matrix A has rank 3. Then it suffices to find some invertible matrices Y and Z, together with $a, b, c, d \in \mathbb{C}$ with $ad \neq bc$, such that

$$Y(aA + cB)Z^T = A^{(k)} \text{ and} \tag{A.9}$$

$$Y(bA + dB)Z^T = B^{(k)}. \tag{A.10}$$

Here $A^{(k)} = [\langle 0ij|\psi_k\rangle]_{ij}$ and $B^{(k)} = [\langle 1ij|\psi_k\rangle]_{ij}$. Let S be an invertible matrix, such that $B' = SA^{-1}BS^{-1}$ has Jordan normal form. Then $A' \equiv SA^{-1}AS^{-1} = \mathbb{1}_3$ and B' is

in either of the following forms,

$$\begin{aligned}
&\text{(a)}\ \begin{pmatrix}\lambda & 1 & 0\\ 0 & \lambda & 1\\ 0 & 0 & \lambda\end{pmatrix}, \quad \text{(b)}\ \begin{pmatrix}\lambda & 1 & 0\\ 0 & \lambda & 0\\ 0 & 0 & \lambda\end{pmatrix},\\
&\text{(c)}\ \begin{pmatrix}\lambda & 1 & 0\\ 0 & \lambda & 0\\ 0 & 0 & \mu\end{pmatrix}, \quad \text{(d)}\ \begin{pmatrix}\lambda & 0 & 0\\ 0 & \lambda & 0\\ 0 & 0 & \mu\end{pmatrix},\\
&\text{(e)}\ \begin{pmatrix}\lambda & 0 & 0\\ 0 & \mu & 0\\ 0 & 0 & \nu\end{pmatrix}, \quad \text{(f)}\ \begin{pmatrix}\lambda & 0 & 0\\ 0 & \lambda & 0\\ 0 & 0 & \lambda\end{pmatrix},
\end{aligned} \tag{A.11}$$

where $\lambda \neq \mu$, $\lambda \neq \nu$, and $\mu \neq \nu$.

Case (a) corresponds to class 17, case (b) to class 16, and case (f) to class 3 via $Y = SA^{-1}$, $Z = (S^{-1})^T$, and $(a, b, c, d) = (1, -\lambda, 0, 1)$. It can be verified that case (c) corresponds to class 13 via

$$Y = \begin{pmatrix}1 & \delta & 0\\ 0 & 0 & \delta\\ 0 & 1 & 0\end{pmatrix} SA^{-1}, \quad Z = \begin{pmatrix}0 & 1 & 0\\ 0 & 0 & 1\\ 1 & 0 & 0\end{pmatrix} (S^{-1})^T, \tag{A.12}$$

and $(a, b, c, d) = (-\lambda, \delta\mu, 1, -\delta)$, where $\delta = 1/(\mu - \lambda)$. For case (d) we choose $Y = SA^{-1}$, $Z = (S^{-1})^T$, and $(a, b, c, d) = (\delta\lambda + 1, -\delta\lambda, -\delta, \delta)$ to transform $|\psi\rangle$ to $|\psi_{10}\rangle$ Finally, case (e) corresponds to class 15 when we let

$$\begin{aligned}
&Y = \mathrm{diag}(\mu - \nu, \lambda - \nu, \mu - \lambda) SA^{-1},\\
&Z = (S^{-1})^T/(\mu - \nu),\\
&a = \nu/(\nu - \lambda), \quad b = \mu/(\mu - \lambda),\\
&c = 1/(\lambda - \nu), \text{ and } d = 1/(\lambda - \mu).
\end{aligned} \tag{A.13}$$

9. **Proof of Lemma A.1**

We consider 3×3 matrices A and B with (i) $\det(\lambda A + \mu B) = 0$ for all $\lambda, \mu \in \mathbb{C}$, and (ii) $Av = 0 = Bv$ and $A^T w = 0 = B^T w$ implies $v = 0$ and $w = 0$ for $v, w \in \mathbb{C}^3$.

We first show that $\mathrm{rank}\, A = \mathrm{rank}\, B = 2$. For this we assume the contrary, $B = x\, y^\dagger$ for some $x, y \in \mathbb{C}^3$. Due to condition (i) there exists a vector $v \neq 0$ with $Av + x\, y^\dagger v = 0$, and hence either $Av = 0$ and $Bv = 0$ or x is in the range of A. The latter implies that for any vector $w \neq 0$ with $A^T w = 0$, also $x^T w = 0$ holds. Either case contradicts condition (ii) and therefore both matrices have rank 2.

Using the singular value decomposition, it is always possible to find an invertible matrix Y_1 and a unitary matrix Z_1, such that $A' = Y_1 A Z_1^T = \mathrm{diag}(1, 1, 0)$ while $B' = Y_1 A Z_1^T$ still has arbitrary form. Then, the upper left 2×2 submatrix of B' can always be brought to Jordan normal form, resulting in from B_{J1} or B_{J2},

$$B_{J1} = \begin{pmatrix}b_{00} & 0 & b_{02}\\ 0 & b_{11} & b_{12}\\ b_{20} & b_{21} & b_{22}\end{pmatrix}, \; B_{J2} = \begin{pmatrix}b_{00} & 1 & b_{02}\\ 0 & b_{00} & b_{12}\\ b_{20} & b_{21} & b_{22}\end{pmatrix}, \tag{A.14}$$

where $|b_{11}| \geq |b_{00}|$ can always be achieved by interchanging both, the first and second row and the first and second column. The matrix A' is left unchanged under this transformation. Note, that $b_{22} = 0$ as it follows from condition (i) via $\det(\lambda A + B) = \lambda^2 b_{22} + \mathcal{O}(\lambda)$.

We use $\det(B_{J1}) = 0$ and $\det(B_{J2}) = 0$ to further restrict the entries b_{ij}, yielding 7 different cases:

$$\begin{aligned} B_1 &= \begin{pmatrix} b_{00} & 0 & b_{02} \\ 0 & b_{11} & b_{12} \\ b_{20} & b_{21} & 0 \end{pmatrix}, B_2 = \begin{pmatrix} 0 & 0 & 0 \\ 0 & b_{11} & b_{12} \\ b_{20} & b_{21} & 0 \end{pmatrix}, \\ B_3 &= \begin{pmatrix} 0 & 0 & b_{02} \\ 0 & 0 & b_{12} \\ b_{20} & b_{21} & 0 \end{pmatrix}, B_4 = \begin{pmatrix} 0 & 0 & b_{02} \\ 0 & b_{11} & b_{12} \\ 0 & b_{21} & 0 \end{pmatrix}, \\ B_5 &= \begin{pmatrix} b_{00} & 1 & b_{02} \\ 0 & b_{00} & b_{12} \\ b_{20} & b_{21} & 0 \end{pmatrix}, B_6 = \begin{pmatrix} 0 & 1 & b_{02} \\ 0 & 0 & 0 \\ b_{20} & b_{21} & 0 \end{pmatrix}, \\ \text{and } B_7 &= \begin{pmatrix} 0 & 1 & b_{02} \\ 0 & 0 & b_{12} \\ 0 & b_{21} & 0 \end{pmatrix}. \end{aligned} \tag{A.15}$$

where for B_1, $|b_{00}| > 0$ and $b_{02}b_{11}b_{20} + b_{00}b_{12}b_{21} = 0$ must hold and for B_5 the conditions $|b_{00}| > 0$ and $b_{00}b_{02}b_{20} - b_{12}b_{20} + b_{00}b_{12}b_{21} = 0$ are in place.

For simplicity, we restrict $(\tilde{Y}, \tilde{Z})$, which defines the set of all pairs of invertible 3×3 matrices, to a subset $(Y, Z) \subset (\tilde{Y}, \tilde{Z})$ such that $YA'Z^T = A'$ implies

$$Y = \begin{pmatrix} \frac{1}{z_{00}} & 0 & y_{02} \\ -\frac{z_{01}}{z_{11}z_{00}} & \frac{1}{z_{11}} & y_{12} \\ 0 & 0 & y_{22} \end{pmatrix}, \; Z = \begin{pmatrix} z_{00} & z_{01} & z_{02} \\ 0 & z_{11} & z_{12} \\ 0 & 0 & z_{22}. \end{pmatrix} \tag{A.16}$$

For all B_k, $k \in 1, 2, \ldots, 9$ one can, by solving the linear system of equations, find ILOs (Y, Z) such that $YB_kZ^T = \tilde{B}_n$, where $\tilde{B}_n$ are the parameter free matrices

$$\begin{aligned} \tilde{B}_1 &= \begin{pmatrix} 1 & 0 & 0 \\ 0 & 1 & 0 \\ 0 & 0 & 0 \end{pmatrix}, \tilde{B}_2 = \begin{pmatrix} 0 & 0 & 0 \\ 0 & 0 & 1 \\ 1 & 0 & 0 \end{pmatrix} \\ \tilde{B}_3 &= \begin{pmatrix} 0 & 0 & 1 \\ 0 & 0 & 0 \\ 1 & 0 & 0 \end{pmatrix}, \tilde{B}_4 = \begin{pmatrix} 1 & 0 & 0 \\ 0 & 0 & 0 \\ 0 & 0 & 1 \end{pmatrix} \\ \tilde{B}_5 &= \begin{pmatrix} 0 & 0 & 0 \\ 0 & 1 & 0 \\ 0 & 0 & 1 \end{pmatrix}. \end{aligned} \tag{A.17}$$

The case $YB_kZ^T = \tilde{B}_1 \equiv A'$ is sorted out due to condition (ii). Similarly, the cases $YB_kZ^T = \tilde{B}_n$ with $n = 3, 4, 5$ have $\det(A' + \tilde{B}_n) \neq 0$, which contradicts condition (i). Hence only the case $YB_kZ^T = \tilde{B}_2 \equiv A'$ remains, which hereby proves Lemma A.1.

10. **Allowed transformations in Fig A.1**
    According to Fig. A.1, there are 14 SLOCC transformations from the classes 10, 13–17 to the classes 3, 8, and 11. In the table below, we provide for each of the transformations matrices X, Y, and Z.

k	$\to$	ℓ	X	Y	Z
10	$\to$	3	$\begin{pmatrix}1&1\\0&0\end{pmatrix}$	$\mathbb{1}_3$	$\mathbb{1}_3$
13	$\to$	3	$\begin{pmatrix}1&1\\0&0\end{pmatrix}$	$\begin{pmatrix}0&0&1\\0&1&0\\1&0&-1\end{pmatrix}$	$\mathbb{1}_3$
15	$\to$	3	$\begin{pmatrix}1&1\\0&0\end{pmatrix}$	$\begin{pmatrix}\frac{1}{2}&0&0\\0&1&0\\0&0&1\end{pmatrix}$	$\mathbb{1}_3$
16	$\to$	3	$\begin{pmatrix}1&0\\0&0\end{pmatrix}$	$\mathbb{1}_3$	$\mathbb{1}_3$
17	$\to$	3	$\begin{pmatrix}1&0\\0&0\end{pmatrix}$	$\mathbb{1}_3$	$\mathbb{1}_3$
10	$\to$	8	$\mathbb{1}_2$	$\begin{pmatrix}1&0&1\\0&1&0\\0&0&0\end{pmatrix}$	$\mathbb{1}_3$
13	$\to$	8	$\mathbb{1}_2$	$\begin{pmatrix}1&0&0\\0&1&0\\0&0&0\end{pmatrix}$	$\mathbb{1}_3$
14	$\to$	8	$\mathbb{1}_2$	$\begin{pmatrix}0&1&0\\1&0&0\\0&0&0\end{pmatrix}$	$\begin{pmatrix}0&1&0\\1&0&0\\0&0&1\end{pmatrix}$
15	$\to$	8	$\mathbb{1}_2$	$\begin{pmatrix}1&0&1\\0&1&0\\0&0&0\end{pmatrix}$	$\begin{pmatrix}1&0&-1\\0&1&0\\0&0&1\end{pmatrix}$
16	$\to$	8	$\mathbb{1}_2$	$\begin{pmatrix}1&0&0\\0&0&1\\0&0&0\end{pmatrix}$	$\begin{pmatrix}1&0&0\\0&0&1\\0&1&0\end{pmatrix}$
17	$\to$	8	$\mathbb{1}_2$	$\begin{pmatrix}1&0&0\\0&0&1\\0&0&0\end{pmatrix}$	$\begin{pmatrix}1&0&0\\0&0&1\\0&1&0\end{pmatrix}$
13	$\to$	11	$\mathbb{1}_2$	$\begin{pmatrix}0&1&1\\1&0&0\\0&0&0\end{pmatrix}$	$\begin{pmatrix}0&1&0\\1&0&0\\0&0&1\end{pmatrix}$

15	→	11	$\mathbb{1}_2$	$\begin{pmatrix} 1 & -1 & 0 \\ 1 & 0 & 1 \\ 0 & 0 & 0 \end{pmatrix}$	$\begin{pmatrix} 0 & -1 & 0 \\ 1 & 1 & -1 \\ 0 & 0 & 1 \end{pmatrix}$	
17	→	11	$\mathbb{1}_2$	$\begin{pmatrix} 1 & 0 & 0 \\ 0 & 1 & 0 \\ 0 & 0 & 0 \end{pmatrix}$	$\mathbb{1}_3$	

One verifies that with the local operators $\tilde{\alpha} = \sum_{ij} X_{ij}|i\rangle\langle j|$, $\tilde{\beta} = \sum_{ij} Y_{ij}|i\rangle\langle j|$, and $\tilde{\gamma} = \sum_{ij} Z_{ij}|i\rangle\langle j|$ a transformation $k \to \ell$ of the representative vectors is given by $(\tilde{\alpha} \otimes \tilde{\beta} \otimes \tilde{\gamma})\,|\psi_k\rangle = |\psi_\ell\rangle$. Finally, there are also 6 transformations from the classes 10, 13–17 to the classes 9 and 12. The according transformations can be constructed from the transformations to classes 8 and 11, respectively, since the classes 10, 13–17 are symmetric under exchange of the parties of B and C, while classes 8 and 9 as well as classes 11 and 12 are interchanged.

Bibliography

[1] E.Schroedinger, Die Naturwissenschaften **23**, 807–812, 823–828, 844–849 (1935).

[2] A. Einstein, B. Podolsky, N. Rosen, Phys. Rev. Lett. **47**, 777–780 (1935).

[3] J. S. Bell, Physics **1**, 195–200 (1964).

[4] J.F. Clauser, M.A. Horne, A. Shimony, R.A. Holt, Phys. Rev. Lett. **23**, 880–884 (1969).

[5] J.F. Clauser, M.A. Horne, Phys. Rev. D **10**, 526–535 (1974).

[6] S.J. Freedman, J.F. Clauser, Phys. Rev. Lett. **28**, 938 (1972).

[7] A. Aspect, P. Grangier, G. Roger, Phys. Rev. Lett. **47**, 460 (1981).

[8] A. Aspect, J. Dalibard, G. Roger, Phys. Rev. Lett. **49**, 1804–1807 (1982).

[9] G. Weihs, T. Jennewein, C. Simon, H. Weinfurter, A. Zeilinger, Phys. Rev. Lett. **81**, 5039 (1998).

[10] J.-W. Pan, D. Bouwmeester, M. Daniell, H. Weinfurter and A. Zeilinger, Nature **403** 515–519 (2000).

[11] S. Wiesner, SIGACT News **15**, 78–88 (1983).

[12] C.H. Bennett and G. Brassard, Proceedings of IEEE International Conference on Computers, Systems and Signal Processing, 175–179 (1984).

[13] W. Wootters, W. Zurek, Nature **299**, 802–803 (1982).

[14] D. Dieks, Phys. Lett. A **92**, 271–272 (1982).

[15] C.H. Bennett, Phys. Rev. Lett. **68**, 3121–3124 (1992).

[16] A.K. Ekert, Phys. Rv. Lett. **67**, 661–663 (1991).

[17] C. H. Bennett and S. J. Wiesner, Phys. Rev. Lett. **69**, 2881 (1992).

[18] C. H. Bennett, G. Brassard, C. Crepeau, R. Jozsa, A. Peres, W. K. Wootters, Phys. Rev. Lett. **70**, 1985 (1993).

[19] Anton Zeilinger. et al., Nature **390**, 575–579 (1997).

[20] Boschi, Branca, De Martini, Hardy, Popescu, Phys. Rev. Lett. **80**, 1121 (1998).

[21] M. D. Barrett, J. Chiaverini, T. Schaetz, J. Britton, W. M. Itano, J. D. Jost, E. Knill, C. Langer, D. Leibfried, R. Ozeri, D. J. Wineland, Nature **429**, 737-739 (2004).

[22] M. Riebe, H. Haeffner, C. F. Roos, W. Haensel, J. Benhelm, G. P. T. Lancaster, T. W. Koerber, C. Becher, F. Schmidt-Kaler, D. F. V. James, R. Blatt, Nature **429**, 734–737 (2004).

[23] Xian-Min Jin et. al., Nature Photonics **4**, 379–381 (2010).

[24] X.S. Ma, T. Herbst, T. Scheidl, D. Wang, S. Kropatschek, W. Naylor, B. Wittmann, A. Mech, et al., Nature **489**, 269–273 (2010).

[25] D.Deutsch, Proceedings of the Royal Society A **400**, 97–107 (1985).

[26] P. W. Shor, SIAM Journal on Computing **26**, 1484–1509 (1997).

[27] Lieven M. K. Vandersypen, Matthias Steffen, Gregory Breyta, Costantino S. Yannoni, Mark H. Sherwood und Isaac L. Chuang,

[28] L. K. Grover, Phys. Rev. Lett. **78**, 325–328 (1997).

[29] Y. H. Wang, Y. Zhang, Commun Theoretical Physics **49**, 1487–1490 (2008).

[30] A. Peres, Phys. Rev. Lett. **77**, 1413–1415 (1996).

[31] M. Horodecki, P. Horodecki, R. Horodecki, Phys. Rev. A **223**, 1 (1996).

[32] Raussendorf, H. J. Briegel, Phys. Rev. Lett. **86** (2001).

[33] M. Hein, J. Eisert, and H. J. Briegel, Phys. Rev. A **69**, 062311 (2004).

[34] M. Rossi, M. Huber, D. Bruß, and C. Macchiavello, New Journal of Physics **15**, 113022 (2013).

[35] R. Raussendorf, D. E. Browne, and H. J. Briegel, Phys. Rev. A **68**, 022312 (2003).

[36] D. Schlingemann and R. F. Werner, Phys. Rev. A **65**,012308 (2002).

[37] M. Gachechiladze, C. Budroni, and O. Gühne, Phys. Rev. Lett. **116**, 070401 (2016).

[38] Kruszynska and Kraus, Phys. Rev. A **79**, 052304 (2009).

[39] Qu, Ri and Ma, Yi-ping and Wang, Bo and Bao, Yan-ru, Phys. Rev. A **87**, 052331 (2013)

[40] A. Bouchet, J. Combin, Theory Ser. B **45**,58–76 (1988).

[41] Maarten Van den Nest, Jeroen Dehaene, Bart De Moor, Phys. Rev. A **69**, 022316 (2004).

[42] M. Bahramgiri and S. Beigi, arXiv:quant-ph/0610267 (2006).

[43] O. Gühne, M. Cuquet, F.E.S. Steinhoff, T. Moroder, M. Rossi, D. Bruß, B. Kraus, C. Macchiavello, J. Phys. A **47**, 335303 (2014).

[44] M.Gachechiladze, N. Tsimakuridzet, C. Budroni, O. Gühne, QPL (2016)

[45] H. J. Briegel, D. E. Browne, W. Dür, R. Raussendorf and M. Van den Nest, Nat. Phys. 5, 19 (2009)

[46] M. A. Nielsen, I. L. Chuang, 'Quantum computation and Quantum information, Cambrige Univ. Press (2010).

[47] J. J. Sakurai, Modern Quantum Mechanics, Revised ed. (Addison-Wesley, New York, 1994).

[48] O. Gühne and G. Tóth, "Entanglement detection," Physics Reports **474**, 1-–75 (2009).

[49] E. Schmidt, Math. Ann. **63**, 433 (1907).

[50] A. Peres, 'Quantum theory:concepts and methods', 193 (Kluwer, Dordrecht, 1993).

[51] M. A. Nielsen, "Conditions for a Class of Entanglement Transformations," Phys. Rev. Lett. **83**, 436 (1999).

[52] W. F. Stinespring, "Positive Functions on C*-Algebras," Proc. Americ. Math. Soc. **6**, 211 (1955).

[53] E. C. G. Sudarshan, P. M. Mathews, and J. Rau, "Stochastic Dynamics of Quantum-Mechanical Systems," Phys. Rev. **121**, 920 (1961).

[54] K. Kraus, "General state changes in quantum theory," Ann. Phys. **64**, 311 (1971).

[55] A. K. Pati, Phys. Rev. A **278**, 118–122 (2000).

[56] J. von Neumann, Mathematical Foundations of Quantum Mechanics (Princeton University Press 1955).

[57] M. Born, 'Quantenmechanik der Stoßvorgänge', Z. Phys. **38**, 803-827 (1926).

[58] C. W. Helstrom, Quantum detection and estimation theory (Academic Press, New York, 1976).

[59] D. Dieks, Phys. Lett. A **126**, 303 (1988).

[60] A. Peres, Phys. Lett. A **128**, 19 (1988)

[61] M. A. Naimark, Izv. Akad. Nauk SSSR Ser. Mat. **4**, 53–104 (1940).

[62] C. H. Bennett, S. Popescu, D. Rohrlich, J. A. Smolin, and A. V. Thapliyal, Phys. Rev. A **63**, 012307 (2001).

[63] P. Kómár, E. M. Kessler, M. Bishof, L. Jiang, A. S. Sørensen, J. Ye and M. D. Lukin, Nature Physics **10**, 582-–587 (2014).

[64] Monz, T. et al. Phys. Rev. Lett. **106**, 130506 (2011).

[65] N. Friis, O.Marty, C. Maier, C. Hempel, M. Holzäpfel, P.Jurcevic, M. B. Plenio, M. Huber, C. Roos, R.Blatt, and B. Lanyon, Phys. Rev. X **8**, 021012 (2018)

[66] S. Pironio, A. Acin, S. Massar, A. B. Giroday, D. N. Mat- sukevich, P. Maunz, S. Olmschenk, D. Hayes, L. Luo, T. A. Manning and C. Monroe, Nature **464**, 1021 (2010).

[67] T. Lunghi, J. B. Brask, C. C. W. Lim, Q. Lavigne, J. Bowles, A. Martin, H. Zbinden and N. Brunner, Phys. Rev. Lett. **114**, 150501(2015).

[68] Z. Huang, C. Macchiavello, L. Maccone, Phys. Rev. A **94**, 012101 (2016).

[69] M. Horodecki R. Horodecki, P. Horodecki and K.Horodecki, Rev. Mod. Phys. **81**, 865-–942 (2009).

[70] J. Uffink M. Seevinck, Phys. Rev. A **78**, 032101 (2008).

[71] F. Yan Y. Hong, T. Gao, Phys. Rev. A **86** 062323 (2012).

[72] R.F. Werner, Phys. Rev. A **40**, 4277–4281 (1989).

[73] Eggeling et al. (2008).

[74] C.Eltschka, J. Siewert, Phys. Rev. Lett. **108**, 020502 (2012).

[75] The LIGO Scientific Collaboration (J. Abadie et al.), Nature Physics **7**, 962 (2011).

[76] B. C. Sanders, Phys. Rev. A **40**, 2417 (1989).

[77] G. Vidal, J.Mod.Opt. **47** 355 (2000).

[78] Martin B. Plenio, S. Virmani, Quant.Inf.Comput. **7**, 1–51 (2007).

[79] V. Vedral and M. Plenio, Phys. Rev. A **57**, 1619 (1998).

[80] I. Bengtsson and K. Zyczkowski, (Cambridge University Press, 2006).

[81] Charles H. Bennett, Herbert J. Bernstein, Sandu Popescu, and Benjamin Schumacher, Phys. Rev. A, **53** 2046–2052 (1996).

[82] C. H. Bennett, D. P. DiVincenzo, J. A. Smolin, and W. K. Wootters, Phys. Rev. A **54**, 3824 (1996).

[83] C. H. Bennett, G. Brassard, S. Popescu, B. Schumacher, J. A. Smolin, W. K. Wootters, Phys. Rev. Lett. **76**, 722–725 (1996).

[84] Coffman, Kundu and Wootters, Phys. Rev. A **61**, 052306 (2000).

[85] Wong and Christensen, Phys. Rev. A **63**, 044301 (2001).

[86] W.K. Wootters, Phys. Rev. Lett. **80**, 2245 (1998).

[87] G. Vidal, R. F.Werner, Phys. Rev. A **65**, 032314 (2002);
M.B.Plenio, Phys. Rev. Lett. **95**, 090503 (2005).

[88] V. Vedral, M. B. Plenio, M. A. Rippin, and P. L. Knight, Phys. Rev. Lett. **78**, 2275 (1997).

[89] A. Shimony, Ann. NY. Acad. Sci. **755**, 675 (1995).

[90] A. Uhlmann, Open Syst. Inf. Dyn. **5**, 209 (1998).

[91] S. Popescu and D. Rohrlich, Physical Review A **56**, 3319–3322 (1997).

[92] A. Peres Phys. Rev. Lett. **77**, 1413 (1996).

[93] C. Eltschka, J. Siewert, J. Phys. A **47**, 424005 (2014).

[94] C. H. Bennett, H. J. Bernstein, S. Popescu, B. Schumacher, Phys.Rev.A **53**, 2046–2052 (1996).

[95] A. Acin, A. Andrianov, E. Jane, R. Tarrach, J. Phys. A **34**, 6725 (2001).

[96] H. Verschelde F. Verstaete J. Dehaene, B. De Moor, Phys. Rev. A. **65**, 052112 (2002).

[97] Gurvits, L., in Proceedings of the 35th ACM Symposium on Theory of Computing, (ACM Press, New York, 2003).

[98] M. Horodecki, P. Horodecki, and R. Horodecki, (1996).

[99] M. Horodecki and P. Horodecki, Phys. Rev. A. **59** (1999).

[100] M. A. Nielsen and J. Kempe, Phys. Rev. Lett. **86**, 5184 (2001).

[101] Kai Chen, Ling-An Wu, Quantum Information and Computation **3**, 193–202 (2003).

[102] H. Hahn, Journal für die reine und angewandte Mathematik **157**, 214–229 (1997).

[103] S. Banach, Studia Mathematica **1**, 211–216 (1929).

[104] E. C. G. Sudarshan, P. M. Mathews, and J. Rau, Phys. Rev. **121**, 920 (1961);
A. Jamio?kowski, Rep. Math. Phys. **3**, 275 (1972);
M.-D. Choi, Linear Alg. Appl. **10**, 285 (1975); K. Kraus, States, Effects, and Operations: Fundamental Notions of Quantum Theory, Lecture notes in Physics, vol. 190 (Spring-Verlag, New York, 1983).

[105] D. Schlingemann, arXiv preprint quant-ph/0305170, (2003).

[106] E. Hostens, J. Dehaene, and B. De Moor, Phys. Rev. A **71**, 042315 (2005).

[107] M. Bahramgiri and S. Beigi, arXiv preprint quant-ph/0610267, (2006).

[108] S. Y. Looi, L. Yu, V. Gheorghiu, and R. B. Griffiths, Phys. Rev. A **78**, 042303 (2008).

[109] A. Keet, B. Fortescue, D. Markham, and B. C. Sanders, Phys. Rev. A **82**, 062315 (2010).

[110] Theory of Graphs, Proc. Colloq., Tihany, 219–230 (Academic Press, New York, 1968).

[111] H. J. Briegel, D. E. Browne, W. Dür, R. Raussendorf and M. Van den Nest, Nat. Phys. **5**, 19-–26 (2009).

[112] L. Vandenberghe and S. Boyd, "Semidefinite Programming," SIAM Rev. **38**, 49 (1996).

[113] W. Dür, G. Vidal, and J. I. Cirac, Phys. Rev. A **62**, 062314 (2000).

[114] F. Verstraete, J. Dehaene, B. De Moor, and H. Verschelde, Phys. Rev. A **65**, 052112 (2002).

[115] E. Briand, J. Luque, J. Thibon, and F. Verstraete, J. Math. Phys. **45**, 4855 (2004).

[116] L. Chen, Y.-X. Chen, and Y.-X. Mei, Phys. Rev. A **74**, 052331 (2006).

[117] P. Horodecki, Phys. Lett. A **232**, 333 (1997)

[118] K. Chen and L.-A. Wu, Quant. Inf. Comp. **39**, 193 (2003)

[119] J. I. de Vicente, Quant. Inf. Comput. **7**, 624 (2007).

[120] L. Gurvits, *Classical deterministic complexity of Edmonds? problem and quantum entanglement*, Proceedings of the 35th Annual ACM Symposium on Theory of Computing (ACM Press, 2003), 10, see also arXiv:quant-ph/0303055.

[121] M. Horodecki, P. Horodecki, and R. Horodecki, Phys. Lett. A **223**, 1 (1996).

[122] B. M. Terhal, Phys. Lett. A **271**, 319 (2000).

[123] A. Acín, D. Bruss, M. Lewenstein, and A. Sanpera, Phys. Rev. Lett. **87**, 040401 (2001).

[124] T. Bastin, P. Mathonet, and E. Solano, Phys. Rev. A **91**, 022310 (2015).

[125] F. Hulpke, D. Bruss, M. Lewenstein, and A. Sanpera, Quant. Inf. Comp. **4**, 207 (2004).

[126] E. Chitambar, R. Duan, and Y. Shi, Phys. Rev. Lett. **101**, 140502 (2008).

[127] L. Vandenberghe and S. Boyd, SIAM Rev. **38**, 49 (1996).

[128] M. Piani and C. Mora, Phys. Rev. A **75**, 012305 (2007).

[129] Bogoljubov, Il Nuovo Cimento **7**, 794–805 (1958).

[130] R. Horodecki, P. Horodecki, M. Horodecki and K. Horodecki, Rev. Mod. Phys. **81**, 865 (2009).

[131] O. Gühne and G. Tóth, Phys. Rep. **474**, 1 (2009).

[132] M. Hein, J. Eisert, and H.J. Briegel, Phys. Rev. A **69**, 062311 (2004); M. Hein, W. Dür, J. Eisert, R. Raussendorf, M. van den Nest and H. -J. Briegel, in *Quantum Computers, Algorithms and Chaos*, edited by G. Casati, D.L. Shepelyansky, P. Zoller, and G. Benenti (IOS Press, Amsterdam, 2006), quant-ph/0602096.

[133] R. Raussendorf, D. E. Browne, and H. J. Briegel, Phys. Rev. A **68**, 022312 (2003).

[134] D. Gottesman, *Stabilizer Codes and Quantum Error Correction*, PhD thesis, CalTech, Pasadena (1997); D. Schlingemann, Quantum Inf. Comp. **2**, 307 (2002).

[135] D. Greenberger, M. Horne, A. Shimony, and A. Zeilinger, Am. J. Phys. **58**, 1131 (1990); N. D. Mermin, Rev. Mod. Phys. **65**, 803 (1993); D.P. DiVincenzo and A. Peres, Phys. Rev. A **55**, 4089 (1997); O. Gühne and A. Cabello, Phys. Rev. A **77**, 032108 (2008).

[136] B. Jungnitsch, T. Moroder and O. Gühne, Phys. Rev. A **84**, 032310 (2011).

[137] A. Kitaev, Ann. Phys. **321**, 2 (2006).

[138] R. Qu, J. Wang, Z. Li, and Y. Bao, Phys. Rev. A **87**, 022311 (2013); M. Rossi, M. Huber, D. Bruß, and C. Macchiavello, New J. Phys. **15**, 113022 (2013).

[139] B. Yoshida, Phys. Rev. B **93**, 155131 (2016); J. Miller and A. Miyake, npj Quantum Information **2**, 16036 (2016).

[140] O. Gühne, M. Cuquet, F. E. S. Steinhoff, T. Moroder, M. Rossi, D. Bruß, B. Kraus, and C. Macchiavello J. Phys. A: Math. Theor. **47**, 335303 (2014).

[141] M. Gachechiladze, C. Budroni, and O. Gühne, Phys. Rev. Lett. **116**, 070401 (2016).

[142] T. Carle, B. Kraus, W. Dür, and J. I. de Vicente, Phys. Rev. A **87**, 012328 (2013); C. Kruszynska and B. Kraus, Phys. Rev. A **79**, 052304 (2009).

[143] C.E. Mora, H.J. Briegel, and B. Kraus, Int. J. Quant. Inf. **5**, 729 (2007).

[144] A. Vourdas, Rep. Prog. Phys. **67**, 267 (2004).

[145] W. Tang, S. Yu, and C.H. Oh, Phys. Rev. Lett. **110**, 100403 (2013).

[146] D. Schlingemann, Quantum Inf. Comp. **4**, 287 (2004); E. Hostens, J. Dehaene, and B. de Moor, Phys. Rev. A **71**, 042315 (2005); M. Bahramgiri, and S. Beigi, arxiv:quant-ph/0610267; S. Y. Looi, L. Yu, V. Gheorghiu, and R. B. Griffiths, Phys. Rev. A **78**, 042303 (2008); A. Keet, B. Fortescue, D. Markham, and B. C. Sanders, Phys. Rev. A **82**, 062315 (2010).

[147] M. A. Nielsen, M. J. Bremner, J. L. Dodd, A. M. Childs, and C. M. Dawson Phys. Rev. A **66**, 022317 (2002).

[148] D. M. Appleby, J. Math. Phys. **46**, 052107 (2005).

[149] T.-C. Wei and P. M. Goldbart, Phys. Rev. A **68**, 042307 (2003).

[150] B. Jungnitsch, T. Moroder and O. Gühne, Phys. Rev. Lett. **106**, 190502 (2011).

[151] L. Vandenberghe and S. Boyd, SIAM Review 38, 49 (1996).

[152] L. Lamata J. Leon, D. Salgado, and E. Solano, Phys. Rev. A **74**, 052336 (2006).

[153] G. H. Hardy, E. M. Wright, *An introduction to the theory of numbers*, Oxford: Clarendon Press (1938).

[154] I. Niven, H. S. Zuckerman, and H. L. Montgomery, *An introduction to the theory of numbers*, Wiley (1991).

[155] W. Son, C. Brukner, and M. S. Kim, Phys. Rev. Lett. **97**, 110401 (2006); A. Asadian, C. Budroni, F. E. S. Steinhoff, P. Rabl, and O. Gühne, Phys. Rev. Lett. **114**, 250403 (2015).

[156] B. Kraus, Phys. Rev. Lett. **104**, 020504 (2010); B. Liu, J.-L. Li, X. Li, and C.-F. Qiao, Phys. Rev. Lett. **108**, 050501 (2012); T.-G. Zhang, M.-J. Zhao, M. Li, S.-M. Fei, and X. Li-Jost, Phys. Rev. A **88**, 042304 (2013).

[157] A. Peres, Phys. Rev. Lett. **77** 1413 (1996) M. Horodecki, P. Horodecki, and R. Horodecki, Phys. Lett. A **223**, (1996).

[158] P. Horodecki, Phys. Lett. A **232** 333 (1997).

[159] R. D. Carmichael, Am. Math. Mont. **19** 22 (1917); P. Erdős, C. Pomerance, and E. Schmutz, Acta Arithmetica **58**, 363 (1991).

[160] A more elementary way of proving is noticing that $qk = q'k$ iff $q = q'\ mod(d/gcd(d,k))$.

[161] N. Miklin 'Characterizing classical and quantum systems from marginal correlations', PhD Thesis (2017).

[162] M. Krenn, M. Huber, R. Fickler, R. Lapkiewicz, and A. Zeilinger, Proc. Natl. Acad. Sci. USA **111**, 6243 (2014).

[163] G. A. Howland, S. H. Knarr, J. Schneeloch, D. J. Lum, and J. C. Howell, Phys. Rev. X **6**, 021018 (2016).

[164] A. Martin, T. Guerreiro, A. Tiranov, S. Designolle, F. Fröwis, N. Brunner, M. Huber, and N. Gisin, Phys. Rev. Lett. **118**, 110501 (2017).

[165] H. Bechmann-Pasquinucci and W. Tittel, Phys. Rev. A **61**, 062308 (2000).

[166] N. J. Cerf, M. Bourennane, A. Karlsson, and N. Gisin, Phys. Rev. Lett. **88**, 127902 (2002).

[167] A. Sanpera, D. Bruß, and M. Lewenstein, Phys. Rev. A **63**, 050301 (2001).

[168] G. Sentís, C. Eltschka, O. Gühne, M. Huber, and J. Siewert, Phys. Rev. Lett. **117**, 190502 (2016).

[169] N. Brunner, S. Pironio, A. Acin, N. Gisin, A. Allan Methot, and V. Scarani, Phys. Rev. Lett. **100**, 210503 (2008).

[170] Y. Cai, Quantum sizes: Complexity, Dimension and Many-box Locality, PhD thesis, Singapore (2015).

[171] W. Cong, Y. Cai, J.-D. Bancal, and V. Scarani, arXiv:1611.01258.

[172] The Appendices can be found in the supplemental material.

[173] B. M. Terhal, Phys. Lett. A **271**, 319 (2000).

[174] O. Gühne and G. Tóth, Phys. Reports **474**, 1 (2009).

[175] H. Georgi, "Lie Algebras In Particle Physics", *Westview Press*, 2nd ed. (1999).

[176] S. Jevtic, D. Jennings, and T. Rudolph, Phys. Rev. Lett. 108, 110403 (2012).

[177] A. Peres, Phys. Lett. A **202**, 16 (1995).

[178] M. Huber and R. Sengupta, Phys. Rev. Lett. **113**, 100501 (2014).

[179] C.-M. Li, K. Chen, A. Reingruber, Y.-N. Chen, and J.-W. Pan, Phys. Rev. Lett. **105**, 210504 (2010).

[180] A. Keet, B. Fortescue, D. Markham, and B. C. Sanders, Phys. Rev. A **82**, 062315 (2010).

[181] M. Hein, W. Dür, J. Eisert, R. Raussendorf, M. Van den Nest, and H.-J. Briegel, quant-ph/0602096.

[182] M. Rossi, M. Huber, D. Bruß, and C. Macchiavello, New J. Phys. **15**, 113022 (2013).

[183] O. Gühne, and N. Lütkenhaus, Phys. Rev. Lett. **96**, 170502 (2006).

[184] L. Mirsky, Monatshefte für Mathematik **79**, 303 (1975).

[185] F.E.S. Steinhoff, C.Ritz, N. Miklin and O. Gühne, Phys. Rev. A **95**, 052340 (2017).

[186] C. Ritz, T. Kraft, N. Brunner, M. Huber and O. Gühne, Phys. Rev. Lett. **120**, 060502 (2018)

[187] C. Bennett, S. Popescu, D. Rohrlich, J. Smolin and A. Thapliyalet, Phys. Rev. A **63**, 012307 (2000).

[188] W. Dür, G. Vidal and J.I. Cirac, Phys. Rev. A **62**, 062314 (2000).

[189] Daniel M. Greenberger, Michael A. Horne and Anton Zeilinger, Bell's Theorem, Quantum Theory, and Conceptions of the Universe (1989).

[190] Akimasa Miyake and Frank Verstraete, Phys. Rev. A **69**, 012101 (2004).

[191] F. Verstraete, J. Dehaene, B. De Moor, and H. Verschelde, Phys. Rev. A **65**, 052112 (2002).

[192] Akimasa Miyake, Phys. Rev. A **67**, 012108 (2003).

[193] Marcio F. Cornelio and A. F. R. de Toledo Piza, Phys. Rev. A **73**, 032314 (2006).

[194] Yang Xin-Gang, Wang Zhi-Xi, Wang Xiao-Hong and Fei Shao-Ming, Commun. Theor. Phys. **50**, 651 (2008).

[195] Noah Linden, Milán Mosonyi and Andreas Winter, Proc. Roy. Soc. Lond. A **469**, 20120737 (2013).

[196] Marcus Huber and Julio I. de Vicente, Phys. Rev. Lett. **110**, 030501 (2013).

[197] Rodger A. Horn and Charles R. Johnson, Cambridge University Press (1985).

[198] Mehul Malik, Manuel Erhard, Marcus Huber, Mario Krenn, Robert Fickler and Anton Zeilinger, Nat. Photon. **10**, 248–252 (2016).

Declaration of Authorship

Erklärungen
gemäß §7 der Promotionsordnung vom 8. Juni 2017

Ich erkläre(,)

1. dass mir die Promotionsordnung vom 8. Juni 2017 bekannt ist und von mir anerkannt wird.

2. dass ich weder früher noch gleichzeitig bei einer anderen Hochschule oder in einer anderen Fakultät ein Promotionsverfahren beantragt habe.

3. hiermit an Eides statt, dass ich die vorliegende Arbeit ohne unzulässige Hilfe Dritter und ohne Benutzung anderer, nicht angegebender Hilfsmittel angefertigt habe. Die aus anderen Quellen direkt oder indirekt übernommenen Daten und Konzepte sind unter Angabe der Quelle gekennzeichnet
   Die Arbeit wurde bisher weder im In- noch im Ausland in gleicher oder ähnlicher Form einer anderen Prüfungsbehörde vorgelegt.
   Es wurden keine Dienste eines Promotionsvermittlers oder einer ähnlichen Organisation in Anspruch genommen.

4. dass zu den vorgeschlagenen Mitgliedern der Promotionskommission keine verwandtschaftlichen Beziehungen, keine Verwandtschaft ersten Grades, Ehe, Lebenspartnerschaft oder eheähnliche Gemeinschaft besteht.

5. dass in meiner Dissertation Forschungsergebnisse verwendet worden sind, die in Zusammenarbeit mit den folgenden Wissenschaftlern gewonnen wurden:

   - Frank E. S. Steinhoff, Dr. , Univ. Fed. de Goias
   - Nikolai Miklin, Dr., Univ. of Gdansk
   - Tristan Kraft, M.Sc., Univ. Siegen
   - Nicolar Brunner, Assoc. Prof. Dr., Univ. de Geneve
   - Marcus Huber, Dr., IQOQI Vienna
   - Cornelia Spee, Dr., Univ. Siegen
   - Otfried Gühne, Prof. Dr., Univ. Siegen

Signed:

_____

Date:

_____